University of Naples Federico II

Department of Agricultural Sciences

Ph.D. in Sustainable Agricultural and Forestry Systems and Food Security

XXXVI Cycle

Humic biostimulants from *green* compost and synergies with mycorrhizal fungi

Ph.D dissertation by

Claudia Savarese

Tutor: Prof. Alessandro Piccolo **Coordinator: Prof. Albino Maggio**

Co-Tutor: Prof. Vincenza Cozzolino

Academic years: 2018-2021

INDEX

SUMMARY

Currently, agricultural intensification is considered as the main strategy to ensure the growing need for food production. However, conventional agriculture already has major global environmental and human impacts such as soil fertility and biodiversity reduction, about one-quarter of global greenhouse gas (GHG) emission, and environmental pollution by the extensive use of chemical products (i.e. fertilizer and pesticides). Therefore, the present thesis work aimed to evaluate various approaches to provide a truly effective solution for maintaining crop productivity and food security, thus supporting the development of sustainable agriculture to replace conventional agronomic practices.

The deterioration of soil health is the main negative aspect of conventional agriculture, since traditional agronomic practices can drastically reduce the quantity and quality of soil organic matter (SOM), as well as the storage of soil organic carbon (SOC). SOM plays a fundamental role in the agro-ecosystems, as it regulates the global carbon and nitrogen cycle, the development of plants and microorganisms, the fertility and stabilization of soil structure. Despite its importance for the development of a sustainable agriculture, the molecular dynamics of soil organic matter under different cropping systems is still poorly understood. Hence, in the first two studies of this research the molecular dynamics of organic matter in soils subjected to long-term field experiments (20 years) under conventional maize monoculture or maize-leguminous crop rotation, were evaluated by both traditional analytical techniques and an innovative chemical sequential fractionation named Humeomics. The application of off-line pyrolysis TMAH-GC-MS (thermochemolysis) and solid-state ^{13}C NMR spectroscopy for the direct molecular characterization of OM components of both the bulk soils and their humic extracts revealed that the long-term cultivation under conventional tillage destabilizes SOM molecular conformation, though to a different extent, as a function of the cropping system. In particular, 20 consecutive years of maize mono-cultivation led to a decrease in alkyl and aliphatic compounds, and an increase in hydrophilic labile components, while the crop-rotated soils

showed a partial preservation of the pristine SOM composition by maintaining the content of hydrophobic and lipid constituents. The application of Humeomics technique, coupled to characterization of separated fractions by GC-MS and high-resolution Orbitrap LC-MS, on the same soils confirmed these results. Particularly, Humeomics showed that the ratio of organosoluble to hydrosoluble components significantly decreased passing from untreated to long-term cultivated soils, thus revealing that the loss of humic hydrophobic compounds such as long-chain esters and fatty acids, rendered more physically and chemically fragile the protection of organic matter in soil. Moreover, most of N-containing compounds in cropped soils were found to be bound to iron, thus implying that different forms of nitrogen entering soil are progressively sequestered into recalcitrant organic pools. These findings highlight that a detailed knowledge on the molecular dynamics of soil Humeome can be archive by Humeomics fractionation, which could be an innovative tool to identify new environmentally sustainable technologies in agriculture.

Another objective of this thesis was to estimate the effectiveness of mixed plant biostimulants as an eco-friendly strategy to increase plant growth while concomitantly ensuring high levels of agricultural productivity and environmental security. To this purpose, the bioactivity of two different humic materials, a potassium humate from leonardite (KH) and compost tea (CT) from a green compost made of coffee husks, and their combination (1:1), was evaluated toward basil seeds germination and maize early growth. After their thorough chemical and molecular characterization, a relation between structure and bioactivity was also investigated. The results of this experiment showed that the high polar CT stimulated both the epicotyl and root development of basil seeds, while the mostly hydrophobic KH exerted a significant bioactivity on maize early growth. On the other hand, the application of a mixed solution of both humic materials to hydroponically grown maize plantlets resulted in a biostimulant effect similar to KH but greater than the individual CT treatment. The molecular characterization of the humic materials allowed to explain these results by a cage effect of the readily bioavailable CT compounds, such as oxidized lignin fragments, saccharides, and peptides within the hydrophobic domains of the mainly apolar KH. These findings thus indicate that

a calibrated mixture of humic materials of selected molecular composition may represent an innovative and ecologically viable method to build up sustainable products with diverse mechanisms of plant biostimulation. Moreover, in a second experiment the bioactivity of the same mixed humic biostimulants was investigated in synergy with microbial bioeffectors (Micosat TABPLUS, M+) on lettuce productivity, nutritional status and metabolism. The synergistic interaction between KH, CT and M+ significantly increased lettuce biomass production and uptake of both macro- and micronutrients compared to the individual application of the biostimulants. Furthermore, the humic-microbial combination (MIX_M+) positively affect the overall plants metabolism. In particular, the GC-MS analysis of leaves primary metabolites revealed an improve in the biosynthesis of essential amino acids and saccharides following the MIX_M+ treatment, thus suggesting the potential role of humic substances in supporting the survival of beneficial microorganisms in the soil environment, as well as in promoting their colonization capacity. Similarly, the UHPLC-MS-IT-TOF analysis of lettuce polyphenols metabolism showed an accumulation of important antioxidant compounds in plants treated with mixed humic materials, thereby supporting the cage effect of bioavailable CT compounds in the hydrophobic components of KH that may enhance the conformational stability of the humic assembly essential for the release of bioactive molecules and the effectiveness of their biological activity. Hence, the findings of this second experiment indicate that a calibrate mixture of humic extracts, containing different type of bioactive molecules, in combination with microbial consortia is a potential tool to improve plants both productivity and nutritional status, as well as to modulate plants metabolome for the development of novel functional crops.

Finally, an additional goal of this doctoral research was to investigate the possible applications of innovative hydrogels based on humic matter from green compost to improve plant growth. The potential use of a hydrogel containing sodium alginate and humic extracts from green compost cross-linked by calcium nitrate and able of maintaining shape after 3D bio printing, as a substrate for soilless cultivation was explored. The preliminary results of this experimentation showed that the addiction of humic substances improved the printability of the alginate gel, ensuring the right mechanical

proprieties essential for 3D printing, and thus resulting in well-assembled and easly printable structures. Furthermore, the biostimulant activity of humic extracts toward plants development allowed an increased growth of both basil and lettuce seedlings in the hydrogel bio-composite compared to the sodium alginate alone. These findidings may indicate that humic-hydrogels could be innovative biomaterials for several agricultural applications.

CHAPTER 1

1.1. The necessity of sustainable agriculture

The world population is estimated to rise from seven to nine billion people by 2050 (Ray et al., 2013), requiring an increase in global food production of between 60 and 110 % (Pardey et al., 2014). In this scenario, agricultural intensification is considered as the main strategy to ensure the growing need for food production (Shennan et al., 2017). However, conventional agriculture already has major global environmental and human impacts: soil fertility and biodiversity reduction (Bai et al., 2018), about one-quarter of global greenhouse gas (GHG) emission (Sanz-Cobena et al., 2017), water, soil and air pollution by the extensive use of chemical products (i.e. fertilizer and pesticides) (Rasmussen et al., 2015; Sun et al., 2018).

The deterioration of soil quality and fertility is the main negative aspect of conventional agriculture, since soil is a vital resource for plant life in the environment, thus representing the major natural not-renewable resource that underpins the survival and development of human beings. Traditional cultivation drastically reduces the quantity and quality of soil organic matter (SOM), as well as the storage of soil organic carbon (SOC) (Piccolo and Mbagwu, 1990; Ogle et al., 2005; Celik, 2005; Ostle et al., 2009), despite their fundamental role in the soil agro-ecosystems (See Paragraph 1.1.1.). Conventional tillage (CT) practices can mechanically break soil aggregates, thus exposing the accumulated organic material to chemical and microbial oxidation and leading to faster losses of soil organic carbon (Six et al. 1999, 2000; Piccolo et al., 2005; Spaccini et al., 2006). Soil disaggregation by CT has extreme consequences, since aggregates not only physically protect soil organic matter (SOM) (Tisdall and Oades, 1982; Piccolo, 1996), but also influence microbial community structure (Drążkiewicz, 1994), limit oxygen diffusion (Sexstone et al., 1985), regulate water flow (Prove et al., 1990), determine nutrient adsorption and desorption (Wang et al., 2001), and reduce run-off and erosion (Barthes and Roose, 2002; Six et al., 2004). Moreover, conventional agricultural practices negatively affect soil biota biodiversity (Spedding et al. 2004), leading to a reduction of

microorganisms density, mainly fungi, which are essential in the linking of soil particles together (Beare et al. 1997). The massive GHG emission and the extensive use of chemical products are other dangerous outcomes of traditional agriculture. Sanz-Cobena et al. (2017) well described that conventional management practices increase the emission of CO_2, CH_4 and N_2O in the atmosphere, while Sun et al. (2018) reported that the considerable amount of sinthetic fertilizer and pesticides used in traditional agriculture is the major couse of soil pollution.

A A mitigation of soil degradation can be achieved by tillage or cultivation practices that ensure SOC sequestration and SOM stabilization, such as conservation tillage, reduced- or no-tillage, crop rotation, and strategy involving the return of crop residues and agroindustry by- products (i.e. manure, compost, biochar) to soil. These practices have several co-benefits, such as the improvement of soil physical, chemical and biological quality (Lal, 2011; Lassaletta and Aguilera, 2015), the enhancement of crop productivity, the reduction in both dependence on external inputs (Smith and Olesen, 2010) and soil erosion rates. Conservation tillage, in contrast to conventional tillage systems, positively affects soil microbiome, by significantly sustaining greater microbial biomass C in the long term, and increases the share of microbial biomass C in total soil organic C (Balota et al. 2003). On the other hand, the absence of tillage (NT) compared to CT, reduces soil disaggregation, thereby increasing the stabilization of SOC within soil aggregates (Álvaro-Fuentes et al., 2008; Plaza-Bonilla et al., 2010), and enhancing both soil microorganism's biodiversity (Kladivko, 2001) and water retention potential (Lampurlanés et al., 2016). Loss of SOC can also be reduced by changing from monoculture to rotation cropping (West and Post, 2002). Long crop rotations improve C sequestration, while restoring soil fertility and structure (Benlhabib et al., 2014). In particular, the introduction of leguminous species in crop rotation was found to stabilize soil organic matter more efficiently than cereals (Carranca et al., 2009), in addition to the reduction of required fertilizers and their high-crop-value in forage production (Rochon et al., 2004).

It has been recently underlined the role of compost biomasses in stabilizing organic matter in soil and reducing SOC losses (Spaccini et al., 2009, 2013; Piccolo, 2012). Compost application leads

to multiple benefits for agricultural soils such as the overall increase of porosity, structural stability, biological activity, and resistance to erosion (Garcia-Gil et al., 2000; Weber et al., 2007; Pane et al., 2015; Cozzolino et al., 2016). Agricultural practices not only influence SOM quantity (organic C, total N) and soil biological status (microbial biomass C), but also the stability of its hydrophobic and hydrophilic components (Piccolo et al., 2004; Šimon et al., 2009). Therefore, in the following two paragraphs it is discussed both the fundamental role of the molecular features of soil organic matter in agro ecosystems, and the evaluation of its molecular dynamics in soil by innovative techniques.

1.1.1. Soil Organic Matter: the fundamental role in soil fertility

Organic matter (OM) or humus is the organic constituent of soil, sediments and of dissolved OM in water, consisting of the product of microbial decomposition of plant materials and animals, which hence evolve towards a higher entropy state (Hayes and Swift, 1978). Soil OM plays a fundamental role in the agro-ecosystems, as it regulates the global carbon and nitrogen cycle, the development of plants and microorganisms, the fate and transport of anthropogenic compounds and metals heavy, the fertility and stabilization of soil structure (Piccolo, 1996; Nardi, 2002). The presence of organic matter in soils also serves as a carbon pool capable to "sequester" the atmospheric CO_2 and reduce its release in the atmosphere. Soil organic carbon (SOC) represents a significant reservoir of carbon within the global carbon cycle that has been estimated to account for 1,200–1,550 Pg C to a depth of 1 m and for 2370–2450 Pg C to a depth of 2 m (Lal, 2004). The essential role of SOM in the stabilization of soil aggregates and consequently in the protection of SOC from oxidation and microbial degradation is mainly related to organic matter hydrophobicity (Piccolo and Mbagwu, 1994, 1999; Piccolo, 1996). This feature of soil organic matter is of fundamental importance, as practices that promote soil hydrophobicity could be used to reduce SOC losses and GHG emission from conventional agriculture (Fonte et al., 2009). Knowledge of SOM molecular composition is hence necessary to understand its dynamics in soils subjected to agricultural management.

The major characteristic of SOM is its remarkably heterogeneity, that leads to an extremely variable composition as a function of several factors, such as climatic conditions, origin of organic compounds reaching the soil and their different nature, as well as the variability of the transformation processes that occur in soil (Saiz-Jimenezs, 1996; Piccolo, 1996). Heterogeneous groups of compounds, identified through their residence times in soil and ranging from the undecomposed organic residues to simple products of decomposition but yet recalcitrant, make up organic matter in soil (Andreux, 1996). The organic residues represent the labile fraction of SOM and mainly consist of simple molecules such as amino acids, sugars, dicarboxylic organic acids, and compounds with greater molecular weight (MW) as polysaccharides, proteins, nucleic acids, lipids and lignins (Piccolo, 1996). Carbohydrates are qualitatively and quantitatively the most important component (Cambrardella and Elliot, 1992) and are estimated to represent up to 25 % of SOM (Stevenson, 1994), being an important source of available energy for the maintenance and development of soil microbial community (Insam, 1996).

Humic substances (HS) represent the more recalcitrant and abundant (50-70 % of SOM) component of soil organic matter (Piccolo, 1996). Humic substances have been divided, based on their solubility, in fulvic acids (FA), humic acids (HA) and humin (HU) (Stevenson, 1994). FA are soluble in aqueous solutions in acidic, neutral, and basic conditions and are the most highly hydrophilic fraction, with the highest acidity. HA are instead solubilized in alkaline conditions but become insoluble again at pH < 3. Humic acids are more hydrophobic, less acidic and poorer in oxygen content (O / C close to 0.5) than FA. Humin is insoluble in either alkaline or acidic conditions, highly hydrophobic and most recalcitrant pool of soil humic substances, with a larger H / C index around 1.5 than those of HA and FA close to 1.0 (Stevenson, 1994).

Several theories on the molecular composition and structure of HS have been formulated over the years. It was initially assumed that HS were polymeric structures consisting of high molecular weight molecules stabilized by covalent bonds (Schnitzer, 1972; Gosh and Schnitzer, 1980). Subsequently, Wershaw (1986) proposed a "micellar" vision, according to which HS would be

amphiphilic structures with highly organized micellar conformation, whose hydrophilic part faces outwards to interface with soil minerals or water of hydration, while the hydrophobic chains form an apolar microenvironment in which other hydrophobic substances could enter to minimize contact with water. The interactions involved would therefore be mainly hydrogen bonds, van der Waals and hydrophobic forces. Finally, several studies conducted by Piccolo and collaborators (1996, 1999b, 2000, 2001) showed that HS appeared as clusters of only apparently large MW, in which small heterogeneous molecules with MW less than 1000 Da, are held together by weak interactions. Therefore, humic substances are nowadays regarded as the self-assemblage of relatively small heterogeneous molecules (< 1000 Da) held together in a supramolecular association by relatively weak interactions such as hydrogen bonds, hydrophobic and van der Waals bonds (Piccolo, 2002). This novel knowledge of HS structural conformation is essential to understand their key role in both soil health and plants development (See Paragraph 1.2.1.). In particular, the main positive function of HS in soils is the long-term stabilization of aggregates by hydrophobic bonding (Piccolo, 1996), which ensure the organic matter separation from soil solution and concomitantly protection from microbial degradation activity, thus favouring the stabilization of organic carbon in soil (Piccolo and Mbagwu, 1999). This "hydrophobic effect" enables a mitigation of SOM degradation and SOC losses as CO_2 emission when humic substances are reinstated in the organic matter of soils (Piccolo et al. 1997a,b, 1999a). In particular, the higher is the hydrophobicity of the employed humic material, the larger the "sequestration" of organic carbon in soil (Piccolo and Mbagwu, 1990; Spaccini et al., 2002). Similarly, it has recently been demonstrated that mature compost possesses the same ability to hydrophobic stabilize organic matter in soil, thus reducing GHG emission (Spaccini et al., 2009). This positive effect of composted biomass on the overall soil bio-humeome is due to compost alkyl components, mainly lipids, waxes, biopolyesters, and lignin-derived aromatic structures, which represent hydrophobic domains where soil labile organic molecules can be protected from microbial mineralization (Piccolo et al, 2004; Spaccini and Piccolo, 2007, 2009). In fact, Spaccini and Piccolo (2012) reported that compost treatments fixed in soils from 3 to 22 ton ha^{-1} more OC than for

conventional tillage. Moreover, Nuzzo er al. (2016, 2017) and Piccolo et al., (2018a) lately showed that the same SOC accumulation can be achieved by photopolymerization of dissolved humic molecules with biomimetic catalysis (metal-porphyrins), which increases the molecular size of soil Humeome (Šmejkalová and Piccolo, 2005, 2006; Nuzzo and Piccolo, 2013a,b) thus promoting the overall stabilization of organic carbon. This evidence on the role of SOM components in agricultural soils quality underlines that the comprehension of Humeome molecular dynamics in soil is a fundamental prerequisite for identifying alternative management practices to reduce the negative impact of conventional agriculture (See Paragraph 1.1.2).

1.1.2. Humeomics as an innovative tool to reveal the impact of agricultural practices

The novel understanding proposed by Piccolo et al. (2001, 2002) of soil Humeome as a supramolecular association of heterogeneous and relatively small (<1000 Da) molecules held together by weak dispersive forces (See Paragraph 1.1.1.) unveiled the possibility to isolate single humic molecules by a progressive breakdown of those inter- and intramolecular interactions, thus facilitating their structural characterization (Piccolo et al., 2019). Based on this concept, it has recently been developed a methodology named Humeomics that consists of "*a stepwise separation of molecules from the complex bulk suprastructure of soil Humeome by progressively cleaving esters and ether bonds and characterizing the separated molecules by advanced analytical instrumentation*" (Piccolo et al., 2018b).

Nebbioso and Piccolo (2011) applied Humeomics for the first time to a humic acid isolated from an Italian soil. The authors obtained both organo- and hydro-soluble fractions by four steps of sequential fractionation, and then characterized their molecular composition, as well as the bulk HA, by chromatography-mass spectrometric techniques (GC–MS and LC–MS) and NMR spectroscopy. In particular, the first fraction of Humeomics (ORG1), derived from an organic solvent extraction (dichloromethane and methanol solution) of free or unbound humic molecules associated with the humic suprastructure only by weak dispersive interactions, showed a greater visibility of alkyl and

saturated components mainly comprising alkanoic (saturated, unsaturated and hydroxylated), hydroxydioic and cyclic acids. On the other hand, the second organosoluble (ORG2) and hydrosoluble (AQU2) fractions, obtained by the cleavage of weakly bound esters by a mild boron trifluoride-methanol (BF3-MeOH) transesterification, were respectively characterized by similar unsaturated compounds but of a lesser degree of unsaturation, plus a larger oxygen substitution than for bulk HA. Moreover, the authors found a large content of N-containing molecules in AQU2 that implied the greater affinity of these humic nitrogenous components to the aqueous phase (Nebbioso and Piccolo, 2011). The third Humeomics step in the study of Nebbioso and Piccolo (2011) was the clearage of strongly bound esters by an alkaline solvolysis reaction (KOH-MeOH), and produced components separated into organosoluble (ORG3) and hydrosoluble (AQU3) fractions. The molecular characterization of ORG3 revealed that this fraction consisted mainly of aliphatic and polyhydroxylated acids, while the low amount of AQU2 prevented its characterization. Finally, the authors applied a treatment with hydroiodic acid (HI) to cleave both strong ether and glycosidic bonds, following a classic mechanism of protonation of the organic ether and subsequent nucleophilic substitution (SN) by iodide with an alcohol acting as a good leaving group. Although the little amount of this extracted fraction (AQU4) prevented its analysis, the molecular characterization of the resulting final residue showed a predominance of totally substituted or condensed aromatic carbons as the end product of the Humeomics fractionation, and a complete disappearance of alkanodioic acids instead detected in the bulk HA (Nebbioso and Piccolo, 2011). Nebbioso and Piccolo (2011) showed in their study that the Humeomic technique succeeded to identify up to 60% of the Humeome, while the unaccounted 40% was attributed to losses of occluded hydration water and small volatile organic compounds, and to decarboxylation.

The same authors then applied the Humeomics fractionation to three size-fractions of the same HA after their separation by preparative HPSEC (high preformation size exclusion chromatography) and identified a greater number of compounds compared to the unfractionated HA (Nebbioso and Piccolo, 2012). The larger overall analytical response of the three size-fractions was explained by the

weakening of conformational stability of the humic suprastructures during the HPSEC separation, and the consequent isolation of less complex humic fractions (Nebbioso and Piccolo, 2012). This study also confirmed the pivotal role of hydrophobic interaction in the stabilization of soil Humeome (See Paragraph 1.1.1.), since the authors found that hydrophobic compounds were mainly distributed in the largest size- fraction, while hydrophilic components were eluted in the smallest size-fraction (Nebbioso and Piccolo, 2012). In two following studies, Nebbioso et al. (2014 a,b) subjected the residual product of a Humeomics fractionation to a preparative HPSEC that yielded ten size separated fractions, which were characterized by high-resolution Orbitrap ESI-MS and different NMR techniques. The results of Orbitrap ESI-MS indicated that long-chain saturated acids were more abundant in large-sized fractions than in short-chain homologues, whereas unsaturated, hydroxylated, and most cyclic acids were prevalent in small-sized fractions (Nebbioso et al., 2014a). On the other hand, the NMR spectra showed that the diffusion coefficients for the size-fractions differed from those of the bulk HA, thus confirming the profound changes in conformational structure induced by HPSEC separation (Nebbioso et al., 2014b). Furthermore, the application of Humeomics fractionation on the un-extractable humin fraction (HU) of the same soil, after removal of minerals by HF/HCl treatment, revealed that HU contained similar components of the bulk HA, thus suggesting more differences in the supramolecular conformation of the humic pool rather than in the molecular composition (Nebbioso et al., 2015).

Following the evidence that Humeomics may lead to a thorough knowledge of humic molecular composition and conformational architecture, necessary to understand their role in agro-ecosystems (See Paragraph 1.1.1.), Drosos et al. (2017) applied the sequential fractionation directly on an agricultural soil, thus comparing this approach to the traditional alkaline extraction used to study SOM dynamics in soils. The authors found that Humeomics fractionation was greatly more efficient in extracting and identifying humic molecules than the traditional alkaline extraction, thus suggesting the potentiality of this technique in the study of the overall soil Humeome. In fact, Humeomics appeared able to progressively release humic molecules from the protective domains

composed of highly hydrophobic materials (ORG fractions), which are surround or are contiguous to hydrophilic moieties (AQU fractions) (Drosos et al., 2017; Piccolo et al., 2018b). Moreover, it was shown that these domains in soil stabilized by organo-mineral complexes through covalent bonds between humic molecules and either Fe or Al-Si components in oxides, hydroxides, and clay minerals (Drosos et al., 2017).

Another important molecular information revealed by Humeomics applied directly to soil was the potential use of the organosoluble to hydrosoluble organic carbon ratio (CPR) in the evaluation of OC stabilization in soil (Drosos et al., 2017). The authors explained that the greater OC amount separated in the ORGs than in the AQUs was due to the abundance of lipidic compounds, which are responsible for the hydrophobic protection of carbon compounds from mineralization and microbial degradation (See Paragraph 1.1.1.), thereby resulting in greater CPR values. They concluded that larger the CPR of a soil Humeome, the greater is the chemical stabilization of soil humus (Drosos et al., 2017). Drosos and Piccolo (2018) confirmed this hypothesis by applying Humeomics on an agricultural soil after 1 and 3 years of conventional tillage under maize cropping. This study revealed a decrease in the overall aliphaticity of SOM in the third year of conventional cultivation, with a consequent significant decrease of the CPR ratio. Moreover, the results of Drosos and Piccolo (2018) further supported the organo-iron complexes formation as the major mechanism of persistent fixation in soil for specific molecules, since they found that nitrogen-rich compounds were persistent in soil after three years of traditional tillage practices. Recently, Drosos et al. (2020) showed that the hydrophobic protection and the organo-minerals fixation of organic materials in soils also change with different cropping systems. In fact, the application of Humeomics revealed that three consecutive years of conventional wheat cropping destabilized the soil Humeome by hydrolyzing the esterified matrices and displacing the humic molecules from iron complexes, thus suggesting that SOM molecular composition is extremely dynamic even after a short-term cultivation.

In recent years, the acknowledgement that Humieomics is a potential tool for revealing the influence of different environmental and agricultural conditions on the soil Humeome (Piccolo et al.,

2019) has promoted the application of this technique for the characterization and differentiation of complex organic matrices. For example, Vinci et al. (2020) applied for the first time the Humeomics fractionation to peat samples collected in two different countries (Canada and Swiss) and at different depths. The authors found less chemical stabilization of humic suprastructures in Canadian peat compared to Swiss peat and greater recalcitrance of both peat humus when collected from the deeper layer as compared to that of the surface horizon. The main difference between the two peat samples was the amount of aromatic and terpenoid compounds in their ORG2 extracts, thus suggesting that the molecular composition of the weakly bound ester fraction may be used to differentiate samples based on geographical origin or environmental conditions (Vinci et al., 2020). The same authors showed in a subsequent work that the content of phenolic and benzoic acids, detected in ORG2 and attributable to lignin or suberin monomers, was the principal difference between two calcareous French soils (Vinci et al., 2021). These findings further confirmed that the "Humeomic" approach provides not only information on the molecular composition of the humic pool, but also on the strength by which organic compounds are retained in the complex supramolecular structure of the soil Humeome (Piccolo et al., 2019; Vinci et al., 2021). Therefore, the understanding of organic matter molecular dynamics in soil by the employment of Humeomics sequential fractionation could be an efficient strategy to identify alterative practices to the conventional agriculture, thus reducing its negative impact (See Paragraph 1.1).

1.2. Plant Biostimulants: an eco-friendly strategy

Recently, the agricultural sector is facing concomitant challenges of rising the productivity to feed the growing global population and reducing the environmental and human health negative impact of conventional agriculture practices (See Paragraph 1.1.). Plant Biostimulants (PB) represent a promising and eco-friendly strategy to stimulate plant growth at very low dosages while concomitantly ensuring high levels of agricultural productivity and food security (du Jardin, 2015; Yakhin et al., 2017; Rouphael and Colla, 2020). The definition of PB appeared for the first time in a

bibliography analysis of scientific literature by du Jardin (2012), which described plant biostimulants as "*substances and materials, with the exception of nutrients and pesticides, which, when applied to plant, seeds or growing substrates in specific formulations, have the capacity to modify physiological processes of plants in a way that provides potential benefits to growth, development and/or stress responses*". In this study du Jardin (2012) proposed eight categories of substances that acts as biostimulants: humic substances, complex organic materials, beneficial chemical elements, inorganic salts, seaweed extracts, chitin, and chitosan derivates, antitranspirants, free amino acids and N-containing substances, though he did not include any microbial biostimulants. Three years later PB were defined by the same author as follows: "*A plant biostimulant is any substance or microorganism applied to plants with the aim to enhance nutrition efficiency, abiotic stress tolerance and/or crop quality traits, regardless of its nutrient content*" (du Jardin, 2015). Recently, the new Regulation (EU) 2019/ 1009 introduced the following definition "*A plant biostimulant shall be an EU fertilizing product the function of which is to stimulate plant nutrition processes independently of the product's nutrient content with the sole aim of improving one or more of the following characteristics of the plant or the plant rhizosphere: i) nutrient use efficiency, ii) tolerance to abiotic stress, iii) quality traits, or iv) availability of confined nutrients in the soil or rhizosphere*" (EU, 2019). Nowadays, PB are tools to enhance agricultural production as progressively shown by scientific publications and the constant expansion of their market. France, Italy, and Spain are the leading EU countries in the production of biostimulants (Traon, 2014). It has been demonstrated that PB application resulted in multiple benefits, since they not only stimulate plant development and productivity, but also enhance plant nutrient uptake and assimilation, promote resistance to several abiotic and biotic stresses, and directly influence plant physiology and metabolism (both primary and secondary) (Bulgari et al., 2015; Yakhin et al., 2017; De Pascale et al., 2017). Moreover, the attention to the potential boost effect on plants of the synergistic combination between different biostimulants drastically increased (Rouphael and Colla, 2018; Castiglione et al., 2021). However, the mechanisms of action by which these bioactive products promote plants growth are difficult to identify and still under investigation

(Ertani et al., 2011; Olivares et al., 2017). Plant biostimulants are generally classified in the following major groups:

Humic substances (HS): they include fulvic acids, humic acids and humin. HS are naturally bioactive molecules of relatively small molecular weight (< 1000 Da) derived from the microbial decomposition of plants and animal tissues, and arranged together in a supramolecular assembly by multiple week interactions (Piccolo, 2002). Humic substances have a fundamental role in the agro-ecosystems (See Paragraph 1.1.1.), since they participate in the maintenance of soil physical, chemical and biological quality (Piccolo, 1996). HS increase plant development, productivity, and tolerance to abiotic/biotic stresses through their interaction with different bio-chemical mechanisms and physiological processes in plants (Nardi et al. 2007; García et al., 2012; Canellas and Olivares, 2014; Canellas et al., 2015a). This biostimulant activity of HS has been related to the incorporation of hormone-like molecules into their supramolecular structure, which can be destroyed by low molecular weight organic acid, like those commonly exuded by plants (Piccolo et al., 2001; Smejkalova and Piccolo, 2008; Savy et al. 2017; Piccolo et al. 2019).

Seaweed extracts (SWE): they are available on the biostimulant market as powder, granular form and as liquid extracts from brown, red, and green macro-algae, which can be applied as foliar sprays or side-dressed near the root. SWE consisted of a several bioactive molecules, such as polysaccharides, phenols, vitamins precursors, osmolytes (mannitol), phytohormones, and hormone-like compounds (Battacharyya et al., 2015). Seaweed extracts are widely used as PB for their enhancement of plant productivity, abiotic stress tolerance, photosynthetic activity, postharvest quality and shelf life (Sharma et al., 2014; Rouphael et al., 2017).

Protein hydrolysates (PH): they are a mixture of free amino acids, oligo- and polypeptides extracted from plant or animal residues. PH are mainly applied as foliar spray and to a lesser extent as a substrate drench and as seed treatment (Colla et al., 2015a). The application of PH resulted in multiple benefits such as increase in plants development, nutrient uptake, and resistance to abiotic

stresses (Ertani et al., 2009; Colla et al., 2017; Sestili et al., 2018). Moreover, the PH direct influence on plants metabolism has recently been underlined (Nardi et al., 2016; Lucini et al., 2018).

Beneficial microorganisms: this group include plant growth-promoting bacteria (PGPB), arbuscular mycorrhizal fungi (AMF) and *Trichoderma spp*. The main positive effect of these beneficial microorganisms is the increase of both macro- (mainly N and P) and micronutrients (i.e. Fe) availability in soil, thus promoting their uptake and use efficiency by plants, which leads to a higher photosynthetic activity and productivity (Backer et al., 2018; Bitterlich et al., 2018; Woo and Pepe, 2018).

1.2.1. Humic biostimulants

Humic substances (HS) are the subject of study in various areas of agriculture, such as soil chemistry and plant physiology, because of the multiple roles played by these materials that can greatly benefit plant growth (Piccolo, 1996; Nardi et al., 2002). HS are one of the main categories of PB, since they can positively affect several plants physiological and metabolic processes as hormone-like molecules, thus stimulating root system development, biomass production, nutrient uptake and resistance to stress condition (Nardi et al. 2007; García et al., 2012; Canellas and Olivares, 2014; Canellas et al., 2015). The main humic substances commercially on the market, called potassium humates (KH), derive from geochemical sources (e.g. lignite, leonardite). KH are widely used both as fertilizers to improve soil chemical, physical and biological proprieties, and as biostimulants to promote plant productivity and resistance to stress conditions (Piccolo et al. 1997a; Kumar and Singh 2017; Conselvan et al. 2017; Ertani et al. 2019). However, the recent necessities of alternative sustainable technologies to reduce the negative impact of conventional agriculture (See Paragraph 1.1.) strongly increased the application of HS from renewable resources, such as composted biomasses, agro-food by-products, or bio-refinery wastes (Savy et al. 2015; Monda et al. 2017; Spaccini et al., 2019). The composting process is a low-cost and sustainable technology to recycle organic biomasses into stabilized products with a significant amount of humified components, which

act as valuable alternative to synthetic chemicals fertilizers (Spaccini and Piccolo, 2009; Piccolo et al., 2012). Recently, it has been shown that the water-soluble fraction of composted biomasses, named compost tea (CT), has multiple beneficial effects as plant biostimulant (Pane et al., 2016; Zaccardelli et al. 2018), bio-pesticide or antimicrobial product (Koné et al. 2010; Verrillo et al. 2021a). CTs are obtained by water immersion of compost, from few days or up to two weeks, with or without active aeration, to produce aerated or non-areated compost teas, respectively (Eudoxie and Martin, 2019).

The promotion of plant growth by humic substances is well documented in the literature (Piccolo et al., 1992; Nardi et al., 2002, 2007; Canellas and Olivares, 2014). The most reported beneficial effect of HS is the promotion of plant root system (Canellas et al., 2015). Many studies have reported that the primary biological activity of HS is the induction of lateral roots emergence and development (Canellas et al., 2002, 2012; Jindo et al., 2012). Roots formation is related to the activity of the H^+-ATPase pumping across the root plasma membrane (PM), since it generates the proton motive force that is necessary to promote the active and passive transport of ions and metabolites through the symplastic pathway (Morsomme and Boutry, 2000). Hager (2003) showed that H+ pumping also lowers the pH of the cell wall (apoplast), activates pH-sensitive enzymes and proteins associated with the wall, and initiates cell wall loosening and extension growth. This mechanism, called acid growth theory, is induced by auxin (Hager, 2003). Canellas et al. (2002) reported that plasma membrane vesicles isolated from maize roots treated with HS exhibited a clear stimulation of the vanadate-sensitive ATPase activity. Similarly, Quaggiotti et al. (2004) found that humic substance induced the overexpression of the major isoform of the maize PM H+-ATPase (Mha2). The authors attributed this stimulatory effect to the presence of auxin-like molecules (i.e. indolacetic acid) into the supramolecular structure of HS (Piccolo, 2002), which access cell receptors to trigger cell signalling (Muscolo et al., 1998, 1999). Another possible mechanism involved in increasing root hair length and density following HS application is the promotion of nitric oxide (NO) accumulation in sites of lateral root emergence (Zandonati et al., 2007). In fact, NO is a bioactive molecule involved in root development (Lamattina et al., 2003), and its regulation by HS has been

shown to be related to morphological root changes such as increase in the number of secondary roots, root thickness and fresh weight (Mora et al., 2012). The promotion of H+-ATPase activity may also lead to the enhancement in root exudation of organic acids observed for HS-treated maize seedlings (Canellas et al., 2008; Puglisi et al., 2008). Actually, the disruption of HS supramolecular assembly by organic acids such as those extruded by plants (Piccolo et al., 2001; Smjkalova and Piccolo, 2008) is in line with the release of bioactive molecules with auxin-like activity. Moreover, Ramos et al. (2015) provided the first evidence for HS upregulation of genes involved in H+-Ca2+ cell signalling, which is in line with the overexpression of calcium-dependent protein kinase (CDPK) responsible for phosphorylation reactions that regulated PM H+-ATPase activity (Morsomme and Boutry, 2000). The promotion of primary root elongation and lateral roots formation was also found in maize seedlings treated with humic-like substances (HLS), such as those extracted from bio-refinery wastes of composted biomasses, thus confirming the biostimulant activity of humic materials (Savy et al., 2015, 2016, 2017; Monda et al., 2017, 2018). In particular, the correlation between the stimulatory activity of both HS and HLS on root system development and their molecular features pointed out that the hydrophobicity of these materials is the property most related to their biological effect (Canellas et al., 2010, 2012), thus revealing the potential use of an efficient structure-activity relationship (See Paragraph 1.2.3.).

Humic materials have found to promote the uptake and accumulation of both macro- and micronutrients by plants (Jannin et al., 2012; Jindo et al., 2016; Priya et al., 2021). Nitrate is considered the most important source of mineral N for plants growth (Wang et al., 2018). Many authors observed a significant enhancement of nitrate transport induced by HS application (Piccolo et al., 1992; Nardi et al., 2000a,b; Huertas Tavares et al., 2019), which is in line with the stimulation of the PM H+-ATPase activity that generates the electrochemical gradient necessary for the uptake of nitrate ions. Moreover, Jannin et al. (2012) demonstrated an induction of genes encoding nitrate and sulphur transporters in roots of plants treated with HS. On the other hand, Jindo and colleagues (2016) recently reported the role of humic substances in the upregulation of high-affinity P transporter

genes in treated roots, while Aguirre and collaborators (2009) previously showed that the expression of genes encoding the Fe(III) chelate-reductase and a Fe(II) root transporter were also affected by HS. Similarly, it is widely reported in literature the role of compost teas in increasing both nutrients uptake and use efficiency in several crops, which is related to the presence in these extracts of both nutrients and hormone-like substances (Pane et al., 2016; Morales-Corts et al., 2018; Priya et al., 2021). This biostimulant activity of CTs on the nutritional status of treated leaves is positively correlated to an improvement in plants growth and photosynthetic activity (Naidu et al., 2013; Zaccardelli et al., 2018).

The stimulatory activity of humic materials on plants growth is also related to their influence on both primary and secondary metabolism. The activity of key enzymes linked to N uptake and assimilation is found to be upregulated by HS (Vaccaro et al., 2015). Ertani et al. (2011) reported that HS application on maize seedlings increased the activity of glutamine synthetase (GS) by 65 % in roots, as well as improved glutamate synthase (GOGAT) functionality by 176 % in the roots and 204 % in leaves, respectively. These results were in accordance with the previously observed enhancement in the activity of N metabolism key enzymes following treatments with humic substances, such as malate dehydrogenase, glutamate dehydrogenase and phosphoenolpyruvate carboxylase (Panuccio et al., 2001). Many studies subsequentaly described the potential role of humic materials in the regulation at transcriptional and post-transcriptional levels of genes involved in the major metabolic plant functions such as carbon and photosynthesis, general cell metabolism, nitrogen/sulphur, phytohormones, plant development, responses to stress and transport of ions and water (Carletti et al., 2008; Trevisan et al., 2011; Jannin et al., 2012). Other essential function in plant physiology that are influence by humic substances are glycolysis and tricarboxylic acids cycle (TCA). Nardi et al. (2007) reported a positive effect of HS application on glycolysis enzymes such as glucokinase, phosphoglucose isomerase, PPi-dependent phosphofructokinase and pyruvate kinase, which depending on humic molecular size, molecular characteristic and concentration. Moreover, early evidence of humic substances influence on carbohydrate metabolism showed that leaf starch

content decreased in plants treated with HS, while the level of soluble sugars concomitantly increased (Merlo et al., 1991). Ertani et al. (2011) then confirmed these results, by correlated the decrease of starch and the increase of soluble sugars to the improvement of rubisco (D-ribulose-1,5-bisphosphate carboxylase/oxygenase activity) in plants treated with leonardite HS. Likewise, it has been recently shown that CTs also influence plants primary metabolism, mainly by improving the photosynthetic process and carbohydrate metabolism with a consequent increase of soluble sugars in treated leaves (Ibraheim et al., 2020; Abou-el-hassan et al., 2020).

Humic substances also strongly influence secondary metabolism. In particular, Schiavon et al (2010) showed for the first time that HS increase the expression of the phenylalanine (tyrosine) ammonialyase (PAL/TAL) that catalyses the first main step in the biosynthesis of phenolics, by converting phenylalanine to trans-cinnamic acid and tyrosine to p-coumaric acid, with a consequent accumulation of phenols in leaves. This evidence consequently increased the attention on humic materials as potential tool in regulation of plants resistance to stress conditions. In fact, Olivares et al. (2015) observed a significant enhancement of PAL activity in tomato leaves treated with humates isolated from vermicompost and a decrease of the field incidence of Phytophora infectans, while Azevedo and Lea (2011) previously showed the capacity to an osmotic adjust by maintaining water absorption and cell turgor of HS treated plants under drought stress. Generation of reactive oxygen species (ROS) is potentially harmful under stress conditions, since it can induce enzyme inhibition, chlorophyll degradation, and damage to organic molecules, including DNA, and lipid peroxidation (Apel and Hirt, 2004). In different studies, García et al. (2012, 2016) have well documented that humic substances applications increase the activity of antioxidant enzymes in plants, thus leading to a decrease in the ROS contents and a better tolerance to oxidative stresses. This regulation of redox homeostasis by HS seems to generate a state of stress that results in a beneficial effect on plants growth (García et al., 2016; van Tol de Castro et al., 2021). Following the evidence that HS play a biostimulanting role on plants secondary metabolism, many authors have reported the application of HS and CTs as an innovative tool not only to increase the resistance of crops to stress condition, but

also to improve the accumulation of important antioxidant compounds for the production of functional foods (Siddiqui et al., 2011; Haghighi et al., 2013; Ros et a., 2020; Verrillo et al., 2021b).

1.2.2. Molecular characterization of humic materials

The molecular characterization of humic materials is of fundamental importance to evaluate their biostimulant activity on plants. Non-destructive spectroscopic methods such as diffuse reflectance infrared Fourier transform (DRIFT) and ^{13}C cross-polarization magic-angle-spinning nuclear magnetic resonance (^{13}C-CPMAS-NMR) have already been applied to characterized complex organic matrices (Spaccini and Piccolo, 2007, 2009). The main advantage of these techniques is the direct analyses of solid organic samples without any preliminary treatments. The Fourier transform infrared spectroscopy (FTIR) has found widespread use for the characterization of HS, since it elucidates the distribution of main functional groups in humified organic materials (Spaccini and Piccolo, 2009; Aguiar et al., 2013). Recently, The IR spectroscopy has also been applied to study the molecular feature of humic-like substances, such as extracts from bio-refinery wastes or water-fractions of composted biomasses (Savy et al., 2015; Monda et al., 2017, 2018; Verrillo et al., 2021a). Typically, HS and HSL bear functional groups that contain oxygen (O), primarily in carbonyl (−C=O), carboxyl (C(=O-)OH) attached to an alkyl group, and hydroxyl (-OH) groups in alcohols and phenols; nitrogen (N) is set in functional groups of amines and amides, while sulfur (S−) in sulfhydryl groups (Ertani et al., 2011; Nardi et al., 2021).

CPMAS-NMR spectroscopy is a non-destructive technique widely used in environmental Sciences as it informs on the nuclei distribution in samples by reducing the interactions that prevent the acquisition of spectra of solids, such as the strong dipolar interactions among homologs and quadrupolar interaction) (Duer, 2002). In fact, Mazzei and Piccolo (2015) recently reported that this technique induces significant signals enhancement exploiting the strong heteronuclear dipolar couplings that can lead to efficient through-space magnetization transfer, called cross-polarization. The same authors also showed that CP-MAS technique increases the sensitivity for less abundant

nuclei with low gyromagnetic ratio γ, such as ^{13}C, ^{15}N, and ^{29}Si, via polarization transfer from the large γ and most abundant ^{1}H nucleus, thus providing an appropriate study of organic matrices composition (Mazzei and Piccolo, 2015). Currently, ^{13}C CPMAS NMR represents the most suitable analytical tool for the rapid investigation of heterogeneous and complex organic materials, since it allows determining the qualitative and relative quantitative distribution of main C functionalities (Conte et al., 2004, Mazzei and Piccolo, 2015). In ^{13}C CPMAS-NMR spectra of humic materials is possible to identify regions belonging to alkyl-C assigned to aliphatic compounds, methoxyl-C or C-N associated to lignin fragments or peptide moieties, O-alkyl-C groups carbohydrates, aryl-C derived from both aromatic and phenolic structures, and carboxyl-C associated to carboxylic acids, aldehydes, or ketones (Piccolo et al., 2005; Spaccini et al., 2006, 2007). These spectral signatures and structural patterns are similar for HS and HSL substances (Spaccini et al., 2008, 2019; Savy et al., 2015, 2016, 2017; Monda et al., 2017, 2018), which usually contain fragments of the same chemical nature but in different quantities. The differentiation in the relative quantities of C functionalities is mainly related to the humification process, since it is a function of soil mineralogy, biota, climate, pH, and deposited organic material, thus determining the incorporation of different quantities of humic fragments in the supramolecular assembly (Piccolo et al., 2018, 2019). Therefore, ^{13}C CPMAS-NMR spectroscopy represents one of the most useful techniques to distinguish different humic materials, as well as for correlating their molecular features to the biological activity on plants (Cozzolino et al., 2018; García et al., 2019; Savy et al., 2020).

A more detailed molecular information on complex organic matrices can be obtained by a thermochemolysis based on an offline pyrolysis in the presence of tetramethylammonium hydroxide (TMAH) followed by gas chromatography-mass spectrometry (TMAH-Pyr-GC-MS). In respect to on-line flash-pyrolysis method, the applications of off-line pyrolysis in the presence of tetra-methyl ammonium hydroxide (TMAH) involves the thermal breaking up of bound components with a simultaneous solvolysis and methylation of ester and ether bonds present in natural organic materials (Spaccini and Piccolo, 2009). This pre-treatment of humified materials enhances the thermal stability

of polar compounds and allows a better quantitative chromatographic determination of pyrolytic products (Spaccini et al., 2013). Major compounds classes detected in the pyrolytic products of humic materials are short and long-chain fatty acids, n-alkane/alkene, alcohols, and lignin derivatives, following by aromatic and phenolic structures, phytosterols, nitrogen residues and some carbohydrates (Spaccini and Piccolo, 2009; Tadini et al., 2015; de Aquino et al., 2019). Moreeover, it was found possible to identify fatty acids of microbial origin, thus distinguishing the contribution of different microorganisms in humified materials (Guignard et al., 2005). The application of TMAH-Pyr-GC-MS analysis for the molecular characterization of humic-like substances revealed that these materials have a similar molecular composition as HS but a different relative abundance (Monda et al., 2017, 2018; Spaccini et al., 2019; Verrillo et al., 2021a). One of the main advantages of this technique, similarly to CPMAS-NMR spectroscopy, is the possibility to calculate structural indices, which can be used as a potential tool to discriminate among humic materials and correlate their molecular features to their bioactivity properties (Nardi et al., 2007; Canellas et al., 2012; Cozzolino et al., 2018).

1.2.3. The structure-activity relationship of humic materials

The attention to the relationship between the molecular features of humic materials and their bioactivity on plants has increased significantly in recent years. Visser et al (1986) reported the first evidence that the molecular composition of humic substances, particularly the low molecular size HS components (LMS-HS), exerts a different biological effect. Subsequently, Piccolo et al. (1992) and Nardi et al. (2000, 2002, 2007) confirmed these results, suggesting that the effectiveness of LMS was due to a larger number of functional groups, mainly aromatic, carboxylic, and phenolic ones. These authors also showed that the larger the hydrophobic components in humic samples, the lesser becomes the activity of HS on plant physiology. They concluded that the biological activity of HS on plants may be attributed to the relative content of specific classes of humic components, such as larger number of hydrophilic molecules (mainly carbohydrates) and smaller content of residual lignin

moieties. This activity appeared to be due to a specific arrangement of humic molecules in solution, where the distribution of hydrophilic components within a hydrophobic environment, maintains a sufficient degree of conformational flexibility to allow the interaction of active humic molecules with root cells (Piccolo et al., 2001; Nardi et al., 2007). Following this evidence, Canellas et al. (2010, 2012) applied statistical tools, such as principal component analysis (PCA), to better correlate the molecular information obtained from CPMAS-NMR spectra of humic substances to their stimulating activity on maize seedlings growth. These studies revealed that two main features arising from NMR spectra correlated with the ability of humic materials to induce lateral root emergence: 1. the 40–110 ppm signal interval comprising O-alkyl and methoxyl/N- alkyl species, and, 2. the hydrophobic index (HB/HI) calculated as the ratio between hydrophobic and hydrophilic components in NMR spectra HS. In particular, the HB/HI index and the 40-110 ppm region (HI components) positively correlated with lateral roots formation, while the content of hydrophobic (HB) carbon in humic samples was negatively correlated to the induction of lateral root hair. Therefore, the authors suggested that the ability of humic materials to act in solution as growth promoters of plants root at small concentrations is related to polar molecular bio-fragments preserved by the hydrophobic domains into humic supramolecular associations (Canellas et al., 2010, 2012). Afterwards, Aguiar et al. (2013) employed statistical analysis such as PCA and PCR (principal component regression) to predict the bioactivity of humic acids from vermicompost trough molecular data obtained from spectroscopy measurements (NMR and DRIFT). The main functionalities/structures to positively correlate with the bioactivity were the methoxyl, aryl and O-aryl-C (from lignin) and carboxyl-C, while O-alkyl and di-O-alkyl (from carbohydrates/cellulose) and C-alkyl were negatively correlated. These results further supported the hypothesis that the polar fragments trapped in the HS supramolecular structure determine the bioactivity of these materials on plants growth, as well as that hydrophobic compounds play a key role in their preservation in solution (Canellas et al., 2012; Aguiar et al., 2013). Similarly, Cozzolino et al. (2018) recently applied PCA analysis to correlate the molecular characteristics of humic acids extracted from different composted biomasses to their biostimulation on early growth of

maize. This study revealed that the abundance of lipid compounds and aromatic structure in the corresponding HA extracted from cauliflower (CAV) and artichoke (CYN) composts determined their significant adhesion to plant roots, leading to a closer and more effective interaction with root cells, and allowing these substrates to better express their biological activity (Canellas and Olivares 2014). Moreover, the presence in the supramolecular assembly of bioactive molecules, such as heterocyclic nitrogen compounds in HA-CYN and aromatic acids in HA-CAV significantly contributed to their bio-stimulation of maize early growth (Cozzolino et al., 2018). The same approach was also used to analyze the biostimulant proprieties of humic-like materials as a function of their molecular features. In several studies, Savy and colleagues (2015, 2016, and 2017) observed that water-soluble lignins isolated from different bio-energy wastes exhibited distinct molecular composition that influenced their bioactivity on maize early growth. Recently, the same author used the published information on the molecular composition of these humic-like substances to create several statistical regression s (PLS) in order to define a quantitative structure-activity relationship between HLS and their bioactivity (Savy et al., 2020). The developed models suggested the relevant positive role of aryl-containing molecules and O-alkyl groups of lignin origin on root and coleoptile elongation and indicated a negative role of alkyl groups and free carboxyl/esterified functions on plant development (Savy et al., 2020). Similarly, Monda and collaborators (2017, 2018) reported that the molecular features and the biological effect of water extracts from compost were related to the specific biomasses used in the composting process. In particular, the authors observed that the biostimulant proprieties of compost extracts resulted from a balanced composition of hydrophobic and hydrophilic components. These findings further confirmed that a certain degree of hydrophobicity is essential for the stability of the supramolecular assembly to ensure the adhesion of humic materials to root surface and the release of trapped bioactive molecules with a hormone-like activity (Savy et al., 2017a,b; Monda et al., 2017; Piccolo et al., 2019). The structure-activity relationship is also useful to understand the effect of humic materials on plant metabolism. In fact, Monda et al. (2021) have recently shown that the stimulation by humic extracts of secondary metabolites production in leaves,

that increase the resistance of plants to stress conditions, is related to their molecular features, mainly aromatic bioactive molecules such as flavonoids and quinones. Furthermore, García et al. (2019) and Nardi et al. (2021) recently reviewed the scientific literature on both the biostimulant proprieties and the molecular composition of humic sbstances derived from different raw materials. The authors concluded that, although the sources of origin are different, HS have a unique structural pattern that is different from that of any other group of soil compounds, and these distinctive molecular features allow humic biostimulants to positively affect plants productivity and several metabolic processes. Therefore, the structure-activity relationship represents a potential tool to develop tailored humic biostimulants for specific agronomic and industrial uses.

1.2.4. Microbial bioeffectors

Microbial bioeffectors are innovative technologies capable to ensure agricultural yield with high nutritional values, overcoming the negative effects of conventional agriculture (See Paragraph 1.1.). The development of this bioeffectors is based on the multiple benefits deriving from the interaction of plants with beneficial microorganisms such as arbuscular mycorrhizal fungi (AMF) and plant growth-promoting bacteria (PGPB) (Thonar et al., 2017; Castiglione et al., 2021).

AMFs are fungi belonging to the Glomeromycota phylum, which includes more than 200 species (Tedersoo et al., 2018). The available commercial inocula contain species almost exclusively belonging to *Rhizophagus* and *Funneliformis* genera that are generalist symbionts (Giannini et al., 2021). On the other hand, PGPB is a very heterogeneous group of endophytic bacteria, which most studied genera are *Aeromonas*, *Arthrobacter*, *Azospirillum*, *Azotobacter*, *Bacillus*, *Pseudomonas*, and *Rhizobium* (Pathania et al., 2020). The main beneficial effect of AMF and PGPB is the improvement of mineral uptake by plants, thus affecting the nutrient use efficiency (Cozzolino et al., 2013; Bargaz et al., 2018). In particular, AMF facilitate the uptake and transfer of mineral nutrients from the soil to their host plants by means of the extraradical mycelium (ERM) extending from colonized roots into soil (Smith et al., 2008). On the other hand, the effect of PGPB on nutrients uptake is related to

different mechanisms, such as their ability to increase mineral availability by N fixation or P solubilization and mineralization, as well as the secretion of hormone-like molecules that modulate roots development (Li et al., 2018; Kour et., 2020; Hii et al., 2020). In fact, it has been demonstrated that PGPB are able to produce inole-3-acetic acid (IAA), the major endogenous auxin in plants that regulates several cell processes, including cell elongation and division, root development, and root hair formation (Rudawska et al., 1997; Huang et al., 2015; Lally et al., 2017). Another important characteristic of PGPMs is the ability to produce ion-chelating compounds known as siderophores, thus enhancing the availability and the uptake by plants of essential micronutrients such as Fe (Radzki et al., 2013). Moreover, microbial bioeffectors have been widely used to increase plants resistance to several stress conditions (Moreira et al., 2020; Moradtalab et al., 2020; Nephali et al., 2021; Miceli et al., 2021). Different studies reported that plants inoculated with PGPB or AMF had a greater scavenging activity against both reactive oxygen (ROS) and nitrogen (RNS) species (Pauly et al., 2006; Abd-Allah et al., 2015; Chiappero et al., 2019). This stress-induced resistance in plants by microbial bioeffectors has been ascribed to their upregulation of important antioxidant enzymes, as well as to the stimulation of production of antioxidant compounds such as polyphenols, vitamins, carotenoids, and glutathione (Hashem et al., 2018; Chandra et al., 2018; Nawaz et al., 2020). Another possible explanation is the enhancement by these beneficial microorganisms of the levels of stress-related hormones, such as salicylic (SA) and jasmonic acid (JA) (Kang et al., 2014; Pedranzani et al., 2016; Quiroga et al., 2018). Recently, many studies focused on the synergistic interaction between PGPB and AMF, to find the appropriate tools capable of exerting the most effective bioactivity on plants (Saia et al., 2020; Diagne et al., 2020; Laranjeira et al., 2021). PGPB can behave like a mycorrhizal helper by producing cell wall-degrading enzymes that facilitate AMF establishment, as well as by releasing secondary metabolites that enhance the root exudation rates, resulting in greater cell permeability and hyphal growth increase (Agnolucci et al., 2019; Giannini et al., 2020). Vice versa, AMF can also enhance the activities of nitrogen fixing and phosphorus solubilizing bacteria (Nadeem et al., 2014). Consequently, the application of combined microbial bioeffectors is a potential

tool to achieve a boost effect on plants productivity, nutritional status, photosynthetic activity, and several physiological and metabolic processes (Cely et al., 2016; Cocetta et al., 2021).

Another important class of microbial bioeffectors are *Trichoderma*-based products, since they displayed multiple beneficial effects such as promotion of plants productivity and nutritional quality, as well as improvement of stress resistance (Lorito et al., 2010; Fiorentino et al., 2018). *Trichoderma* is present as active ingredients in over 200 agricultural products such as biopesticides, biofertilizers, biogrowth enhancers and biostimulants (Woo et al., 2014). The improvement of plants development and productivity by *Trichoderma* application has been noted in terms of both root growth promotion and increase in aboveground vegetative growth such as stem length and thickness, leaf area, chlorophyll content and yield (size and/or number of flowers and/or fruits) (Woo et al., 2014; Fiorentino et al., 2018; Brenda et al., 2020). The phytostimulation of *Trichoderma* has been attributed to several direct and indirect effects on plants, including the release of substances with auxin activity (i.e., IAA), small peptides and volatile organic compounds, which improve root system architecture and assimilation/solubilization of macro- (P) and micronutrients (Fe, Mn, and Zn) (Lorito and Woo, 2015; Brenda et al., 2020). Moreover, the beneficial effects to plants can be attributed to the capacity of many *Trichoderma spp*. to produce specific metabolites that are antimicrobial, thus contribute to phytopathogen control, and/or positively affect the plant in aspects of growth promotion, increased yield and other desirable characters i.e. augmented anti-oxidant properties (Vinale et al., 2009, 2010). Recently, the attention to the development of microbial inoculants that emulate the structured biological networks in native soils, thus replenishing the natural microbiome reduced by crop domestication, has increased scientific curiosity to the synergistic effect of *Trichoderma spp*. and other beneficial microorganisms (Woo and Pepe, 2018; Bradáčová et al., 2019). Many studies have shown that the co-inoculation of *Trichoderma spp* and AMF lead to multiple benefits, such as the improvement of both growth parameters (leaf height, leaf number, shoot and root dry weight) and performance after transplanting in several crops, as well as the increase in nutritional status, chlorophyll content and photosynthetic activity of treated plants (Colla et al., 2015b; Saia et al., 2019).

On the other hand, the combined application of *Trichoderma spp* and PGPB have also been reported to boost plants productivity through the production of growth-promoting substances or by increasing the availability of nutrients and their uptake (López-Bucio et al., 2015).

1.2.5. The synergistic effect of mixed humic biostimulants – microbial bioeffectors

The ever-growing need for sustainable agriculture (See Paragraph 1,1), has focused attention on the mixing of different types of bioactive products, such as microorganisms and biologically active matrices, in order to employ their synergistic interaction to obtain a boost effect on crops productivity and nutritional quality. Compost and vermicompost are considered important raw materials for biostimulant formulations (Xu and Geelsen, 2018). Several investigations reported that compost and beneficial microorganisms, when mixed, can determine a positive synergistic effect on plant growth. For example, Bharti et al. (2016) bserved a significant positive effect on basil growth after the inoculation of a PGPB and AMF with vermicompost, while Thonar et al. (2017) showed that the co-inoculation of two beneficial bacteria and *Trichoderma spp* with manure compost in soils depleted in nutrients improved maize root growth, biomass production and uptake of N and P. However, the same authors not always observed a positive effect of the compost-microorganisms combination, thus confirming previous results of Cozzolino et al. (2016) on the need for compost characterization before application, since some molecular components of compost can induce the activity of antagonistic microflora in soil thus minimizing the effect of beneficial microorganisms. Recently, Vinci and colleagues (2018a,b) in two similar studies reported that combined application of compost with beneficial bacteria or *Trichoderma spp* resulted in an efficient compost-microorganisms synergism that significantly increased maize biomass production, nutrient uptake (N and P) and photosynthetic activity. This synergism has also positively affected the metabolome of treated plants, improving the production of essential metabolites involved in N assimilation, photosynthesis process, carbohydrate metabolisms and biosynthesis of secondary metabolites (Vinci et al., 2018a,b). It was also pointed out that the combination of compost and AMF affects the resistance of plants to stressful conditions

by increasing antioxidant enzyme activities and proline content (Ait-El-Mokhtar et al., 2020). Moreover, the mixture of compost extracts (i.e. humic substances) and microbial bioeffectors can achieve a potential boost effect on plants. In fact, it has been reported that the combined application of humic acids and PGPB was able to significant increase both productivity and performance of different crops, such as sugarcane (Canellas et al., 2013), maize (Canellas et al., 2015b; Canellas and Olivares, 2017), tomato (Olivares et al., 2015), and potato (Ekin et al., 2019). This synergistic effect of humic materials and beneficial bacteria is related to several mechanisms of action (Olivares et al., 2017). It is well known that HS induce morphological adaptation of plants root, such as the stimulation of both lateral roots formation and border cells release from tips, that can promotes the colonization ability of microorganisms (Canellas et al., 2002, 2017). Moreover, physiological changes as the increase of organic acids exudation by plants treated with HS could also favour the survival of beneficial microorganisms in the soil environmental, supporting their growth as a carbon substrate (Nardi et al., 2021). Furthermore, Aguiar et al. (2018) and Canellas et al. (2019) showed that the combined application of PGPB and humic materials positively affect important primary and secondary metabolic pathways in treated plants, thus underlining the potential use of mixed biostimulants for a wild range of agronomic needs. This synergism between HS and PGPB has also been observed with other beneficial microorganisms. In a recent study, Cozzolino and collaborators (2021) reported that the combined application of humic extracts, PGPB and AMF determined a boost effect on maize biomass production and nutritional status. The same authors also detected that this positive effect was correlated to the shifts in the microbial community composition, thus indicating the potential employ of mixed humic-microbial bioeffectors to emphasize and exploit the natural biological fertility of soils. In fact, humic materials can behave as a potential vehicle for the microbial survival in soils and the enhancement of plants colonization by beneficial microorganisms (da Silva et al., 2021), probably thanks to the protection in the recalcitrant hydrophobic domains present in supramolecular structure of humic matter (Piccolo et al., 2001; Piccolo, 2002). Therefore, further investigation are needed on all potential benefits of the synergistic combination between humic

biostiomulants and microbial bioeffectors to understand the implicit mechanisms, and to develop novel efficient products for specific agronomic and industrial uses.

1.3. Innovative application of humic biostimulants

Conventional agriculture in different countries, especially the developing ones, depends on mineral fertilizers and chemical/synthetic pesticides, which have several side effects on human, animal and plant health (See Paragraph 1.1,). Hence, natural strategies for protecting the environment as well as plant, animal and human health is considered one of the main goals of developed countries. In recent years, the application of superabsorbent polymers, also identified as hydrogels, in the agricultural field has increasingly been investigated as a potential innovative technology to alleviate several agricultural problems (Neethu et al., 2018; Elshafie and Camele, 2021). Hydrogels are macromolecular materials having a water-hyper accumulation capacity of up to 100% of their own weights through osmosis property (Hüttermann et al., 2009). These materials are widely use in the biomedical fields, since their highly organized three-dimensional networks mimic physiological tissue environments, enabling effective delivery of therapeutic agents (Forget et al., 2013, 2016, 2017). In the agricultural field, the use of superabsorbent polymers has several benefits, such as conservation of soil water-holding capacity, lowering surface runoff, avoiding soil erosion and improving the performance of different fertilizers and pesticides (Abobatta, 2018). At present, most of the hydrogel products in the market are made from monomers or polymers of acrylic acid and polyacrylamide, which are derived from petroleum productions and difficult to degrade in soil or whose degradation products are potentially biologically toxic (Song et al., 2020). Therefore, in order to avoid potential toxicity and protect environment, natural polymers have attracted increasing attention due to their unique properties such as biodegradability, environmental and ecological friendliness, low cost and abundant sources (Guilherme et al., 2015). Among all materials used, alginate is considered as the most common experimental polymer in agriculture and is one of the most commonly used material for the encapsulation of beneficial microorganisms (Bashan et al., 2002,

2014; Meftah Kadmiri et al., 2020). Similarly, recent evidences showed that pectin could be an excellent natural polymer to build eco-compatible hydrogels. In particular, Nuzzo et al. (2020 a,b) lately reported that the combination of humic or humic-like substances with pectin in the formulation of humo-pectin hydrogels allows a slow-release of a previously incorporated model compound such as phloroglucinol. In fact, the molecular features of humic materials and their supramolecular associations seem to affect the morphological and rheological properties of pectin hydrogels, thus improving the capacity to control the release of the encapsulated substances (Nuzzo et al., 2020 a,b). These results confirmed the previous observed ability of HS to stabilize alginate hydrogel network, thereby increasing the protection and survival of encapsulated microorganisms (Young et al., 2006), and suggested that humic materials could be an innovative tool for the formulation of bio-composites. Moreover, recent studies have reported the potential application of hydrogel composites as an alternative to the common methods used in soilless cultivation, since their porous structure, sufficient oxygen functional groups and suitable mechanical properties could be useful for promoting seed germination and plant growth (Tang et al., 2014; Cao and Li, 2021). However, the possible applications of hydrogel bio-composites in agriculture are still poorly investigated, especially in combination with humic biostimulants.

CHAPTER 2

2.2. Work objectives

The challenges associated with the development of sustainable agriculture to replace conventional agronomic practices require the integration of various approaches to provide a truly effective solution for maintaining crop productivity and food security.

One of the aims of the present thesis work was to evaluate the effects of different agricultural managements on both soil organic matter (SOM) and organic carbon (SOC). To this purposes, **Chapter 3** reports the molecular characterization of SOM of soils under long-term conventional monoculture and crop-rotation system, as evaluated by pyrolysis GC-MS applied directily on soils. In **Chapter 4,** the molecular dynamics of the overall soil Humeome were investigated in the same long-term field samples by applying a sequential chemical fractionation, named Humeomics, to obtain the molecular details of humus changes under crop-rotation system.

Another objective of this thesis was to estimate the effectiveness of the combination of humic biostimulants with microbial bioeffectors in improving plants health and development. Therefore, **Chapter 5** reports the stimulatory effect of different humic materials and their combination on maize early growth. The molecular features of these materials were characterized in details and then correlated to their biological activity, in order to attempt to build up a structure-activity relationship. Moreover, **Chapter 6** comprises a study on the synergistic effects of mixed humic biostimulants with microbial bioeffectors on lettuce productivity and nutritional status. In this chapter, changes in primary and secondary metabolisms of treated plants were evaluated by gas chromatography coupled with mass spectrometry (GC-MS) and ultra-high performance liquid chromatography coupled to a time-of-flight mass spectrometer (UHPLC-MS-IT-TOF).

Finally, an additional goal of this doctoral research was to investigate the possible applications of innovative hydrogels based on humic matter from green compost to improve plant growth. The preliminary results on the formulation of a hydrogel containing sodium alginate and humic extracts

from green compost cross-linked by calcium nitrate as cross-linking agent and extruded by a 3D printer, as a substrate for soilless cultivation, are reported in **Chapter 7**.

CHAPTER 3

Molecular characterization of soil organic matter and its extractable humic fraction from long-term field experiments under different cropping systems

(Published in Geoderma Journal)

Geoderma 383 (2021) 114700

Contents lists available at ScienceDirect

Geoderma

journal homepage: www.elsevier.com/locate/geoderma

Molecular characterization of soil organic matter and its extractable humic fraction from long-term field experiments under different cropping systems

Claudia Savarese[b], Marios Drosos[a,*], Riccardo Spaccini[b,c], Vincenza Cozzolino[b,c], Alessandro Piccolo[b,c,*]

[a] Institute of Resource, Ecosystem and Environment of Agriculture (IREEA), Nanjing Agricultural University, 1 Weigang Road, 210095 Nanjing, China
[b] Department of Agricultural Sciences. Università di Napoli Federico II, Via Università 100, 80055 Portici, Italy
[c] Interdepartmental Research Centre of Nuclear Magnetic Resonance for the Environment, Agro-Food and New Materials (CERMANU). University of Naples Federico II, Via Università 100, 80055 Portici, Italy

ARTICLE INFO

Handling Editor: Jan Willem Van Groenigen

Keywords:
Soil organic matter
Molecular characterization
Humic substances
Soil management
Long-term cultivation
Crop-rotation

ABSTRACT

Soil Organic Matter (SOM) is essential for soil stability, fertility and crop productivity. Recent findings showed that SOM supramolecular structure is strongly influenced by cultivation and land management. In this study, we investigated the molecular dynamics of organic matter in soils from three long-term field-experiments which were subjected for 20 consecutive years to the following crop managements: i) non cultivated (Control); ii) maize mono-culture; and iii) maize-leguminous (*Vicia Faba*) rotation. Off-line pyrolysis TMAH-GC-MS (thermochemolysis) and solid-state ^{13}C NMR spectroscopy were applied for the direct molecular characterization of OM components in both the bulk soils and their humic extracts. While 20 consecutive years of Maize mono-cultivation led to alteration of the SOM hydrophobic composition, with a decrease in alkyl and aliphatic compounds (e.g. 47.4% reduction in fatty acids), and an increase in hydrophilic labile components (42.2%), the crop-rotated soils showed a partial preservation of the pristine SOM composition by maintaining the content of hydrophobic and lipid constituents (only 1.8% reduction). Our results suggest that different cropping systems change the SOM molecular dynamics and stability in long-term field experiments by primarily altering the hydrophobic components of SOM. In particular, Maize mono-cultivation leads to a progressive degradation of SOM quality. Yet, the introduction of a leguminous species in crop rotation with Maize maybe an advantageous strategy to preserve SOM quality while reducing SOC losses.

1. Introduction

Soil organic matter (SOM) is the end product of the microbial transformation of biomolecules released by dead cells of plant and animal biomass (Piccolo, 1996; Nebbioso et al., 2015). SOM plays a fundamental role in the ecosystem, by regulating global carbon and nitrogen cycles, vegetal and microbial growth, and soil functions (Spaccini et al., 2002; Nardi et al., 2002). Similarly, the maintenance of SOM in agricultural ecosystems is necessary not only to support soil fertility and crop productivity (Lal, 2004; Pan et al., 2004; 2009a), but also to stabilize soil organic carbon (SOC) and reduce greenhouse gases (GHG) emissions (Piccolo et al., 2004; Pan et al., 2009b; Zhou et al., 2009, 2010). Nevertheless, the growing pressure for an upshift in food production increases the risk of SOC depletion in cropland soils, thereby leading to soil degradation, erosion, and desertification (Ostle et al., 2009). In fact, it is ascertained that long-term cultivation with traditional tillage accelerates SOM degradation, with consequent reduction of soil fertility, structural stability, and biodiversity (Celik, 2005; Fontaine et al., 2007). Several decades of continuous cultivation has shown to affect soil biological quality and to degrade soil aggregation (Gupta and Germida, 1988; Dick, 1992), resulting in acceleration of SOM abiotic and biotic oxidation (Piccolo, 1996; Doran and Werner, 1990), and in enhancement of soil nutrients depletion (Elliott, 1986; Burke et al., 1995) and GHG emissions (Jobbagy and Jackson, 2000;

Abbreviations: SOM, Soil organic matter; SOC, Soil organic carbon; eSOM, alkaline extractable soil organic matter; Pyr-TMAH-GC-MS, Pyrolysis in the presence of tetramethylammonium hydroxide followed by gas chromatography-mass spectroscopy; ^{13}C-CPMAS, ^{13}C-Cross Polarization-Magic Angle Spinning NMR spectroscopy; NMR, Nuclear Magnetic Resonance; HB, Hydrophobicity; HI, Hydrophilicity; ARM, Aromaticity; PCA, Principal component analysis

* Corresponding authors at: Institute of Resource, Ecosystem and Environment of Agriculture (IREEA), Nanjing Agricultural University, 1 Weigang Road, 210095 Nanjing, China (M. Drosos). Department of Agricultural Sciences. Università di Napoli Federico II, Via Università 100, 80055 Portici, Italy (A. Piccolo).
E-mail addresses: drosos.marios@gmail.com, drososmarios@njau.edu.cn (M. Drosos), alessandro.piccolo@unina.it (A. Piccolo).

https://doi.org/10.1016/j.geoderma.2020.114700
Received 4 March 2020; Received in revised form 30 July 2020; Accepted 30 August 2020
Available online 18 September 2020

Baker et al., 2007; Smith et al., 2014).

The mitigation of SOM losses is achieved by alternative management practices, such as crop rotation, addition of organic fertilizers and/or biochar, green manuring, and no-till or reduced tillage (Smith et al., 2014; Piccolo et al., 2018a). In fact, while conventional tillage promotes the availability of the organic forms of nutrients (Chivenge et al., 2007) and SOC dynamics (Six et al., 2002a, 2002b), no-till practices favor the accumulation of organic matter and nutrients in soil (Dick and Daniel, 1987). Similarly, the substitution of mono-cultivation with crop rotation reduces the losses of organic material and improves soil microbial biodiversity (Dick, 1984; McGill et al., 1986). However, while the quantitative depletion of SOM in cropped soils has been repeatedly acknowledged, it is not yet clear the molecular variation of the OM composition under different soil managements and cropping systems. In fact, both accumulation and decomposition of SOC have been shown to depend not only on the quantity of incorporated SOM but also on its molecular composition (Puglisi et al., 2008; Song et al., 2013; Spaccini et al., 2013).

Following the new understanding of SOM as a supramolecular assembly of relatively small (< 1000 Da) heterogeneous molecules held together by multiple relatively weak interactions (Piccolo, 1996; 2001; 2002; 2018a; Piccolo et al., 2001), an innovative, though complex, method of chemical fractionation combined with advanced analytical techniques, called Humeomics, was recently introduced in order to thoroughly characterize the molecular composition of both humic extracts and organic matter in soil (Nebbioso and Piccolo, 2011; Drosos et al., 2017, 2018; Drosos and Piccolo, 2018). However, a rapid and still adequate molecular characterization of SOM can be achieved by the pyrolysis gas chromatography-mass spectrometry (Pyr-GC/MS) technique, that is directly applicable to heterogeneous organic solid matrices (soils, humic substances, composts, and plant tissues) (Spaccini et al., 2013; Song et al., 2013; Tadini et al., 2015). The addition of tetramethyl ammonium hydroxide (TMAH) as derivatizing agent prior to an *off-line* pyrolysis, favors the solvolysis and methylation of ester and ether bonds present in the organic matrix, thereby enhancing both thermal stability and chromatographic detection of compounds holding polar groups (Spaccini et al., 2009; Zhou et al., 2010; Tadini et al., 2015). Moreover, the derivatization reaction combined with the use of lower temperature contributes to limit the clay catalytic interactions, thus enabling a more effective quantitative and qualitative measurement of pyrolytic products (Spaccini and Piccolo, 2009; Spaccini et al., 2013).

The aim of this work was to apply the *off-line* Pyr-TMAH-GC-MS technique to understand the molecular changes of OM in soils from three long-term field-experiments which were subjected for 20 consecutive years to the following crop managements: i) non cultivated (Control); ii) maize mono-culture; and iii) maize-leguminous (*Vicia Faba*) rotation. The thermochemolysis pyrograms were obtained on both the whole soils and the humic matter extracted (eSOM) by the traditional alkaline/pyrophosphate solution. The changes in the eSOM samples were also evaluated by solid-state NMR spectroscopy.

2. Materials and methods

2.1. Soil samples

Samples of a Vertic Xerofluvent soil, with silty-clay loam texture (18.3% sand, 31.3% silt, and 50.4% clay), and pH of 8.3, were collected from the experimental farm of the University of Napoli Federico II at Castel Volturno (CE). Soils were sampled from 20 year-long field experiments under conventional tillage and three different cropping systems: i) untilled control soil without cultivation (2.62% OC); ii) Maize (*Zea mais* L.) monoculture (1.00% OC); iii) Maize-Broad bean (*Vicia faba* L.) crop rotation (1.17% OC). The following specific criteria ensured that the differences between control and each of cropped soils were referred to long-term cultivation: a. the control and cropped plots were distant at least 80 m from roads or other cultivated soils in order to limit possible contamination arising from any other source; b. all topographical aspects of control and cropped soils were similar; c. parent materials of cropped and control soils were identical as inferred by physical closeness, pedological maps of the experimental station, and similarity of general properties of soils. Each cropping experiment was conducted on a 50 m × 50 m plot, by a randomized blocks design. Composite soil samples, comprising ten sub-samples within a radius of 10 m, were randomly collected from the ploughed horizon (20 cm) of each plot, air dried, sieved under 2 mm, and placed in a glass bottle (100 mL transparent duran glass, with PP screw cups from Carl Roth) for subsequent analysis.

2.2. Extractable SOM (eSOM) in alkaline solution

Triplicates of 25 g of each soil were suspended in 225 mL of a 0.5 M NaOH and 0.1 M $Na_4P_2O_7$ solution. Samples were shaken overnight, centrifuged for 10 min at 10000 rpm, and filtered through a Whatman 42 filter. The pH of the supernatant was adjusted to 7 with a 37% HCl solution. Then, eSOM was dialyzed against distilled water until Cl-free using Amicon C membrane (1000 Da cutoff) and freeze-dried. The eSOM extracts had an average weight yield of 250 (± 50) mg.

2.3. ^{13}c-CPMAS-NMR

The characterization of eSOM extracts was conducted in the solid-state by the Cross Polarization Magic Angle Spinning (CPMAS) NMR technique using a 300 MHz Bruker Avance wide-bore magnet (Bruker Bio Spin GmbH, Rheinstetten, Germany). This was equipped with a CPMAS probe, working at ^{13}C frequency of 75.47 MHz. Samples were loaded into 4-mm zirconia rotors, which were closed with Kel-F caps and spun at a rate of 13000 ± 1 Hz. The ^{13}C-CPMAS-NMR spectra were acquired by applying a cross-polarization technique and consisted of 1814 time domain points, a spectral width of 300 ppm (22,727.3 Hz), a recycle delay of 2 s, 5000 scans and 1 ms of contact time. The ^{13}C-CPMAS pulse sequence was conducted by using a ^{1}H RAMP pulse to account for the non-homogeneity of the Hartmann–Hahn condition. A TPPM15 scheme was applied to perform the ^{13}C–^{1}H decoupling. The Free Induction Decay (FID) was transformed by applying a 4 k zero filling and an exponential function with a line broadening of 100 Hz. All NMR spectra were acquired at a temperature of 298 ± 1 K and processed by using MestReC NMR Processing Software (v.4.8.6.0, Cambridgesoft, Cambridge, Massachusetts, USA).

The ^{13}C-CPMAS-NMR spectra were evaluated by dividing the overall chemical shift range into the following main resonance intervals: alkyl-C (0–45 ppm); methoxy-C and N-alkyl-C (45–60 ppm); O-alkyl-C (60–110 ppm); unsubstituted and alkyl-substituted aromatic-C (110–145 ppm); O-substituted aromatic-C (145–160 ppm); carboxyl- and carbonyl-C (160–200 ppm). The percent relative contribution of a specific functional group (*i*) was determined by dividing the area of each spectral region (Res*i*) by the sum of all spectral areas: Rel*i* % = (Res*i* / Σ Res*i*) × 100.

2.4. Off-line pyrolysis TMAH-GC–MS

1 g of soil sample was placed in a quartz boat, and was moistened with 1 mL of 25% methanol TMAH solution (*Alfa Aesar*). Subsequently it was left to dry for 2 h, and then was analyzed by thermochemolysis as reported earlier (Spaccini and Piccolo, 2007; Spaccini et al., 2009, 2013). Briefly, the quartz boat was placed in Pyrex tubular reactor (50 cm × 3.5 cm i.d.), and heated at 400 °C (10 min isothermal) in a Barnstead Thermolyne 21,100 tubular furnace for 30 min. The freed vapors of thermochemolysis were collected in chloroform into two consecutive traps. The trapping solvent was rotoevaporated down to 2 mL of chloroform and transferred in a glass vial for GC–MS analysis. The same procedure was applied to 100 mg of each eSOM fraction using

400 μL of TMAH solution. Two analytical replicates were obtained for each sample.

2.5. Elemental composition

Elemental Composition (C, H, N) was determined for 20–25 mg of the original soils and 1–2 mg of eSOM extracts by a Fisons Instruments EA 1108 Elemental Analyzer, using Eager 200 Ver. 3.09 calculation software.

2.6. GC–MS spectrometry

For the GC–MS analysis, a Perkin-Elmer Autosystem XL was equipped with an RTX-5MS WCOT capillary column (Restek, 30 m × 0.25 mm i.d.; film thickness = 0.25 μm), and a heated transfer line (250 °C), coupled with a PE Turbomass-Gold quadruple mass spectrometer, was used following a protocol reported earlier (Spaccini and Piccolo, 2007; Spaccini et al., 2009, 2013). Nonadecanoic acid (≥98% GC purity from Sigma Aldrich, CAS no. 646-30-0) was used as internal standard, and an external calibration curve of specific standards was built for the different classes of compounds. Methylated and silylated compounds were converted into their nominal masses by adding the H + mass and by removing the methylated and silylated groups were needed. The signals selected for identification were those exceeding the cut-off limit of 0.05% of the overall area. Chemical structures were obtained using the NIST library (Spaccini et al., 2013; Drosos et al., 2018).

2.7. Statistical analysis

In order to detect the effects of different cropping systems (No cultivation, Maize mono-culture, Maize-Broad bean cultivation) on the molecular composition of soil organic matter, the GC/MS data of the three pyrolyzed bulk soils and their eSOM fractions were evaluated by Principal Components Analysis (PCA). The Principal Component Analysis (PCA) was used to highlight the analytical results expressed in term of variable variance. The XLStat software, version 9.0 (Addinsoft) was used to process the PCA of relative (%) abundance for the selected 16 classes of compounds (alcohols, amides, alkanes/alkenes, amines, benzoic esters, dicarboxylic acids, esters, fatty acids, aromatic hydrocarbons, nitrogen/oxygen heterocyclic compounds, ketones, phenolic acids, phenols, sterols and sugar derivatives) which were identified by GC-MS both for soil samples and eSOM extracts. A One-Way ANOVA (Tukey's test at a significant level of 0.05) was carried out in order to assess the statistical significance of the differences in the relative (%) abundance of the 16 aforementioned compound classes among the three different cropping systems. All data were previously found to be normally distributed according to the Shapiro-Wilk test. All statistical tests were performed by using XLStat software, version 9.0 (Addinsoft).

3. Results

3.1. Soil samples

The elemental composition of the three soils from the long-term field experiment are shown in Table 1. The tilled soil without cultivation (Control) maintained the largest carbon content of about 2.62%. As expected, the carbon content decreased in soils under cropping management for 20 consecutive years. In particular, the tilled soil under Maize mono-cultivation showed the least carbon content (1%), that increased slightly (1.12%) for the tilled soil under Maize-Broad bean rotation (Mix).

The Pyr-TMAH-GC-MS pyrograms of the three bulk soils revealed 177 most abundant molecules for the Control sample, 76 for the Maize mono-cultivation sample, and 100 for the Mix sample (Table S1 in Supporting Information). The empirical formulae of the identified compounds allowed the calculation of the H/C and O/C ratios, which were used to build the corresponding van Krevelen and relative abundance plots (Fig. 1, Fig. 2, and Fig. 3). In particular, the van Krevelen plots of all soils indicated a relatively large content of condensed material and long-chain hydrocarbon (left side) and a small presence of partially oxidized materials (right side) (Fig. 1a, Fig. 2a, and Fig. 3a). In all soils, the majority of identified compounds were phenols, fatty acids, aromatic hydrocarbons, long-chain alcohols and alkanes/alkenes (Fig. 1b, Fig. 2b, and Fig. 3b). Some differences among soils were found for the content of less abundant compounds. More amides, amines, nitrogen and oxygen heterocyclic compounds, and less alkanes/alkenes and alcohols were observed for the Control than for the other two cropped soils (Fig. 1b). Conversely, soils from both Maize mono-cultivation and Mix crop rotation showed a greater content of long chain alcohols, alkanes/alkenes and aromatic hydrocarbons, and a minority of nitrogenated compounds, esters and ethers (Fig. 2b, Fig. 3b). Moreover, in all three soils small quantities of sterols, steroids, and saccharide compounds were also found (Fig. 1b, Fig. 2b, and Fig. 3b). It is interesting to note that 53.2% of the identified molecules in soil under Maize mono-cultivation were unique to that specific soil, whereas 46.8% were common with Control (Fig. 4b). In the Mix crop rotation soil, 68.3% and 4.8% of the identified molecules were common with Control and Maize soils, respectively (Fig. 4c), but only 26.9% were unique to the Mix soil under crop rotation (Fig. 4c).

The GC/MS data from *off-line* Pyr-TMAH analysis of the three soils were managed as a unique data matrix by Principal Components Analysis (PCA). The PCA was used here to relate the molecular composition of the three soils with the different cultivation systems (No cultivation, Maize mono-culture, Mix crop rotation). The resulting PCA score-plot (Fig. 5) showed that the three soil samples were distinctly separated based on the content of 16 identified compound classes (alcohols, amides, alkanes/alkenes, amines, benzoic esters, dicarboxylic acids, esters, fatty acids, aromatic hydrocarbons not assigned in another group, nitrogen/oxygen heterocyclic compounds, ketones, phenolic acids, phenols, sterols and sugar derivatives). Along PC1 (60.59% of the total variance) the Maize mono-cultivated soil was neatly separated from the soil under Maize-leguminous crop rotation (Mix), mainly due to the content of aromatic compounds (phenols, phenolic acids and aromatic hydrocarbons), amines, oxygenated compounds (positive loadings) and fatty acids, alkanes/alkenes and sterols (negative loadings) (Fig. 5). The differences in the relative abundance (%) of such compounds were assessed by means of One-Way ANOVA test, and were found to be statistically significant by showing P-values lower than 0.05 and F-values greater than the F-critic value 5.143 ($df_1 = 2$, $df_2 = 6$, at significant level of 0.05). On the other hand, the content of esters, ketones, dicarboxaylic acids, N-compounds (amides, heterocyclic N compounds) benzoic esters and sugar derivatives accounted for the separation by positive values along the PC2 (34.80% of the total variance) and resulted to be most abundant for the Control soil than for the soil under long-term Maize cultivation (Fig. 5). Even in this case, the differences in the content (%) of these compounds were statistically significant ($P < 0.05$, $F > 5.143$).

3.2. Extractable soil organic matter (eSOM)

The eSOM isolated from soil by the same alkaline pyrophosphate solution commonly applied to extract humic substances (Piccolo et al., 2005) contained both humic and fulvic acids. Such combined humic matter extract (eSOM) yielded 1014, 696 and 815 mg for Control, Maize and Mix samples, respectively, and gave the elemental composition shown in Table 1. A progressive reduction of OC extracted in eSOM was found passing from Control (22.3%) to Maize (12.6%) and Mix (11.3%) samples (Table 1).

^{13}C-CPMAS-NMR spectra of humic matter extracted from the three different cultivated soils (Control, Maize mono-cultivation, Mix crop rotation) are shown in Fig. 6, whereas the relative distribution of signal

Table 1
Elemental composition (C, H, N) and C/N ratios of the three soil samples and their eSOM extracts from long-term field plots: Uncultivated soil (CONTROL), soil under Maize mono-cultivation (MAIZE), and soil under Maize-Broad bean crop rotation (MIX).

	C (%)	H (%)	N (%)	Mass (mg)	C (mg)	N (mg)	H (mg)	C/N
Soil Samples								
CONTROL	2.62 ± 0.06	n.d.	0.28 ± 0.01	100,000.0	2623.0 ± 3.5	280.0 ± 1.5	n.d.	9.4
MAIZE	1.0 ± 0.03	n.d.	0.11 ± 0.01	100,000.0	1000.0 ± 1.5	110.0 ± 1.1	n.d.	9.1
MIX	1.12 ± 0.03	n.d.	0.14 ± 0.01	100,000.0	1117.0 ± 1.5	140.0 ± 1.1	n.d.	8.0
eSOM								
CONTROL	22.3 ± 0.05	4.01 ± 0.02	2.34 ± 0.03	1013.6 ± 15	225.6 ± 2.5	40.6 ± 1.0	23.7 ± 0.1	9.5
MAIZE	12.6 ± 0.03	3.21 ± 0.03	1.44 ± 0.03	696.0 ± 10	87.7 ± 1.5	22.4 ± 0.5	10.0 ± 0.1	9.5
MIX	11.3 ± 0.05	2.99 ± 0.02	1.47 ± 0.05	815.2 ± 15	92.1 ± 2.0	24.4 ± 0.5	12.0 ± 0.1	8.0

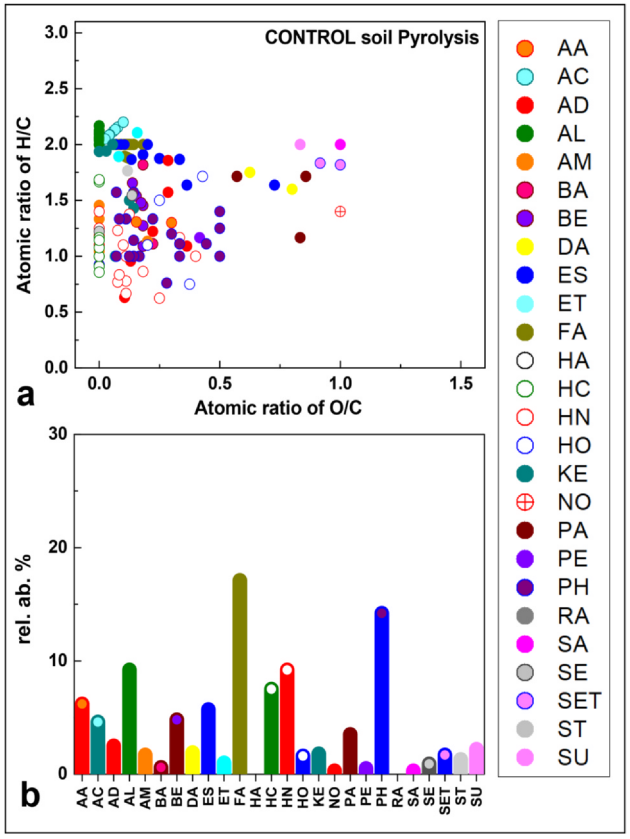

Fig 1. Van Krevelen Plot (a) of various molecular components identified in pyrolyzed bulk uncultivated soil (CONTROL) and their relative (%) abundance (b). AA: Aromatic acids, AC: Alcohols, AD: Amides, AL: Alkanes/alkenes, AM: Amines, BA: Benzoic Acids, BE: Benzoic Esters, DA: Dicarboxylic Acids, ES: Esters, ET: Ethers, FA: Fatty Acids, HA: Hydroxy Acids, HC: Aromatic hydrocarbons not assigned in another group, HN: Heterocyclic Nitrogen compounds, HO: Heterocyclic Oxygen compounds, KE: Ketones, NO: Nitroxides, PA: Phenolic Acids, PE: Phenolic Esters, PH: Phenols, RA: Resin Acids, SA: Sugar Acids, SE: Steroids, SET: Sugar Ethers/Esters, ST: Sterols, SU: Sugars. Standard deviation for all classes of compounds was ≤ 1.

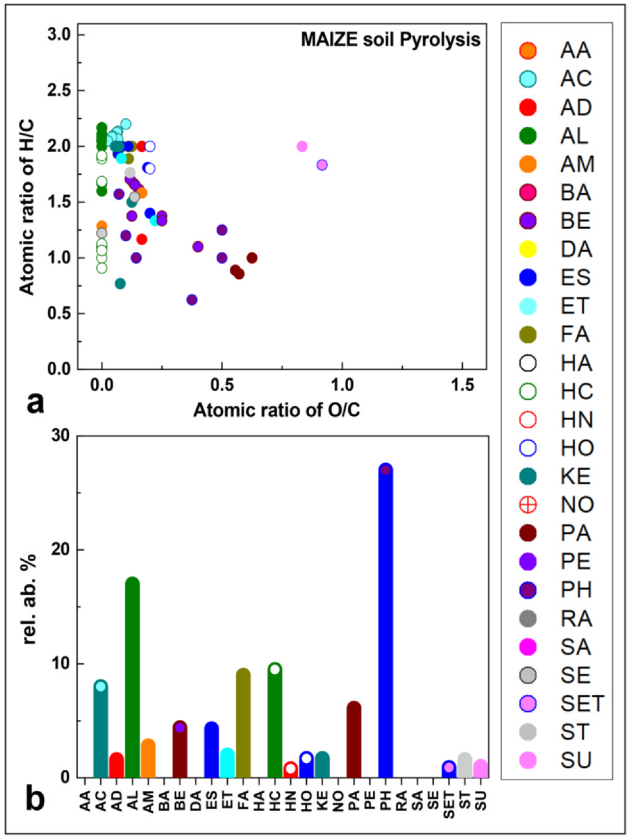

Fig 2. Van Krevelen Plot (a) of various molecular components identified in pyrolyzed bulk soil under Maize mono-cultivation (MAIZE) and their relative (%) abundance (b). AA: Aromatic acids, AC: Alcohols, AD: Amides, AL: Alkanes/alkenes, AM: Amines, BA: Benzoic Acids, BE: Benzoic Esters, DA: Dicarboxylic Acids, ES: Esters, ET: Ethers, FA: Fatty Acids, HA: Hydroxy Acids, HC: Aromatic hydrocarbons not assigned in another group, HN: Heterocyclic Nitrogen compounds, HO: Heterocyclic Oxygen compounds, KE: Ketones, NO: Nitroxides, PA: Phenolic Acids, PE: Phenolic Esters, PH: Phenols, RA: Resin Acids, SA: Sugar Acids, SE: Steroids, SET: Sugar Ethers/Esters, ST: Sterols, SU: Sugars. Standard deviation for all classes of compounds was ≤ 1.

areas is reported in Table 2. The spectra revealed a predominance of Alkyl-C (0–45 ppm) and O-Alkyl–C (60–110 ppm) regions in all three eSOM extracts, which accounted for > 50% of total area in each sample (Table 2). The aromatic carbons, responsible for the 110–160 ppm spectral region were the second most abundant compounds in the humic extracts of all samples (Table 2). The same difference were found in the OCH_3/CN (45–60 ppm) and carbonyl/carboxyl-C (160–190 ppm) intervals (Fig. 6), which resulted more abundant in the Maize eSOM extract (Table 2). Moreover, the relative carbon distribution in the spectra allowed to calculate the variation in the hydrophobicity (HB/HI) and aromaticity (ARM) in the different eSOM extracts. Both these structural indexes resulted smaller in the Maize eSOM fractions than for those of the Control and the Mix, while the HB/HI even increased under the Mix system (Table 2).

The pyrograms of the three eSOM extracts revealed 108 most abundant molecules in Control, 81 in Maize and 111 in Mix samples (Table S2 in Supporting Information). The Van Krevelen plots of the eSOM extracts built by using the H/C and O/C ratios (Fig. 7a, Fig. 8a, and Fig. 9a) calculated from the empirical formulae of detected molecules (Table S2 in Supporting Information), presented small percentages of oxidized materials (right side), and an abundance of condensed material and long-chain hydrocarbons (left side). In Control, the

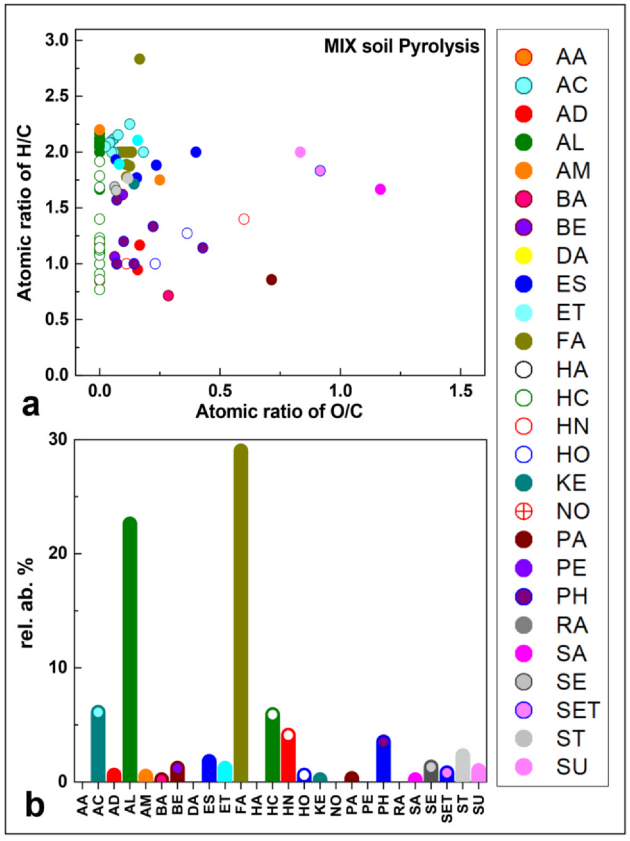

Fig 3. Van Krevelen Plot (a) of various molecular components identified in pyrolyzed bulk soil under Maize-Broad bean crop rotation. (MIX) and their relative (%) abundance (b). AA: Aromatic acids, AC: Alcohols, AD: Amides, AL: Alkanes/alkenes, AM: Amines, BA: Benzoic Acids, BE: Benzoic Esters, DA: Dicarboxylic Acids, ES: Esters, ET: Ethers, FA: Fatty Acids, HA: Hydroxy Acids, HC: Aromatic hydrocarbons not assigned in another group, HN: Heterocyclic Nitrogen compounds, HO: Heterocyclic Oxygen compounds, KE: Ketones, NO: Nitroxides, PA: Phenolic Acids, PE: Phenolic Esters, PH: Phenols, RA: Resin Acids, SA: Sugar Acids, SE: Steroids, SET: Sugar Ethers/Esters, ST: Sterols, SU: Sugars. Standard deviation for all classes of compounds was ≤ 1.

majority of compounds were long-chain alcohols, alkanes/alkenes and fatty acids (Fig. 7), while in the other two eSOM extracts most of identified compounds were phenols and fatty acids, with a prevalence of nitrogen and oxygen heterocyclic compounds in the eSOM of Maize mono-cultivated soil (Fig. 8), and of phenolic acids in the eSOM extract of Mix sample (Fig. 9). The second abundant group of compounds included nitrogen-containing molecules and sugar derivatives for the Control eSOM, amides and sterols for the Maize eSOM, alcohols and alkanes/alkenes for the Mix eSOM (Fig. 7b, Fig. 8b, and Fig. 9b).

The identified molecules in the Maize eSOM sample, also visible in the Control eSOM sample, reached 82.6% of total, while only 17.4% of the molecules were present to the Maize SOM extract specifically (Fig. 10b). Conversely, the extracted SOM from the long-term Mix soil revealed that 69.2% and 13.6% of total identified molecules were common to the Control and the Maize eSOM, respectively (Fig. 10c), while up to 17.2% were unique to the Mix eSOM fraction (Fig. 10c).

The GC/MS data of the three pyrolyzed eSOM fractions were evaluated by Principal Components Analysis (PCA). The PCA score-plot (Fig. 11) of the 16 abundant identified compound classes accounted for 86.95% of the total variance and showed a large degree of separation among the eSOM extracts of the three soil samples. The content of heterocyclic N-compounds, amides, fatty acids and sterol accounted for the separation by positive values along the PC1 and resulted more abundant in the eSOM fraction of Maize mono-cultivated soil than in the uncultivated soil (Control eSOM) (Fig. 11). Actually, the One-Way ANOVA test showed the statistically significance of the differences in the relative (%) abundance of such compounds, by determining P-values lower than 0.05 and F-values greater than the F-critic value 5.143 ($df_1 = 2$, $df_2 = 6$, at significant level of 0.05). The same variables separated the Maize eSOM from Mix eSOM along the PC2 (negative loadings) (Fig. 11). This splitting was also due to the greater content of amines, phenols, oxygen contained compounds and phenolic acids (positive loadings) in the Mix eSOM (Fig. 11), and the differences in the relative (%) abundance were found to be statistically significant ($P < 0.05$, $F > 5.143$).

4. Discussion

4.1. Molecular profiles of bulk soils

As expected, the decrease of organic C and N when passing from Control to Maize soil sample (Table 1) is due to the organic matter mineralization induced by the long-term Maize cultivation under conventional tillage (Chivenge et al., 2007). Conversely, a small increase of OC content was noticed in soil under long-term maize-leguminous rotation (Table 1), in line with reports showing that crop rotation could decrease the rate of OC decomposition in soils (West and Post, 2002).

In all three soils from field experiments, the pyrograms indicated a prevalence of alkyl compounds, such as long chain alcohols, alkanes/alkenes and fatty acids (Fig. 1, Fig. 2, and Fig. 3). Alkyl C derive from plant biopolymers (cutin and wax) and microbial metabolites (Ussiri and Johnson, 2003; Rumpel et al., 2005) and their hydrophobicity is related to the most stable and recalcitrant OM in soils (Buurman et al., 2007; Song et al., 2013; Zhang et al., 2019). In fact, the preservation in soil of alkyl compounds, like fatty acids and alkanes/alkenes, is

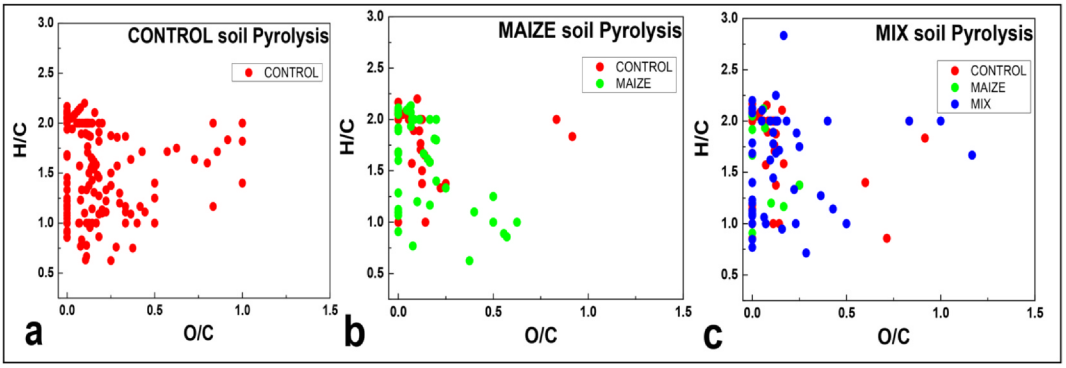

Fig 4. Van Krevelen Plots of common molecular components identified in pyrolyzed bulk soil samples. Molecules identified in the uncultivated soil sample (CONTROL) are noted in red, whereas molecules present only in Maize mono-cultivated soil (MAIZE) are marked in green, and molecules present only in soil under Maize-Broad bean crop rotation (MIX) are shown in blue.

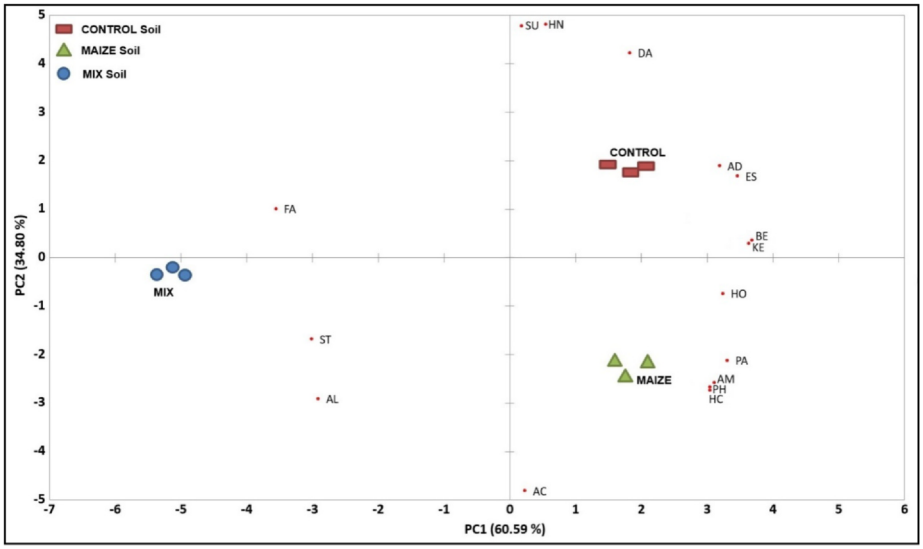

Fig 5. PCA score plot of compounds classes relative (%) abundance recognized in pyrolyzed bulk soil samples: i) No-cultivation (CONTROL); ii) Maize mono-cultivation (MAIZE); iii) Maize-Broad bean crop rotation (MIX). AC: Alcohols, AD: Amides, AL: Alkanes/alkenes, AM: Amines, BE: Benzoic Esters, DA: Dicarboxylic Acids, ES: Esters, FA: Fatty Acids, HC: Aromatic hydrocarbons not assigned in another group, HN: Heterocyclic Nitrogen compounds, HO: Heterocyclic Oxygen compounds, KE: Ketones, PA: Phenolic Acids, PH: Phenols, ST: Sterols, SU: Sugars.

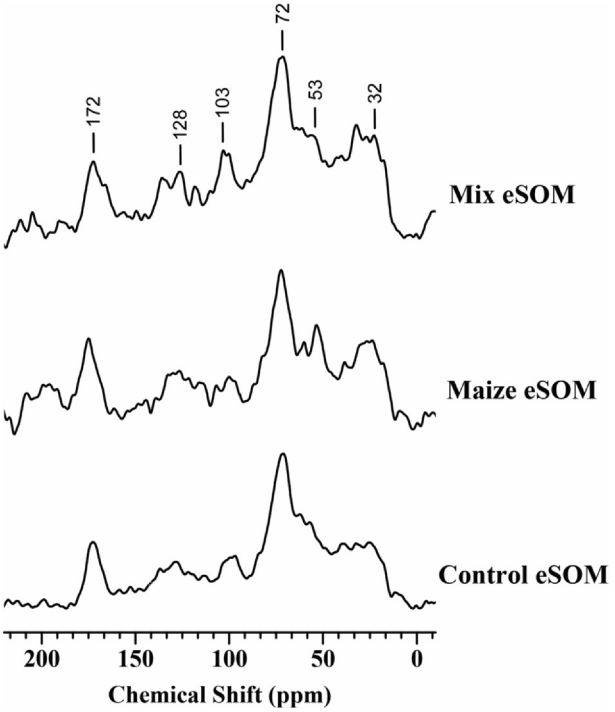

Fig 6. ^{13}C-CPMAS-NMR spectra of eSOM extracts. Control = uncultivated soil; Maize = soil under Maize mono-cultivation; Mix = soil under Maize-Broad bean crop rotation; eSOM = alkaline extractable soil organic matter.

believed to enhance the accumulation of SOM (Guignard et al., 2005; Piccolo et al., 2005; Jandl et al., 2012) by a mechanism based on sequestration of organic carbon into the progressively greater hydrophobic domains of SOM (Spaccini et al., 2000; 2002; Piccolo et al., 2004, 2018b; Feng et al., 2008). Hence, the observed decrease of hydrophobic alkyl content passing from Control to the soil under the long-term Maize cultivation appears in line with the reported instability of SOM under such cropping system (Mann et al., 2002; Celik, 2005; Jandl et al., 2007). Conversely, the soil under the Maize-Bean crop rotation showed a larger content of SOM alkyl compounds, such as long-chain alcohols, alkanes/alkenes and fatty acids, than for continuous Maize soil (Fig. 3b). The presence of long-chain lipids in a crop-rotation system has been already interpreted as an index of SOM stabilization (Jandl et al., 2012). Therefore, our results confirm that a long-term crop rotation of Maize with a leguminous species prevented an excessive degradation of soil hydrophobic components, thereby favoring the increase of SOM content (Table 1) by incorporating even labile organic compounds within the soil hydrophobic domains and protecting them from microbial mineralization (Piccolo and Mbagwu, 1999; Smith et al., 2014; Drosos and Piccolo, 2018; Piccolo et al., 2018b).

Thermochemolysis also revealed a great content of aromatic components, such as phenolic acids, phenols, benzoic esters and aromatic hydrocarbons, in all three soils organic matter (Fig. 1, Fig. 2, and Fig. 3). A reason for this abundance may be due to an uncontrolled condensation and aromatization reactions of pristine compounds catalyzed by clay minerals during pyrolysis (Saiz-Jimenez, 1994; Spaccini et al., 2013). However, the predominance of aromatic compounds in the soil under Maize mono-cultivation (Fig. 2b) may be also caused by either a more rapid degradation of lignin components under Maize and a consequent accumulation of aromatic-rich compounds in soil (Dignac et al., 2005; Rasse et al., 2006; Thevenot et al., 2010), or a selective

Table 2
Relative distribution (%) of signals area over chemical shift regions (ppm) in ^{13}C-CPMAS-NMR Of eSOM extracts.

eSOMfractions	Alkyl (0–45)	CH_3O/CN (45–60)	O-alkyl (60–110)	Aromatic (110–145)	O-aryl (145–160)	Carbonyl/Carboxyl (160–190)	HB/HI[a]	ARM[b]
CONTROL[1]	21.37	12.04	40.99	13.71	3.07	8.81	0.62	0.17
MAIZE[2]	22.43	12.81	37.08	13.70	1.67	12.31	0.61	0.15
MIX[3]	23.40	11.28	40.15	13.17	2.80	9.20	0.65	0.16

[1] Uncultivated soil.
[2] Soil under Maize mono-cultivation.
[3] Soil under Maize-Broad bean crop rotation.
[a] HI/HB = Hydrophobicity index = Hydrophobic carbons/hydrophilic carbons = [(0–45) + (110–160)/(45–110) + (110–190)].
[b] ARM = Aromaticity index = (110–160)/Σ(0–190).

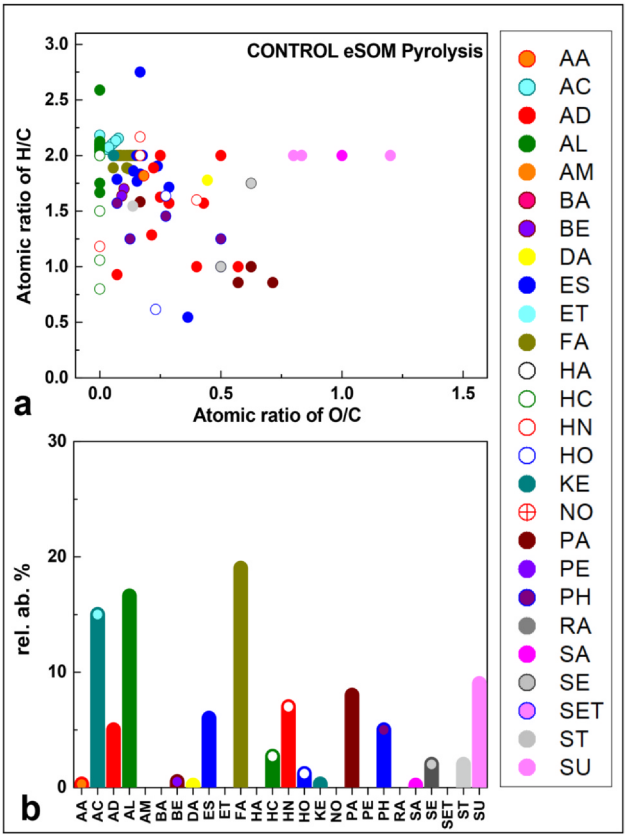

Fig 7. Van Krevelen Plot (a) of various molecular components identified in pyrolyzed eSOM extract of uncultivated soil (CONTROL) and their relative (%) abundance (b). eSOM = alkaline extractable soil organic matter. AA: Aromatic acids, AC: Alcohols, AD: Amides, AL: Alkanes/alkenes, AM: Amines, BA: Benzoic Acids, BE: Benzoic Esters, DA: Dicarboxylic Acids, ES: Esters, ET: Ethers, FA: Fatty Acids, HA: Hydroxy Acids, HC: Aromatic hydrocarbons not assigned in another group, HN: Heterocyclic Nitrogen compounds, HO: Heterocyclic Oxygen compounds, KE: Ketones, NO: Nitroxides, PA: Phenolic Acids, PE: Phenolic Esters, PH: Phenols, RA: Resin Acids, SA: Sugar Acids, SE: Steroids, SET: Sugar Ethers/Esters, ST: Sterols, SU: Sugars. Standard deviation for all classes of compounds was ≤ 1.

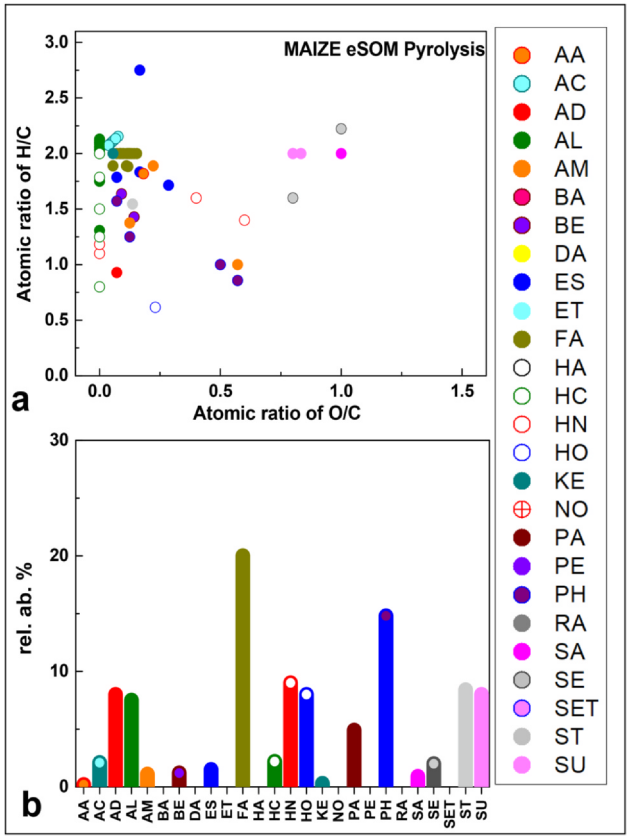

Fig 8. Van Krevelen Plot (a) of various molecular components identified in pyrolyzed eSOM extract of soil under Maize mono-cultivation (MAIZE) and their relative (%) abundance (b). eSOM = alkaline extractable soil organic matter. AA: Aromatic acids, AC: Alcohols, AD: Amides, AL: Alkanes/alkenes, AM: Amines, BA: Benzoic Acids, BE: Benzoic Esters, DA: Dicarboxylic Acids, ES: Esters, ET: Ethers, FA: Fatty Acids, HA: Hydroxy Acids, HC: Aromatic hydrocarbons not assigned in another group, HN: Heterocyclic Nitrogen compounds, HO: Heterocyclic Oxygen compounds, KE: Ketones, NO: Nitroxides, PA: Phenolic Acids, PE: Phenolic Esters, PH: Phenols, RA: Resin Acids, SA: Sugar Acids, SE: Steroids, SET: Sugar Ethers/Esters, ST: Sterols, SU: Sugars. Standard deviation for all classes of compounds was ≤ 1.

preservation of aromatic components of SOM due to the effects of root exudates under Maize monoculture (Drosos and Piccolo, 2018).

The predominance of long-chain alkyl compounds and condensed material in bulk soils from the long-term field experiments was shown by the Van Krevelen Plots of Fig. 1, Fig. 2, and Fig. 3. Nevertheless, partially oxidized materials, such as dicarboxylic acids and sugar derivatives were also detected more in Control and Mix soils (Fig. 1a, Fig. 3a) than in the Maize mono-cultivation soil (Fig. 2a), and may derive from an increased microbial activity under a crop rotation system (Kahle et al. 2010).

Small amounts of carbohydrate derivatives were found in soil samples (Fig. 1, Fig. 2, and Fig. 3), as products of easily decomposed polysaccharides from plant residues (Grandy and Neff, 2008; Song et al., 2013). The smaller content of carbohydrates in Maize mono-cultivated soil than in the other two samples (Fig. 1, Fig. 2, and Fig. 3), contrary to the demonstrated increase of sugar derivatives in long-term cultivated soil (Schnitzer et al., 2006; Drosos et al., 2020), is suspected due to the low efficacy of thermochemolysis to detect polysaccharides in complex matrices (Chefetz et al., 2000; Song et al., 2013).

Interestingly, the pyrogram of the Maize mono-cultivated soil reveled 41 molecules (53.2% of the total area) specific to this cropping system (Fig. 4b), which were for the most part esters, alkanes/alkenes and aromatic hydrocarbons (Table S1 in Supporting Information). These compounds are believed to be originated from the external protective wax layers of plant tissues and microbial by-products (Naafs et al, 2004; Spaccini et al., 2009). In the Mix soil after 20 consecutive years, 42 molecules (26.9% of total area) were identified as specific to the leguminous crop rotation (Fig. 4c), and belonged mainly to fatty acids and aromatic compounds classes (Table S1 in Supporting Information). In particular, the long-chain fatty acids were already reported as abundant molecules in a crop-rotation system (Jandl et al., 2012) and were considered as an indicator of SOM stabilization (Jandl et al., 2007).

The PCA analysis confirmed the molecular differences found in the pyrolytic products of soils from the three different long-term cultivation systems. Along the first PC, the Maize mono-cultivated soil was separated from the soil under Maize-leguminous crop rotation (Mix) (Fig. 5). This differentiation was due to the larger content of fatty acids and alkanes/alkenes in the soil subjected to 20 consecutive years of Maize-Broad bean rotation, and confirm the increase of SOM stabilization by hydrophobic protection in a crop-rotation system (Jandl et al., 2007; 2012; Piccolo et al., 2018b). Moreover, the splitting of Control and Maize soil samples along the PC2 (Fig. 5), based on the larger abundance of heterocyclic oxygen, amines and phenolic acids in the Maize continuous cultivation soil, suggests a less hydrophobic preservation of labile organic components against the microbial mineralization in the mono-culture system (Drosos and Piccolo, 2018).

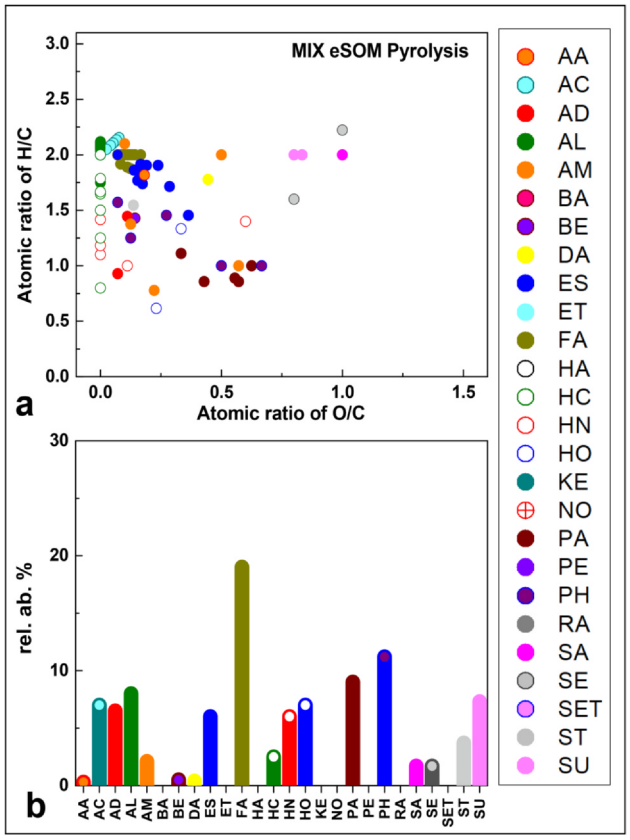

Fig 9. Van Krevelen Plot (a) of various molecular components identified in pyrolyzed eSOM extract of soil under Maize-Broad bean crop rotation (MIX) and their relative (%) abundance (b). eSOM = alkaline extractable soil organic matter. AA: Aromatic acids, AC: Alcohols, AD: Amides, AL: Alkanes/alkenes, AM: Amines, BA: Benzoic Acids, BE: Benzoic Esters, DA: Dicarboxylic Acids, ES: Esters, ET: Ethers, FA: Fatty Acids, HA: Hydroxy Acids, HC: Aromatic hydrocarbons not assigned in another group, HN: Heterocyclic Nitrogen compounds, HO: Heterocyclic Oxygen compounds, KE: Ketones, NO: Nitroxides, PA: Phenolic Acids, PE: Phenolic Esters, PH: Phenols, RA: Resin Acids, SA: Sugar Acids, SE: Steroids, SET: Sugar Ethers/Esters, ST: Sterols, SU: Sugars. Standard deviation for all classes of compounds was ≤ 1.

4.2. Molecular differences in the extractable soil organic matter (eSOM)

The Control soil produced the largest eSOM extraction yield followed in the order by the Mix crop rotation and continuous Maize soils (Table 1), thus confirming the occurrence of significant SOM losses during a long-term cultivation under traditional tillage (Spaccini et al., 2002; Piccolo et al., 2004; Jandl et al., 2007). Moreover, the decrease of OC content from Control (22.3%) to Maize (12.6%) and Mix (11.3%) eSOM extracts (Table 1), suggests an alteration of SOC molecular composition in the two cropped soils under long-term conventional cultivation in respect to control, that may have increased the loss of most labile compounds during the eSOM extraction process (Drosos et al., 2018).

^{13}C-CPMAS-NMR spectra showed some differences in the molecular features of the three eSOM fractions. The predominance of alkyl-C and O-alkyl-C in the 0–45 and 60–110 ppm intervals, respectively, revealed that all humic extracts were dominated by both aliphatic compounds and carbohydrates (Fig. 6). The intense signal around 32 ppm can be attributed to methylenic chains deriving from lipid compounds, plant waxes/biopolyester, and peptidic materials (Spaccini and Piccolo, 2007; 2009). The broad signal at 72 ppm was assigned to the presence of carbohydrates and compounds derived from cellulose and hemicelluloses, whereas the 103 ppm absorbance is commonly assigned to sugar anomeric carbons (Spaccini and Piccolo, 2009; Tadini et al., 2015). The spectra also revealed an abundance of aromatic/phenolic carbons in the three eSOM extracts, responsible for the 110–160 ppm spectral interval (Fig. 6). In this region, the signal at around 128 ppm may be related to both partially degraded lignin structure and condensed aromatic carbons (Spaccini and Piccolo, 2009). Moreover, the 45–60 and 160–190 ppm ranges were more abundant in humic fraction of Maize mono-cultivated soil (Table 2), being the former interval attributable to carbons in methoxyl groups or linked to nitrogen, whereas the latter one is related to carbons in carboxyl/carbonyl groups (Spaccini and Piccolo, 2009; Tadini et al., 2015). In particular, the intense peak at 172 ppm may indicate a large content of carboxyl groups in aliphatic acids of plant and microbial origin and/or amide groups in amino acid moieties (Spaccini and Piccolo, 2009). Furthermore, a slightly decrease of hydrophobicity (HB/HI) and aromaticity (ARM) index values was found when passing from Control to Maize humic extracts (Table 2). This is associated to a loss of SOM hydrophobic components due to the long-term maize mono-cultivation (Jandl et al., 2007; Spaccini et al., 2013) and a probable reduction of the organic matter stability in the Maize soil (Piccolo et al., 2018b). Conversely, the noticed enhancement of HB/HI values in the Mix eSOM extract, resulted in accordance with the increase of aromatic/phenolic compounds under leguminous cultivation (Zohaib et al., 2014; Amb and Ahluwalia, 2016) and with the already reported maintenance of the degree of SOM hydrophobicity and, hence, stability, in the crop-rotation system (Jandl et al., 2012).

Thermochemolysis of the three eSOM extracts confirmed the molecular differences in their composition. The majority of identified molecules in eSOM from the Control soil were alkyl hydrophobic compounds, such as long-chain alcohols, alkanes/alkenes and fatty acids (Fig. 7), which are selectively accumulated in soil by aggregating

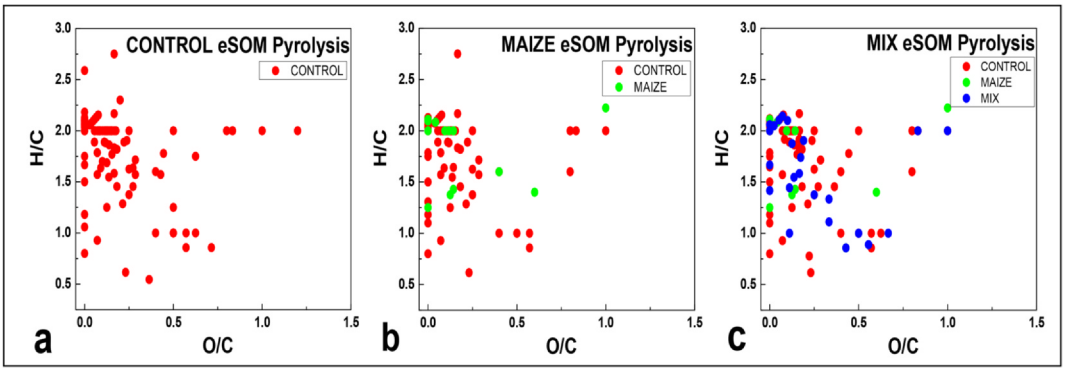

Fig 10. Van Krevelen Plots of common molecular components identified in pyrolyzed extractable soil organic matter (eSOM). Molecules identified in the uncultivated soil sample (CONTROL) are noted in red, whereas molecules present only in Maize mono-cultivated soil (MAIZE) are marked in green, and molecules present only in soil under Maize-Broad bean crop rotation (MIX) are shown in blue.

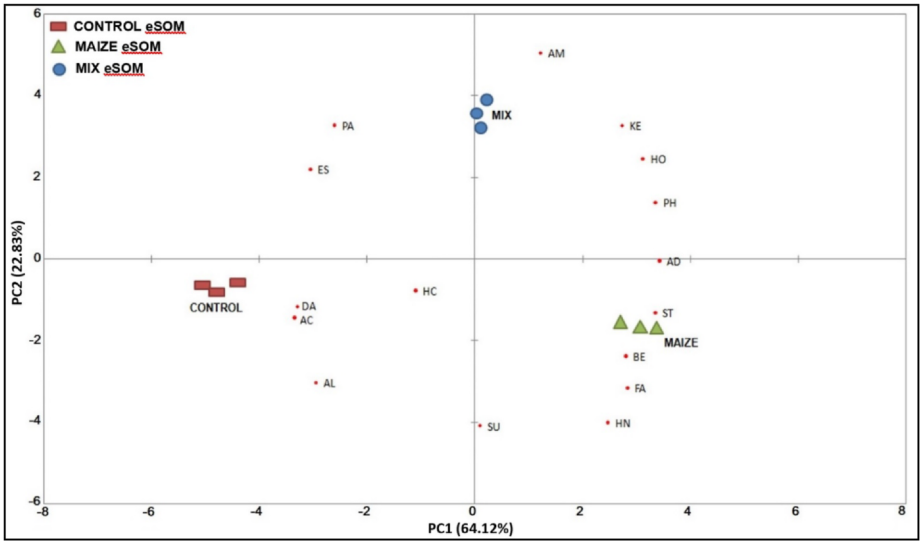

Fig 11. PCA score-plot of compounds classes relative (%) abundance recognized in pyrolyzed alkaline extractable soil organic matter (eSOM): i) No-cultivation (CONTROL); ii) Maize mono-cultivation (MAIZE); iii) Maize-Broad bean crop rotation (MIX). AC: Alcohols, AD: Amides, AL: Alkanes/alkenes, AM: Ammines, BE: Benzoic Esters, DA: Dicarboxylic Acids, ES: Esters, FA: Fatty Acids, HC: Aromatic hydrocarbons not assigned in another group, HN: Heterocyclic Nitrogen compounds, HO: Heterocyclic Oxygen compounds, KE: Ketones, PA: Phenolic Acids, PH: Phenols, ST: Sterols, SU: Sugars.

into microbially resistant hydrophobic domains (Spaccini et al., 2002; Buurman et al., 2007; Piccolo et al., 2018b). The molecular profile of this eSOM extract is in line with the results obtained by thermochemolysis on the bulk Control soil (Fig. 1) that was assumed to contain the most stable OM pool.

In the eSOM extract of Maize mono-cultivated soil the main compound class was represented by fatty acids (Fig. 8), originating from microorganisms or plant residues (Jandl et al., 2005; Spaccini et al., 2009), whose abundance was larger than in the Control eSOM fraction (Fig. 7). This is somewhat contrary to the results obtained on the whole Maize soil discussed above (Fig. 2). The difference may be due to the alkaline hydrolysis of complex esters during the eSOM extraction that may have released in solution long-chain acids and alcohols otherwise undetectable by thermochemolysis on the bulk soil samples (Drosos et al., 2017; Drosos and Piccolo, 2018). A larger content of phenols and N-compounds (amides and heterocyclic N compounds) were also found in pyrolytic products of Maize eSOM extract as compared to the Control eSOM fraction (Fig. 7, Fig. 8). An increase in aromaticity and an enrichment in N-containing compounds passing from virgin to long-term cultivated soils was likewise reported by Schnitzer et al. (2006) and can be associated to an extensive degradation of SOM as a result of cultivation.

Greater amount of long-chain alcohols, alkanes/alkenes and fatty acids were instead identified in the eSOM from the cultivated soil under Maize-Bean rotation (Fig. 7b, Fig. 9b). This is in line with the above thermochemolysis results from the corresponding whole sample of the Mix soil (Fig. 3), in which the identification of hydrophobic alkyl components were interpreted as an index of a more stable SOM under the long-term crop rotation system than for the Maize mono-cultural experiment (Spaccini et al., 2002; Jandl et al., 2007; 2012; Zhang et al., 2019; Spaccini and Piccolo, 2019). Additionally, a large percent of phenols and phenolic acids were found in the Mix eSOM (Fig. 7b, Fig. 9b), which probably derive from either the polyphenolic root exudates or residual biomass of leguminous roots left in soil (Zohaib et al., 2014; Amb and Ahluwalia, 2016).

The predominance of long/chain alkyl and condensed compounds is revealed in the Van Krevelen Plots of Fig. 7, Fig. 8, and Fig. 9. However, contrary to the results obtained for the bulk soil samples (Fig. 1, Fig. 2, and Fig. 3), partially oxidized materials, such as heterocyclic oxygen compounds, dicarboxylic and phenolic acids were also shown in all three eSOM extracts (Fig. 7, Fig. 8, and Fig. 9), which were presumably derived from the hydrolysis of complex esters during the alkaline extraction (Drosos et al., 2017; Drosos and Piccolo, 2018). Moreover, saccharide compounds were found among the pyrolysis products of the three eSOM fractions (Fig. 7, Fig. 8, and Fig. 9), that probably derived from microbial and plant carbohydrates, as observed also in other studies (Schnitzer et al., 2006; Song et al., 2013).

It is to be noted that 16 molecules (17.4% of the total area) were identified in the pyrogram of Maize eSOM extract belonging only to Maize (Fig. 10b), which were mainly fatty acids possibly released from the Maize residual biomasses (Spaccini et al., 2013). Conversely, 26 molecules (17.2% of total area) mainly phenolic acids (Table S2 in Supporting Information) were recognized in the pyrolytic products of Mix eSOM as specific of this cropping system (Fig. 10c) and associated to roots exudates and plant residues of the leguminous crop rotation (Zohaib et al., 2014).

The PCA score-plot of pyrolysis results of eSOM extracts from the soils of three long-term experiments showed the molecular differences among the samples (Fig. 11). The separation of Control from Maize eSOM extract along the PC1 (Fig. 11) was principally due to a greater content of N-containing compounds (amides, heterocyclic N compounds), fatty acids and sterols in the Maize sample, which are likely derived from microbial activity (Schnitzer et al., 2006) and plant lipid components (Spaccini et al., 2013). The separation may be also attributed to a larger quantity in the Control than in the maize extract of alkyl compounds, such as long-chain alcohols and alkanes/alkenes, thereby confirming the alteration of the SOM hydrophobic stability occurred under maize cultivation during 20 years (Spaccini et al., 2002; Zhang et al., 2019). Furthermore, the distance of the Mix eSOM sample from the other two extracts along the PC2 (Fig. 11) was mainly due to the larger abundance of phenols and phenolic acids in the crop-rotated Mix soil, and supported the hypothesis of an enrichment in polyphenolic components of SOM as a result of the maize-leguminous rotation (Zohaib et al., 2014).

5. Conclusions

Despite its importance for the development of a sustainable agriculture, the molecular dynamics of soil organic matter under different cropping systems is still poorly understood. Our findings suggest that the long-term cultivation under conventional tillage destabilizes SOM molecular conformation, though to a different extent, as a function of the cropping system. In particular, 20 consecutive years of Maize mono-cultivation led to alteration of the SOM hydrophobic composition, with a decrease in alkyl compounds, and an increase in hydrophilic labile components. The introduction of a leguminous species in rotation with maize partially preserved the original SOM composition by maintaining the content of hydrophobic lipid constituents throughout the 20 years

of the experiment (Piccolo et al., 2005, 2018b; Jandl et al., 2007; 2012).

Our results on the molecular dynamics of SOM in long-term field experiments under different cropping systems are in line with the concept that the process of stabilization of organic matter in soil occurs through a progressive accumulation of hydrophobic compounds, which contribute to separate the humic supramolecular structure from water, and, consequently, from the degrading microbial activity (Drosos and Piccolo, 2018; Piccolo et al., 2018b).

Declaration of Competing Interest

The authors declare that they have no known competing financial interests or personal relationships that could have appeared to influence the work reported in this paper.

Appendix A. Supplementary data

Supplementary data to this article can be found online at https://doi.org/10.1016/j.geoderma.2020.114700.

References

Amb, M.K., Ahluwalia, A.S., 2016. Allelopathy: Potential Role to Achieve New Milestones in Rice Cultivation. Rice Sci. 23, 165–183. https://doi.org/10.1016/j.rsci.2016.06.001.

Baker, J.M., Ochsner, T.E., Venterea, R.T., Griffis, T.J., 2007. Tillage and soil carbon sequestration-What do we really know? Agric. Ecosyst. Environ. 118, 1–5. https://doi.org/10.1016/j.agee.2006.05.014.

Burke, I.C., Lauenroth, W.K., Coffin, D.P., 1995. Soil organic matter recovery in semiarid grasslands: Implications for the conservation reserve program. Ecol. Appl. 5, 793–801. https://doi.org/10.2307/1941987.

Buurman, P., Schellekens, J., Fritze, H., Nierop, K.G.J., 2007. Selective depletion of organic matter in mottled podzol horizons. Soil Biol. Biochem. 39, 607–621. https://doi.org/10.1016/j.soilbio.2006.09.012.

Celik, I., 2005. Land-use effects on organic matter and physical properties of soil in a southern Mediterranean highland of Turkey. Soil Till Res 83, 270–277. https://doi.org/10.1016/j.still.2004.08.001.

Chefetz, B., Chen, Y., Clapp, C.E., Hatcher, P.G., 2000. Characterization of organic matter in soils by thermochemolysis using tetramethylammonium hydroxide (TMAH). Soil Sci. Soc. Am. J. 64, 583–589. https://doi.org/10.2136/sssaj2000.642583x.

Chivenge, P.P., Murwira, H.K., Giller, K.E., Mapfumo, P., Six, J., 2007. Long-term impact of reduced tillage and residue management on soil carbon stabilization: Implications for conservation agriculture on contrasting soils. Soil Till Res 94, 328–337. https://doi.org/10.1016/j.still.2006.08.006.

Dick, W.A., 1984. Influence of long-term tillage and crop rotation combinations on soil enzyme activities. Soil Sci. Soc. Am. J. 48, 569–574. https://doi.org/10.2136/sssaj1984.03615995004800030020x.

Dick, W.A., Daniel, T.C., 1987. Soil chemical and biological properties as affected by conservation tillage: Environmental impacts. In: Logan, T.J. (Ed.), Effects of Conservation Tillage on Groundwater Quality: Nitrates and Pesticides. Lewis Publishers Inc,, Chelsen, MI, USA.

Dick, R.P., 1992. A review: long-term effects of agricultural systems on soil biochemical and microbial parameters. Agric. Ecosyst. Environ. 40, 25–36. https://doi.org/10.1016/0167-8809(92)90081-L.

Dignac, M., Bahri, H., Rumpel, C., Rasse, D.P., Bardoux, G., Balesdent, J., Girardin, C., Chenu, C., Mariotti, A., 2005. Carbon-13 natural abundance as a tool to study the dynamics of lignin monomers in soil : an appraisal at the Closeaux experimental field (France). Geoderma 128, 3–17. https://doi.org/10.1016/j.geoderma.2004.12.022.

Doran, J.W., Werner, M.R., 1990. Management and soil biology. In: Francis, C.A., Flora, C.B., King, L.D. (Eds.), Sustainable agriculture in temperate zones. John Wiley and Sons, New York, USA, pp. 205–230.

Drosos, M., Nebbioso, A., Mazzei, P., Vinci, G., Spaccini, R., Piccolo, A., 2017. A molecular zoom into soil Humeome by a direct sequential chemical fractionation of soil. Sci. Total Environ. 586, 807–816. https://doi.org/10.1016/j.scitotenv.2017.02.059.

Drosos, M., Nebbioso, A., Piccolo, A., 2018. Humeomics: A key to unravel the humusic pentagram. Appl. Soil Ecol. 123, 513–516. https://doi.org/10.1016/j.apsoil.2017.07.027.

Drosos, M., Piccolo, A., 2018. The molecular dynamics of soil humus as a function of tillage. Land Degrad. Dev. 29, 1792–1805. https://doi.org/10.1002/ldr.2989.

Drosos, M., Vinci, G., Spaccini, R., Piccolo, A., 2020. Molecular dynamics of organic matter in a tilled soil under short term wheat cultivation. Soil Tillage Res. 196, 104448. https://doi.org/10.1016/j.still.2019.104448.

Elliott, E.T., 1986. Aggregate structure and carbon, nitrogen, and phosphorus in native and cultivated soils. Soil Sci. Soc. Am. J. 50, 627–633. https://doi.org/10.2136/sssaj1986.03615995005000030017x.

Feng, X., Simpson, A.J., Wilson, K.P., Dudley Williams, D., Simpson, M.J., 2008. Increased cuticular carbon sequestration and lignin oxidation in response to soil warming. Nat. Geosci. 1, 836–839. https://doi.org/10.1038/ngeo361.

Fontaine, S., Barot, S., Barré, P., Bdioui, N., Mary, B., Rumpel, C., 2007. Stability of organic carbon in deep soil layers controlled by fresh carbon supply. Nature 450, 277–280. https://doi.org/10.1038/nature06275.

Grandy, A.S., Neff, J.C., 2008. Molecular C dynamics downstream: The biochemical decomposition sequence and its impact on soil organic matter structure and function. Sci. Total Environ. 404, 297–307. https://doi.org/10.1016/j.scitotenv.2007.11.013.

Guignard, C., Lemée, L., Amblès, A., 2005. Lipid constituents of peat humic acids and humin. Distinction from directly extractable bitumen components using TMAH and TEAAc thermochemolysis. Org Geochem. 36, 287–297. https://doi.org/10.1016/j.orggeochem.2004.07.016.

Gupta, V.V.S.R., Germida, J.J., 1988. Distribution of microbial biomass and its activity in different soil aggregate size classes as affected by cultivation. Soil Biol. Biochem. 20, 777–786. https://doi.org/10.1016/0038-0717(88)90082-X.

Jandl, G., Leinweber, P., Schulten, H.R., Ekschmitt, K., 2005. Contribution of primary organic matter to the fatty acid pool in agricultural soils. Soil Biol. Biochem. 37, 1033–1041. https://doi.org/10.1016/j.soilbio.2004.10.018.

Jandl G, Leinweber P, Schulten HR (2007) Origin and fate of soil lipids in a Phaeozem under rye and maize monoculture in Central Germany. 321–332. https://doi.org/10.1007/s00374-006-0109-2.

Jandl G, Baum C, Blumschein A, Leinweber P (2012) The impact of short rotation coppice on the concentrations of aliphatic soil lipids. 163–177. https://doi.org/10.1007/s11104-011-0892-x.

Jobbagy, E.G., Jackson, R.B., 2000. The Vertical Distribution of Soil Organic Carbon and Its Relation to Climate and Vegetation. Ecol. Appl. 10, 423. https://doi.org/10.2307/2641104.

Kahle, P., Baum, C., Boelcke, B., Kohl, J., Ulrich, R., 2010. Vertical distribution of soil properties under short-rotation forestry in Northern Germany. J. Plant Nutr. Soil Sci. 173, 737–746. https://doi.org/10.1002/jpln.200900230.

Lal, R., 2004. Soil carbon sequestration impacts on global climate change and food security. Science 304, 1623–1627. https://doi.org/10.1126/science.1097396.

Mann, L., Tolbert, V., Cushman, J., 2002. Potential environmental effects of corn (Zea mays L.) stover removal with emphasis on soil organic matter and erosion. Agric. Ecosyst. Environ. 89, 149–166. https://doi.org/10.1016/S0167-8809(01)00166-9.

McGill, W.B., Cannon, K.R., Robertson, J.A., Cook, F.D., 1986. Dynamics of soil microbial biomass and water-soluble organic C in Breton L after 50 years of cropping to two rotations. Can. J. Soil Sci. 66, 1–19. https://doi.org/10.4141/cjss86-001.

Naafs, D.F.W., Van Bergen, P.F., De Jong, M.A., Oonincx, A., De Leeuw, J.W., 2004. Total lipid extracts from characteristic soil horizons in a podzol profile. Eur. J. Soil Sci. 55, 657–669. https://doi.org/10.1111/j.1365-2389.2004.00633.x.

Nardi, S., Pizzeghello, D., Muscolo, A., Vianello, A., 2002. Physiological effects of humic substances on higher plants. Soil Biol. Biochem. 34, 1527–1536. https://doi.org/10.1016/S0038-0717(02)00174-8.

Nebbioso, A., Piccolo, A., 2011. Basis of a humeomics science: Chemical fractionation and molecular characterization of humic biosuprastructures. Biomacromolecules 12, 1187–1199. https://doi.org/10.1021/bm101488e.

Nebbioso, A., Vinci, G., Drosos, M., Spaccini, R., Piccolo, A., 2015. Unveiling the molecular composition of the unextractable soil organic fraction (humin) by humeomics. Biol. Fertil. Soils 51, 443–451. https://doi.org/10.1007/s00374-014-0991-y.

Ostle, N.J., Levy, P.E., Evans, C.D., Smith, P., 2009. UK land use and soil carbon sequestration. Land use policy 26, 274–283. https://doi.org/10.1016/j.landusepol.2009.08.006.

Pan, G., Li, L., Wu, L., Zhang, X., 2004. Storage and sequestration potential of topsoil organic carbon in China's paddy soils. Glob. Change Biol. 10, 79–92. https://doi.org/10.1111/j.1365-2486.2003.00717.x.

Pan, G., Zhou, P., Li, Z., Smith, P., Li, L., Qiu, D., Zhang, X., Xu, X., Shen, S., Chen, X., 2009a. Combined inorganic/organic fertilization enhances N efficiency and increases rice productivity through organic carbon accumulation in a rice paddy from the Tai Lake region, China. Agric. Ecosyst. Environ. 131, 274–280. https://doi.org/10.1016/j.agee.2009.01.020.

Pan, G., Smith, P., Pan, W., 2009b. The role of soil organic matter in maintaining the productivity and yield stability of cereals in China. Agric. Ecosyst. Environ. 129, 344–348. https://doi.org/10.1016/j.agee.2008.10.008.

Piccolo A (1996) Humus and Soil Conservation. In: Humic Substances in Terrestrial Ecosystems. pp. 225–264. https://doi.org/10.1016/b978-044481516-3/50006-2.

Piccolo, A., Mbagwu, J.S.C., 1999. Role of hydrophobic components of soil organic matter on the stability of soil aggregates. Soil Sci. Soc. Am. J. 63, 1801–1810. https://doi.org/10.2136/sssaj1999.6361801x.

Piccolo, A., 2001. The supramoleular structure of humic substances. Soil Sci. 166, 810–832.

Piccolo, A., Conte, P., Cozzolino, A., 2001. Chromatographic and spectrophotometric properties of dissolved humic substances compared with macromolecular polymers. Soil Sci. 166, 174–185. https://doi.org/10.1097/00010694-200103000-00003.

Piccolo, A., 2002. The Supramolecular structure of humic substances. A novel understanding of humus chemistry and implications in soil Science. Adv. Agron. 75, 57–134. https://doi.org/10.1016/S0065-2113(02)75003-7.

Piccolo, A., Spaccini, R., Nieder, R., Richter, J., 2004. Sequestration of a biologically labile organic carbon in soils by humified organic matter. Clim. Change 67, 329–343. https://doi.org/10.1007/s10584-004-1822-1.

Piccolo, A., Conte, P., Spaccini, R., Mbagwu, J.S.C., 2005. Influence of land use on the characteristics of humic substances in some tropical soils of Nigeria. Eur. J. Soil Sci. 56, 343–352. https://doi.org/10.1111/j.1365-2389.2004.00671.x.

Piccolo, A., Spaccini, R., Cozzolino, V., Nuzzo, A., Drosos, M., Zavattaro, L., Grignani, G., Puglisi, E., Trevisan, M., 2018a. Effective carbon sequestration in Italian agricultural soils by in situ polymerization of soil organic matter under biomimetic photocatalysis. L Degrad Dev 29, 485–494. https://doi.org/10.1002/ldr.2877.

Piccolo, A., Spaccini, R., Drosos, M., Vinci, G., Cozzolino, V., 2018b. The molecular composition of humus carbon: recalcitrance and reactivity in soils. In: Garcia, C., Nannipieri, P., Hernandez, T. (Eds.), The Future of Soil Carbon: Its Conservation and Formation. Academic Press Elsevier, 125 London Wall London (UK), pp. 87–124.

Puglisi, E., Fragoulis, G., Del Re, A.A.M., Spaccini, R., Piccolo, A., Gigliotti, G., Said-Pullicino, D., Trevisan, M., 2008. Carbon deposition in soil rhizosphere following amendments with compost and its soluble fractions, as evaluated by combined soil-plant rhizobox and reporter gene systems. Chemosphere 73, 1292–1299. https://doi.org/10.1016/j.chemosphere.2008.07.008.

Rasse, D.P., Dignac, M.F., Bahri, H., Rumpel, C., Mariotti, A., Chenu, C., 2006. Lignin turnover in an agricultural field: from plant residues to soil-protected fractions. Eur. J. Soil Sci. 57, 530–538. https://doi.org/10.1111/j.1365-2389.2006.00806.x.

Rumpel, C., Seraphin, A., Dignac, M.-F., Michaelis, W., Eusterhues, K., Kögel-Knabner, I., 2005. Effect of base hydrolysis on the chemical composition of organic matter of an acid forest soil. Org. Geochem. 36, 239–249. https://doi.org/10.1016/j.orggeochem.2004.08.001.

Saiz-Jimenez, C., 1994. Production of alkylbenzenes and alkylnaphthalenes upon pyrolysis of unsaturated fatty acids. Naturwissenschaften 81, 451–453. https://doi.org/10.1007/bf01136646.

Schnitzer, M., McArthur, D.F.E., Schulten, H.-R., Kozak, L.M., Huang, P.M., 2006. Long-term cultivation effects on the quantity and quality of organic matter in selected Canadian prairie soils. Geoderma 130, 141–156. https://doi.org/10.1016/j.geoderma.2005.01.021.

Six, J., Conant, R.T., Paul, E.A., Paustian, K., 2002a. Stabilization mechanisms of soil organic matter: Implications for C-saturation of soils. Plant Soil 241, 155–176. https://doi.org/10.1023/A:1016125726789.

Six, J., Feller, C., Denef, K., Ogle, S.M., de Moraes Sa, J.C., Albrecht, A., 2002b. Soil organic matter, biota and aggregation in temperate and tropical soils - Effects of no-tillage. Agronomy 22, 755–775. https://doi.org/10.1051/agro:2002043.

Smith P, Bustamante M, Ahammad H, Clark H, Dong H, Elsiddig EA, House J (2014) In O. R. Edenhofer, et al. (Eds.), Climate change 2014: Mitigation of climate change. Contribution of working group III to the fifth assessment report of the intergovernmental panel on climate change (IPCC), Cambridge: Cambridge University Press, pp. 816–887.

Song, X.Y., Spaccini, R., Pan, G., Piccolo, A., 2013. Stabilization by hydrophobic protection as a molecular mechanism for organic carbon sequestration in maize-amended rice paddy soils. Sci. Total Environ. 458–460, 319–330. https://doi.org/10.1016/j.scitotenv.2013.04.052.

Spaccini, R., Piccolo, A., Haberhauer, G., Gerzabek, M.H., 2000. Transformation of organic matter from maize residues into labile and humic fractions of three European soils as revealed by 13 C distribution and CPMAS-NMR spectra. Eur. J. Soil Sci. 51, 583–594. https://doi.org/10.1111/j.1365-2389.2000.00341.x.

Spaccini, R., Piccolo, A., Conte, P., Haberhauer, G., Gerzabek, M.H., 2002. Increased soil organic carbon sequestration through hydrophobic protection by humic substances. Soil Biol. Biochem. 34, 1839–1851. https://doi.org/10.1016/S0038-0717(02)00197-9.

Spaccini, R., Piccolo, A., 2007. Molecular characterization of compost at increasing stages of maturity. 2. Thermochemolysis-GC-MS and 13C-CPMAS-NMR spectroscopy. J. Agric. Food Chem. 55, 2303–2311. https://doi.org/10.1021/jf0625407.

Spaccini, R., Piccolo, A., 2009. Molecular characteristics of humic acids extracted from compost at increasing maturity stages. Soil Biol. Biochem. 41, 1164–1172. https://doi.org/10.1016/j.soilbio.2009.02.026.

Spaccini, R., Sannino, D., Piccolo, A., Fagnano, M., 2009. Molecular changes in organic matter of a compost-amended soil. Eur. J. Soil Sci. 60, 287–296. https://doi.org/10.1111/j.1365-2389.2008.01108.x.

Spaccini, R., Song, X.Y., Cozzolino, V., Piccolo, A., 2013. Molecular evaluation of soil organic matter characteristics in three agricultural soils by improved off-line thermochemolysis: The effect of hydrofluoric acid demineralisation treatment. Anal. Chim. Acta 802, 46–55. https://doi.org/10.1016/j.aca.2013.09.031.

Spaccini, R., Piccolo, A., 2019. Amendments with humified compost effectively sequester organic carbon in agricultural soils. Land Degrad. Dev. https://doi.org/10.1002/ldr.3524.

Tadini, A.M., Pantano, G., de Toffoli, A.L., Fontaine, B., Spaccini, R., Piccolo, A., Moreira, A.B., Bisinoti, M.C., 2015. Off-line TMAH-GC/MS and NMR characterization of humic substances extracted from river sediments of northwestern São Paulo under different soil uses. Sci. Total Environ. 506–507, 234–240. https://doi.org/10.1016/j.scitotenv.2014.11.012.

Thevenot, M., Dignac, M.F., Rumpel, C., 2010. Fate of lignins in soils: A review. Soil Biol. Biochem. 42, 1200–1211. https://doi.org/10.1016/j.soilbio.2010.03.017.

Ussiri, D.A.N., Johnson, C.E., 2003. Characterization of organic matter in a northern hardwood forest soil by 13 C NMR spectroscopy and chemical methods of organic matter could account for variations in the structure and chemistry of organic matter in these forest soils. Geoderma 111, 123–149. https://doi.org/10.1016/S0016-7061(02)00257-4.

West, T.O., Post, W.M., 2002. Soil organic carbon sequestration rates by tillage and crop rotation: A global data analysis. Soil Sci. Soc. Am. J. 66, 1930–1946. https://doi.org/10.2136/sssaj2002.1930.

Zhang, J., Chi, F., Wei, D., Zhou, B., Cai, S., Li, Y., Kuang, E., Sun, L., Li, L.-J., 2019. Impacts of Long-term Fertilization on the Molecular Structure of Humic Acid and Organic Carbon Content in Soil Aggregates in Black Soil. Sci. Rep. 9, 11908. https://doi.org/10.1038/s41598-019-48406-8.

Zhou, P., Song, G., Pan, G., Li, L., Zhang, X., 2009. Role of chemical protection by binding to oxyhydrates in SOC sequestration in three typical paddy soils under long-term agro-ecosystem experiments from South China. Geoderma 153, 52–60. https://doi.org/10.1016/j.geoderma.2009.07.018.

Zhou, P., Pan, G.X., Spaccini, R., Piccolo, A., 2010. Molecular changes in particulate organic matter (POM) in a typical Chinese paddy soil under different long-term fertilizer treatments. Eur. J. Soil Sci. 61, 231–242. https://doi.org/10.1111/j.1365-2389.2009.01223.x.

Zohaib, A., Tanveer, A., Khaliq, A., Safdar, M.E., 2014. Phytotoxic effect of water soluble phenolics from five leguminous weeds on germination and seedling growth of rice. Pakistan J Weed Sci Res 20, 417–429. https://doi.org/10.28941/pjwsr.v20i4.556.

Supporting Information

Molecular characterization of soil organic matter and its extractable humic fraction from long-term field experiments under different cropping systems

Claudia Savarese[b], Marios Drosos[a]*, Riccardo Spaccini[b,c], Vincenza Cozzolino[b,c], Alessandro Piccolo[b,c]*

[a] Institute of Resource, Ecosystem and Environment of Agriculture (IREEA). Nanjing Agricultural University, 1 Weigang Road, 210095 Nanjing, China.

[b] Department of Agricultural Sciences. Università di Napoli Federico II, Via Università 100, 80055 Portici, Italy.

[c] Interdepartmental Research Centre of Nuclear Magnetic Resonance for the Environment, Agro-Food and New Materials (CERMANU). University of Naples Federico II, Via Università 100, 80055 Portici, Italy.

*** Corresponding authors. E-mail address: drosos.marios@gmail.com; alpiccol@unina.com**

Two tables (S1 and S2)

Table S1. Retention time (RT), empirical formula, molecular group assigned, and relative abundance (%) of molecules detected by thermochemolysis GC-MS in the three bulk soils from long-term field plots (Control, Maize: monoculture, and Mix: Maize-Bean rotation). The samples were categorized in 26 distinct molecular groups (AA: Aromatic acids, AC: Alcohols, AD: Amides, AL: Alkanes/alkenes, AM: Amines, BA: Benzoic Acids, BE: Benzoic Esters, DA: Dicarboxylic Acids, ES: Esters, ET: Ethers, FA: Fatty Acids, HA: Hydroxy Acids, HC: Aromatic hydrocarbons not assigned in another group, HN: Heterocyclic Nitrogen compounds, HO: Heterocyclic Oxygen compounds, KE: Ketones, NO: Nitroxides, PA: Phenolic Acids, PE: Phenolic Esters, PH: Phenols, RA: Resin Acids, SA: Sugar Acids, SE: Steroids, SET: Sugar Ethers/Esters, ST: Sterols, SU: Sugars).

RT	Empirical Formula	Group	Relative Abundance (%)		
			CONTROL soil sample (no cultivation. no tillage)	**MAIZE soil sample** (maize mono-cultivation. traditional tillage)	**MIX soil sample** (maize-broad bean rotation. traditional tillage)
5.27	C6H12ON2	AD	-	0.3	-
5.31	C6H6O	PH	1.3	-	-
5.41	C11H12N	AM	-	-	0.1
5.46	C9H11N2	HN	0.4	-	-
5.52	C12H25	AL	-	0.5	-
5.54	C16H34	AL	-	-	0.3
5.70	C7H8O	PH	1.6	-	-
5.73	C12H19O2N	AM	-	0.4	-
5.87	C12H18O3	HO	0.2	-	-
5.95	C10H20O2	HO	-	1.3	-
5.97	C7H10O	KE	0.3	-	-
6.07	C7H9N	AM	-	2.5	-
6.09	C8H18O	AC	-	-	0.4
6.16	C6H6O	PH	1.1	-	-
6.17	C7H12O	KE	-	-	0.2
6.37	C8H12O	KE	1.0	0.7	-
6.61	C10H13O3N	AA	6.1	-	-
6.88	C9H11O2N	AD	0.3	-	-
7.01	C7H12O3	HO	0.4	-	-

7.07	C10H12ON2	AD	-	0.7	-
7.13	C11H14O2	BE	3.9	-	-
7.14	C9H12O2	PH	-	-	0.5
7.33	C11H12O4N2	AD	0.7	-	-
7.41	C5H8O4	DA	1.4	-	-
7.42	C10H16	AL	-	0.3	-
7.63	C5H5O2N	HN	1.4	-	-
7.63	C10H22N2	AM	-	-	0.2
7.82	C7H6O4	PA	-	3.3	-
7.95	C14H14O2	PH	0.8	2.3	1.4
8.31	C10H10	HC	0.3	0.3	0.1
8.41	C8H8O	PH	0.3	-	-
8.47	C10H10	HC	0.4	0.5	-
8.56	C9H12O2	ET	0.2	1.5	-
8.62	C6H6O2	PH	0.3	-	-
8.73	C10H14	HC	-	-	0.2
8.94	C8H14O5	DA	0.5	-	-
9.23	C17H34	AL	2.2	1.0	0.4
9.44	C12H26	AL	0.2	0.4	-
9.55	C6H8N2	AM	0.7	-	-
9.58	C6H7ON	AD	-	0.6	0.2
9.80	C9H12O	PH	0.5	-	-
9.93	C7H11O2N	AD	0.6	-	-
10.03	C6H7O2N	HN	0.2	-	-
10.22	C5H7N3	HN	0.2	-	0.3
10.62	C13H16ON4	HN	0.2	-	-
10.71	C13H17O2N	AA	0.1	-	-
10.94	C24H24N2	HN	0.4	-	-
11.09	C12H14O5	PE	0.5	-	-
11.14	C11H12	HC	-	0.4	0.7

11.29	C10H10	HC	1.8	-	-
11.38	C11H12	HC	-	1.2	-
11.44	C9H10O2	BA	0.1	-	-
11.51	C7H14O7	SA	0.3	-	-
11.61	C10H12O	PH	-	0.4	0.1
11.71	C6H12O5	SU	0.6	0.4	0.2
11.85	C16H32	AL	0.4	-	-
12.08	C11H10	HC	1.3	-	-
12.14	C6H6O3	PH	-	10.0	-
12.15	C14H26O4N2	AD	0.2	-	-
12.26	C14H14O	BE	-	-	0.5
12.34	C6H6O3	PH	0.3	-	-
12.70	C11H10	HC	0.6	0.6	0.5
12.82	C11H20O2	BA	0.4	-	-
12.88	C12H34O2	FA	-	-	0.1
12.98	C8H14O2N2	AM	-	-	0.2
13.17	C5H7O5N	NO	0.3	-	-
13.53	C23H22O3N2	AD	0.4	-	-
13.86	C11H16N2	AM	0.1	-	-
13.95	C16H22O2N2	HN	1.3	-	-
14.07	C6H6O3	PH	0.5	-	-
14.13	C11H12	HC	-	-	0.2
14.18	C12H14	HC	0.3	-	-
14.33	C19H15O2N	AD	0.4	-	-
14.38	C7H8O3	PH	-	-	0.6
14.45	C6H12O5	SU	0.3	-	-
14.51	C15H28O5	ES	0.2	-	-
14.60	C6H12O5	SU	-	-	0.1
14.66	C19H38O2	ES	1.5	-	-
14.74	C17H36O	AC	-	1.0	0.2

14.76	C11H18O4	ES	0.1	-	-
14.89	C10H18O2	HO	-	0.4	-
14.90	C18H36	AL	0.2	-	-
14.91	C11H22O2	SU	-	-	0.2
14.99	C22H24O4	BE	0.2	-	-
15.13	C10H11ON	HN	0.4	-	-
15.24	C5H10O5	SU	0.3	-	-
15.32	C6H10O7	SA	-	-	0.1
15.36	C11H18O4	ES	0.2	-	-
15.49	C12H12	HC	0.3	-	-
15.60	C16H12O6	HO	0.5	-	-
15.60	C12H12	HC	-	-	0.1
15.70	C8H5O2N	HN	0.1	-	-
15.76	C13H13O3	HO	-	-	0.3
16.14	C9H9ON	HN	0.8	-	0.4
16.28	C12H16O	PH	0.1	-	-
16.47	C12H12	HC	0.6	-	0.4
16.64	C10H20O2	ES	0.1	-	-
16.80	C11H20O11	SET	1.1	-	-
16.91	C8H5O3	PH	-	4.1	-
17.27	C20H22O4	HO	0.1	-	-
17.40	C10H11O2N	HN	0.1	-	-
17.49	C6H12O6	SU	0.2	-	-
17.63	C11H18O8	ES	1.5	-	-
17.78	C18H38	AL	0.4	-	-
17.81	C17H36	AL	-	-	0.1
17.85	C18H36O2	ES	-	0.3	-
18.03	C14H22O	PH	1.6	2.4	0.6
18.17	C13H16	HC	-	-	0.2
18.45	C10H11N	HN	1.4	0.8	-

18.55	C10H11N	HN	-	-	1.0
18.66	C14H14O	PH	0.4	-	-
18.75	C13H14	HC	-	-	0.2
18.89	C6H12O6	SU	0.6	-	-
19.04	C13H14	HC	0.1	-	-
19.22	C13H14	HC	0.3	-	-
19.72	C11H14O4	HO	-	-	0.3
19.73	C7H12O6	PA	1.1	-	-
19.75	C20H28O4	ES	-	0.9	-
19.95	C30H30O2	KE	0.3	-	-
20.17	C9H12O2	PH	0.9	-	-
20.21	C12H16O3	BE	-	0.5	-
20.27	C13H10	HC	-	-	0.2
20.38	C7H12O4	PA	1.3	-	-
20.40	C19H40O	AC	-	-	0.4
20.44	C18H34	HC	-	1.0	-
20.59	C18H38	AL	0.3	-	-
20.73	C15H18	HC	-	-	0.4
21.02	C13H12O	PH	0.1	-	-
21.27	C11H13N	HN	0.3	-	0.9
21.35	C15H17O3N	AM	0.4	-	-
21.50	C8H10O4	PH	-	7.6	-
21.78	C10H12O3	PH	0.3	-	-
21.87	C9H10O3	PH	0.4	-	-
22.55	C9H7ON	HN	0.1	-	-
22.67	C22H23N	AM	0.5	-	-
22.69	C21H34O2	BE	-	-	0.5
22.73	C18H18	HC	-	0.5	-
22.73	C18H18	HC	-	-	0.2
22.83	C14H16	HC	0.1	-	0.4

22.96	C14H28O2	FA	0.2	-	-
23.05	C13H28O	AC	0.1	-	0.4
23.22	C14H12	HC	0.1	-	-
23.32	C16H34	AL	0.2	-	-
23.35	C17H32O4	ES	-	-	0.2
23.42	C14H12	HC	0.1	-	0.3
23.45	C 14H14O	PH	-	-	0.2
23.56	C9H6ON4	HN	0.2	-	-
23.74	C7H6O5	PA	1.1	-	0.3
23.96	C14H28O2	FA	0.5	-	-
24.00	C15H30O2	FA	-	-	1.8
24.05	C22H44O2	ES	0.3	-	-
24.07	C15H32O	AC	-	0.6	-
24.33	C20H4O	AL	0.2	-	0.1
24.43	C28H5O	PH	-	-	0.1
24.55	C9H10O4	PH	0.1	-	-
24.68	C28H24	HC	0.1	-	-
24.81	C12H15N	HN	0.2	-	-
25.06	C12H15N	HN	0.3	-	-
25.22	C13H10ON2	HN	0.4	-	-
25.28	C32H34O2	BE	-	-	0.2
25.38	C22H19O4N	HN	0.1	-	-
25.61	C10H14O5	PH	1.9	-	-
25.65	C13H11N	HN	-	-	1.6
25.68	C15H16	HC	-	0.3	-
25.79	C16H34O	AC	-	0.9	-
25.80	C18H36O2	FA	1.1	-	-
25.83	C16H32O2	FA	-	-	1.0
25.96	C8H10O4	PH	0.8	-	-
25.98	C25H52	AL	-	-	0.8

26.08	C13H10O	KE	-	0.3	-
26.54	C19H32	HC	-	0.4	0.2
26.57	C15H30O2	FA	0.1	-	0.3
26.66	C17H36O	AC	0.6	-	-
26.71	C26H46	HC	-	0.8	0.2
26.88	C15H28O2	ES	0.1	-	-
26.99	C18H36O	KE	0.2	0.3	-
27.02	C14H28O	KE	-	0.3	-
27.63	C19H32	HC	0.2	-	-
28.06	C18H30	HC	0.1	-	-
28.17	C16H32O2	FA	0.9	-	0.3
28.31	C12H10ON2	HN	0.6	-	-
28.37	C14H10O4	BA	-	-	0.2
28.49	C18H38	AL	-	0.9	-
28.52	C16H30O2	FA	0.9	-	1.8
28.64	C18H32	HC	0.8	3.1	1.2
28.78	C16H30O2	FA	0.6	-	0.4
29.09	C16H32O2	FA	5.2	2.5	11.1
29.27	C9H8O5	PA	-	1.3	-
29.95	C15H30O2	FA	-	-	0.4
29.97	C17H32O2	FA	0.2	-	-
30.13	C17H34O2	FA	0.5	2.4	1.0
30.30	C14H28O2	FA	0.2	-	-
30.38	C10H22O	AC	0.1	0.4	-
30.62	C17H34O2	FA	0.4	0.5	0.4
30.75	C20H40	AL	0.1	-	-
30.77	C18H34O2	FA	-	-	0.2
30.81	C17H34O2	FA	0.1	-	-
30.90	C28H56O2	ES	0.7	-	-

30.92	C40H82	AL	-	1.1	0.6
31.13	C17H32O2	FA	0.3	-	-
31.14	C38H36O6N2	AD	-	-	0.4
31.15	C20H22O8	BE	-	1.0	-
31.56	C15H32O	AC	1.1	-	-
31.57	C21H42O2	FA	-	-	0.4
31.58	C22H46O	AC	-	0.7	-
31.81	C12H26	AL	0.2	0.5	0.2
32.23	C15H30O	AC	0.2	-	-
32.33	C17H34O	AC	1.1	1.5	2.0
32.65	C8H8O5	PA	-	1.4	-
33.02	C18H32O2	FA	-	-	9.9
33.19	C18H34O2	FA	1.6	-	12.5
33.24	C36H72O3	ES	-	2.0	-
33.32	C18H34O2	FA	0.5	0.4	-
33.82	C18H36O2	FA	1.8	2.4	4.7
34.48	C37H70O3	ET	0.5	0.5	0.9
34.67	C19H38O2	FA	0.1	-	-
34.81	C11H22O2	FA	0.1	-	-
34.83	C20H40O	AC	-	-	0.2
35.10	C19H40O3	ET	0.2	-	0.3
35.32	C27H56O	AC	0.1	-	-
35.33	C30H58O2	FA	-	0.3	0.7
35.46	C43H88	AL	0.5	1.4	0.7
35.66	C30H58O2	ES	-	0.3	1.0
35.73	C19H36O2	FA	1.0	-	-
35.73	C21H38O4	ES	-	0.7	-
36.79	C10H20O4	ES	-	-	0.4
36.87	C5H10O5	SU	0.2	-	-

37.00	C28H56O2	FA	0.1	-	-
37.23	C32H62O	KE	0.1	-	-
37.58	C35H72	AL	0.2	0.8	0.3
37.65	C12H22O11	SET	0.7	0.7	0.6
38.02	C34H66O	KE	0.1	-	-
38.16	C20H40O2	FA	0.3	-	0.2
38.58	C26H46O4	ES	-	-	0.2
38.59	C30H62O2	AC	-	1.1	-
38.89	C40H82	AL	0.1	-	-
39.39	C22H42O4	ES	0.7	-	-
39.65	C44H90	AL	0.3	0.6	0.9
40.23	C23H48O	AC	0.4	-	1.2
41.61	C22H46	AL	1.0	1.4	1.5
43.64	C36H74	AL	-	-	1.5
44.18	C24H50O	AC	0.3	0.6	1.5
45.42	C30H62	AL	0.7	4.8	2.6
45.96	C24H48O2	FA	0.2	0.5	0.5
46.22	C24H48O2	FA	0.3	-	-
46.31	C32H54O2	SE	-	-	0.2
47.33	C30H50	AL	0.4	5.0	9.2
47.70	C41H84O	AC	0.6	1.0	0.9
47.99	C29H48O4	BE	0.2	2.9	-
48.49	C29H48O2	SE	-	-	0.7
48.88	C21H44	AL	0.8	-	2.7
49.40	C16H30O4	ES	0.3	-	-
50.54	C54H110	AL	0.4	-	-
51.12	C17H30O2	ST	1.3	1.0	1.6
51.66	C25H19O7N	PH	0.4	-	-
51.95	C14H22O2	PH	0.1	-	-

52.15	C34H70	AL	0.7	-	-
52.23	C39H80	AL	-	0.8	0.5
52.47	C14H22O	HO	0.4	-	-
52.59	C26H40O4	BE	0.2	-	-
52.90	C22H32O4	BE	0.1	-	-
53.12	C23H34O4	BE	0.3	-	-
54.02	C14H22O2	PH	0.1	-	-
54.21	C14H22O2	PH	0.1	-	-

Table S2. Retention time (RT), empirical formula, molecular group assigned, and relative abundance (%) of molecules detected by thermochemolysis GC-MS of the three eSOM extracts obtained from long-term cultivated soil (Control, Maize: monoculture, and Mix: Maize-Bean rotation). The samples were categorized in 26 distinct molecular groups (AA: Aromatic acids, AC: Alcohols, AD: Amides, AL: Alkanes/alkenes, AM: Amines, BA: Benzoic Acids, BE: Benzoic Esters, DA: Dicarboxylic Acids, ES: Esters, ET: Ethers, FA: Fatty Acids, HA: Hydroxy Acids, HC: Aromatic hydrocarbons not assigned in another group, HN: Heterocyclic Nitrogen compounds, HO: Heterocyclic Oxygen compounds, KE: Ketones, NO: Nitroxides, PA: Phenolic Acids, PE: Phenolic Esters, PH: Phenols, RA: Resin Acids, SA: Sugar Acids, SE: Steroids, SET: Sugar Ethers/Esters, ST: Sterols, SU: Sugars).

RT	Empirical Formula	Group	Relative Abundance (%)		
			CONTROL eSOM (no cultivation. no tillage)	**MAIZE eSOM** (maize mono-cultivation. traditional tillage)	**MIX eSOM** (maize-broad bean rotation. traditional tillage)
9.29	C8H11ON	AM	-	0.5	0.4
9.62	C17H36O	AC	9.3	0.2	4.2
9.85	C5H8O2N2	AD	6.4	2.5	4.1
10.05	C5H7N3	AM	-	0.5	-
10.15	C26H46O4	ES	0.5	-	0.9
10.24	C6H6O3	PH	-	-	0.8
10.39	C6H13ON3	HN	0.9	0.5	0.5
10.43	C9H13ON	AM	-	-	0.4
10.48	C7H11O3N	AD	0.2	-	-
10.68	C6H12ON2	HN	0.2	-	0.2
11.06	C21H44	AL	0.2	0.2	0.8
11.19	C7H14O7	SA	-	-	0.5
11.34	C24H44O4	ES	0.3	0.5	0.6
11.39	C5H10O5	SU	-	-	0.7
11.43	C8H14O5	SE	2.0	-	-
11.58	C6H6O3	PH	-	-	0.3
11.74	C7H14O7	SA	0.2	0.9	1.3
11.99	C13H28O	AC	0.4	0.6	0.2

12.21	C29H54O4	ES	0.2	-	0.3
12.33	C20H42O	AC	0.7	0.2	0.2
12.61	C10H16O4N2	AD	-	0.6	-
12.63	C4H8ON2	AD	0.5	0.2	0.8
12.77	C5H7O3N	HN	-	7.3	4.1
12.89	C7H6O3	PA	-	-	2.6
13.11	C4H8O2N2	AD	1.2	-	1.2
13.77	C6H6O3	PH	0.3	1.1	2.3
13.93	C7H6O3	PA	-	-	1.2
14.01	C11H6O4	ES	0.3	-	-
14.16	C5H10O4	SU	2.6	3.7	2.2
14.29	C14H30O	AC	-	-	1.0
14.31	C6H12O5	SU	1.0	0.6	0.4
14.4	C5H10O6	SU	0.9	-	-
14.48	C9H12O3	HO	-	-	0.7
14.75	C12H17N	HN	-	-	0.4
14.91	C11H20O2	AA	0.3	0.2	0.3
15.16	C23H46O2	FA	0.3	0.3	0.6
15.25	C9H17O2N	AD	0.4	1.2	1.3
15.42	C10H8	HC	0.4	0.2	0.8
15.67	C6H6O4	PH	-	-	0.4
15.75	C9H9ON	HN	-	-	0.5
15.9	C12H18	HC	0.6	0.2	0.4
16.06	C14H24O4	ES	0.3	0.6	0.7
16.33	C5H5O2N2	AD	0.1	0.2	0.7
16.39	C11H24O	AC	1.5	-	-
16.50	C6H12O5	SU	0.2	-	0.2
16.58	C16H16O8	SE	0.1	-	-
16.61	C10H16O8	SE	-	0.8	1.0

16.84	C6H12O5	SU	-	-	0.7
17.01	C31H64	AL	0.5	0.2	0.2
17.26	C9H20O9	SE	-	0.6	0.7
17.33	C21H40O5	ES	0.5	-	0.8
17.57	C14H22O	PH	3.9	11.2	5.9
18.07	C14H22O4	ES	0.8	-	-
18.08	C10H11N	HN	-	0.9	1.1
18.28	C13H28O	AC	0.7	-	0.3
18.57	C15H32O	AC	0.2	-	0.1
18.73	C9H16O4	DA	0.2	-	0.4
18.84	C10H20	AL	-	-	0.2
19.30	C14H18O3N2	AD	0.5	0.4	0.4
19.98	C24H38O4	PA	3.2	4.9	4.5
20.16	C18H38	AL	-	0.5	1.3
20.22	C7H6O4	PA	0.9	1.0	-
20.66	C20H34O2	BE	0.3	-	-
20.96	C8H13O2N	AD	0.2	1.5	0.7
21.28	C17H28	HC	0.3	-	0.2
21.42	C34H70	AL	-	-	1.3
21.59	C7H11O2N	AD	0.3	1.8	-
21.68	C11H18O3	HO	1.0	-	-
21.73	C11H13N	HN	0.2	1.0	0.6
21.89	C17H34O3	ES	0.2	-	-
22.22	C8H8O4	PH	0.2	1.0	0.6
22.29	C11H22	AL	0.1	-	-
22.62	C14H28O2	FA	0.1	-	0.2
22.7	C28H50O2	ES	2.3	-	0.2
22.89	C21H40O4	ES	-	0.2	0.2
23.22	C13H8O3	HO	0.2	10.6	6.8

23.44	C7H6O5	PA	3.7	-	-
23.52	C14H28O2	FA	-	1.8	1.2
23.6	C18H36	AL	0.2	-	0.8
23.87	C12H24	HC	1.1	-	-
23.97	C18H30	HC	-	-	0.1
24.00	C19H40	AL	0.4	-	-
24.23	C8H8O5	PA	0.2	-	0.5
24.58	C24H66O4	ES	0.6	0.2	0.3
24.96	C8H10O	PH	0.1	0.5	0.6
25.22	C16H32O2	FA	1.6	2.5	4.5
25.33	C20H40	AL	1.3	-	-
25.36	C21H42O2	FA	-	1.4	3.3
25.41	C15H30O2	FA	1.4	-	-
25.52	C26H54	AL	0.5	1.6	0.7
25.6	C8H10O4	PH	0.4	-	-
25.75	C11H16O3	PH	0.2	-	0.1
25.80	C9H8O5	PA	-	-	0.1
26.07	C15H30O2	FA	0.1	0.7	0.1
26.20	C19H40O	AC	-	-	0.2
26.23	C20H40O3	ES	0.2	-	-
26.42	C35H72O	AC	1.0	-	-
26.43	C14H20O2	BE	-	0.5	0.5
26.57	C18H36O	KE	0.3	0.3	-
27.17	C22H36O2	BE	0.2	0.7	-
27.61	C12H24	AL	0.4	-	-
27.7	C9H8O5	PA	-	-	0.3
27.75	C13H26O2	FA	0.2	0.4	-
27.87	C7H7O4N	AD	1.5	1.1	1.2
28.05	C31H66	AL	0.8	2.3	-

28.1	C16H32O2	FA	-	-	1.6
28.2	C14H13ON	AD	0.9	0.9	0.8
28.66	C16H32O2	FA	8.6	6.8	3.5
29.61	C47H94	AL	0.3	0.5	0.4
30.18	C28H56O2	FA	0.4	0.6	0.5
30.27	C24H50O	AC	-	0.6	0.4
30.30	C20H40	AL	0.7	-	-
30.34	C17H3402	FA	-	0.3	-
30.44	C32H56	AL	1.2	0.5	0.3
30.65	C17H32O2	FA	0.2	0.3	-
30.67	C9H10O3	PA	-	-	0.3
30.76	C16H20	HC	-	1.0	0.6
31.10	C17H34O2	FA	0.2	0.5	0.2
31.86	C17H34O	AC	0.6	-	0.3
32.6	C18H34O2	FA	0.2	1.1	0.6
32.75	C43H88	AL	1.0	-	-
32.88	C18H34O2	FA	0.3	0.8	0.7
33.37	C18H36O2	FA	3.3	3.5	1.1
33.81	C23H40O4	ES	-	-	0.2
34.08	C30H62	AL	0.3	-	-
34.34	C11H22	AL	0.1	-	0.1
34.63	18H36	HC	-	0.1	-
34.85	C15H32O	AC	1.0	0.3	-
34.97	C21H44	AL	0.8	0.4	-
35.23	C18H34O2	FA	1.2	0.2	0.2
37.10	C33H68	AL	1.0	0.2	0.2
37.54	C18H36	HC	-	0.2	0.2
37.68	C20H40O2	FA	0.2	0.2	0.1
38.94	C22H34O3	ST	-	-	2.0
39.05	C27H56O	AC	0.6	0.2	-

39.15	C35H72	AL	0.3	0.3	0.3
39.72	C25H50	HC	0.2	0.5	0.2
40.29	C10H21ON	AM	-	-	0.2
41.1	C17H36	AL	2.6	0.4	0.2
41.68	C22H34O3	ST	1.2	5.1	-
43.01	C20H42	AL	2.0	0.2	0.2
43.57	C23H46O2	FA	0.1	0.2	0.1
43.90	C40H82	AL	0.5	-	-
44.87	C54H110	AL	2.9	0.2	0.3
45.39	C24H48O2	FA	0.2	0.2	0.3
46.59	C25H52	AL	0.2	0.1	0.2
46.73	C30H50	AL	0.1	-	0.1
47.14	C25H50O2	FA	0.2	-	0.1
47.38	C41H84O	AC	-	-	0.1

CHAPTER 4

The impact of long-term field experiments under different cropping systems on the molecular dynamics and stability of the soil Humeome

(Published in Agriculture, Ecosystems and Environment Journal)

Agriculture, Ecosystems and Environment 331 (2022) 107928

Contents lists available at ScienceDirect

Agriculture, Ecosystems and Environment

journal homepage: www.elsevier.com/locate/agee

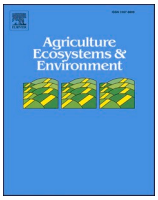

The impact of long-term field experiments under different cropping systems on the molecular dynamics and stability of the soil Humeome

Claudia Savarese [a,b], Li Xiong [b,c,d], Marios Drosos [c,*], Paola Vitaglione [a], Antonio Scopa [e], Alessandro Piccolo [a,b,**]

[a] Department of Agricultural Sciences, Università di Napoli Federico II, Via Università 100, 80055 Portici, Italy
[b] Interdepartmental Research Centre of Nuclear Magnetic Resonance for the Environment, Agri-Food and New Materials (CERMANU). University of Naples Federico II, Via Università 100, 80055 Portici, Italy
[c] Institute of Resource, Ecosystem and Environment of Agriculture (IREEA), Nanjing Agricultural University, 1 Weigang Road, 210095 Nanjing, China
[d] Institute of Soil and Fertilizer & Resources and Environment, Jiangxi Academy of Agricultural Sciences, 330200 Nanchang, China
[e] Scuola di Scienze Agrarie, Forestali, Alimentari ed Ambientali (SAFE), Università della Basilicata, Viale dell'Ateneo Lucano, 10, 85100 Potenza, Italy

ARTICLE INFO

Keywords:
Soil organic matter
Humic matter
Humeomics fractionation
GC-MS
Orbitrap-LC-MS
Long-term field experiments
Monoculture
Crop-rotation

ABSTRACT

Cultivation practices alter the molecular status of the soil Humeome, meant as the ensemble of all heterogeneous humic molecules, whose changes need to be understood and monitored in order to maintain the sustainability of agricultural soils. We applied the Humeomics sequential chemical fractionation, coupled to characterization of separated fractions by GC-MS and high-resolution Orbitrap LC-MS, on soils subjected for 20 consecutive years to the following treatments: i) non cultivated and untilled soil (Control); ii) maize monoculture (Maize); iii) maize-leguminous (*Vicia faba*) rotation (Mix). Humeomics fractions revealed a greater amount of organic carbon (OC) than for the traditional alkaline humus extraction (eSOM), double chromatographic visibility and one order of magnitude more detectable empirical formulae. Humeomics indicated that the ratio of organosoluble to hydrosoluble components decreased significantly passing from Control to Mix and Maize soils, thus unveiling that the loss of humic hydrophobic compounds, such as long-chain esters and fatty acids, rendered more physically and chemically fragile soils under long-term maize monoculture than under crop rotation. Saccharides undetectable in eSOM became instead visible after cleavage of esters weakly bound to the humic matrix, confirming a mechanism of protection of polar compounds by hydrophobic humic components. The same was observed for nitrogen-containing compounds, such as amides and heterocyclic nitrogen, which were significantly detected in Humeomics fractions of cropped soils only after the HI step disrupted ether linkages and organo-mineral complexes. Most of N-containing compounds in cropped soils were found to be bound to iron, thus implying that different forms of nitrogen entering soil by either synthetic fertilizer or nitrogen fixation are progressively sequestered into recalcitrant organic pools. Our findings highlight that a detailed knowledge on the molecular dynamics of the Humeome of soils under long-term field trials allowed a further understanding of the organic matter molecular distribution and the mechanisms of its stabilization.

1. Introduction

Soil organic matter (SOM) or Humus, that is stored mainly in the upper soil layers as the molecular end product of plant and animal decomposition, represents a key function in soil fertility and in the organic carbon (OC) global cycle (Lal, 2004), thus ensuring crop

Abbreviations: SOM, Soil organic matter; SOC, Soil organic carbon; OC, Organic carbon; CPR, Chemical protection ratio; eSOM, alkaline extractable soil organic matter.; CONTROL, Uncultivated, untilled soil; MAIZE, Maize mono-cultivated soil with conventional tillage; MIX, Maize-Broad bean crop-rotated soil with conventional tillage; ORG1, Organosoluble unbound fraction; ORG2, Organosoluble weakly ester bound fraction; AQU2, Hydrosoluble weakly ester bound fraction; ORG3, Organosoluble strongly ester bound fraction; AQU3, Hydrosoluble strongly ester bound fraction; AQU4, Hydrosoluble strongly ether bound fraction; RESOM, Residual alkaline-extractable organic matter; RESORG, Residual organo-soluble matter.

* Corresponding author.
** Corresponding author at: Department of Agricultural Sciences, Università di Napoli Federico II, Via Università 100, 80055 Portici, Italy.
E-mail addresses: drosos.marios@gmail.com (M. Drosos), alessandro.piccolo@unina.it (A. Piccolo).

https://doi.org/10.1016/j.agee.2022.107928
Received 20 November 2021; Received in revised form 9 February 2022; Accepted 21 February 2022
Available online 26 February 2022

productivity and SOC stability (Pan et al., 2009a; Zhou et al., 2009, 2010). The increased food needs for the rapidly growing population, will lead to an intensification of traditional agriculture and to an excessive SOM degradation, thus leading to a reduction of soil physical, chemical, and biological qualities, while enhancing organic matter oxidation and greenhouse gasses emission (Jobbagy and Jackson, 2000; Smith et al., 2014). Land use and management of agricultural systems is known to affect the storage of organic carbon in soil humus (Ogle et al., 2005; Kuzyakov and Zamanian, 2019). It has been shown that prolonged cultivation under conventional tillage decreases soil biodiversity (Dick, 1984; Kahle et al., 2010), depletes nutrients and enhances soil OC losses (Celik, 2005; Fontaine et al., 2007), whereas abandonment of cultivation determines OC stabilization and restoration of general soil qualities (Deng et al., 2018; Piccolo et al., 2018a). Mitigation of SOM losses and GHG emission may be achieved by practices that sequester carbon and favor accumulation of organic matter and nutrients in soils, such as crop rotation, organic manuring, no-till or reduced tillage (Smith et al., 2014; Wertebach et al., 2017).

There have been attempts to relate changes in soil use and management to variations of organic matter molecular composition (Puglisi et al., 2008; Zhou et al., 2010; Song et al., 2013; Mao et al., 2016; Kalinina et al., 2019; Zhang et al., 2019; Nuzzo et al., 2020; Mielnik et al., 2021). While it has been suggested the important role of SOM aliphatic components in restoring and stabilizing soil organic carbon under different land uses (Jandl et al., 2012; Savarese et al., 2021), the adopted analytical methods, based on either mass spectrometric or spectroscopic techniques, failed to usefully resolve the complex heterogeneity of humus when extracted from soil by the traditional alkaline solution (Olk et al., 2019).

Conversely, it has been shown that an advanced molecular understanding of the soil Humeome, which is the ensemble of organic molecules in soil humus, can be achieved by a chemical fractionation sequence, named Humeomics (Nebbioso and Piccolo, 2011, 2012; Nebbioso et al., 2014a, 2014b, 2015). This extraction technique was developed following the novel concept of soil humus that, rather than being constituted by macropolymers as traditionally believed (Piccolo, 2002), is now regarded as a supramolecular association of small heterogeneous molecules held together by weak linkages such as van der Waals, π-π, hydrogen, and metal bridged electrostatic bonds (Piccolo, 2002; Lehmann and Kleber, 2015; Wells, 2019; Piccolo et al., 2018b). Humeomics allows the progressive breaking of inter- and intra-molecular interactions within the humic matrix to progressively isolate more homogeneous fractions, in which single humic molecules may be structurally identified by advanced analytical methods (Nebbioso and Piccolo, 2011). Recently, the Humeomics fractionation was applied directly on peats to distinguish their geographical origin (Vinci et al., 2020), on different grassland soils to characterize their Humeome (Drosos et al., 2018a; Vinci et al., 2021), and on tilled soils to reveal changes in organic matter molecular composition even under different short-term cultivation (Drosos et al., 2017, 2018b, 2020).

Herein, we applied the Humeomics technique on cultivated soils from three long-term field-experiments, which were subjected for 20 consecutive years to the following crop systems: i) non-cultivated (Control); ii) maize monoculture (Maize); and iii) maize-leguminous rotation (Mix). Hence, the aim of this work was to utilize Humeomics to characterize in detail the molecular composition of the Humeome of soils that have been subjected to different long-term cropping systems and thus understand the molecular mechanism of SOC stability under either crop monoculture or rotation.

2. Materials and Methods

2.1. Soil samples

Samples of soil, classified as a Vertic Xerofluvent according to USDA soil taxonomy (USDA United States Department of Agriculture - Soil Survey Staff, 1999), were collected at the experimental farm of the University of Napoli Federico II at Castel Volturno (CE), from a long-term field experiment (20 years) managed with conventional tillage and under three different cropping systems: i) untilled soil without cultivation (2.62% OC); ii) Maize (*Zea mais* L.) monoculture (1.00% OC); iii) Maize-Broad bean (*Vicia faba* L.) rotation (1.17% OC). The soil had a silty-clay loam texture (18.3% sand, 31.3% silt, and 50.4% clay), and a pH of 8.3. Each long-term experiment was conducted on a 50 m × 50 m plot, by a randomized blocks design. Composite soil samples, comprising ten sub-samples within a radius of 10 m, were randomly collected from the ploughed horizon (20 cm) of each plot, air dried, sieved under 2 mm, and placed in a glass bottle (100 mL transparent duran glass, with PP screw cups from Carl Roth) for subsequent analysis.

2.2. Extractable SOM in alkaline solution (eSOM)

The eSOM fraction was extracted in triplicates from 100 g of soil using 0.9 L of an alkaline solution (0.5 M NaOH and 0.1 M $Na_4P_2O_7$), as by the methods recommended by the International Humic Substances Society (IHSS) (Hayes, 1985; Stevenson, 1994; Zaccone et al., 2007; Drosos et al., 2009). After overnight shaking, the supernatant was separated by centrifugation (15 min at 7000 rpm / 7080 x g), and filtration through a Whatman 41 filter. The pH of the supernatant was adjusted to 7 with a 37% HCl solution. eSOM was then dialyzed against distilled water until Cl-free using Amicon C membrane (1000 Da cutoff) and freeze-dried.

2.3. Humeomics sequential fractionation

Triplicates of 100 g of each soil sample were placed in 300 mL of 0.1 M HCl and shaken overnight. The samples were centrifuged (15 min, 7000 rpm / 7080 x g), water-washed until neutrality and freeze-dried. The Humeomics fractionation was applied as previously described (Drosos et al., 2018) to obtain eight fractions.

2.3.1. Unbound fraction (ORG1)

100 g of washed soil (Res0) was suspended in 300 mL of a 2:1 v/v dichloromethane (DCM) and methanol (MeOH) solution and stirred for 24 h at room temperature. The supernatant (ORG1) was separated by centrifugation (15 min, 7500 rpm / 8128 x g) and filtration (with two Whatman 41 filters). The residue left on the filters was merged with the residual soil and was air-dried.

2.3.2. Weakly bound ester fractions (ORG2-AQU2)

The residue from the previous step (Res1) was placed in a Teflon tube added with 12% BF_3-MeOH (1 g of soil/1 mL of solution) and kept overnight in stove at 85 °C. This reaction was repeated twice. The supernatants were centrifuged (15 min, 7500 rpm / 8128 x g) and combined. The resulting solution was added with water to quench the residual BF_3, rotoevaporated to remove MeOH, and extracted three times with a total of 150 mL chloroform. The organic phase was separated (ORG2), dried with anhydrous Na_2SO_4, filtered on a Whatman 41 filter, and rotoevaporated. The aqueous phase (AQU2) was rotoevaporated to remove residual MeOH and chloroform traces, dialyzed against distilled water using Amicon C membranes (1000 Da cutoff) until Cl-free, and freeze-dried. The soil residue was air-dried before the next step.

2.3.3. Strongly bound ester fractions (ORG3-AQU3)

The residue from the previous step (Res2) was suspended (1 g/mL) in 1 M KOH-MeOH solution, refluxed for 2 h at 70 °C under N_2 atmosphere. After cooling, the supernatant was recovered by centrifugation (10 min, 7000 rpm / 7080 x g). The residue was washed with 50 mL of MeOH and centrifuged. The supernatants were combined and then liquid-liquid extracted three times with a total of 150 mL (50:50, v/v) of DCM/water mixture. The organosoluble (ORG3) and hydrosoluble (AQU3)

extracts were purified as for ORG2 and AQU2. The solid residue soil was air-dried before the next step.

2.3.4. Strongly bound ether fractions (AQU4)

A suspension of 1 mL of 47% HI aqueous solution per g of soil residue from the previous step (Res3) was stirred for 48 h at 75 °C under N_2 atmosphere. After cooling, 100 mL of distilled water were added, stirred, and filtered. The solution was neutralized by saturated $NaHCO_3$ solution, freeze-dried, and dialyzed (1000 Da cut-off Amicon C membranes) first against saturated $Na_2S_2O_3$ solution to neutralize I_2, and then against distilled water to remove residual $Na_2S_2O_3$. The resulting suspension (AQU4) was freeze-dried. The residual soil was washed extensively with water and air-dried.

2.3.5. Residual alkaline Organic Matter (RESOM)

The residue from the previous step (Res4) was extracted by shaking overnight with an alkaline solution, as for eSOM, to remove humic molecules remained still bound to the soil inorganic matrix. The supernatant was then treated as in the case of eSOM. The residual soil was extensively water-washed and air-dried.

2.3.6. Residual Organosoluble fraction (RESORG)

The final residue from the previous step (Res5) was suspended in a 2:1 v/v solution of dichloromethane (DCM) and methanol (MeOH), as for ORG1, to further extract a residual organosoluble fraction (RESORG).

2.4. Elemental Analysis

Elemental Composition (C, H, N) was determined by a Fisons Instruments EA 1108 Elemental Analyzer (Eager 200 Ver. 3.09 calculation software) using 20–25 mg of the original soils and of the solid residues left after extraction of both eSOM and Humeomics, as well as weighing 1–2 mg of eSOM extracts and Humeomics separated fractions.

2.5. GC–MS spectrometry

Organosoluble fractions (ORG1 to RESORG) were derivatized before GC–MS analysis using acetyl chloride/methanol as methylating agent, followed by silylation with N,N-bis [trimethylsilyl] trifluoracetamide/1% trimethylchlorosilane. A Perkin-Elmer Autosystem XL equipped with an RTX-5MS WCOT capillary column (Restek, 30 m × 0.25 mm i.d.; film thickness = 0.25 μm), a heated transfer line (250 °C), coupled with a PE Turbomass-Gold quadruple mass spectrometer, was used for the GC-MS analysis as reported earlier (Nebbioso and Piccolo, 2011). Nonadecanoic acid was used as internal standard, and an external calibration curve was built of known standards such as derivatized tridecanoic, ω-hydroxyhexadecanoic, docosandioic acids, and sitosterol. Methylated and silylated compounds were converted into their nominal masses by adding the H^+ mass and by removing the methylated and silylated groups when needed. The signals selected for identification were those exceeding the cut-off limit of 0.05% of the highest peak area. Chemical structures were finally identified using the NIST library.

2.6. High resolution ESI-Orbitrap-MS

The eSOM, hydrosoluble fractions (AQU2, AQU3 and AQU4) and RESOM were analyzed by high resolution ESI-*Orbitrap*-Mass Spectroscopy as described earlier (Drosos et al., 2018). Briefly, few milligrams of each fraction were spiked with 20 μg each of the two internal standards 16-d3-hexadecanoic acid and ring^{13}C labeled hydroxybenzoic acid, and then dissolved using diluted ammonia (0.05 M) LC-MS grade (Fluka) to reach a final volume of 1 mL. Two 40 μL replicates of each sample were injected by an Agilent 1200 G1367 autosampler. Mass spectra were obtained with an LTQ Orbitrap (Thermo Electron, Waltham, MA) equipped with a HESI-II source, using negative mode for AQUs, eSOM and RESOM samples, 140–2000 *m/z* mass scan range, and 1.0 s scan time. N_2 was the sheath gas (50 AU) and He was the collision gas (5 AU). Ion spray, capillary and tube lens voltages were set to 4000, 200 and 75 V, respectively. The ion source vaporizer was set to 350 and capillary temperatures to 275 °C, respectively. High Performance Size Exclusion Chromatography (HPSEC) was used to reduce sample complexity before entering mass spectrometry (Nebbioso and Piccolo, 2011). The HPSEC system comprised an Agilent 1200 G1312 Binary Pump set to output 0.5 mL min^{-1} of a 55/45 A/B solution (A: 5 mM $AcONH_4$ in Milli-Q water and 5% MeCN, pH 7; B: 100% MeCN) for a total of 70 min in a Phenomenex Bio-Sep SEC-S 2000 column (300 × 7.8 mm) and precolumn (30 × 7.8 mm), both thermostatted at 30 °C by an Agilent 1200 G1316 unit. UV chromatograms were recorded by an Agilent 1200 G1315 DAD spectrophotometer set at 254 nm wavelength. The averaged *m/z* values measured by Orbitrap MS were extracted from the Xcalibur software, corrected on the basis of the internal standards, and converted to nominal masses by adding the mass of H^+ and removing the masses of Fe when necessary. Possible chemical structures corresponding to empirical formulae of detected masses were found by the ChemSpider database (http://www.chemspider.com).

2.7. Total organic matter calculation

As earlier described (Drosos et al., 2017), a specific empirical formula $C_xH_yO_zN_aFe_b$ obtained from MS spectra, was turned into its Formula Molecular Weight (FMW) by multiplying the number of corresponding atoms in each compound (FMW=12x+1 y + 16z+14a+56b). Hence, the percent of total carbon (C_{tot}) for all the identified compounds in each fraction was obtained by the following equation:

$$C_{tot} = \sum_{i=1}^{n} = \frac{12x_i \times (abundance_i \%)}{100}$$

where ($12x_i$) and ($abundance_i$ %) were the total atomic weight and the relative percentage of each i^{th} molecule over all visible compounds in the mass spectrogram for every fraction, respectively (Table S1, S2 and S3 in Supporting Information section).

Similarly, the total OM (OM_{tot}) for all the identified compounds in each fraction, and then, the percent of OM identified in each Humeomic fraction (% OM) was calculated by taking into account the FMW of each fraction (FMW_i) and the percent carbon found in that fraction by elemental analysis (C_i), respectively:

$$OM_{tot} = \sum_{i=1}^{n} = \frac{FMW_i \times (abundance_i \%)}{100}$$

$$\%OM = \frac{OMtot \times C_i}{Ctot}$$

The actual OM weight (mg) in each fraction (m_{OMi}) was then obtained:

$$m_{OMi} = \frac{(\%OM) \times m_i}{100}$$

Thereafter, the OM chromatographic visibility of each fraction ($m_{OMi,vis}$) for both ESI-Orbitrap and GC measurements was calculated by multiplying m_{OMi} with the percent visibility reported in Table 2:

$$m_{OMi,vis} = m_{OMi} \times \%\ visibility$$

Finally, the total chromatographic OM as well as the total visible chromatographic OM was respectively calculated:

$$\sum_{i=1}^{n} m_{OMi} = m_{OM1} + m_{OM2} + \ldots + m_{OMn}$$

$$\sum_{i=1}^{n} m_{OMi,vis} = m_{OM1}, vis + m_{OM2}, vis + \ldots + m_{OMn}, vis$$

Table 1
Elemental composition (C, H, N) and C/N ratios of eSOM extracts and Humeomics fractions of the three soil samples from long-term field plots: Uncultivated soil (Control), soil under Maize monoculture (Maize), soil under Maize-Broad bean crop rotation (Mix). Humeomics and eSOM extractions were conducted in triplicates, and reported values are averages.

SAMPLE	C%	H%	N%	C/N	Mass (mg)	C (mg)	H (mg)	N (mg)
CONTROL SOIL								
Bulk soil	**2.62±0.06**	**n.d.**	**0.28±0.01**	**9.4±0.1**	**100000.0**	**2623.0±3.5**	**n.d.**	**280.0±1.5**
eSOM	**22.3±0.05**	**4.01±0.02**	**2.34±0.03**	**9.5±0.3**	**1013.60±15**	**225.60±2.5**	**40.6±0.1**	**23.70±1.0**
Res[a] after eSOM	1.49±0.1	n.d.	0.08±0.01	18.7±0.5	84059.20±10	1254.30±2.0	n.d.	67.20±2.0
Loss[b] of Material	7.66±0.1	n.d.	1.27±0.01	6.0±0.1	14927.20±10	1143.10±2.0	n.d.	189.10±2.0
ORG1	27.87±2.3	7.81±0.9	0.11±0.1	248.3±135	133.60±20.9	37.24±2.2	10.43±0.2	0.15±0.2
AQU2	34.55±3.5	5.08±0.9	3.42±0.1	10.1±0.8	39.80±18.9	13.75±8.6	2.02±1.5	1.36±0.7
ORG2	27.69±1.6	4.93±0.4	0.66±0.1	42.2±3.3	1422.60±176	393.89±73.8	70.07±15.6	9.33±2.7
AQU3	35.24±11.7	6.67±2.2	3.57±1.2	9.9±0.1	4.20±2.1	1.48±1.48	0.28±0.28	0.15±0.15
ORG3	41.21±8.4	4.62±0.5	0.83±0.3	49.7±10	39.80±22.3	16.40±4.0	1.84±0.7	0.33±0,01
AQU4	0.81±0.1	1.72±0.04	0.19±0.02	4.2±0.9	17661.00±4711	142.69±11.8	303.49±73	34.09±12.6
RESOM	11.42±0.5	1.10±0.02	1.03±0.03	11.1±0.2	481.20±92.2	54.93±13.3	5.27±1.1	4.96±1.1
RESORG	26.94±7.4	4.81±0.7	1.62±0.2	16.6±2.6	21.60±10.7	5.82±0.5	1.04±0.3	0.35±0.1
Total ORGs[c]	28.03±1.6	5.15±0.4	0.63±0.1	44.6±4.0	1617.60±185	453.34±80.5	83.38±16.3	10.16±3.0
Total AQUs[d]	1.17±0.2	1.71±0.03	0.22±0.01	5.3±1.0	18186.20±4643	212.85±14.4	311.05±73	40.56±12.8
Total[e] Humeomics	**3.36±0.3**	**1.99±0.2**	**0.26±0.01**	**13.1±1.6**	**19803.80±4828**	**666.19±95**	**394.43±57**	**50.72±15.7**
Res[f] after Humeomics	1.17± 0.04	n.d.	0.10±0.01	15.5±0.7	43714.00±6123	512.75±90	n.d.	33.0±7.7
Loss[g] of material	3.96±0.9	n.d.	0.54±0.1	7.4±0.3	36482.20±10952	1444.05±4.7	n.d.	196.28±8.0
MAIZE SOIL								
Bulk Soil	**1.00±0.03**	**n.d.**	**0.11±0.01**	**9.1±0.1**	**100.000.0**	**1000.00±1.5**	**n.d.**	**110.00±1.1**
eSOM	**12.6±0.03**	**3.21±0.03**	**1.44±0.03**	**8.8±0.3**	**696.00±10**	**87.70±1.5**	**22.4±0.1**	**10.00±0.5**
Res[a] after eSOM	0.97±0.05	n.d.	0.002±0.001	371.3±1.0	91825.60±15	891.002.0	n.d.	2.40±0.01
Loss[b] of Material	0.28±0.05	n.d.	1.17±0.01	0.2±0.06	7478.40±15	21.30±2.0	n.d.	87.60±1.0
ORG1	4.46± 0.6	5.48± 0.8	0.10±0.05	45.1±20	161.60±75.2	7.21± 1.9	8.86± 5.9	0.16±0.05
AQU2	21.17± 1.5	4.20± 0.04	2.01±0.3	10.5±0.8	54.80±19.8	11.60± 3.1	2.30± 0.8	1.10±0.2
ORG2	12.07± 1.5	3.31±0.2	0.32±0.1	38.0±1.5	484.40±146	58.49± 8.0	16.03± 3.4	1.54±0.1
AQU3	39.39± 0.7	6.84± 0.2	4.08±0.03	9.7±0.1	9.80±4.8	3.86± 2.0	0.67± 0.3	0.40±0.2
ORG3	31.25± 5.2	3.52±1.5	1.14±0.5	27.5±5.2	8.80±3.4	2.75± 1.7	0.31± 0.3	0.10±0.1
AQU4	0.94± 0.07	1.38±0.2	0.10±0.01	9.1±1.0	12010.8±1842	196.96± 1.8	289.94± 73	21.67±3.0
RESOM	4.41±1.2	3.48±0.2	0.78±0.1	5.6±2.0	2447.60±967	107.90± 1.3	85.08± 42	19.21±11
RESORG	31.40±1.4	6.10±1.3	0.61± 0.1	51.5±9.0	16.40±3.9	5.15± 1.5	1.00± 0.5	0.10±0.01
Total ORGs[c]	10.97±2.0	3.90±0.7	0.27±0.04	41.1±1.1	671.20±221	73.60± 6.0	26.19±2.3	1.79±0.2
Total AQUs[d]	2.21±0.1	2.60±0.05	0.29±0.04	7.6±1.2	14523.00±891	320.33± 0.6	377.99±31	42.38±8.0
Total[e] Humeomics	**2.59±0.07**	**2.66±0.07**	**0.29±0.04**	**8.9**±1.3	**15194.20±670**	**393.93±6.6**	**404.18±29**	**44.8±8.2**
Res[f] after Humeomics	0.41±0.02	n.d.	0.05±0.01	9.0±0.8	58620.00±4718	237.91±31.5	n.d.	26.55±6.3
Loss[g] of material	1.41±0.1	n.d.	0.15±0.01	9.4±0.1	26185.80±4048	368.16±24.9	n.d.	39.28±2.0
MIX SOIL								
Bulk Soil	**1.12±0.03**	**n.d.**	**0.14±0.01**	**7.9**±0.1	**100.000.0**	**1117.00±1.5**	**n.d.**	**140.00±1.1**
eSOM	**11.3±0.05**	**2.99±0.0**	**1.47±0.05**	**7.7**±0.2	**815.20±15**	**92.10±2.0**	**24.4±0.1**	**12.00±0.5**
Res[a] after eSOM	1.02±0.01	n.d.	0.002±0.001	501.5±1.0	97852.00±15	1002.90±1.0	n.d.	2.00±0.01
Loss[b] of Material	1.65±0.1	n.d.	11.72±1.0	0.2±0.02	1332.80±15	22.00±1.0	n.d.	126.00±.0
ORG1	8.42±0.2	8.40±3.2	0.10±0.01	87.7±7.5	104.20±2.6	8.77±0.05	8.75±3.6	0.10±0.01
AQU2	28.00±2.9	4.61±0.7	5.28±0.4	5.3±0.9	18.00±5.7	5.04±0.9	0.83±0.1	0.95±0.4
ORG2	16.07±0.4	2.56±0.3	0.57±0.1	28.0±3.7	552.20±96	88.75±18	14.16±4.2	3.17±0.2
AQU3	31.88±2.5	5.63± 1.5	2.08±0.2	15.3±3.2	4.80±1.1	1.53±0.5	0.27±0.15	0.10±0.01
ORG3	35.67±1.2	3.06±0.4	1.42±0.2	25.2±4.4	13.40±9.9	4.78± 3.8	0.41±0.4	0.19±0.1
AQU4	1.00±0.3	1.25±0.1	0.09±0.01	10.7±2.6	12837.60±127	128.62±38	160.08±12	12.01±0.8
RESOM	2.86±0.2	2.86±0.5	0.32± 0.1	8.8±1.4	564.00±187	16.12±7.1	16.11±1.9	1.83±1.3
RESORG	36.50±7.8	4.30±2.4	2.60± 0.3	14.0±1.1	10.00±2.3	3.65±1.8	0.43±0.4	0.26± 0.1
Total ORGs[c]	15.59±0.1	3.50±0.5	0.53± 0.01	29.3±0.1	679.80±81	105.95±12	23.76±7.0	3.62± 0.4
Total AQUs[d]	1.13±0.3	1.32± 0.1	0.11± 0.02	10.3±1.2	13424.40±55	151.31±45	117.29±14	14.74± 2.4
Total[e] Humeomics	**1.82±0.4**	**1.43±0.04**	**0.13±0.01**	**14.0±1.4**	**14104.20±26**	**257.26±58**	**201.05±6.5**	**18.41±2.0**
Res[f] after Humeomics	0.53±0.05	n.d.	0.10±0.01	8.1±0.2	62068.60±243	325.92±32	n.d.	40.35±4.5
Loss[g] of material	2.24±0.1	n.d.	0.34±0.01	6.6±0.1	23827.20±218	533.82±25	n.d.	81.24±2.5

[a] Res corresponds to residual material after eSOM extraction.
[b] Loss of material after eSOM extraction based on original soil excluding eSOM CHN yields.
[c] Total ORGs refers to the overall of ORG1. ORG2. ORG3 and RESORG.
[d] Total AQUs refers to the overall of AQUE. AQU3. AQU4 and RESOM.
[e] Total Humeomics refers to the addition of all ORGs and AQUs fractions.
[f] Res correspond to residual material after Humeomics sequential fractionation.
[g] Loss of material after Humeomics extraction based on original soil excluding Total Humeomics CHN yields.

3. Results and discussion

3.1. Soil organic carbon dynamics

The traditional alkaline extraction recommended by the International Humic Substances Society (IHSS) was applied to extract the humic matter (eSOM) from the three soil samples of long-term field experiments. The elemental composition of the eSOM extracts (Table 1) showed that the OC content decreased passing from Control (225.60 mg) to Maize (87.70 mg), and was slightly increased in the humic fraction extracted from the Mix soil (92.10 mg). As previously indicated (Savarese et al., 2021), these results suggest that the long-term field experiment under continuous maize leads, as compared to control, to a significant SOC depletion, that is diminished by the crop-rotation system.

Table 2
Percent visibility of organic matter in eSOM extracts and Humeomics fractions as evaluated by reference to internal standards in GC-MS and ESI-Orbitrap-MS.

Sample	Total chromatographic OM (OM_{tot})[a] (mg)	Visible chromatographic OM (OM_{vis})[b] (mg)	Visibility (%)
CONTROL SOIL[c]			
eSOM	**419.40**	**66.86**	**15.9**
ORG1	50.41	17.31	34.3
AQU2	26.88	4.47	16.6
ORG2	584.33	76.60	13.1
ORG3	23.11	1.71	7.4
AQU4	279.17	167.74	60.1
RESOM	80.59	39.93	49.5
RESORG	8.04	1.13	14.0
Total Humeomics	**1052.53**	**308.89**	**29.4**
MAIZE SOIL[d]			
eSOM	**157.42**	**15.24**	**9.7**
ORG1	10.32	1.78	17.3
AQU2	21.75	3.83	17.6
ORG2	87.71	10.21	11.6
ORG3	5.38	0.59	11.0
AQU4	242.89	31.49	13.0
RESOM	219.50	27.84	12.7
RESORG	7.43	0.80	10.7
Total Humeomics	**594.98**	**76.54**	**12.9**
MIX SOIL[e]			
eSOM	**167.32**	**15.27**	**9.1**
ORG1	12.52	3.36	26.8
AQU2	10.06	2.24	22.3
ORG2	133.78	10.28	7.7
ORG3	6.81	3.83	56.3
AQU4	279.28	47.58	17.0
RESOM	30.40	4.73	15.6
RESORG	5.14	1.56	30.5
Total Humeomics	**477.99**	**73.58**	**15.4**

[a] OM_{tot} calculation is explained in section 2.8.
[b] OM_{vis} calculation is based on internal standard.
[c] Uncultivated soil.
[d] Soil under Maize mono-cultivation.
[e] Soil under Maize-Broad bean crop rotation.

The application of Humeomics on the same samples allowed the separation of eight fractions (ORG1–3, AQU2–4, RESOM and RESORG), whose elemental composition is reported in Table 1. The sum of the separated humic fractions yielded an OC content of 666.19 mg for the uncultivated soil (Control), 393.93 mg for the soil under Maize mono-culture, and 257.26 mg for the Mix soil. The OC increase in the sum of fractions for all soils, as compared to eSOM extracts (Table 1), confirms once again the already observed capacity of Humeomics to extract significantly more SOC than by the traditional IHSS alkaline method (Nebbioso and Piccolo, 2011; Drosos et al., 2017).

Moreover, the progressive decrease in OC of total Humeomics when passing from Control to Maize and Mix samples suggests that the long-term cropped soils were subjected to an alteration of SOM physical and chemical protection (Fu et al., 2000; Celik, 2005; Fontaine et al., 2007), with a consequent release of hydrosoluble small-size polar molecules (Piccolo et al., 2004, 2005) mostly lost during dialysis (Drosos and Piccolo, 2018). Concomitantly, the residual OC still retained in soil after Humeomics fractionation was 512.75, 325.92 and 237.91 mg for Control, Maize, and Mix samples, respectively, which corresponded, in respect to the uncultivated control, to a significant OC decrease after 20 years-long cultivation of 53.6% for Maize and 36.4% for Mix, (Table 1).

The information obtained on the OC content in the Humeomic fractions of the three different long-term cropping experiments can be used to draw an index related to C stabilization in soil. In fact, since lipidic compounds are assumed to protect hydrophilic components from mineralization and microbial degradation (Spaccini et al., 2002; Piccolo et al., 2004), the larger the organosoluble/hydrosoluble carbon ratio of the soil Humeome, the greater is the chemical protection of organic matter in soil. Hence, SOM stability can be described by the Chemical Protection Ratio (CPR) as the ratio of OC solubilized in ORG and RESORG fractions over the OC extracted in AQU and RESOM fractions (Piccolo et al., 2018b). The CPR of the Humeome for the three long-term experiments of this study revealed a decrease of the organosoluble to hydrosoluble OC ratio passing from Control (2.13) to the Mix (0.70), and to the Maize (0.23) soils, thereby indicating that the Maize monoculture determined a significant availability of hydrophilic components, as released in the AQU and RESOM fractions, as compared to the other two soil treatments (Table 1). These results are in line with earlier studies (Savarese et al., 2021), which suggested a reduction of the chemical hydrophobic protection of SOM after two decades of continuous maize cultivation, and a concomitant easier release of labile/hydrophilic humic molecules. Moreover, our findings agree with a previous report that indicated a loss of hydrophobic molecules from the Humeome of a soil under Maize even after only three years of cultivation (Drosos and Piccolo, 2018). An additional indication of our study is that the Maize-Faba bean rotation experiment mitigated the depletion from soil Humeome of the hydrophobic molecules, which are mainly responsible for SOM protection (Spaccini et al., 2002; Piccolo et al., 2018b), thus giving molecular bases to the well-known gains of soil quality provided by crop rotation versus monoculture.

3.2. *Molecular differences of compounds classes in the extractable SOM (eSOM)*

The ESI-Orbitrap-MS spectrograms revealed 42, 39 and 44 molecules in the eSOM extracts for the Control, Maize and Mix soil samples, respectively (Table S1, S2 and S3 in Supporting Information). In all humeomic fractions of the three soil samples, the most abundant compounds belonged to the amines (AM) class, followed by heterocyclic nitrogen compounds (HN), fatty acids (FA) and phenols (PH) (Fig. 1 A; Fig. S1 in SI). Similar percentages of amides (AD) in all eSOM extracts, regardless of the cropping system (Tables 3, 4 and 5), suggest a degree of

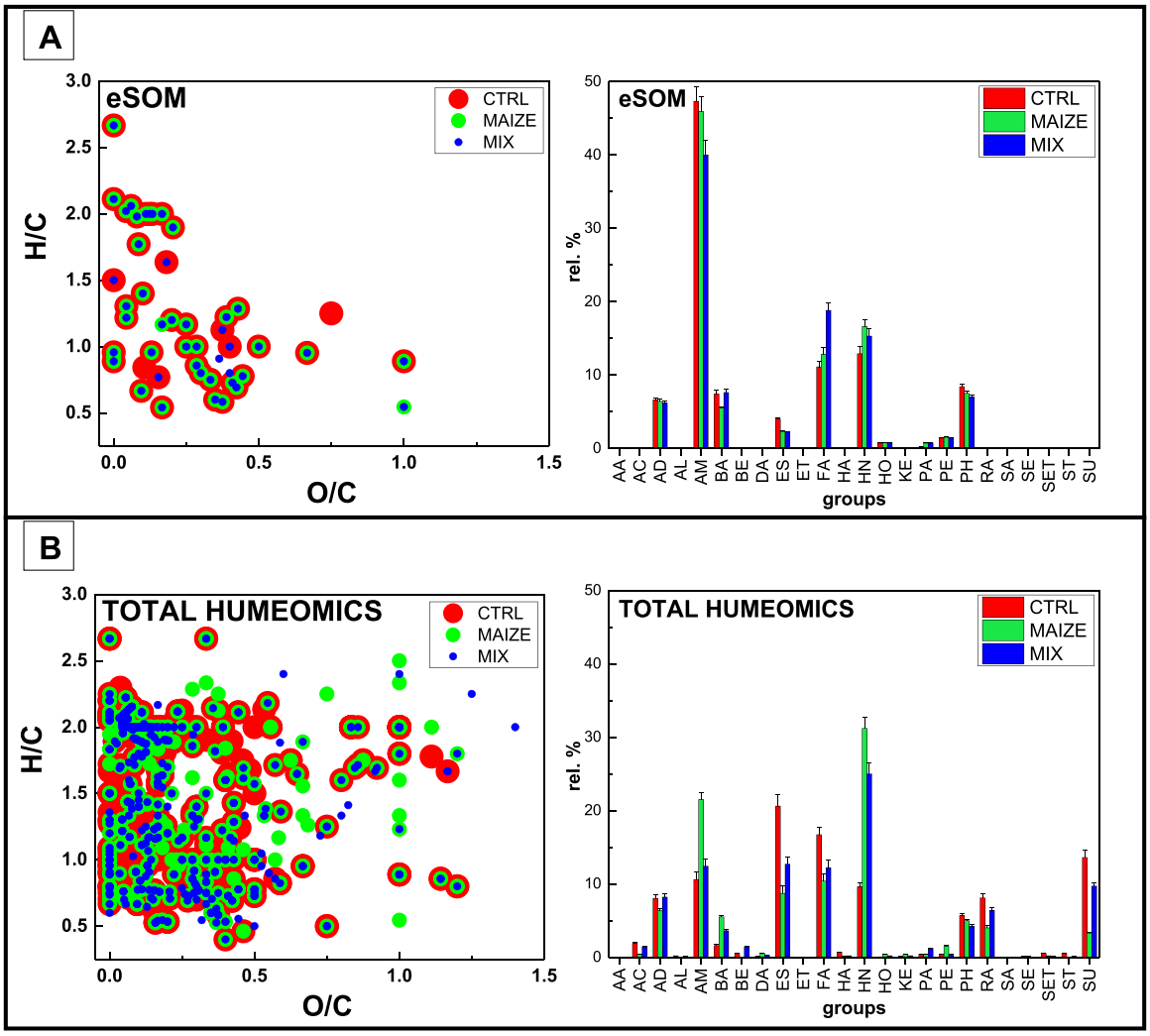

Fig. 1. Van Krevelen Plots of various molecular components identified in eSOM (**A**) extracts and Humeomics fractions (sum of all fractions) (**B**) of soil samples and their relative (%) abundance. Molecules identified in the uncultivated Control soil (CTRL) are noted in red, whereas molecules found in Maize monoculture soil (MAIZE) are marked in green, and molecules detected in soil under Maize-Broad bean crop rotation (MIX) are shown in blue. AA: Aminoacids; AC: Alcohols; AD: Amides; AL: Alkanes/alkenes/alkynes; AM: Amines; BA: Benzoic Acids; BE: Benzoic Esters; DA: Dicarboxylic Acids; ES: Esters; ET: Ethers; FA: Fatty Acids; HA: Hydroxy Acids; HN: Heterocyclic Nitrogen compounds; HO: Heterocyclic Oxygen compounds; KE: Ketones; PA: Phenolic Acids; PE: Phenolic Esters; PH: Phenols; RA: Resin Acids; SA: Sugar Acids; SE: Sterols; SET: Sugar Ethers/Esters; ST: Steroids; SU: Sugars.

recalcitrance of such compounds to cultivation and tillage alteration (Drosos and Piccolo, 2018). On the other hand, the relative increase in percentage of HN when passing from the uncultivated (Control) to both long-term Maize and Mix cropped soils (Fig. 1 A), agrees with the previously reported enrichment of N-containing compounds after several years of soil cultivation (Schnitzer et al., 2006). Moreover, Maize and Mix humeomic fractions showed a high relative abundance of C_{12}-C_{18} saturated fatty acids (Table S2 and S3), which may derive from either soil microorganisms or plant residues (Jandl et al., 2005; Spaccini et al., 2013). In particular, the largest FA percentage observed in the Mix soil (Fig. 1 A) confirms earlier findings, in which the identification of hydrophobic alkyl components was interpreted as an index of a more stable SOM under the long-term crop rotation than for Maize monoculture (Savarese et al., 2021).

3.3. Molecular dynamics of Humeomics fractions

The organosoluble fractions (ORG1, ORG2, ORG3 and RESORG) separated by Humeomics were characterized by GC-MS, while high-resolution ESI-Orbitrap-MS was employed for characterizing the hydrosoluble fractions (AQU3, AQU4 and RESOM), with the exception of AQU3 whose yield was insufficient for the analysis (Table 1). The structural assignments for the sum of Humeomics fractions accounted for 601, 521 and 506 different molecules in soils of Control, Maize and Mix, respectively, that is an order of magnitude larger than the number of molecules identified in the traditional eSOM separates (Table S1, S2 and S3). Moreover, the OM chromatographic visibility increased five-fold passing from eSOM extracts to total Humeomics (Table 2), while in the latter 24 diverse compounds classes were identified, as compared to only 11 classes observed in the eSOM separates (Fig. 1; Fig. S1; Tables 3, 4 and 5).

Such an advanced insight in the molecular dynamics of the soil Humeome under different cropping systems, indicated that in the uncultivated soil (Control) there was an abundance of long-chain esters (ES) and fatty acids (FA), followed by sugar derivatives (SU), resin acids (RA) and N-containing compounds (HN, AM, AD) (Fig. 1B; Fig. S1). These compounds were depleted in the soils cultivated with both continuous maize and maize-bean rotation, except for the N-containing compounds, such as amines (AM) and heterocyclic nitrogen compounds (HN), which were among the most representative compounds classes in these long-term cropped experiments (Fig. 1B; Fig. S1). Hence, the accurate molecular assessment provided by Humeomics confirms previous

Table 3
mg OC and (%) of compounds classes in eSOM and Humeomic fractions of the no-tilled soil (Control), as determined by GC-MS and Orbitrap-MS.

Group	eSOM	ORG1	AQU2	ORG2	ORG3	AQU4	RESOM	RESORG	Total ORGs[a]	Total AQUs[b]	Total Humeomics[c]
CONTROL SOIL											
Aminoacids (AA)	–	–	–	–	–	–	0.01(0.0)	–	–	**0.01(0.0)**	**0.01(0.01)**
Alcohols (AC)	–	1.38 (3.7)	–	9.25(2.4)	1.69 (10.3)	–	–	0.40(6.9)	**12.72 (2.8)**	–	**12.72(1.9)**
Amides (AD)	**14.93 (6.6)**	1.27 (3.4)	1.32 (9.6)	36.44 (9.3)	2.62 (16.0)	10.70 (7.5)	0.49(0.9)	0.32(5.5)	**40.65 (9.0)**	**12.51 (5.9)**	**53.16(8.0)**
Alkanes/alkenes/ alkynes (AL)	–	0.87 (2.4)	–	–	–	–	–	0.22(3.8)	**1.09(0.2)**	–	**1.09(0.2)**
Amines (AM)	**106.46 (47.3)**	0.05 (0.1)	3.67 (26.7)	–	–	23.19 (16.3)	43.51 (79.2)	–	**0.05 (0.03)**	**70.37 (33.3)**	**70.42(10.6)**
Benzoic acids (BA)	**16.78 (7.4)**	–	0.60 (4.4)	–	–	9.36 (6.7)	0.64(1.2)	–	–	**10.60 (5.0)**	**10.60(1.6)**
Benzoic esters (BE)	–	–	0.08 (0.6)	–	–	3.19 (2.2)	–	–	–	**3.27(1.6)**	**3.27(0.5)**
Dicarboxylic acids (DA)	–	0.06 (0.2)	0.11 (0.8)	–	–	0.62 (0.4)	Traces	0.03(0.5)	**0.09 (0.04)**	**0.73(0.4)**	**0.82(0.1)**
Esters (ES)	**9.02(4.0)**	11.06 (29.6)	0.20 (1.5)	117.24 (29.8)	4.38 (26.7)	2.54 (1.8)	0.12(0.2)	1.60 (27.5)	**134.28 (29.6)**	**2.86(1.4)**	**137.14(20.6)**
Ethers (ET)	**Traces**	0.06 (0.2)	Traces	–	–	Traces	Traces	–	**0.06 (0.03)**	**Traces**	**0.06(0.02)**
Fatty acids total[d] (FA)	**24.98 (11.1)**	10.26 (27.6)	2.40 (17.5)	81.74 (20.7)	2.54 (15.5)	9.58 (6.7)	2.89(5.3)	1.49 (25.6)	**96.03 (21.2)**	**14.87 (7.0)**	**110.90(16.7)**
Saturated Fatty acids	**24.98 (11.1)**	8.94 (24.0)	1.87 (13.6)	75.83 (19.2)	2.33 (14.2)	8.14 (5.7)	2.52(4.6)	1.38 (23.7)	**88.48 (19.5)**	**12.53 (5.9)**	**101.01(15.2)**
Unsaturated Fatty acids	–	1.32 (3.6)	0.53 (3.9)	5.91(1.5)	0.21 (1.3)	1.44 (1.0)	0.37(0.7)	0.11(1.9)	**7.55(1.7)**	**2.34(1.1)**	**9.89(1.5)**
Hydroxy acids (HA)	–	1.79 (4.8)	0.01 (0.1)	1.92(0.5)	0.52 (3.2)	0.03 (0.0)	–	0.65 (11.1)	**4.88(1.1)**	**0.04(0.0)**	**4.92(0.7)**
Heterocyclic N compounds (HN)	**29.08 (12.9)**	–	4.20 (30.5)	–	–	53.43 (37.4)	6.27 (11.4)	–	–	**63.90 (30.2)**	**63.90(9.6)**
Heterocyclic O compounds (HO)	**1.69(0.7)**	–	0.02 (0.1)	–	–	0.12 (0.1)	0.03(0.1)	–	–	**0.17(0.1)**	**0.17(0.06)**
Ketones (KE)	–	–	0.07 (0.5)	–	–	0.39 (0.3)	0.06(0.1)	–	–	**0.52(0.3)**	**0.52(0.1)**
Phenolic acids (PA)	**0.44(0.2)**	0.09 (0.2)	0.03 (0.2)	1.28(0.3)	–	1.48 (1.0)	0.01(0.0)	0.04(0.7)	**1.41(0.3)**	**1.52(0.7)**	**2.93(0.4)**
Phenolic esters (PE)	**3.18(1.4)**	–	0.17 (1.2)	–	–	2.50 (1.7)	0.11(0.2)	–	–	**2.78(1.3)**	**2.78(0.4)**
Phenols (PH)	**19.04 (8.4)**	0.14 (0.4)	0.74 (5.4)	10.92 (2.8)	–	25.41 (17.8)	0.78(1.4)	–	**11.06 (2.4)**	**26.93 (12.7)**	**37.99(5.7)**
Resin acids (RA)	–	4.81 (12.9)	–	45.50 (11.5)	2.88 (17.6)	–	–	0.71 (12.3)	**53.90 (11.9)**	–	**53.90(8.1)**
Sugar acids (SA)	–	–	0.02 (0.1)	–	–	Traces	–	–	–	**0.02(0.0)**	**0.02(0.01)**
Sterols (SE)	–	0.48 (1.3)	0.02 (0.1)	–	–	0.02 (0.0)	0.01(0.0)	–	**0.48(0.1)**	**0.05(0.0)**	**0.53(0.1)**
Sugar esters/ethers (SET)	–	–	0.09 (0.7)	2.85(0.7)	–	0.13 (0.1)	–	Traces	**2.85(0.6)**	**0.22(0.1)**	**3.07(0.5)**
Steroids (ST)	–	3.34 (9.0)	–	–	0.10 (0.6)	–	–	0.05(0.9)	**3.49(0.8)**	–	**3.49(0.5)**
Sugars (SU)	–	1.58 (4.2)	–	86.75 (22.0)	1.67 (10.2)	–	–	0.31(5.2)	**90.31 (19.9)**	–	**90.31(13.6)**
TOTAL	**225,82**	36.64	13.75	391.31	16. 4	142,69	54.93	5.82	**443.86**	**211.37**	**655.23**

[a] Total ORGs refers to the overall of ORG1, ORG2, ORG3 and RESORG.
[b] Total AQUs refers to the overall of AQU2, AQU4 and RESOM.
[c] Total Humeomics refers to the sum of all ORGs and AQUs fractions.
[d] Fatty acids total are referring to the sum of the saturated and unsaturated fatty acids.

reports (Drosos and Piccolo, 2018; Savarese et a, 2021) in indicating a preferential loss of mostly hydrophobic molecules and a concomitant accumulation of hydrosoluble nitrogen-rich compounds in soils subjected to 20 consecutive years of conventional cultivation. However, the long-term soil management under Mix cropping reduced the depletion of long-chain esters and fatty acids also in eSOM (Fig. 1B; Fig. S1), suggesting that the hydrophobic protection of SOM was somewhat maintained in comparison to the continuous maize experiment and so was the organic matter stability (Piccolo et al., 2004; Spaccini and Piccolo, 2019).

3.3.1. *Organosoluble fractions*

The most significant constituents of the first organo-soluble fraction ORG1, as revealed by GC-MS, accounted to 99, 29 and 28 molecules for the Control, Maize and Mix experiments, respectively (Table S1, S2, and S3). Among the unbound humic molecules separated in ORG1 fractions of the three soils, the most abundant compounds were long-chain esters (ES), fatty acids (FA), sugar derivatives (SU), and resin acids (RA) (Fig. 2; Fig. S2). However, the Humeome extracted in the ORG1 fraction of both the cropped Maize and Mix soils revealed, as compared to the uncultivated Control soil, a significant decrease in the content of alkanoic acids (FA), while ES and RA content were relatively enhanced (Fig. 2; Tables 3, 4 and 5).

Table 4
mg OC and (%) of compounds classes in eSOM and Humeomic fractions of soil under long-term maize mono-cultivation and traditional tillage (**Maize**), as determined by GC-MS and Orbitrap-MS.

Group	eSOM	ORG1	AQU2	ORG2	ORG3	AQU4	RESOM	RESORG	Total ORGs[a]	Total AQUs[b]	Total Humeomics[c]
MAIZE SOIL											
Aminoacids (AA)	–	–	–	–	–	–	–	–	–	–	–
Alcohols (AC)	–	0.15 (2.1)	–	1.07 (1.8)	0.02 (0.8)	–	Traces	0.32(6.2)	**1.56(2.1)**	–	**1.56(0.4)**
Amides (AD)	**5.59 (6.4)**	0.53 (7.4)	1.12 (9.7)	5.91 (10.1)	0.12 (4.3)	15.34 (7.8)	1.62(1.5)	0.41(8.0)	**6.97(9.5)**	**18.08 (5.7)**	**25.05(6.4)**
Alkanes/alkenes/ alkynes (AL)	–	0.10 (1.4)	–	–	–	–	–	0.03(0.6)	**0.13(0.2)**	–	**0.13(0.0)**
Amines (AM)	**40.29 (45.9)**	–	3.37 (29.0)	–	–	47.56 (24.1)	32.94 (30.5)	–	–	**83.87 (26.5)**	**83.87(21.5)**
Benzoic acids (BA)	**4.84 (5.5)**	–	0.56 (4.8)	–	–	16.28 (8.3)	4.66(4.3)	–	–	**21.50 (6.8)**	**21.50(5.5)**
Benzoic esters (BE)	–	–	0.08 (0.7)	–	–	–	–	–	–	**0.08(0.0)**	**0.08(0.0)**
Dicarboxylic acids (DA)	–	–	0.24 (2.1)	–	–	1.41(0.7)	0.14(0.1)	0.01(0.2)	**0.01(0.0)**	**1.79(0.6)**	**1.80(0.5)**
Esters (ES)	**2.02 (2.3)**	3.91 (54.2)	0.19 (1.6)	22.70 (38.9)	0.02 (0.7)	4.17(2.1)	1.42(1.3)	1.60 (31.1)	**28.23 (38.3)**	**5.78(1.8)**	**34.01(8.7)**
Ethers (ET)	**Traces**	–	Traces	–	–	Traces	0.01(0.0)	–	–	**0.01(0.0)**	**0.01(0.0)**
Fatty acids total[d] (FA)	**11.20 (12.8)**	0.36 (5.0)	2.10 (18.1)	3.93 (6.7)	0.32 (11.6)	18.85 (9.6)	14.12 (13.1)	0.90 (17.4)	**5.51(7.5)**	**35.07 (11.1)**	**40.58(10.4)**
Saturated Fatty acids	**11.20 (12.8)**	0.34 (4.7)	1.67 (14.4)	3.93 (6.7)	0.32 (11.6)	14.91 (7.6)	13.88 (12.9)	0.78 (15.1)	**5.37(7.3)**	**30.46 (9.6)**	**35.83(9.2)**
Unsaturated Fatty acids	–	0.02 (0.3)	0.43 (3.7)	–	–	3.94(2.0)	0.24(0.2)	0.12(2.3)	**0.14(0.2)**	**4.61(1.5)**	**4.75(1.2)**
Hydroxy acids (HA)	–	0.06 (0.8)	0.02 (0.2)	–	–	0.14(0.1)	–	0.28(5.4)	**0.34(0.5)**	**0.16(0.1)**	**0.50(0.1)**
Heterocyclic N compounds (HN)	**14.56 (16.6)**	–	2.45 (21.1)	–	0.02 (0.7)	74.68 (37.9)	44.47 (41.3)	–	**0.02(0.0)**	**121.60 (38.4)**	**121.62(31.2)**
Heterocyclic O compounds (HO)	**0.74 (0.8)**	–	0.04 (0.3)	–	–	0.78(0.4)	0.62(0.6)	–	–	**1.44(0.5)**	**1.44(0.4)**
Ketones (KE)	–	–	0.07 (0.6)	–	–	0.68(0.3)	0.69(0.6)	–	–	**1.44(0.5)**	**1.44(0.4)**
Phenolic acids (PA)	**0.63 (0.7)**	–	0.03 (0.3)	0.62 (1.1)	–	0.42(0.2)	0.43(0.4)	0.02(0.4)	**0.64(0.9)**	**0.88(0.3)**	**1.52(0.4)**
Phenolic esters (PE)	**1.27 (1.5)**	–	0.31 (2.7)	–	–	4.55(2.3)	0.88(0.8)	–	–	**5.74(1.8)**	**5.74(1.5)**
Phenols (PH)	**6.56 (7.5)**	0.03 (0.4)	0.87 (7.5)	1.48 (2.5)	–	11.81 (6.0)	5.50(5.1)	–	**1.51(2.1)**	**18.18 (5.7)**	**19.69(5.0)**
Resin acids (RA)	–	1.94 (26.9)	–	12.69 (21.7)	0.01 (0.3)	–	–	0.98 (19.0)	**15.62 (21.2)**	–	**15.62(4.0)**
Sugar acids (SA)	–	–	0.01 (0.1)	–	–	Traces	–	0.03(0.6)	**0.03(0.0)**	**0.01(0.0)**	**0.04(0.0)**
Sterols (SE)	–	–	0.02 (0.2)	–	–	0.05(0.1)	0.40(0.4)	–	–	**0.47(0.1)**	**0.47(0.1)**
Sugar esters/ethers (SET)	–	–	0.12 (1.0)	0.24 (0.4)	–	0.24(0.1)	–	0.01(0.2)	**0.25(0.3)**	**0.36(0.1)**	**0.61(0.2)**
Steroids (ST)	–	0.04 (0.6)	–	–	–	–	–	0.04(0.8)	**0.08(0.1)**	–	**0.08(0.0)**
Sugars (SU)	–	0.09 (1.2)	–	9.85 (16.8)	2.24 (81.6)	–	–	0.52 (10.1)	**12.70 (17.3)**	–	**12.70(3.3)**
TOTAL	**87.7**	7.21	11.6	58,49	2.75	197.05	93.77	5.15	**67.55**	**302.42**	**369.97**

[a] Total ORGs refers to the overall of ORG1, ORG2, ORG3 and RESORG.
[b] Total AQUs refers to the overall of AQU2, AQU4 and RESOM.
[c] Total Humeomics refers to the addition of all ORGs and AQUs fractions.
[d] Fatty acids total are referring to the sum of the saturated and unsaturated fatty acids.

When the esters weakly-bound to the humic matrix were broken to solubilize the resulting molecules in the ORG2 fraction, this accounted to 54, 32 and 24 molecules for the Control, Maize and Mix soils, respectively, while those liberated in ORG3 from the strongly-bound esters amounted to 32, 24, and 70 molecules for the same soil series (Table S1, S2 and S3). However, long-chain ES, FA, RA and SU remained the main components of all ORG2 fractions and did not change substantially among the different soil treatments (Fig. 2; Fig. S2), whereas in ORG3 the percentage of polysaccharides increased significantly in the Maize soil, as compared to control, and the same was observed for the percent of fatty acids in the Mix soil (Fig. 2; Tables 4 and 5). This suggests that humic molecules solubilized by the BF_3-based acidic hydrolysis in the ORG2 fraction may well represent a recalcitrant organic carbon in soils, regardless of its land use and management. Moreover, it is noted that sugar molecules, that are extracted in this fraction, and even more so in the ORG3 fraction following an alkaline hydrolysis, were not at all visible in the eSOM fractions (Fig. 2; Fig. S1), thereby once more indicating the conformational complexity of the soil Humeome and the sequestering role played by apolar components in regard to polar compounds potentially more liable of biodegradation (Piccolo et al., 2018b).

Differently from recent applications of Humeomics to soils (Vinci et al., 2020, 2021), here we further extracted Res5 by a DCM/MeOH solution, as done for the extraction of ORG1 from Res0, to obtain a final

Table 5
mg OC and (%) of compounds classes in eSOM and Humeomic fractions of soil under long-term maize-broad bean crop rotation and traditional tillage (**Mix**), as determined by GC-MS and Orbitrap-MS.

Group	eSOM	ORG1	AQU2	ORG2	ORG3	AQU4	RESOM	RESORG	Total ORGs[a]	Total AQUs[b]	Total Humeomics[c]
MIX SOIL											
Aminoacids (AA)	–	–	Traces	–	–	–	–	–	–	**Traces**	**Traces**
Alcohols (AC)	–	0.25 (2.9)	–	2.65 (3.0)	0.36 (7.5)	–	–	0.38 (10.4)	**3.64(3.4)**	–	**3.64(1.4)**
Amides (AD)	**5.70 (6.2)**	0.66 (7.5)	0.50 (9.9)	11.11 (12.5)	0.08 (1.7)	8.36(6.5)	0.17(1.1)	0.10(2.7)	**11.95 (11.3)**	**9.03(6.0)**	**20.98(8.2)**
Alkanes/alkenes/ alkynes (AL)	–	–	–	–	0.02 (0.4)	–	–	0.12(3.3)	**0.14(0.1)**	–	**0.14(0.1)**
Amines (AM)	**36.78 (40.0)**	–	1.32 (26.2)	–	–	25.34 (19.7)	5.19 (32.2)	–	–	**31.85 (21.2)**	**31.85(12.4)**
Benzoic acids (BA)	**7.02 (7.6)**	–	0.08 (1.6)	–	–	8.56(6.7)	0.65(4.0)	–	–	**9.29(6.1)**	**9.29(3.6)**
Benzoic esters (BE)	–	–	0.02 (0.5)	–	–	3.62(2.8)	–	–	–	**3.64(2.4)**	**3.64(1.4)**
Dicarboxylic acids (DA)	–	–	0.10 (1.9)	–	–	0.73(0.6)	–	0.01(0.3)	**0.01(0.0)**	**0.83(0.6)**	**0.84(0.3)**
Esters (ES)	**2.04 (2.2)**	4.59 (52.4)	0.01 (0.2)	24.46 (27.6)	0.48 (10.0)	2.20(1.7)	0.13(0.8)	0.68 (18.6)	**30.21 (28.5)**	**2.34(1.6)**	**32.55(12.7)**
Ethers (ET)	**0.01 (0.0)**	–	Traces	–	–	–	Traces	–	–	**Traces**	**Traces**
Fatty acids total[d] (FA)	**17.25 (18.8)**	0.73 (8.3)	0.87 (17.1)	10.68 (12.0)	2.01 (42.2)	12.94 (10.1)	2.60 (16.1)	1.30 (35.6)	**14.72 (13.9)**	**16.41 (11.0)**	**31.13(12.2)**
Saturated Fatty acids	**17.25 (18.8)**	0.70 (8.0)	0.69 (13.6)	10.68 (12.0)	1.01 (21.1)	10.83 (8.5)	2.22 (13.8)	0.98 (26.8)	**13.37 (12.6)**	**13.74 (9.2)**	**27.11(10.6)**
Unsaturated Fatty acids	–	0.03 (0.3)	0.18 (3.5)	–	1.00 (21.0)	2.11(1.6)	0.38(2.3)	0.32(8.8)	**1.35(1.3)**	**2.67(1.8)**	**4.02(1.6)**
Hydroxy acids (HA)	–	0.16 (1.9)	0.01 (0.2)	–	0.10 (2.1)	0.07(0.1)	–	0.06(1.6)	**0.32(0.3)**	**0.08(0.1)**	**0.40(0.2)**
Heterocyclic N compounds (HN)	**14.11 (15.3)**	–	1.67 (33.1)	–	0.05 (1.0)	56.48 (43.8)	5.94 (36.8)	–	**0.05(0.1)**	**64.09 (42.7)**	**64.14(25.0)**
Heterocyclic O compounds (HO)	**0.76 (0.8)**	–	0.01 (0.3)	–	–	0.41(0.3)	0.02(0.1)	–	–	**0.44(0.3)**	**0.44(0.2)**
Ketones (KE)	–	–	0.03 (0.6)	–	–	0.37(0.3)	0.06(0.4)	–	–	**0.46(0.3)**	**0.46(0.2)**
Phenolic acids (PA)	**0.68 (0.7)**	–	0.01 (0.3)	–	0.36 (7.5)	2.61(2.0)	0.01(0.1)	–	**0.36(0.3)**	**2.63(1.8)**	**2.99(1.2)**
Phenolic esters (PE)	**1.28 (1.4)**	–	0.06 (1.1)	–	–	0.89(0.7)	0.03(0.2)	–	–	**0.98(0.7)**	**0.98(0.4)**
Phenols (PH)	**6.47 (7.0)**	–	0.28 (5.6)	3.15 (3.5)	0.15 (3.1)	5.88(4.6)	1.27(7.9)	–	**3.30(3.1)**	**7.43(5.0)**	**10.73(4.2)**
Resin acids (RA)	–	2.18 (24.8)	–	13.66 (15.4)	0.21 (4.4)	–	–	0.21(5.8)	**16.26 (15.3)**	–	**16.26(6.4)**
Sugar acids (SA)	–	–	0.01 (0.3)	–	0.02 (0.4)	–	–	0.01(0.3)	**0.03(0.1)**	**0.01(0.0)**	**0.04(0.0)**
Sterols (SE)	–	–	0.01 (0.1)	–	–	0.04(0.0)	0.05(0.3)	–	–	**0.10(0.1)**	**0.10(0.0)**
Sugar esters/ethers (SET)	–	–	0.05 (1.0)	–	–	0.12(0.1)	–	–	–	**0.17(0.1)**	**0.17(0.1)**
Steroids (ST)	–	0.08 (0.9)	–	–	0.04 (0.8)	–	–	0.07(1.9)	**0.19(0.2)**	–	**0.19(0.1)**
Sugars (SU)	–	0.12 (1.3)	–	23.04 (26.0)	0.90 (18.9)	–	–	0.71 (19.5)	**24.77 (23.4)**	–	**24.77(9.7)**
TOTAL	**92.1**	8.77	5.04	88.74	4.78	120.06	16.12	3.65	**105.95**	**149.78**	**255.73**

[a] Total ORGs refers to the overall of ORG1, ORG2, ORG3 and RESORG.
[b] Total AQUs refers to the overall of AQU2, AQU4 and RESOM.
[c] Total Humeomics refers to the addition of all ORGs and AQUs fractions.
[d] Fatty acids total are referring to the sum of the saturated and unsaturated fatty acids.

organosoluble fraction (RESORG) from all three soil samples. The GC-MS analyses of all RESORG fractions revealed an abundance of molecules (80, 65 and 72 for the Control, Maize and Mix soils, respectively) (Table S1, S2 and S3) that was unexpectedly larger for both Maize and Mix samples than that found for ORG1. This shows that, despite the abundant removal of organic compounds by the previous Humeomics steps, there were many unbound components still extractable as organosoluble molecules. Moreover, this finding confirms that the soil Humeome is arranged in a supramolecular assembly of relatively small heterogeneous molecules, which can be progressively liberated by disrupting their conformational arrangements during different and alternate fractionation steps.

All RESORG fractions showed a distribution of compounds classes similar to that of ORG1 (Fig. 2; Fig. S2), except for the relative remarkable increase of long-chain fatty acids found in Mix soil (Fig. 2; Table 5). The similarity between ORG1 and RESORG fractions suggests once again that the most stable part of soil humus is hydrophobic and becomes available to degradation when the complex protecting network of alternate hydrophobic and hydrophilic domains (Nebbioso et al., 2015) is depleted due to continuous tillage. Nevertheless, our findings indicate that some apolar-esterified molecules remained strongly bound to the soil matrix under the 20 years-long tilled Maize monoculture. However, the Maize sample is also characterized by a substantial depletion of organosoluble alkanoic acids (FA), as already observed for

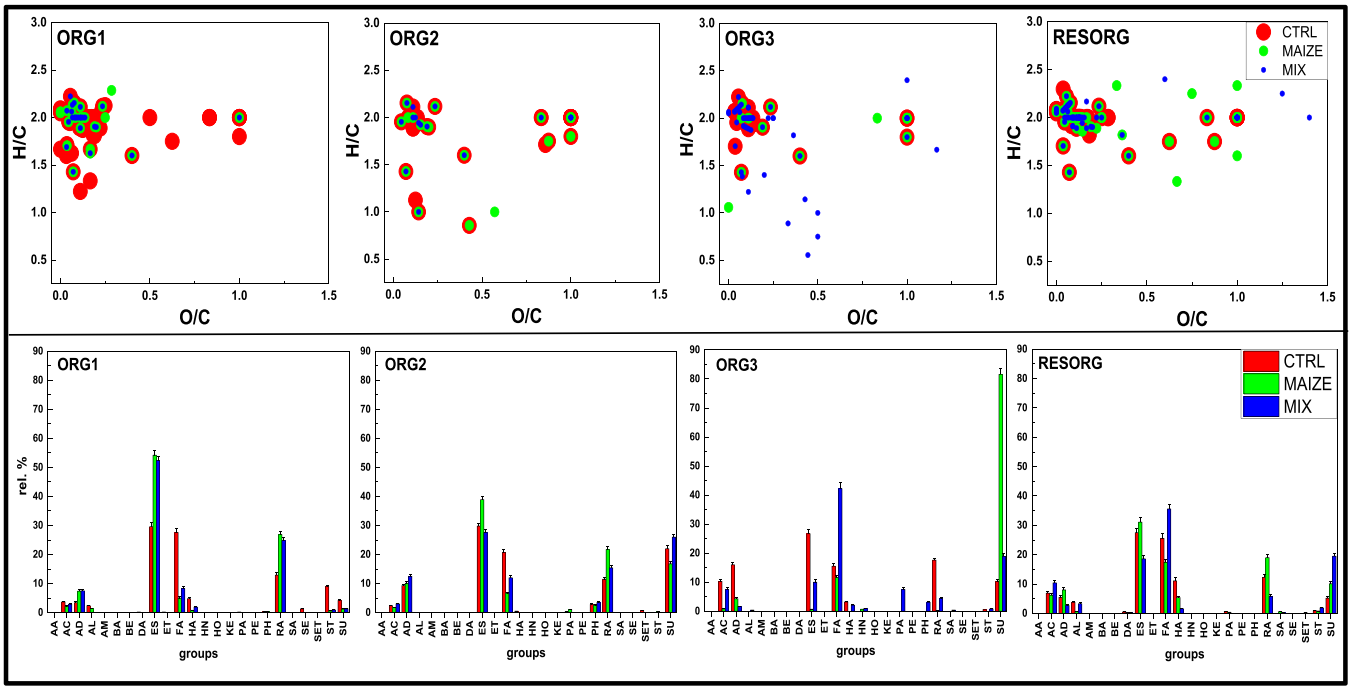

Fig. 2. Van Krevelen Plots of various molecular components identified in organosoluble fractions (ORG) extracted from soil samples and their relative (%) abundance. Molecules identified in the uncultivated Control soil (CTRL) are noted in red, whereas molecules found in Maize monoculture soil (MAIZE) are marked in green, and molecules detected in soil under Maize-Broad bean crop rotation (MIX) are shown in blue. AA: Aminoacids; AC: Alcohols; AD: Amides; AL: Alkanes/alkenes/alkynes; AM: Amines; BA: Benzoic Acids; BE: Benzoic Esters; DA: Dicarboxylic Acids; ES: Esters; ET: Ethers; FA: Fatty Acids; HA: Hydroxy Acids; HN: Heterocyclic Nitrogen compounds; HO: Heterocyclic Oxygen compounds; KE: Ketones; PA: Phenolic Acids; PE: Phenolic Esters; PH: Phenols; RA: Resin Acids; SA: Sugar Acids; SE: Sterols; SET: Sugar Ethers/Esters; ST: Steroids; SU: Sugars. Standard deviation for all classes of compounds was ≤ 2.

soils still under Maize but after a short cultivation period (Drosos and Piccolo, 2018), thereby substantiating the decrease of the corresponding CPR index observed above. The differential loss of hydrophobic components recorded for the soil under maize is instead mitigated in the Mix soil, revealing a relative enhancement of alkyl compounds (FA, AC, AL) (Fig. 2), which are considered as the most stable humic components in soils (Song et al., 2013; Zhang et al, 2019), and responsible for SOM preservation in the crop-rotation system (Savarese et al., 2021).

3.3.2. *Hydrosoluble fractions*

High-resolution ESI-Orbitrap-MS spectrometry was employed to detect humic molecules solubilized in AQU and RESOM fractions (Fig. 3; Fig. S3). In AQU2 fractions, 148, 123 and 130 molecules were revealed in Control, Maize and Mix soils, respectively (Table S1, S2 and S3). The main specific compounds classes in AQU and RESOM fractions were amines (AM) and heterocyclic nitrogen compounds (HN) (Fig. 3; Fig. S3), which were only very poorly present in the organosoluble ORG fractions. These classes were followed in abundance by amides (AD) and fatty acids (FA), benzoic acids (BA), phenols (PH) and phenolic esters (PE). The amount of these compounds was similar in the soils of different treatments, except for HN that was significantly greater in the long-term Maize cultivated soil (Table 3), as it was reported earlier for the Humeome of another soil under maize after a short cultivation period (Drosos et al., 2020).

The AQU4 fraction, resulting from the cleavage of ether bonds in humic molecules, solubilized 112, 123 and 133 molecules for Control, Maize and Mix soils, respectively, while 74, 98 and 84 molecules were detected, respectively, in RESOM, that is the fraction solubilized in a sodium hydroxide/pyrophosphate solution from RES4 (Table S1, S2 and S3). AM, HN and FA remained the main compounds classes in both fractions (Fig. 3; Fig. S3), although the content of amides (AM) in RESOM of Control was significantly greater than for Maize and Mix soils, thus suggesting an enhanced depletion of this nitrogen-containing molecular class in tilled cropped soils. The AQU2, AQU4 and RESOM fractions characterized by Orbitrap-MS showed a peculiar behaviour as for the content of N-containing molecules (AD, AM, HN) in the different long-term treatments (Fig. 3; Tables 3–5). The sum of the latters decreased for AQU2 passing from 9.2 to 6.9 and 3.5 mg C in Control, Maize and Mix samples, respectively, indicating with cultivation a progressive loss of nitrogen compounds liberated from the weakly-bound ester fraction. However, the magnitude of their sum was much larger in the case of AQU4 and RESOM, being 87.3, 137.6, 90.2, and 50.3, 79.0, 11.3 mg C, respectively, for the same series of samples (Fig. 3; Tables 3–5). This means that the N compounds were significantly trapped within the most recalcitrant soil humeome that was released in AQU4 not only after the disruption of ether bonds in organic compounds, but also due to a partial degradation of the soil inorganic components upon the action of HI. Moreover, such alteration of the soil organo-mineral structure allowed a significant release of N-compounds in Total Humeomics (187.5, 231, 117 mg C in Control, Maize and Mix soil, respectively) (Tables 3–5) which corresponded to a 24.6%, 282.5%, and 106.7%, mass increase in Control, Maize and Mix soil, respectively, as compared to those extracted by the single alkaline eSOM extracts. These results suggest that N-containing components of the Humeome are preferentially stabilized within the most chemically recalcitrant organic domains, that are also intimately linked to the inorganic soil constituents (Drosos and Piccolo, 2018).

It is also to be noted that while the weight sum AD, AM, and HN compounds classes in the tilled Maize and Mix soils was significantly smaller than Control for the eSOM fractions, both the AQU4 and RESOM fractions separated by Humeomics showed much larger values for the Maize samples than for Mix and Control soils. This may be possibly explained by the different cropping system, whereby Maize received for 20 years of cultivation a larger nitrogen fertilization than both the maize-leguminous rotation and the uncultivated no-tilled control soil (Schnitzer et al., 2006). Hence, an addition of different amount and forms of N compounds to the long-term field experiments may have produced pools of organic N of diverse stability and recalcitrance in

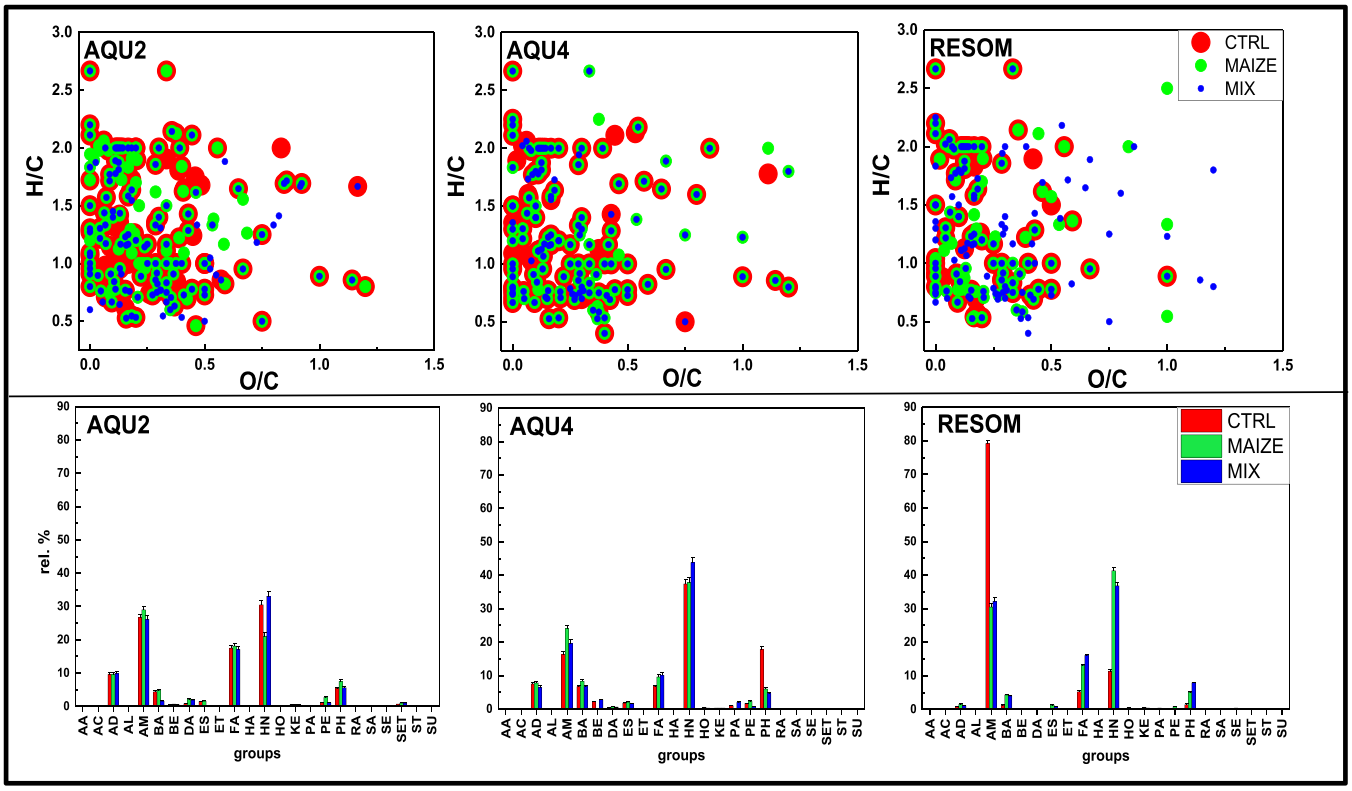

Fig. 3. Van Krevelen Plots of various molecular components identified in hydrosoluble fractions (AQUs) and residual organic matter (RESOM) extracted from soil samples and their relative (%) abundance. Molecules identified in the uncultivated Control soil (CTRL) are noted in red, whereas molecules found in Maize monoculture soil (MAIZE) are marked in green, and molecules detected in soil under Maize-Broad bean crop rotation (MIX) are shown in blue. AA: Aminoacids; AC: Alcohols; AD: Amides; AL: Alkanes/alkenes/alkynes; AM: Amines; BA: Benzoic Acids; BE: Benzoic Esters; DA: Dicarboxylic Acids; ES: Esters; ET: Ethers; FA: Fatty Acids; HA: Hydroxy Acids; HN: Heterocyclic Nitrogen compounds; HO: Heterocyclic Oxygen compounds; KE: Ketones; PA: Phenolic Acids; PE: Phenolic Esters; PH: Phenols; RA: Resin Acids; SA: Sugar Acids; SE: Sterols; SET: Sugar Ethers/Esters; ST: Steroids; SU: Sugars. Standard deviation for all classes of compounds was ≤ 2.

soils. In support to this explanation, we found that most molecules detected in eSOM, AQUs and RESOM fractions of the three soils showed empirical formulae compatible with compounds bound to iron hydroxides (Table S1-S3; Fig. 4). The covalent C–O–Fe bonds were present in molecules solubilized by similar amounts in these fractions in both cropped soils after 20 years of cultivation (Fig. 4B). This result not only confirms the important role played by iron in the stabilization of the soil Humeome (Nuzzo et al., 2013; Lv et al., 2016), but also shows that the amount of AM and HN linked to iron after 20 years of cropping was much larger than that measured in another soil after only 1 and 3 years of maize monoculture (Drosos and Piccolo, 2018). Moreover, the nitrogen-containing compounds appeared to be progressively removed from the humus yearly turnover in tilled soils and immobilized in poorly available and highly recalcitrant pools, as those represented by AQU4 and RESOM fractions. This organic nitrogen that is sequestered in soils due to strong chemical affinity among heterogeneous molecules and to their adsorption on soil inorganic components, may well represent the so-called “unknown nitrogen” that has remained unidentified in agricultural soils (Schnitzer et al., 1983).

4. Conclusions

In this study, the application of Humeomics on soils with a 20 years-long history of different land use and management allowed a more detailed molecular comprehension of the overall dynamics of the soil Humeome. Our findings showed that the organosoluble to hydrosoluble OC ratio of Humeomics fractions dropped significantly in both long-term cropped soils under both continuous Maize and Maize-Broad bean rotation, as compared to the uncropped untilled soil (Table 1). This revealed that 20 years of cultivation under traditional tillage not only reduced the total OC content of soils but also progressively depleted the hydrophobic components of soil humus and the capacity of sequestering the labile/hydrophilic molecules, which were then released in the separated humeomic fractions. The loss of OC hydrophobic protection due to reduction of lipophilic components (such as long-chain fatty acids) under continuous Maize was significantly mitigated in soil cropped with a Maize-Faba bean rotation, thus confirming at molecular level the long-standing perception of a greater ecological sustainability of crop rotation in respect to monoculture.

The Humeomics fractionation enabled not only solubilization and characterization of a significant larger proportion of the soil Humeome than for the traditional single alkaline extraction (eSOM), but also detection of different types of humic molecules when the Humeome complex matrix was unraveled by progressively breaking weakly and strongly bound esters and highly recalcitrant ether linkages. In fact, compounds classes such as saccharides, which were not identified in eSOM, became visible in organosoluble fractions preferentially from soil under continuous Maize that was mostly deprived of SOM hydrophobic components. Moreover, the alteration of the Humeome molecular arrangement by sequential fractionation allowed to further solubilized organosoluble components, which were not extracted in earlier fractionation steps. The same was true for the hydrosoluble components which were detected in AQUs and RESOM fractions when they became accessible after disruption of chemical and physical protection during fractionation steps. This suggests a supramolecular association of the soil Humeome, whose components are more extractable as the protective complex molecular matrix is progressively altered or removed. Hydrosoluble nitrogen-containing compounds classes, such as amides, amines, and heterocyclic nitrogen were revealed in greater amount in the more recalcitrant AQUs and RESOM fractions of both cropped soils,

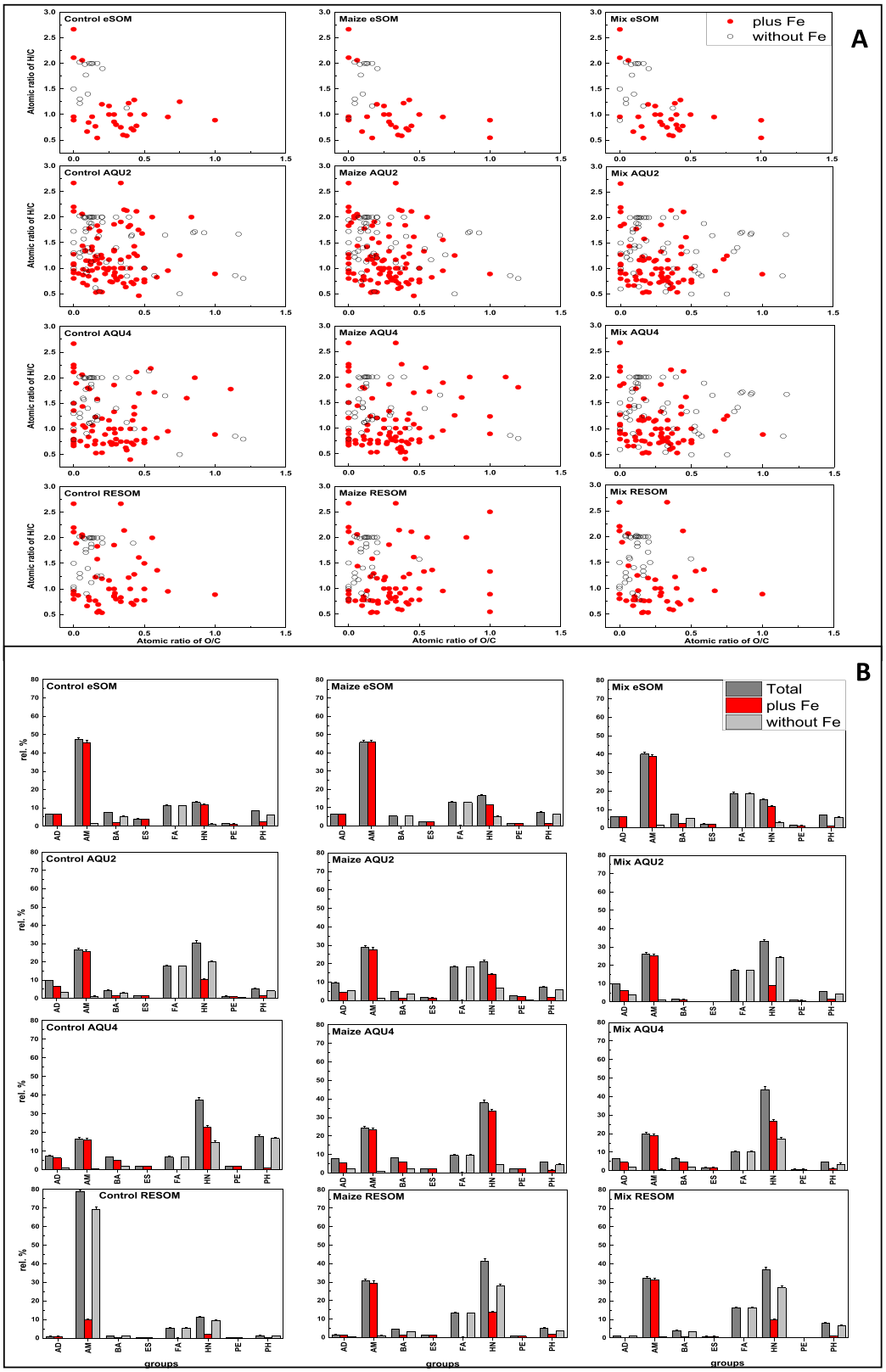

Fig. 4. **A:** Van Krevelen Plots of molecular structures in eSOM. AQUs and RESOM fractions for the three soil samples: Uncultivated soil (Control), soil under Maize monoculture (Maize), soil under Maize-Broad bean crop rotation (Mix). Molecules linked to iron hydroxides are shown in red. **B:** Relative (%) abundance of some significant compound classes (AD: Amides; AM: Amines; BA: Benzoic Acids; ES: Esters; FA: Fatty Acids; HN: Heterocyclic Nitrogen compounds; PE: Phenolic Esters; PH: Phenols) identified in eSOM, AQUs and RESOM fractions of the three soil samples (Control. Maize and Mix). The total amount of molecules for each significant group is noted in dark gray bars, those not linked to iron hydroxides is noted in light gray, while the percentage of Fe-bound molecules is marked in red.

most likely due to their intimate interactions in organo-mineral complexes. In fact, most of the detected amines and heterocyclic nitrogen were bound to iron, thereby indicating that its interaction with different forms of N compounds represents a mechanism of nitrogen sequestration in agricultural soils. This is in agreement with previous studies that related lower C/N ratios with mineral associated organic matter, though based only on physical soil fractionation, (Liang et al., 2019; Lavallee et al., 2020).

Our results showed an unprecedented molecular detail of soil Humeomes in long-term field experiments under different land use, as achieved by a sequential chemical fractionation of SOM coupled to advanced analytical determinations. This approach promises to contribute to elucidate the mechanisms of SOC stabilization, which may become the basis for new environmentally sustainable technologies in Agriculture.

Declaration of Competing Interest

The authors declare that they have no known competing financial interests or personal relationships that could have appeared to influence the work reported in this paper.

Acknowledgements

This work was conducted in partial fulfilment of first author requirements, to achieve a Doctoral degree, funded by the Ministry of University and Research (MUR) of Italy.

Appendix A. Supporting information

Supplementary data associated with this article can be found in the online version at doi:10.1016/j.agee.2022.107928.

References

Celik, I., 2005. Land-use effects on organic matter and physical properties of soil in a southern Mediterranean highland of Turkey. Soil Tillage Res. 83 (2), 270–277. https://doi.org/10.1016/j.still.2004.08.001.

Dick, W.A., 1984. Influence of long-term tillage and crop rotation combinations on soil enzyme activities. Soil Sci. Soc. Am. J. 48, 569–574. https://doi.org/10.2136/sssaj1984.03615995004800030020x.

Drosos, M., Jerzykiewicz, M., Deligiannakis, Y., 2009. H-binding groups in lignite vs. soil humic acids: NICA-Donnan and spectroscopic parameters. J. Col. Inter. Sci. 332, 78–84. https://doi.org/10.1016/j.jcis.2008.12.023.

Drosos, M., Nebbioso, A., Mazzei, P., Vinci, G., Spaccini, R., Piccolo, A., 2017. A molecular zoom into soil Humeome by a direct sequential chemical fractionation of soil. Sci. Tot. Environ. 586, 807–816. https://doi.org/10.1016/j.scitotenv.2017.02.059.

Drosos, M., Savy, D., Spiteller, M., Piccolo, A., 2018a. Structural characterization of carbon and nitrogen molecules in the Humeome of two different grassland soils. Chem. Biol. Technol. Agr. 5, 14. https://doi.org/10.1186/s40538-018-0127-y.

Drosos, M., Nebbioso, A., Piccolo, A., 2018b. Humeomics: A key to unravel the humusic pentagram. Appl. Soil Ecol. 123, 513–516. https://doi.org/10.1016/j.apsoil.2017.07.027.

Drosos, M., Piccolo, A., 2018. The molecular dynamics of soil humus as a function of tillage. Land Degrad. Dev. 29, 1792–1805. https://doi.org/10.1002/ldr.2989.

Drosos, M., Vinci, G., Spaccini, R., Piccolo, A., 2020. Molecular dynamics of organic matter in a tilled soil under short term wheat cultivation. Soil Tillage Res. 196, 104448 https://doi.org/10.1016/j.still.2019.104448.

Fontaine, S., Barot, S., Barré, P., Bdioui, N., Mary, B., Rumpel, C., 2007. Stability of organic carbon in deep soil layers controlled by fresh carbon supply. Nature 450, 277–280. https://doi.org/10.1038/nature06275.

Fu, S., Cabrera, M.L., Coleman, D.C., Kisselle, K.W., Garrett, C.J., Hendrix, P.F., Crossley Jr., D.A., 2000. Soil carbon dynamics of conventional tillage and no-till agroecosystems at Georgia Piedmont - HSB-C models. Ecol. Model. 131, 229–248. https://doi.org/10.1016/S0304-3800(00)00250-7.

Hayes, M.H.B., 1985. Extraction of Humic Substances from Soil. In: Aiken, G.R., McKnight, D.M., Wershaw, R.L., MacCarthy, P. (Eds.), Humic Substances in Soil, Sediment and Water. Wiley, New York, pp. 329–362.

Jandl, G., Leinweber, P., Schulten, H.R., Ekschmitt, K., 2005. Contribution of primary organic matter to the fatty acid pool in agricultural soils. In: Soil Biol. Biochem, 37, pp. 1033–1041. https://doi.org/10.1016/j.soilbio.2004.10.018.

Jandl, G., Baum, C., Blumschein, A., Leinweber, P., 2012. The impact of short rotation coppice on the concentrations of aliphatic soil lipids. Plant Soil 350, 163–177. https://doi.org/10.1007/s11104-011-0892-x.

Jobbagy, E.G., Jackson, R.B., 2000. The Vertical Distribution of Soil Organic Carbon and Its Relation to Climate and Vegetation. Ecol. Appl. 10, 423–436. https://doi.org/10.1890/1051-0761(2000)010[0423:TVDOSO]2.0.CO;2.

Kahle, P., Baum, C., Boelcke, B., Kohl, J., Ulrich, R., 2010. Vertical distribution of soil properties under short-rotation forestry in Northern Germany. J. Plant Nutr. Soil Sci. 173, 737–746. https://doi.org/10.1002/jpln.200900230.

Kalinina, O., Cherkinsky, A., Chertov, O., Goryachkin, S., Kurganova, I., Lopes de Gerenyu, V., Lyuri, D., Kuzyakov, Y., Giani, L., 2019. Post-agricultural restoration: implications for dynamics of soil organic matter pools. Catena 181, 104096. https://doi.org/10.1016/j.catena.2019.104096.

Kuzyakov, Y., Zamanian, K., 2019. Reviews and syntheses: agropedogenesis – Humankind as the sixth soil-forming factor and attractors of agricultural soil degradation. Biogeosciences 16 (24), 4783–4803. https://doi.org/10.5194/bg-16-4783-2019.

Lal, R., 2004. Soil carbon sequestration impacts on global climate change and food security. Science 304, 1623–1627. https://doi.org/10.1126/science.1097396.

Lavallee, J.M., Soong, J.L., Cotrufo, M.F., 2020. Conceptualizing soil organic matter into particulate and mineral-associated forms to address global change in the 21st century. Glob. Change Biol. 26, 261–273. https://doi.org/10.1111/gcb.14859.

Lehmann, J., Kleber, M., 2015. The contentious nature of soil organic matter. Nature 528, 60–68. https://doi.org/10.1038/nature16069.

Liang, C., Amelung, W., Lehmann, J., Kastner, M., 2019. Quantitative assessment of microbial necromass contribution to soil organic matter. Glob. Change Biol. 25, 3578–3590. https://doi.org/10.1111/gcb.14781.

Lv, J., Zhang, S., Wang, S., Luo, L., Cao, D., Christie, P., 2016. Molecular- scale investigation with ESI-FT-ICR-MS on fractionation of dissolved organic matter induced by adsorption on iron oxyhydroxides. Environ. Sci. Technol. 50, 2328–2336. https://doi.org/10.1021/acs.est.5b04996.

Mao, J., Nierop, K.G., Rietkerk, M., Damsté, J.S.S., Dekker, S.C., 2016. The influence of vegetation on soil water repellency-markers and soil hydrophobicity. Sci. Tot. Environ. 566, 608–620. https://doi.org/10.1016/j.scitotenv.2016.05.077.

Mielnik, L., Weber, J., Podlasinski, M., Kocowicz, A., 2021. Fluorescence properties of humic substances transformed in ectohumus horizons of Podzols affected by alkaline fly-ash. Land Degrad. Dev. 32, 3487–3497. https://doi.org/10.1002/ldr.3926.

Nebbioso, A., Piccolo, A., 2011. Basis of a humeomics science: Chemical fractionation and molecular characterization of humic biosuprastructures. Biomacromolecules 12, 1187–1199. https://doi.org/10.1021/bm101488e.

Nebbioso, A., Piccolo, A., 2012. Advances in humeomics: Enhanced structural identification of humic molecules after size fractionation of a soil humic acid. Anal. Chim. Acta 720, 77–90. https://doi.org/10.1016/j.aca.2012.01.027.

Nebbioso, A., Mazzei, P., Savy, D., 2014a. Reduced complexity of multidimensional and diffusion NMR spectra of soil humic fractions as simplified by Humeomics. Chem. Biol. Technol. Agric. 1, 24. https://doi.org/10.1186/s40538-014-0024-y.

Nebbioso, A., Piccolo, A., Lamshöft, M., Spiteller, M., 2014b. Molecular characterization of an end-residue of humeomics applied to a soil humic acid. R. S. C. Adv. 4, 23658–23665. https://doi.org/10.1039/c4ra01619j.

Nebbioso, A., Vinci, G., Drosos, M., Spaccini, R., Piccolo, A., 2015. Unveiling the molecular composition of the unextractable soil organic fraction (humin) by humeomics. Biol. Fertil. Soils 51, 443–451. https://doi.org/10.1007/s00374-014-0991-y.

Nuzzo, A., Sánchez, A., Fontaine, B., Piccolo, A., 2013. Conformational changes of dissolved humic and fulvic superstructures with progressive iron complexation. J. Geochem. Explor. 129, 1–5. https://doi.org/10.1016/j.gexplo.2013.01.010.

Nuzzo, A., Buurman, P., Cozzolino, V., Spaccini, R., Piccolo, A., 2020. Infrared spectra of soil organic matter under a primary vegetation sequence. Chem. Biol. Technol. Agr. 7, 6. https://doi.org/10.1186/s40538-019-0172-1.

Ogle, S.M., Breidt, F.J., Paustian, K., 2005. Land use and management of agricultural systems is known to change the storage of soil organic carbon (SOC) through variation in land use, tillage, cropping practices (intensity and types of crops), irrigation, fertilization, and other activities. Biogeochemistry 72, 87–121. https://doi.org/10.1007/s10533-004-0360-2.

Olk, D.C., Bloom, P.R., De Nobili, M., Chen, Y., McKnight, D.M., Wells, M.J.M., Weber, J., 2019. Using humic fractions to understand natural organic matter processes in soil and water: selected studies and applications. J. Environ. Qual. 48, 1633–1643. https://doi.org/10.2134/jeq2019.03.0100.

Pan, G., Smith, P., Pan, W., 2009a. The role of soil organic matter in maintaining the productivity and yield stability of cereals in China. Agric. Ecosyst. Environ. 129, 344–348. https://doi.org/10.1016/j.agee.2008.10.008.

Piccolo, A., 2002. The Supramolecular structure of humic substances. A novel understanding of humus chemistry and implications in soil Science. Adv. Agron. 75, 57–134. https://doi.org/10.1016/S0065-2113(02)75003-7.

Piccolo, A., Spaccini, R., Nieder, R., Richter, J., 2004. Sequestration of a biologically labile organic carbon in soils by humified organic matter. Clim. Change 67, 329–343. https://doi.org/10.1007/s10584-004-1822-1.

Piccolo, A., Conte, P., Spaccini, R., Mbagwu, J.S.C., 2005. Influence of land use on the characteristics of humic substances in some tropical soils of Nigeria. Eur. J. Soil Sci. 56, 343–352. https://doi.org/10.1111/j.1365-2389.2004.00671.x.

Piccolo, A., Spaccini, R., Cozzolino, V., Nuzzo, A., Drosos, M., Zavattaro, L., Grignani, C., Puglisi, E., Trevisan, M., 2018a. Effective carbon sequestration in Italian agricultural soils by in situ polymerization of soil organic matter under biomimetic photocatalysis. Land Degrad. Dev. 29, 485–494. https://doi.org/10.1002/ldr.2877.

Piccolo, A., Spaccini, R., Drosos, M., Vinci, G., Cozzolino, V., 2018b. The molecular composition of humus carbon: recalcitrance and reactivity in soils. In: Garcia, C., Nannipieri, P., Hernandez, T. (Eds.), The Future of Soil Carbon: Its Conservation and Formation, 125. Academic Press Elsevier, London Wall, London (UK), pp. 87–124.

Puglisi, E., Fragoulis, G., Del Re, A.A.M., Spaccini, R., Piccolo, A., Gigliotti, G., Said-Pullicino, D., Trevisan, M., 2008. Carbon deposition in soil rhizosphere following amendments with compost and its soluble fractions, as evaluated by combined soil-plant rhizobox and reporter gene systems. In: Chemosphere, 73, pp. 1292–1299. https://doi.org/10.1016/j.chemosphere.2008.07.008.

Savarese, C., Drosos, M., Spaccini, R., Cozzolino, V., Piccolo, A., 2021. Molecular characterization of soil organic matter and its extractable humic fraction from long-term field experiments under different cropping systems. Geoderma 383, 114700. https://doi.org/10.1016/j.geoderma.2020.114700.

Schnitzer, M., Marshall, P.R., Hindle, D.A., 1983. The isolation of soil humic and fulvic acid components rich in "unknown nitrogen". Can. J. Soil Sci. 63, 425–433. https://doi.org/10.4141/cjss83-044.

Schnitzer, M., McArthur, D.F.E., Schulten, H.R., Kozak, L.M., Huang, P.M., 2006. Long-term cultivation effects on the quantity and quality of organic matter in selected Canadian prairie soils. Geoderma 130, 141–156. https://doi.org/10.1016/j.geoderma.2005.01.021.

Smith, P., Bustamante, M., Ahammad, H., Clark, H., Dong, H., Elsiddig, E.A., House, J., 2014. Climate change 2014: Mitigation of climate change. In: Edenhofer, O., Pichs-Madruga, R., Sokona, Y., Farahani, E., Kadner, S., Seyboth, K., Adler, A., Baum, I., Brunner, S., Eickemeier, P., Kriemann, B., Savolainen, J., Schlömer, S., von Stechow, C., Zwickel, T., Minx, J.C. (Eds.), Contribution of working group III to the fifth assessment report of the intergovernmental panel on climate change (IPCC). Cambridge University Press, Cambridge, pp. 816–887.

Song, X.Y., Spaccini, R., Pan, G., Piccolo, A., 2013. Stabilization by hydrophobic protection as a molecular mechanism for organic carbon sequestration in maize-amended rice paddy soils. Sci. Tot. Environ. 458–460, 319–330. https://doi.org/10.1016/j.scitotenv.2013.04.052.

Spaccini, R., Piccolo, A., Conte, P., Haberhauer, G., Gerzabek, M.H., 2002. Increased soil organic carbon sequestration through hydrophobic protection by humic substances. Soil Biol. Biochem. 34, 1839–1851. https://doi.org/10.1016/S0038-0717(02)00197-9.

Spaccini, R., Song, X.Y., Cozzolino, V., Piccolo, A., 2013. Molecular evaluation of soil organic matter characteristics in three agricultural soils by improved off-line thermochemolysis: The effect of hydrofluoric acid demineralisation treatment. Anal. Chim. Acta 802, 46–55. https://doi.org/10.1016/j.aca.2013.09.031.

Spaccini, R., Piccolo, A., 2019. Amendments with humified compost effectively sequester organic carbon in agricultural soils. Land Degrad. Dev. 31, 1206–1216. https://doi.org/10.1002/ldr.3524.

Stevenson, F.J., 1994. Humus Chemistry: Genesis, Composition, Reactions, 2nd ed.,. John Wiley & Sons,, New York, p. 1994.

Vinci, G., Mazzei, P., Drosos, M., Zaccone, C., Piccolo, A., 2020. Molecular characterization of ombrotrophic peats by humeomics. Chem. Biol. Technol. Agr. 7, 18. https://doi.org/10.1186/s40538-020-00184-6.

USDA (United States Department of Agriculture - Soil Survey Staff), 1999. Soil Taxonomy: A Basic System of Soil Classification for Making and Interpreting Soil Surveys, 2nd ed.,. Agriculture Handbook No. 436, USDA, Natural Resources Conservation Service,, New York.

Vinci, G., Cangemi, S., Bridoux, M., Spaccini, R., Piccolo, A., 2021. Molecular properties of the Humeome of two calcareous grassland soils as revealed by GC/qTOF-MS and NMR spectroscopy. Chemosphere 279, 130518. https://doi.org/10.1016/j.chemosphere.2021.130518.

Wells, M.J.M., 2019. Supramolecular answers to the organic matter controversy. J. Environ. Qual. 48, 1644–1651. https://doi.org/10.2134/jeq2019.02.0089.

Wertebach, T.M., Hoelzel, N., Kaempf, I., Yurtaev, A., Tupitsin, S., Kiehl, K., Kamp, J., Kleinebecker, T., 2017. Soil carbon sequestration due to post-Soviet cropland abandonment: estimates from a large-scale soil organic carbon field inventory. Glob. Change Biol. 23 (9), 3729–3741. https://doi.org/10.1111/gcb.13650.

Zaccone, C., Cocozza, C., D'Orazio, V., Plaza, C., Cheburkin, A., Miano, T.M., 2007. Influence of extractant on quality and trace elements content of peat humic acids. Talanta 73, 820–830. https://doi.org/10.1016/j.talanta.2007.04.052.

Zhang, J., Chi, F., Wei, D., Zhou, B., Cai, S., Li, Y., Kuang, E., Sun, L., Li, L.J., 2019. Impacts of Long-term Fertilization on the Molecular Structure of Humic Acid and Organic Carbon Content in Soil Aggregates in Black Soil. Sci. Rep. 9, 11908. https://doi.org/10.1038/s41598-019-48406-8.

Zhou, P., Song, G., Pan, G., Li, L., Zhang, X., 2009. Role of chemical protection by binding to oxyhydrates in SOC sequestration in three typical paddy soils under long-term agro-ecosystem experiments from South China. Geoderma 153, 52–60. https://doi.org/10.1016/j.geoderma.2009.07.018.

Zhou, P., Pan, G.X., Spaccini, R., Piccolo, A., 2010. Molecular changes in particulate organic matter (POM) in a typical Chinese paddy soil under different long-term fertilizer treatments. Eur. J. Soil Sci. 61, 231–242. https://doi.org/10.1111/j.1365-2389.2009.01223.x.

Supporting Information

The impact of long-term field experiments under different cropping systems on the molecular dynamics and stability of the soil Humeome

Claudia Savarese[1,2], Li Xiong[2,3,4], Marios Drosos[3]*, Paola Vitaglione[1], Antonio Scopa[5], Alessandro Piccolo[1,2]*

1. Department of Agricultural Sciences, Università di Napoli Federico II, Via Università 100, 80055 Portici, Italy
2. Interdepartmental Research Centre of Nuclear Magnetic Resonance for the Environment, Agri-Food and New Materials (CERMANU). University of Naples Federico II, Via Università 100, 80055 Portici, Italy
3. Institute of Resource, Ecosystem and Environment of Agriculture (IREEA), Nanjing Agricultural University, 1 Weigang Road, 210095, Nanjing, China
4. Institute of Soil and Fertilizer & Resources and Environment, Jiangxi Academy of Agricultural Sciences, 330200, Nanchang, China
5. Scuola di Scienze Agrarie, Forestali, Alimentari ed Ambientali (SAFE), Università della Basilicata, Viale dell'Ateneo Lucano, 10, 85100 Potenza, Italy

*** Corresponding authors. E-mail addresses: drosos.marios@gmail.com; alessandro.piccolo@unina.it.**

Table S1. Empirical formulae and relative abundance (%) of molecules detected by ESI-Orbitrap-MS and GC-MS in eSOM and all Humeomics fractions of the long-term non-cultivated and no-tilled soil (Control).

eSOM		ORG1		AQU2		ORG2		ORG3		AQU4		RESOM		RESORG	
Emp. formula	Rel. Ab. %	Emp. formula	Rel. Ab. %	Emp. formula	Rel. Ab. %	Emp. formula	Rel. Ab. %	Emp. formula	Rel. Ab. %	Emp. formula	Rel. Ab. %	Emp. formula	Rel. Ab. %	Emp. formula	Rel. Ab. %
C10H15N	1,6	C14H20ON2	1.6	C2H2O2N6	16,5	C14H20ON2	3.8	C14H20ON2	8.6	C2H2O2N6	12,8	C14H20ON2	3,6	C14H20ON2	3.6
C8H9O3N	0,1	C6H12O3	0.1	C10H13N	0,3	C6H12O6	0.4	C13H28O	2.9	C10H13N	0,1	C8H16O2	0,1	C8H16O2	0.1
C12H24O2	1,8	C13H28O	0.5	C10H15N	0,8	C14H14O2	1.2	C5H10O5	1.7	C10H15N	0,3	C8H16O2	0,2	C8H16O2	0.2
C9H19N(FeO)	45,6	C5H10O5	0.4	C8H8O3	0,1	C7H8O3	1.3	C5H10O5	0.8	C7H7O3N	0,1	C7H14O2	traces	C7H14O2	traces
C15H30O2	2,4	C5H10O5	0.3	C7H6O4	traces	C13H28O	1.1	C5H9O5	0.7	C5H11N (FeO)	0,9	C6H12O6	traces	C6H12O6	traces
C16H32O2	1,3	C6H12O5	0.2	C5H11N (FeO)	2,3	C5H10O5	1.1	C6H12O6	0.8	C5H4O6	traces	C13H28O	1,2	C13H28O	1.2
C10H12O2N2 (FeO)	2,5	C6H12O6	0.2	C5H4O6	0,1	C5H10O5	1.4	C6H12O6	0.5	C8H9ON3	traces	C15H32O	0,7	C15H32O	0.7
C18H36O2	5,6	C6H12O5	0.1	C8H9ON3	0,1	C5H10O5	0.4	C6H12O6	3.1	C8J9O3N	traces	C5H10O5	0,7	C5H10O5	0.7
C20H28O2	5,4	C5H9O5	0.2	C9H10O3	traces	C6H12O5	1.9	C16H32O2	0.9	C10H20O2	0,3	C5H10O5	0,7	C5H10O5	0.7
C12H14O3N2 (FeO)	5,5	C14H28O2	0.2	C10H20O2	1,0	C6H12O6	0.3	C6H12O6	1.8	C10H20O3	traces	C5H10O5	0,1	C5H10O5	0.1
C9H8N4 (Fe2O2)	1,6	C6H12O6	0.2	C2H8ON4 (FeO)	0,4	C5H10O5	0.5	C16H32O2	1.4	C9H10ON4	traces	C6H12O6	0,2	C6H12O6	0.2
C23H30O	6,1	C15H30O2	0.3	C6H11ON (FeO)	0,1	C6H12O5	0.3	C6H12O6	0.9	C14H11N	traces	C6H12O5	0,1	C6H12O5	0.1
C10H10O4 (Fe2O2)	2,0	C14H28O2	0.2	C10H20O3	0,1	C5H10O5	0.4	C18H38O2	3.7	C8H4O6	2,2	C5H10O5	0,1	C5H10O5	0.1
C14H14O4N2 (FeO)	1,5	C6H12O6	0.2	C7H12O6	0,1	C5H9O5	1.3	C18H34O2	1.3	C12H24O2	0,3	C5H10O5	0,1	C5H10O5	0.1
C9H8O9N2 (FeO)	4,0	C20H40O2	0.3	C6H10O7	0,1	C5H10O5	0.7	C18H36O2	1.5	C14H22O	0,3	C6H12O6	0,1	C6H12O6	0.1
C3H8N8 (Fe3O3)	1,6	C6H12O6	1.3	C8H4O6	0,5	C6H12O6	0.3	C18H40O	1.3	C10H14O3N2	1,1	C7H14O2	traces	C7H14O2	traces
C12H12O3N8 (FeO)	1,8	C16H32O2	0.9	C12H24O2	0,9	C5H10O5	0.3	C18H36O2	3.9	C9H19N (FeO)	10,8	C14H30O	0,1	C14H30O	0.1
C13H10O2N4 (Fe3O3)	1,4	C6H12O6	0.5	C14H22O	0,9	C7H12O6	0.4	C17H36O4	0.6	C11H10ON4	1,1	C6H12O6	0,1	C6H12O6	0.1
C23H28ON6	1,0	C16H30O2	1.2	C10H14O3N2	2,0	C7H12O6	0.3	C22H43ON	7.4	C7H6O8	0,4	C6H12O6	0,2	C6H12O6	0.2
C19H16O2 (Fe2O2)	1,3	C16H30O2	1.9	C9H19N (FeO)	22,4	C6H12O6	2.9	C22H44O2	0.8	C15H24O	0,3	C6H12O6	0,1	C6H12O6	0.1
C14H12O4N8 (FeO)	0,5	C16H32O2	6.4	C11H10ON4	2,6	C6H12O6	0.8	C16H33O	1.0	C14H28O2	0,6	C6H12O6	0,1	C6H12O6	0.1
C21H14O2 (Fe2O2)	1,0	C18H36O	0.1	C7H6O8	0,6	C6H12O6	1.8	C10H16O4	17.6	C15H30O2	0,6	C6H12O6	0,2	C6H12O6	0.2
C8H10O6N8 (Fe2O2)	0,5	C16H34O	0.5	C14H28O2	1,1	C8H14O7	0.7	C22H44O3	0.9	C9H8O2N2 (FeO)	0,3	C15H32O	0,1	C15H32O	0.1
C23H22N2 (Fe2O2)	0,5	C17H34O2	0.3	C3H8ON2 (FeO)	0,1	C6H12O6	0.4	C24H48O2	1.0	C8H6O3N2 (FeO)	18,1	C15H30O2	0,1	C15H30O2	0.1
C16H16O8 (Fe2O2)	0,6	C6H12O6	0.1	C15H30O2	1,2	C5H10O5	0.5	C21H40O4	1.6	C16H30O2	1,0	C8H14O7	0,1	C8H14O7	0.1
C18H14O8N4 (FeO)	0,3	C17H34O2	0.3	C9H8O2N2 (FeO)	0,3	C6H12O6	4.5	C21H40O4	19.7	C16H32O2	2,2	C15H32O	0,1	C15H32O	0.1
C14H18O6 (Fe3O3)	0,4	C17H34O2	0.2	C16H30O2	2,1	C16H32O2	0.5	C22H44O3	2.3	C13H16O2N4	0,1	C6H12O6	1,4	C6H12O6	1.4
C20H16O6N2 (Fe2O2)	0,5	C38H74O2	0.4	C16H32O2	5,5	C6H12O6	1.5	C26H52O2	1.0	C10H12O2N2(FeO)	0,9	C6H12O6	0,8	C6H12O6	0.8
C35H62O3	0,2	C17H32O2	0.1	C10H12O2N2(FeO)	0,1	C6H12O6	0.4	C27H46O	0.6	C17H34O2	0,3	C16H32O2	0,4	C16H32O2	0.4
C23H22O3 (Fe3O3)	0,2	C13H26O2	0.3	C17H34O2	0,8	C16H32O2	2.1	C28H58O	0.6	C18H36O2	1,3	C16H32O2	3,1	C16H32O2	3.1
C21H20O14 (FeO)	0,1	C18H36O2	0.4	C18H34O2	1,8	C6H12O6	0.3	C30H62O	4.5	C18H28O3	1,0	C16H34O	0,5	C16H34O	0.5
C20H12O7 (Fe3O3)	0,3	C18H38O2	0.7	C18H36O2	2,8	C17H34O2	0.3	C35H68O5	4.9	C20H28O2	1,7	C6H12O6	0,1	C6H12O6	0.1
C24H18O8N2 (Fe2O2)	0,2	C16H32O2	0.1	C2H6O4N4 (Fe2O2)	2,1	C18H36O2	0.3			C12H14O3N2(FeO)	1,6	C17H36O	0,2	C17H36O	0.2
C18H22O7N4 (Fe3O3)	0,1	C6H12O5	0.1	C6H5O2N3 (Fe2O2)	0,3	C18H38O2	4.8			C12H14O3N2(FeO)	0,1	C17H36O	traces	C17H36O	traces
C22H16O9 (Fe3O3)	0,2	C18H36O2	2.4	C20H28O2	2,8	C18H34O2	0.8			C23H30O	16,0	C22H44O2	0,5	C22H44O2	0.5
C24H14O9 (Fe3O3)	0,1	C18H40O	0.3	C12H14O3N2(FeO)	2,8	C18H34O2	0.3			C16H29O2N5	0,2	C18H36O2	1,0	C18H36O2	1.0
C26H18O11 (Fe3O3)	0,1	C19H36O2	0.3	C10H20O2N10	0,8	C18H36O2	0.7			C10H10O4 (Fe2O2)	0,8	C16H32O2	0,1	C16H32O2	0.1
C47H95O2N3	traces	C18H36O2	0.4	C9H8N4 (Fe2O2)	0,9	C18H34O2	0.4			C15H32O8	0,1	C18H34O2	0,7	C18H34O2	0.7
C50H99O4N	traces	C16H32O3	0.1	C20H30O3	0,1	C18H36O2	8.9			C14H14O4N2(FeO)	0,5	C18H36O2	3,1	C18H36O2	3.1
C50H103O3N (FeO)	traces	C11H22O	0.3	C23H30O	3,2	C16H18O2	0.3			C14H21N (Fe2O2)	traces	C18H40O	0,9	C18H40O	0.9
C49H93O10N	traces	C18H36O2	0.3	C16H29O2N5	0,4	C20H40O2	0.3			C15H6O6 (FeO)	0,2	C16H32O2	0,4	C16H32O2	0.4
C48H26O8 (Fe3O3)	traces	C20H40O2	0.8	C10H10O4 (Fe2O2)	1,3	C17H36O4	0.5			C9H8O9N2 (FeO)	0,8	C18H36O2	0,1	C18H36O2	0.1

eSOM	ORG1		AQU2		ORG2		ORG3	AQU4		RESOM		RESORG	
	C8H14O5	0.2	C14H14O4N2(FeO)	2,8	C22H43ON	5.4		C15H8O3N4(FeO)	0,2	C18H36O3	0,5	C18H36O3	0.5
	C9H18O9	0.2	C9H18O5(Fe2O2)	0,1	C22H44O2	0.5		C24H48O2	0,1	C20H40O2	0,3	C20H40O2	0.3
	C17H36O4	0.6	C13H22O11	0,4	C6H12O6	0.3		C3H8N8(Fe3O3)	0,4	C8H14O5	0,7	C8H14O5	0.7
	C21H42O2	0.2	C9H8O9N2(FeO)	1,1	C10H16O4	11.6		C24H30O4	0,3	C17H36O4	0,7	C17H36O4	0.7
	C13H27O3N	0.1	C15H8O3N4(FeO)	0,3	C20H38O4	0.4		C8H18N4(Fe3O3)	3,8	C21H42O2	0,2	C21H42O2	0.2
	C16H34O4	0.2	C24H48O2	0,2	C24H48O2	0.4		C12H12O3N8(FeO)	0,7	C17H36O	0,1	C17H36O	0.1
	C18H34O4	0.3	C13H22O12	0,1	C21H40O4	1.3		C16H23ON(Fe2O2)	0,1	C22H43ON	1,8	C22H43ON	1.8
	C22H43ON	1.8	C3H8N8(Fe3O3)	0,9	C21H40O4	22.3		C13H10O2N4(Fe3O3)	0,5	C22H44O2	1,0	C22H44O2	1.0
	C25H52	0.4	C11H12O2N4(Fe2O2)	0,4	C22H44O3	0.5		C18H12N2(Fe2O2)	0,1	C16H33O	1,9	C16H33O	1.9
	C22H44O2	1.6	C18H18O9	0,1	C23O46O2	0.3		C23H28ON6	0,3	C6H12O6	0,3	C6H12O6	0.3
	C16H33O	0.5	C24H30O4	0,5	C35H68O5	1.7		C17H28O11	traces	C10H16O4	12,3	C10H16O4	12.3
	C6H12O6	0.5	C12H12O3N8(FeO)	0,9	C35H68O5	3.6		C20H16N2(Fe2O2)	0,2	C24H48O2	0,8	C24H48O2	0.8
	C10H16O4	12.8	C16H23ON(Fe2O2)	0,1				C11H12N4(Fe3O3)	0,2	C26H52O2	1,0	C21H40O4	2.1
	C19H38O4	0.1	C13H10O2N4(Fe3O3)	0,7				C19H16O2(Fe2O2)	0,5	C26H52O3	0,7	C21H40O4	24.6
	C23H46O2	0.6	C23H28ON6	0,5				C9H19O4N(Fe3O3)	traces	C23H46O4	0,1	C22H40O4	0.5
	C17H34O	0.1	C19H18O2N4(FeO)	0,1				C28H56O2	traces	C24H50	0,2	C22H44O3	9.4
	C21H40O4	0.2	C17H28O11	0,0				C10H18ON4(Fe3O3)	0,1	C25H52O	0,1	C30H62	0.6
	C20H38O4	0.4	C20H16N2(Fe2O2)	0,3				C9H16O10(Fe2O2)	0,4	C27H54O2	0,3	C24H48O3	0.4
	C30H62	0.3	C11H6O2N2(Fe3O3)	0,4				C14H19N7(Fe2O2)	traces	C27H62O	0,1	C26H52O2	1.0
	C18H24O3N2	0.1	C11H12N4(Fe3O3)	0,3				C11H8O3N2(Fe3O3)	0,1	C24H46O2	0,8	C26H52O3	0.7
	C24H48O2	2.8	C11H14N4(Fe3O3)	0,2				C10H16O8N2(Fe2O2)	0,2	C25H52	1,1	C23H46O4	0.1
	C21H40O4	1.5	C19H16O2(Fe2O2)	0,7				C12H9N5(Fe3O3)	traces	C27H46O	0,9	C24H50	0.2
	C21H40O4	24.6	C9H19O4N(Fe3O3)	0,1				C21H14O2(Fe2O2)	0,4	C28H56O2	1,1	C25H52O	0.1
	C26H50O4	0.2	C28H56O2	traces				C15H16O2(Fe3O3)	0,2	C28H58O	0,8	C27H54O2	0.3
	C22H46	0.2	C14H12O4N8(FeO)	0,3				C18H14O9(FeO)	0,2	C40H82	0,4	C27H62O	0.1
	C25H50O2	0.3	C13H6O6N2(Fe2O2)	0,0				C24H28O4N6	0,1	C26H52O2	0,8	C24H46O2	0.8
	C22H40O4	0.2	C11H8O3N2(Fe3O3)	0,2				C23H46O9	traces	C26H54	0,9	C25H52	1.1
	C22H44O3	2.2	C12H14O4(Fe3O3)	0,1				C11H24O6(Fe3O3)	0,4	C30H60O2	6,4	C27H46O	0.9
	C30H62	0.4	C15H16N2(Fe3O3)	traces				C23H22N2(Fe2O2)	0,1	C27H56	0,3	C28H56O2	1.1
	C23O46O2	0.3	C21H14O2(Fe2O2)	0,6				C24H17O5N(FeO)	traces	C28H56O2	0,6	C28H58O	0.8
	C26H52O2	1.0	C18H14O9(FeO)	0,1				C13H16O2N4(Fe3O3)	0,1	C30H62	0,2	C40H82	0.4
	C26H52O3	1.3	C22H20N2(Fe2O2)	0,1				C16H16O8(Fe2O2)	0,2	C21H42O2	2,5	C26H52O2	0.8
	C23H46O4	0.1	C8H10O6N8(Fe2O2)	0,3				C12H19O2N5(Fe3O3)	traces			C26H54	0.9
	C24H50	0.2	C12H14O2N4(Fe3O3)	traces				C15H16ON4(Fe3O3)	traces			C30H60O2	6.4
	C24H48O2	0.1	C23H46O9	0,1				C18H14O8N4(FeO)	0,1			C27H56	0.3
	C27H54O2	0.1	C23H22N2(Fe2O2)	0,3				C27H30O3N6	0,1			C28H56O2	0.6
	C25H48O3	0.7	C12H24O10(Fe2O2)	0,1				C19H12O7(Fe2O2)	0,1			C30H62	0.2
	C25H52	0.7	C13H10O4N2(Fe3O3)	0,1				C14H18O6(Fe3O3)	0,1			C21H42O2	2.5
	C27H46O	0.6	C13H16O2N4(Fe3O3)	0,2				C14H20O6(Fe3O3)	traces				
	C28H56O2	0.8	C16H16O8(Fe2O2)	0,3				C14H26O4N2(Fe3O3)	0,1				
	C28H58O	1.1	C12H19O2N5(Fe3O3)	traces				C17H12N6(Fe3O3)	0,1				
	C24H40O4	0.2	C18H14O8N4(FeO)	0,2				C12H12O4N6(Fe3O3)	traces				
	C40H82	0.2	C30H40O2N4	0,2				C17H14O10(Fe2O2)	3,9				
	C28H48O	1.1	C14H30O5(Fe3O3)	0,1				C20H16O6N2(Fe2O2)	3,9				
	C29H48O	0.9	C19H12O7(Fe2O2)	0,1				C22H16O11(FeO)	traces				

eSOM	ORG1		AQU2		ORG2	ORG3	AQU4		RESOM	RESORG
	C29H49O	2.6	C14H18O6 (Fe3O3)	0,2			C35H62O3	traces		
	C30H50O	0.7	C14H20O6 (Fe3O3)	0,1			C14H24O8 (Fe3O3)	traces		
	C30H50	0.2	C14H26O4N 2(Fe3O3)	0,3			C12H14O5N 6(Fe3O3)	0,3		
	C30H60O2	2.1	C26H29O6N 5	traces			C13H22O6N 4(Fe3O3)	traces		
	C30H49O	0.2	C28H32O3N 2(FeO)	traces			C20H14O6N 4(Fe2O2)	0,1		
	C30H50O	0.5	C12H12O4N 6(Fe3O3)	0,1			C18H32O2N 4(Fe3O3)	0,1		
	C32H52O2	0.7	C17H14O10 (Fe2O2)	traces			C19H10O3N 4(Fe3O3)	0,1		
	C18H22O2	0.2	C20H16O6N 2(Fe2O2)	0,1			C23H22O3 (Fe3O3)	0,1		
	C21H38O4	0.4	C22H16O11 (FeO)	0,1			C21H20O14 (FeO)	traces		
	C30H48O	0.3	C35H60O3	0,1			C20H14O3N 4(Fe3O3)	traces		
	C30H50O	2.4	C35H62O3	0,2			C21H16ON6 (Fe3O3)	0,1		
	C51H102O4	0.7	C28H32O4N 2(FeO)	traces			C21H28O6 (Fe3O3)	traces		
			C16H34O6 (Fe3O3)	0,1			C24H18O8N 2(Fe2O2)	traces		
			C29H26ON6 (FeO)	0,1			C14H28O12 N2(Fe3O3)	traces		
			C18H32O2N 4(Fe3O3)	0,2			C22H16O9 (Fe3O3)	traces		
			C17H12O6N 2(Fe3O3)	traces			C26H18O7 (Fe3O3)	1,1		
			C19H10O3N 4(Fe3O3)	0,2			C24H14O9 (Fe3O3)	traces		
			C28H28O6N 2(FeO)	0,2			C24H22O7N 2(Fe3O3)	traces		
			C23H22O3 (Fe3O3)	0,1			C27H20O7 (Fe3O3)	traces		
			C21H20O14 (FeO)	0,1			C26H18O11 (Fe3O3)	traces		
			C30H26O2N 6(FeO)	0,2			C37H38O3N 4(Fe2O2)	traces		
			C35H46O4N 4	traces			C47H95O2N 3	traces		
			C39H24O6	traces			C50H99O4N	traces		
			C21H28O6 (Fe3O3)	traces			C50H103O3 N(FeO)	traces		
			C36H62N8	traces			C56H106O (Fe2O2)	traces		
			C25H24O6N 4(Fe2O2)	traces						
			C18H22O7N 4(Fe3O3)	traces						
			C22H16O9 (Fe3O3)	0,1						
			C32H52O13	traces						
			C24H42O11 (Fe2O2)	traces						
			C34H39O3N (Fe2O2)	traces						
			C21H40O7N 8(Fe2O2)	traces						
			C29H36O13 (FeO)	traces						
			C24H22O7N 2(Fe3O3)	traces						
			C27H20O7 (Fe3O3)	traces						
			C34H56O14	traces						
			C47H46O4N 2	traces						
			C31H42O4N 6(Fe2O2)	traces						
			C31H44O4N 6(Fe2O2)	traces						
			C36H36O6N 6(FeO)	traces						
			C26H18O11(Fe3O3)	traces						
			C39H38O9 (FeO)	traces						
			C47H95O2N 3	traces						
			C44H24O8N 4	traces						
			C45H32O3N 4(FeO)	traces						
			C28H38O8N 8(Fe2O2)	traces						

eSOM	ORG1	AQU2		ORG2	ORG3	AQU4	RESOM	RESORG
		$C_{25}H_{46}O_{10}N_8(Fe_2O_2)$	traces					
		$C_{31}H_{39}O_6N_3(Fe_3O_3)$	traces					
		$C_{36}H_{48}O_3N_2(Fe_3O_3)$	traces					
		$C_{50}H_{99}O_4N$	traces					
		$C_{33}H_{57}O_6N(Fe_3O_3)$	traces					
		$C_{37}H_{50}O_3N_2(Fe_3O_3)$	traces					
		$C_{31}H_{52}O_{15}(Fe_2O_2)$	traces					
		$C_{50}H_{103}O_3N(FeO)$	traces					
		$C_{42}H_{45}O_5N_5(Fe_2O_2)$	traces					
		$C_{45}H_{38}O_{17}$	traces					
		$C_{49}H_{93}O_{10}N$	traces					
		$C_{45}H_{44}O_3N_6(Fe_2O_2)$	traces					
		$C_{46}H_{46}O_{16}(FeO)$	traces					
		$C_{31}H_{56}O_{12}N_8(Fe_3O_3)$	traces					
		$C_{51}H_{83}O_9N_9$	traces					

Table S2. Empirical formulae and relative abundance (%) of molecules detected by ESI-Orbitrap-MS and GC-MS in eSOM and all Humeomics fractions of soil under long-term maize mono-cultivation and traditional tillage (Maize).

eSOM		ORG1		AQU2		ORG2		ORG3		AQU4		RESOM		RESORG	
Emp. formula	Rel. Ab. %	Emp. formula	Rel. Ab. %	Emp. formula	Rel. Ab. %	Emp. formula	Rel. Ab. %	Emp. formula	Rel. Ab. %	Emp. formula	Rel. Ab. %	Emp. formula	Rel. Ab. %	Emp. formula	Rel. Ab. %
C12H24O2	1,0	C14H20ON2	3.1	C2H2O2N6	2,3	C14H20ON2	4.4	C14H20ON2	4.3	C2H2O2N6	1,8	C2H2O2N6	23,1	C14H20ON2	5.0
C13H12N3	4,0	C8H16O2	0.2	C10H13N	0,3	C6H12O6	0.4	C6H12O6	0.4	C10H13N	0,2	C10H15N	0,9	C3H7O3N	0.3
C9H19N(FeO)	45,9	C13H28O	1.0	C10H15N	0,8	C14H14O2	2.0	C13H28O	0.8	C10H15N	0,5	C5H11N (FeO)	2,6	C8H16O2	0.1
C15H30O2	2,1	C15H32O	0.5	C8H8O3	0,2	C7H6O3	0.5	C6H12O6	0.6	C7H7O3N	0,1	C8H7ON3	0,0	C4H9O3N	0.1
C16H32O2	8,4	C6H12O6	0.2	C6H9O2N3	traces	C13H28O	1.4	C5H10O5	2.8	C5H11N (FeO)	2,0	C10H20O2	1,4	C8H16O2	0.2
C10H12O2N2 (FeO)	2,5	C16H32O2	0.6	C5H11N (FeO)	2,4	C5H10O5	1.1	C5H10O5	1.0	C5H4O6	0,1	C14H11N	0,1	C4H8O4	0.0
C18H36O2	1,2	C18H38O2	1.9	C5H4O6	0,2	C5H10O5	1.2	C6H12O5	0.4	C8H9ON3	traces	C12H24O2	0,8	C13H28O	1.8
C20H28O2	5,5	C18H34O2	0.3	C8H9ON3	0,1	C5H10O5	0.4	C6H12O6	0.9	C7H7O2N3	traces	C9H19N (FeO)	26,6	C15H32O	0.8
C12H14O3N2 (FeO)	5,7	C18H36O2	0.8	C9H10O3	0,1	C6H12O5	0.8	C6H12O6	0.5	C10H20O2	0,1	C11H10ON4	3,0	C5H10O5	1.7
C9H8N4 (Fe2O2)	1,9	C18H36O2	0.5	C10H20O2	0,1	C5H10O5	0.5	C5H9O5	1.7	C10H20O3	0,1	C14H28O2	1,4	C5H10O5	0.7
C23H30O	6,3	C17H36O4	1.0	C2H8ON4 (FeO)	0,8	C5H10O5	0.5	C5H10O5	52.2	C9H10ON4	traces	C3H8ON2 (Fe2O2)	0,1	C6H12O5	0.4
C14H14O4N2 (FeO)	1,6	C22H43ON	4.3	C6H11ON (FeO)	0,2	C7H7O4	1.1	C6H12O6	0.6	C14H11N	traces	C15H30O2	1,5	C6H12O6	0.2
C9H8O9N2 (FeO)	2,3	C16H33O	0.3	C10H20O3	0,2	C5H9O5	1.1	C6H12O6	1.2	C10H13O3N	traces	C16H30O2	0,2	C5H10O5	0.2
C3H8N8 (Fe3O3)	1,8	C6H12O6	1.0	C7H12O6	0,1	C5H10O5	0.5	C6H12O6	15.2	C12H24O2	0,8	C16H32O2	6,5	C6H12O5	0.1
C12H12O3N8 (FeO)	2,0	C10H16O4	26.7	C8H4O6	0,7	C5H10O5	0.4	C6H12O6	3.2	C14H22O	0,6	C10H12O2N 2(FeO)	1,5	C5H10O5	0.2
C23H28ON6	1,0	C20H38O4	0.8	C12H24O2	1,1	C7H12O6	0.4	C28H56O2	5.0	C10H14O3N 2	1,8	C17H34O2	0,9	C5H10O5	0.3
C14H12O4N8 (FeO)	0,6	C24H48O2	0.3	C14H22O	0,9	C6H12O6	1.8	C6H12O6	0.6	C9H19N (FeO)	14,6	C18H36O2	0,4	C5H10O5	0.2
C21H14O2 (Fe2O2)	1,2	C21H40O4	3.1	C10H14O3N 2	3,5	C6H12O6	0.3	C18H36O2	6.3	C11H10ON4	1,7	C6H5O2N3 (Fe2O2)	0,3	C6H12O6	0.5
C11H6O11 (Fe2O2)	0,5	C21H40O4	49.3	C9H19N (FeO)	23,9	C6H12O6	1.4	C18H36O2	0.4	C7H6O8	0,6	C20H28O2	3,2	C14H28O2	0.1
C24H28O4N6	0,2	C22H44O3	0.8	C11H10ON4	2,7	C8H14O7	0.4	C6H12O6	0.3	C6H11N5 (FeO)	0,2	C12H14O3N 2(FeO)	3,1	C14H30O	0.1
C23H22N2 (Fe2O2)	0,6	C27H46O	0.2	C7H6O8	1,8	C6H12O6	4.7	C17H36O4	0.3	C14H28O2	0,9	C9H8N4 (Fe2O2)	1,1	C11H20O4	0.1
C16H16O8 (Fe2O2)	0,7	C28H58O	0.4	C6H11N5 (FeO)	3,2	C6H12O6	1.4	C10H16O4	0.3	C3H8ON2 (Fe2O2)	0,1	C23H30O	3,4	C6H12O6	0.1
C18H14O8N4 (FeO)	0,4	C7H1602	0.4	C14H28O2	1,3	C6H12O6	0.5	C21H40O4	0.4	C15H30O2	0,9	C16H29O2N 5	0,6	C6H12O6	0.1
C14H18O6 (Fe3O3)	0,5	C24H40O4	0.3	C3H8ON2 (FeO)	0,1	C18H36O2	0.6	C17H18	0.7	C9H8O2N2 (FeO)	0,4	C11H22O2N 10	0,3	C6H12O6	0.1
C20H16O6N2 (Fe2O2)	0,5	C40H82	0.7	C15H30O2	1,3	C18H36O2	5.8			C8H6O3N2 (FeO)	25,0	C10H10O4 (Fe2O2)	1,1	C6H12O6	0.1
C35H62O3	0,2	C24H39O4	0.4	C9H8O2N2 (FeO)	0,2	C17H36O4	1.0			C5H9O6N (FeO)	1,4	C20H34O4	0,2	C6H12O6	0.6
C23H22O3 (Fe3O3)	0,3	C33H68	0.4	C16H30O2	1,9	C22H43ON	5.7			C16H30O2	1,4	C22H17O3N	traces	C15H30O2	0.3
C21H20O14 (FeO)	0,1	C30H60O2	0.2	C16H32O2	6,1	C10H16O4	21.7			C16H32O2	4,2	C14H14O4N 2(FeO)	0,9	C9H12O6	0.1
C20H12O7 (Fe3O3)	0,3	C40H82	0.3	C10H12O2N 2(FeO)	1,2	C20H38O4	0.6			C10H12O2N 2(FeO)	1,4	C9H18O5 (Fe2O2)	0,1	C8H14O7	0.3
C24H18O8N2 (Fe2O2)	0,2			C17H34O2	0,9	C24H48O2	0.3			C17H34O2	0,5	C25H26N2	0,2	C6H12O6	2.8
C18H22O7N4 (Fe3O3)	0,1			C18H34O2	1,8	C21H40O4	36.9			C18H36O2	0,1	C14H22O7N 4	0,1	C6H12O6	1.5
C22H16O9 (Fe3O3)	0,2			C18H36O2	3,4	C26H50O4	0.4			C6H5O2N3 (Fe2O2)	0,1	C9H8O9N2 (FeO)	1,3	C16H32O2	0.9
C24H14O9 (Fe3O3)	0,2			C2H6O4N4 (Fe2O2)	2,3					C20H28O2	2,3	C15H8O3N4 (FeO)	0,4	C16H32O2	5.4
C26H18O11 (Fe3O3)	0,1			C6H5O2N3 (Fe2O2)	0,4					C20H30O2	0,6	C3H8N8 (Fe3O3)	1,0	C16H34O	0.4
C47H95O2N3	traces			C20H28O2	3,4					C12H14O5N 6(Fe3O3)	2,7	C6H8O6N4 (Fe2O2)	0,5	C22H44O2	0.4
C50H99O4N	traces			C12H14O3N 2(FeO)	0,4					C9H17O6N (FeO)	0,2	C24H30O4	0,6	C6H14O2	0.2
C50H103O3N (FeO)	traces			C10H20O2N 10	1,1					C9H8N4 (Fe2O2)	0,9	C12H12O3N 8(FeO)	1,3	C18H36O2	1.9
C49H93O10N	traces			C9H8N4 (Fe2O2)	1,1					C23H30O	2,6	C24H34O4	0,1	C5H8O5	0.6
C48H26O8 (Fe3O3)	traces			C23H30O	3,8					C16H29O2N 5	0,3	C12H12O3N 8(FeO)	1,3	C18H34O2	1.4
				C16H29O2N 5	0,5					C13H10O4N 2(FeO)	0,3	C24H34O4	0,1	C18H36O2	3.3
				C13H10O4N 2(FeO)	0,2					C10H10O4 (Fe2O2)	1,0	C16H23ON (Fe2O2)	0,1	C18H40O	1.4

eSOM	ORG1	AQU2		ORG2	ORG3	AQU4		RESOM		RESORG	
		C10H10O4 (Fe2O2)	1,3			C20H34O4	1,0	C4H10O4N4 (Fe3O3)	0,2	C16H32O2	1.7
		C20H34O4	1,3			C13H18O7N 4	0,1	C13H10O2N 4(Fe3O3)	0,5	C8H14O5	0.3
		C13H18O7N 4	0,2			C12H14O4N 2(FeO)	0,5	C27H30ON2	0,1	C18H36O3	0.1
		C14H14O4N 2(FeO)	0,7			C14H21N (Fe2O2)	0,1	C23H28ON6	0,6	C20H40O2	0.2
		C9H18O5 (Fe2O2)	0,2			C15H6O6 (FeO)	0,2	C18H14O2 (Fe2O2)	0,2	C17H36O4	0.6
		C13H22O11	0,5			C15H18O3N 8	0,1	C20H16N2 (Fe2O2)	0,3	C18H34O4	0.2
		C15H18O3N 8	0,2			C9H8O9N2 (FeO)	1,1	C19H16O2 (Fe2O2)	0,8	C22H43ON	2.6
		C9H8O9N2 (FeO)	1,0			C8H18O3N4 (Fe2O2)	0,3	C9H19O4N (Fe3O3)	0,1	C28H52O4	0.1
		C15H8O3N4 (FeO)	0,3			C15H8O3N4 (FeO)	0,3	C14H12O4N 8(FeO)	0,3	C22H44O2	0.8
		C13H22O12	0,2			C3H8N8 (Fe3O3)	0,4	C11H8O3N2 (Fe3O3)	0,3	C16H33O	1.3
		C3H8N8 (Fe3O3)	1,0			C5H12O10 (Fe2O2)	0,4	C6H12O5N4 (Fe3O3)	0,4	C6H12O6	0.5
		C11H12O2N 4(Fe2O2)	0,5			C24H30O4	0,3	C12H9N5 (Fe3O3)	traces	C10H16O4	18.9
		C18H18O9	0,1			C20H28O2N 6	0,1	C21H14O2 (Fe2O2)	0,6	C21H40O4	1.8
		C24H30O4	0,6			C8H18N4 (Fe3O3)	4,9	C29H34O2N 2	0,1	C21H40O4	28.3
		C17H22O3N 8	0,1			C12H12O3N 8(FeO)	1,0	C18H14O9 (FeO)	0,1	C22H44O3	5.2
		C12H12O3N 8(FeO)	1,1			C16H23ON (Fe2O2)	0,1	C11H10O4N 2(Fe3O3)	0,1	C30H62	0.1
		C16H23ON (Fe2O2)	0,1			C5H6N8(Fe3 O3)	0,1	C11H6O11 (Fe2O2)	0,3	C27H54O2	0.0
		C5H6N8 (Fe3O3)	0,3			C13H10O2N 4(Fe3O3)	0,7	C23H22N2 (Fe2O2)	0,4	C25H52	0.1
		C13H10O2N 4(Fe3O3)	0,9			C18H12N2 (Fe2O2)	0,2	C24H17O5N (FeO)	traces	C27H46O	0.9
		C23H28ON6	0,5			C23H28ON6	0,5	C13H16O2N 4(Fe3O3)	0,3	C28H56O2	0.1
		C18H14O2 (Fe2O2)	0,2			C18H14O2 (Fe2O2)	0,1	C16H16O8 (Fe2O2)	0,4	C28H58O	0.4
		C17H28O11	traces			C17H28O11	traces	C12H19O2N 5(Fe3O3)	0,1	C32H66	0.1
		C20H16N2 (Fe2O2)	0,2			C20H16N2 (Fe2O2)	traces	C18H14O8N 4(FeO)	0,1	C33H68	0.3
		C11H6O2N2 (Fe3O3)	0,5			C19H14N2 (Fe2O2)	0,5	C14H30O5 (Fe3O3)	0,1	C30H60O2	0.5
		C11H12N4 (Fe3O3)	0,3			C19H16O2 (Fe2O2)	0,7	C14H18O6 (Fe3O3)	0,3		
		C11H14N4 (Fe3O3)	0,2			C19H10O7 (FeO)	0,1	C14H26O4N 2(Fe3O3)	0,4		
		C19H16O2 (Fe2O2)	0,7			C28H56O2	traces	C13H21O6N (Fe3O3)	0,1		
		C9H19O4N (Fe3O3)	0,1			C10H18ON4 (Fe3O3	0,1	C34H68O2	traces		
		C28H56O2	0,1			C14H12O4N 8(FeO)	0,5	C17H14O5 (Fe3O3)	0,1		
		C14H12O4N 8(FeO)	0,3			C9H18O10 (Fe2O2)	0,1	C17H22O3N 2(Fe3O3)	0,3		
		C13H6O6N2 (Fe2O2)	0,1			C11H8O3N2 (Fe3O3)	0,1	C12H12O4N 6(Fe3O3)	0,1		
		C11H8O3N2 (Fe3O3)	0,3			C10H16O8N 2(Fe2O2)	0,3	C20H16O6N 2(Fe2O2)	0,3		
		C12H14O4 (Fe3O3)	0,1			C13H14O6N 2(Fe2O2)	0,1	C35H60O3	0,1		
		C21H14O2 (Fe2O2)	0,5			C12H9N5 (Fe3O3)	traces	C35H62O3	0,1		
		C29H34O2N 2	0,5			C21H14O2 (Fe2O2)	0,5	C15H20O8 (Fe3O3)	traces		
		C18H14O9 (FeO)	0,1			C15H16O2 (Fe3O3)	0,2	C19H10O3N 4(Fe3O3)	0,2		
		C11H10O4N 2(Fe3O3)	0,1			C18H14O9 (FeO)	0,1	C23H22O3 (Fe3O3)	0,2		
		C22H20N2 (Fe2O2)	0,2			C11H10O4N 2(Fe3O3)	traces	C21H20O14 (FeO)	traces		
		C8H10O6N8 (Fe2O2)	0,2			C13H16O13 (FeO)	0,1	C20H12O7 (Fe3O3)	0,1		
		C12H14O2N 4(Fe3O3)	0,1			C15H8O6N2 (Fe2O2)	0,1	C21H16ON6 (Fe3O3)	0,2		
		C23H46O9	0,1			C8H10O6N8 (Fe2O2)	0,2	C24H18O8N 2(Fe2O2)	0,1		
		C23H22N2 (Fe2O2)	0,3			C24H30O7N 2	0,2	C29H22O6 (Fe2O2)	traces		
		C24H17O5N (FeO)	traces			C24H28O4N 6	0,1	C18H22O7N 4(Fe3O3)	traces		
		C13H10O4N 2(Fe3O3)	0,1			C23H46O9	0,1	C22H16O9 (Fe3O3)	0,1		
		C13H16O2N 4(Fe3O3)	0,2			C11H24O6 (Fe3O3)	0,5	C29H22O5N 4(Fe2O2)	traces		

eSOM	ORG1	AQU2		ORG2	ORG3	AQU4		RESOM		RESORG
		C16H16O8 (Fe2O2)	traces			C23H22N2 (Fe2O2)	0,3	C24H14O9 (Fe3O3)	0,1	
		C12H19O2N 5(Fe3O3)	0,1			C24H17O5N (FeO)	traces	C24H22O7N 2(Fe3O3)	traces	
		C18H14O8N 4(FeO)	0,2			C13H16O2N 4(Fe3O3)	0,2	C31H24O3N 2(Fe3O3)	traces	
		C30H40O2N 4	0,3			C16H16O8 (Fe2O2)	0,3	C26H18O11 (Fe3O3)	traces	
		C14H30O5 (Fe3O3)	0,1			C12H19O2N 5(Fe3O3)	traces	C47H95O2N 3	traces	
		C19H12O7 (Fe2O2)	1,7			C18H14O8N 4(FeO)	0,1	C22H30O13 N2(Fe3O3)	traces	
		C14H18O6 (Fe3O3)	0,2			C27H30O3N 6	0,1	C50H99O4N	traces	
		C14H20O6 (Fe3O3)	0,1			C19H12O7 (Fe2O2)	0,2	C31H38O8N 4(Fe3O3)	traces	
		C14H26O4N 2(Fe3O3)	0,3			C14H18O6 (Fe3O3)	0,2	C50H103O3 N(FeO)	traces	
		C13H21O6N (Fe3O3)	traces			C14H26O4N 2(Fe3O3)	0,4	C49H93O10 N	traces	
		C18H28O12 (FeO)	traces			C17H12N6 (Fe3O3)	0,1	C56H106O (Fe2O2)	traces	
		C17H14O5 (Fe3O3)	0,1			C12H12O4N 6(Fe3O3)	0,1	C48H26O8 (Fe3O3)	traces	
		C19H24O13 N4	traces			C17H14O10 (Fe2O2)	4,8			
		C12H12O4N 6(Fe3O3)	0,1			C20H16O6N 2(Fe2O2)	0,3			
		C17H14O10 (Fe2O2)	traces			C22H16O11 (FeO)	traces			
		C20H16O6N 2(Fe2O2)	0,2			C35H62O3	traces			
		C22H16O11 (FeO)	0,1			C14H24O8 (Fe3O3)	0,1			
		C35H60O3	0,1			C12H14O5N 6(Fe3O3)	0,4			
		C35H62O3	0,2			C13H22O6N 4(Fe3O3)	traces			
		C16H34O6 (Fe3O3)	0,2			C18H32O2N 4(Fe3O3)	0,2			
		C24H28O14	0,1			C19H10O3N 4(Fe3O3)	0,2			
		C15H20O8 (Fe3O3)	0,1			C23H22O3 (Fe3O3)	0,2			
		C29H26ON6 (FeO)	0,1			C21H20O14 (FeO)	0,1			
		C18H32O2N 4(Fe3O3)	0,3			C20H14O3N 4(Fe3O3)	0,1			
		C17H12O6N 2(Fe3O3)	0,3			C20H12O7 (Fe3O3)	0,2			
		C19H10O3N 4(Fe3O3)	0,2			C21H16ON6 (Fe3O3)	0,1			
		C28H28O6N 2(FeO)	0,1			C20H14ON4 (Fe3O3)	traces			
		C23H22O3 (Fe3O3)	0,1			C21H28O6 (Fe3O3)	traces			
		C21H20O14 (FeO)	0,1			C24H18O8N 2(Fe2O2)	0,1			
		C30H35O4N 3(Fe3O3)	traces			C29H22O6 (Fe2O2)	traces			
		C22H24O9 (Fe2O2)	0,1			C14H28O12 N2(Fe3O3)	traces			
		C20H12O7 (Fe3O3)	0,1			C22H16O9 (Fe3O3)	0,1			
		C21H34O6N 4(Fe2O2)	traces			C26H18O7 (Fe3O3)	1,3			
		C21H16ON6 (Fe3O3)	0,1			C24H14O9 (Fe3O3)	0,1			
		C21H28O6 (Fe3O3)	traces			C24H22O7N 2(Fe3O3)	traces			
		C21H24O5N 2(Fe3O3)	0,1			C26H18O11 (Fe3O3)	traces			
		C24H18O8N 2(Fe2O2)	0,1			C50H99O4N	traces			
		C36H62N8	traces							
		C25H24O6N 4(Fe2O2)	traces							
		C18H22O7N 4(Fe3O3)	traces							
		C26H26O6N 4(Fe2O2)	traces							
		C22H16O9 (Fe3O3)	0,1							
		C33H63O6N (FeO)	0,1							
		C32H52O13	traces							
		C46H34O4	traces							

eSOM	ORG1	AQU2		ORG2	ORG3	AQU4	RESOM	RESORG
		C24H22O7N2(Fe3O3)	traces					
		C31H24O3N2(Fe3O3)	traces					
		C31H44O4N6(Fe2O2)	traces					
		C46H66O6	traces					
		C26H18O11(Fe3O3)	traces					
		C39H38O9(FeO)	traces					
		C28H42O6N8(Fe2O2)	traces					
		C44H24O8N4	traces					
		C25H46O10N8(Fe2O2)	traces					
		C31H39O6N3(Fe3O3)	traces					
		C50H99O4N	traces					
		C55H107N	traces					
		C48H97O3N(FeO)	traces					
		C51H88O7	traces					
		C50H99O2N(FeO)	traces					
		C50H103O3N(FeO)	traces					
		C49H93O10N	traces					
		C51H103O2N(Fe2O2)	traces					
		C46H46O16(FeO)	traces					
		C56H106O(Fe2O2)	traces					
		C48H26O8(Fe3O3)	traces					
		C55H107N	traces					

Table S3. Empirical formulae and relative abundance (%) of molecules detected by ESI-Orbitrap-MS and GC-MS in eSOM and all Humeomics fractions of soil under long-term maize-broad bean crop rotation and traditional tillage (Mix).

eSOM		ORG1		AQU2		ORG2		ORG3		AQU4		RESOM		RESORG	
Emp. formula	Rel. Ab. %	Emp. formula	Rel. Ab. %	Emp. formula	Rel. Ab. %	Emp. formula	Rel. Ab. %	Emp. formula	Rel. Ab. %	Emp. formula	Rel. Ab. %	Emp. formula	Rel. Ab. %	Emp. formula	Rel. Ab. %
C10H15N	1,4	C14H20ON2	3.4	C2H2O2N6	20,1	C14H20ON2	8.1	C14H20ON2	1.4	C2H2O2N6	14,9	C2H2O2N6	14,9	C14H20ON2	2.7
C8H9O3N	0,2	C13H28O	1.1	C10H13N	0,3	C6H12O6	0.9	C9H5O4N	0.0	C10H13N	0,2	C10H13N	0,2	C8H16O2	0.1
C12H24O2	1,6	C15H32O	0.6	C10H15N	0,7	C14H14O2	3.5	C8H16O2	0.0	C10H15N	0,4	C10H15N	0,4	C5H12O3	0.1
C9H19N(FeO)	38,5	C6H12O6	0.5	C8H8O3	0,1	C13H28O	3.0	C6H6O3	0.1	C7H7O3N	0,1	C7H7O3N	0,1	C5H14O8	0.1
C15H30O2	2,2	C16H32O2	0.7	C7H6O4	0,1	C5H10O5	2.3	C6H12O6	0.1	C5H11N (FeO)	1,7	C5H11N (FeO)	1,7	C13H28O	0.9
C16H32O2	9,9	C18H38O2	2.4	C6H9O2N3	traces	C5H10O5	2.7	C6H12O6	0.1	C5H4O6	0,1	C5H4O6	0,1	C15H32O	0.5
C10H12O2N2 (FeO)	2,4	C18H34O2	0.3	C5H11N (FeO)	2,2	C5H10O5	0.9	C5H10O5	0.1	C8H9ON3	traces	C8H9ON3	traces	C5H10O5	1.8
C18H36O2	5,0	C18H36O2	1.4	C9H6O3	0,1	C6H12O5	2.3	C7H8O3	2.4	C7H7O2N3	traces	C7H7O2N3	traces	C5H10O5	0.6
C20H28O2	5,2	C18H40O	0.3	C8H4O4	0,1	C5H10O5	1.2	C13H28O	0.5	C10H20O2	1,0	C10H20O2	1,0	C12H26O	0.2
C12H14O3N2 (FeO)	5,5	C18H36O2	1.4	C10H20O2	1,3	C5H10O5	0.9	C6H12O6	0.6	C10H20O3	0,1	C10H20O3	0,1	C5H10O5	0.1
C9H8N4 (Fe2O2)	1,8	C20H40O2	0.2	C2H8ON4 (FeO)	0,7	C5H10O5	1.3	C5H10O5	1.2	C9H10ON4	traces	C9H10ON4	traces	C6H12O6	0.6
C23H30O	5,9	C17H36O4	0.9	C10H20O3	0,1	C6H12O6	2.7	C5H10O5	0.4	C14H11N	traces	C14H11N	traces	C6H12O5	0.3
C10H10O4 (Fe2O2)	2,4	C22H43ON	4.3	C7H12O6	0,1	C6H12O6	1.9	C6H12O6	0.7	C10H13O3N	traces	C10H13O3N	traces	C5H10O5	0.5
C14H14O4N2 (FeO)	1,5	C22H44O2	0.4	C6H10O7	0,1	C6H12O6	6.7	C6H12O6	0.3	C8H4O6	2,8	C8H4O6	2,8	C5H10O5	0.1
C9H8O9N2 (FeO)	2,2	C16H33O	0.4	C8H4O6	0,5	C6H12O6	2.2	C5H10O5	0.0	C12H24O2	0,6	C12H24O2	0,6	C4H9O5	0.2
C3H8N8 (Fe3O3)	1,8	C6H12O6	0.9	C12H24O2	1,0	C16H32O2	1.0	C6H12O6	0.1	C14H22O	0,4	C14H22O	1,1	C14H28O2	1.1
C12H12O3N8 (FeO)	1,9	C10H16O4	24.7	C14H22O	0,8	C18H38O2	6.0	C5H12O5	0.1	C10H14O3N2	1,5	C9H19N (FeO)	28,9	C14H30O	0.5
C13H10O2N4 (Fe3O3)	1,4	C20H38O4	0.8	C10H14O3N2	2,8	C18H36O2	5.1	C5H10O5	0.1	C9H19N (FeO)	11,9	C11H10ON4	2,9	C11H20O4	0.2
C23H28ON6	0,9	C24H48O2	0.7	C9H19N (FeO)	21,6	C17H36O4	0.8	C5H9O5	4.0	C11H10ON4	1,4	C15H24O	2,2	C6H12O6	0.2
C10H8O4N6 (Fe2O2)	1,4	C21H40O4	3.0	C11H10ON4	2,5	C22H43ON	4.4	C5H10O5	1.1	C7H6O8	0,5	C14H28O2	1,3	C16H32O2	0.2
C14H12O4N8 (FeO)	0,6	C21H40O4	47.4	C7H6O8	1,8	C10H16O4	15.4	C9H8O3	0.9	C6H11N5 (FeO)	0,2	C3H8ON2 (Fe2O2)	0,1	C15H30O2	0.3
C21H14O2 (Fe2O2)	1,1	C22H44O3	1.5	C6H11N5 (FeO)	0,3	C21H40O4	21.7	C6H12O6	0.5	C14H28O2	0,7	C15H30O2	1,3	C18H34O3	0.2
C11H10O4N2 (Fe3O3)	0,1	C26H52O3	0.4	C14H28O2	1,2	C26H50O4	0.8	C6H12O6	0.1	C3H8ON2 (Fe2O2)	0,1	C14H21O3N	0,5	C6H12O6	0.6
C11H6O11 (Fe2O2)	0,5	C28H58O	0.5	C15H30O2	1,2	C35H68O5	4.2	C5H10O5	0.3	C15H30O2	0,8	C16H30O2	2,3	C15H30O2	0.9
C24H28O4N6	0,2	C24H39O4	0.3	C9H8O2N2 (FeO)	0,1			C6H12O6	0.2	C9H8O2N2 (FeO)	0,3	C16H32O2	5,5	C5H10O7	0.4
C23H22N2 (Fe2O2)	0,6	C29H49O	0.6	C16H30O2	1,8			C6H12O6	0.1	C8H6O3N2 (FeO)	19,3	C10H12O2N2(FeO)	1,3	C6H12O6	0.6
C16H16O8 (Fe2O2)	0,7	C30H60O2	0.7	C16H32O2	5,3			C14H30O	0.2	C5H9O6N (FeO)	1,0	C17H34O2	0,7	C15H32O	0.1
C18H14O8N4 (FeO)	0,4	C51H102O4	0.2	C10H12O2N2(FeO)	1,0			C6H12O6	0.8	C16H30O2	1,2	C18H36O2	3,3	C6H12O6	11.0
C14H18O6 (Fe3O3)	0,5			C17H34O2	0,8			C9H8O3	5.9	C16H32O2	3,3	C20H28O2	3,4	C6H12O6	2.7
C20H16O6N2 (Fe2O2)	0,5			C18H34O2	1,7			C5H7ON3	0.9	C10H12O2N2(FeO)	1,2	C12H14O3N2(FeO)	3,2	C16H32O2	2.4
C35H62O3	0,2			C18H36O2	2,8			C6H12O6	0.7	C17H34O2	0,4	C9H8N4 (Fe2O2)	0,7	C16H32O2	8.9
C23H22O3 (Fe3O3)	0,3			C2H6O4N4 (Fe2O2)	1,7			C15H30O2	0.6	C18H36O2	1,5	C23H30O	3,5	C16H34O	1.2
C21H20O14 (FeO)	0,1			C6H5O2N3 (Fe2O2)	0,3			C6H10O7	0.4	C18H28O3	1,9	C16H29O2N5	0,5	C13H26O2	0.5
C20H12O7 (Fe3O3)	0,3			C20H28O2	0,3			C6H12O6	5.3	C6H5O2N3 (Fe2O2)	0,1	C11H22O2N10	0,3	C6H12O6	0.4
C24H18O8N2 (Fe2O2)	0,2			C12H14O3N2(FeO)	3,2			C6H12O6	1.9	C20H28O2	1,9	C10H10O4 (Fe2O2)	0,7	C22H46	0.7
C18H22O7N4 (Fe3O3)	0,1			C13H17O4N5	0,3			C16H30O2	1.6	C20H30O2	0,5	C20H34O4	0,2	C22H44O2	0.7
C22H16O9 (Fe3O3)	0,2			C9H8N4 (Fe2O2)	1,0			C16H32O2	9.1	C12H14O5N6(Fe3O3)	2,4	C22H17O3N	traces	C18H36O2	4.2
C24H14O9 (Fe3O3)	0,2			C23H30O	3,3			C16H34O	0.5	C9H17O6N (FeO)	0,2	C14H14O4N2(FeO)	0,8	C18H34O2	2.3
C26H18O11 (Fe3O3)	0,1			C16H29O2N5	0,5			C17H34O2	0.3	C9H8N4 (Fe2O2)	0,7	C25H26N2	0,2	C18H36O2	3.3
C47H95O2N3	traces			C11H22O2N5	0,3			C6H12O6	0.2	C23H30O	2,0	C14H22O7N4	0,1	C18H40O	2.3
C50H99O4N	traces			C13H10O4N2(FeO)	0,1			C18H38O2	3.3	C16H29O2N5	0,3	C9H8O9N2 (FeO)	0,8	C38H78	0.8
C50H103O3N (FeO)	traces			C10H10O4 (Fe2O2)	1,1			C8H6O4	0.6	C13H10O4N2(FeO)	0,3	C15H8O3N4(FeO)	0,3	C16H32O2	2.8

eSOM		ORG1	AQU2		ORG2	ORG3		AQU4		RESOM		RESORG	
C49H93O10N	traces		C12H20O11	traces		C18H34O2	1.5	C10H10O4 (Fe2O2)	0,9	C3H8N8 (Fe3O3)	1,0	C18H36O2	0.2
C48H26O8 (Fe3O3)	traces		C14H14O4N 2(FeO)	0,6		C18H36O2	6.0	C20H34O4	0,9	C24H30O4	0,4	C44H88O2	0.3
			C13H22O11	0,4		C18H40O	1.6	C13H18O7N 4	0,1	C12H12O3N 8(FeO)	1,3	C20H42O	0.1
			C9H8O9N2 (FeO)	0,1		C18H36O2	0.4	C12H14O4N 2(FeO)	0,7		C24H3 4O4	0,1	0.1
			C15H8O3N4 (FeO)	0,3		C11H20O4	0.2	C14H21N (Fe2O2)	traces	C16H23ON (Fe2O2)	0,1	C20H40O2	0.4
			C15H20O7N 4	0,2		C18H38O2	0.2	C15H6O6 (FeO)	0,2	C13H10O2N 4(Fe3O3)	0,5	C20H42O	0.8
			C13H22O12	0,1		C20H40O2	0.2	C15H18O3N 8	0,1	C27H30ON2	0,1	C17H36O4	0.3
			C3H8N8 (Fe3O3)	0,7		C20H42O	0.4	C9H8O9N2 (FeO)	0,9	C23H28ON6	0,3	C17H36O	0.2
			C24H30O4	0,6		C17H36O4	0.2	C15H8O3N4 (FeO)	0,2	C18H14O2 (Fe2O2)	0,1	C21H42O2	0.1
			C15H20O8N 4	0,2		C16H32O4	0.9	C22H38O4	0,2	C20H16N2 (Fe2O2)	0,3	C17H36O	0.1
			C25H15N5	traces		C18H36O4	0.6	C3H8N8 (Fe3O3)	0,3	C19H16O2 (Fe2O2)	0,4	C18H36O4	0.4
			C12H12O3N 8(FeO)	1,0		C22H43ON	0.2	C5H12O10 (Fe2O2)	0,3	C9H19O4N (Fe3O3)	traces	C22H43ON	0.1
			C16H23ON (Fe2O2)	0,1		C22H44O2	1.0	C24H30O4	0,3	C28H56O2	0,1	C22H42O2	0.2
			C15H20O12	0,1		C16H33O	2.5	C20H28O2N 6	0,1	C14H12O4N 8(FeO)	0,2	C24H48O3	0.2
			C17H32O10	0,3		C10H16O4	4.4	C8H18N4 (Fe3O3)	3,7	C21H14O2 (Fe2O2)	0,4	C22H44O2	1.2
			C13H10O2N 4(Fe3O3)	0,8		C20H38O2	0.4	C12H12O3N 8(FeO)	0,9	C29H34O2N 2	0,1	C16H33O	1.8
			C20H29O2N 7	0,1		C22H44O3	0.2	C16H23ON (Fe2O2)	0,1	C18H14O9 (FeO)	0,1	C10H16O4	5.7
			C23H28ON6	0,5		C24H48O2	0.3	C5H6N8 (Fe3O3)	0,1	C15H20O8 (Fe3O3)	traces	C20H38O4	0.2
			C18H14O2 (Fe2O2)	0,2		C24H50O	0.4	C13H10O2N 4(Fe3O3)	0,6	C19H10O3N 4(Fe3O3)	0,1	C24H48O2	0.3
			C17H28O11	traces		C21H40O4	9.8	C18H12N2 (Fe2O2)	0,1	C23H22O3 (Fe3O3)	0,2	C24H50O	0.7
			C20H16N2 (Fe2O2)	0,2		C22H42O2	17.1	C23H28ON6	0,4	C21H20O14 (FeO)	traces	C21H40O4	11.4
			C11H6O2N2 (Fe3O3)	0,4		C24H46O2	0.7	C17H28O11	0,0	C20H12O7 (Fe3O3)	0,1	C22H42O2	3.9
			C11H12N4 (Fe3O3)	0,3		C27H46O	0.7	C20H16N2 (Fe2O2)	0,2	C21H16ON6(Fe3O3)	0,1	C24H48O3	0.2
			C11H14N4 (Fe3O3)	0,2		C28H58O	0.7	C19H14N2 (Fe2O2)	0,4	C24H18O8N 2(Fe2O2)	0,1	C26H52O3	0.1
			C19H16O2 (Fe2O2)	0,6		C18H22O2	0.6	C19H16O2 (Fe2O2)	0,6	C29H22O6 (Fe2O2)	traces	C25H52	0.3
			C9H19O4N (Fe3O3)	0,1		C30H62O	0.4	C19H10O7 (FeO)	0,1	C18H22O7N 4(Fe3O3)	traces	C27H46O	1.8
			C14H12O4N 8(FeO)	0,2		C31H64	0.3	C28H56O2	traces	C22H16O9 (Fe3O3)	0,1	C28H58O	0.8
			C11H8O3N2 (Fe3O3)	0,2		C40H82	0.4	C10H18ON4 (Fe3O3)	0,1	C29H22O5N 4(Fe2O2)	traces	C40H82	1.5
			C20H18O11	0,1				C14H12O4N 8(FeO)	0,4	C24H14O9(Fe3O3)	0,1	C30H60O2	2.0
			C12H14O4 (Fe3O3)	0,1				C14H19N7 (Fe2O2)	traces	C24H22O7N 2(Fe3O3)	traces	C35H68O5	6.2
			C15H16N2 (Fe3O3)	traces				C11H8O3N2 (Fe3O3)	0,1	C42H85O5N	traces		
			C21H14O2 (Fe2O2)	0,4				C10H16O8N 2(Fe2O2)	0,2	C31H24O3N 2(Fe3O3)	traces		
			C29H34O2N 2	0,4				C14H10O2N 6(Fe2O2)	0,1	C47H94O2	traces		
			C22H12O7N 4	0,1				C12H9N5 (Fe3O3)	traces	C26H18O11 (Fe3O3)	traces		
			C18H14O9 (FeO)	0,1				C21H14O2 (Fe2O2)	0,4	C47H95O2N 3	traces		
			C22H34O4N 6	0,1				C15H16O2 (Fe3O3)	0,2	C22H30O13 N2(Fe3O3)	traces		
			C21H20O11	traces				C18H14O9 (FeO)	0,1	C50H99O4N	traces		
			C11H10O4N 2(Fe3O3)	0,1				C11H10O4N 2(Fe3O3)	traces	C50H103O3 N(FeO)	traces		
			C21H22O11	0,1				C13H16O13 (FeO)	traces	C40H50O5N 6(Fe2O2)	traces		
			C17H24O14	traces				C15H8O6N2 (Fe2O2)	0,1	C49H93O10 N	traces		
			C30H60O2	0,1				C8H10O6N8 (Fe2O2)	0,2	C56H106O (Fe2O2)	traces		
			C15H8O6N2 (Fe2O2)	0,2				C24H30O7N 2	0,2	C48H26O8 (Fe3O3)	traces		
			C22H20N2 (Fe2O2)	0,2				C24H28O4N 6	0,1				
			C8H10O6N8 (Fe2O2)	0,2				C23H46O9	traces				
			C12H14O2N 4(Fe3O3)	0,1				C11H24O6 (Fe3O3)	0,4				

eSOM	ORG1	AQU2		ORG2	ORG3	AQU4		RESOM	RESORG
		C23H46O9	0,1			C23H22N2(Fe2O2)	0,3		
		C23H22N2(Fe2O2)	0,3			C24H17O5N(FeO)	traces		
		C24H17O5N(FeO)	traces			C13H16O2N4(Fe3O3)	0,1		
		C13H10O4N2(Fe3O3)	0,1			C16H16O8(Fe2O2)	0,3		
		C13H16O2N4(Fe3O3)	0,2			C12H19O2N5(Fe3O3)	traces		
		C16H16O8(Fe2O2)	0,3			C18H14O8N4(FeO)	0,1		
		C12H19O2N5(Fe3O3)	traces			C27H30O3N6	0,1		
		C31H20O4N2	0,1			C15H26ON4(Fe3O3)	0,1		
		C18H14O8N4(FeO)	0,2			C14H18O6(Fe3O3)	0,1		
		C30H40O2N4	0,1			C14H20O6(Fe3O3)	0,1		
		C14H30O5(Fe3O3)	0,1			C14H26O4N2(Fe3O3)	0,3		
		C19H12O7(Fe2O2)	0,1			C12H12O4N6(Fe3O3)	0,1		
		C14H18O6(Fe3O3)	0,2			C17H14O10(Fe2O2)	3,4		
		C14H20O6(Fe3O3)	0,1			C20H16O6N2(Fe2O2)	0,2		
		C14H26O4N2(Fe3O3)	0,3			C22H16O11(FeO)	traces		
		C13H21O6N(Fe3O3)	traces			C35H62O3	traces		
		C17H14O5(Fe3O3)	0,1			C14H24O8(Fe3O3)	traces		
		C18H12ON4(Fe3O3)	traces			C12H14O5N6(Fe3O3)	0,3		
		C12H12O4N6(Fe3O3)	0,1			C13H22O6N4(Fe3O3)	traces		
		C22H16O11(FeO)	0,1			C20H14O6N4(Fe2O2)	0,1		
		C35H60O3	0,1			C18H32O2N4(Fe3O3)	0,2		
		C35H62O3	0,1			C19H10O3N4(Fe3O3)	0,1		
		C29H26ON6(FeO)	traces			C23H22O3(Fe3O3)	0,2		
		C22H20O3(Fe3O3)	traces			C21H20O14(FeO)	traces		
		C18H32O2N4(Fe3O3)	0,2			C20H14O3N4(Fe3O3)	0,1		
		C17H12O6N2(Fe3O3)	traces			C20H12O7(Fe3O3)	0,1		
		C19H10O3N4(Fe3O3)	0,2			C21H16ON6(Fe3O3)	0,1		
		C11H13O8N5(Fe3O3)	traces			C20H14ON4(Fe3O3)	traces		
		C23H22O3(Fe3O3)	0,1			C21H28O6(Fe3O3)	traces		
		C21H20O14(FeO)	0,1			C24H18O8N2(Fe2O2)	traces		
		C30H35O4N3(Fe3O3)	0,1			C29H22O6(Fe2O2)	traces		
		C20H12O7(Fe3O3)	0,1			C19H22O3N8(Fe3O3)	traces		
		C21H16ON6(Fe3O3)	0,1			C14H28O12N2(Fe3O3)	traces		
		C21H28O6(Fe3O3)	traces			C22H16O9(Fe3O3)	0,1		
		C21H24O5N2(Fe3O3)	0,1			C24H18O7(Fe3O3)	traces		
		C24H18O8N2(Fe2O2)	0,1			C24H14O9(Fe3O3)	0,1		
		C19H22O3N8(Fe3O3)	traces			C24H22O7N2(Fe3O3)	traces		
		C22H16O9(Fe3O3)	0,1			C26H18O7(Fe3O3)	traces		
		C40H75N(FeO)	traces			C27H20O7(Fe3O3)	traces		
		C29H22O5N4(Fe2O2)	traces			C28H22O7(Fe3O3)	traces		
		C24H18O7(Fe3O3)	traces			C26H18O11(Fe3O3)	traces		
		C24H22O7N2(Fe3O3)	traces			C37H38O3N2(Fe2O2)	traces		
		C46H66O6	traces			C47H95O2N3	traces		
						C50H99O4N	traces		
						C50H103O3N(FeO)	traces		
						C52H101O15N	traces		

Figure S1
Van Krevelen Plots of various molecular components identified in eSOM extracts (A) and Humeomics fractions (sum of all fractions) (B) of soil samples and their relative (%) abundance. Control = uncultivated soil; Maize = soil under maize monoculture; Mix =soil under maize-broad bean crop rotation.
AA: Aromatic acids; AC: Alcohols; AD: Amides; AL: Alkanes/alkenes; AM: Amines; BA: Benzoic Acids; BE: Benzoic Esters; DA: Dicarboxylic Acids; ES: Esters; ET: Ethers; FA: Fatty Acids; HA: Hydroxy Acids; HN: Heterocyclic Nitrogen compounds; HO: Heterocyclic Oxygen compounds; KE: Ketones; PA: Phenolic Acids; PE: Phenolic Esters; PH: Phenols; RA: Resin Acids; SA: Sugar Acids; SE: Sterols; SET: Sugar Ethers/Esters; ST: Steroids; SU: Sugars.
Standard deviation for all classes of compounds was ≤ 2.

Figure S2
Van Krevelen Plots of various molecular components identified in organosoluble fractions (ORG) extracted from soil samples and their relative (%) abundance. Control = uncultivated soil; Maize = soil under maize monoculture; Mix = soil under maize-broad bean crop rotation.
AA: Aromatic acids; AC: Alcohols; AD: Amides; AL: Alkanes/alkenes; AM: Amines; BA: Benzoic Acids; BE: Benzoic Esters; DA: Dicarboxylic Acids; ES: Esters; ET: Ethers; FA: Fatty Acids; HA: Hydroxy Acids; HN: Heterocyclic Nitrogen compounds; HO: Heterocyclic Oxygen compounds; KE: Ketones; PA: Phenolic Acids; PE: Phenolic Esters; PH: Phenols; RA: Resin Acids; SA: Sugar Acids; SE: Sterols; SET: Sugar Ethers/Esters; ST: Steroids; SU: Sugars.
Standard deviation for all classes of compounds was ≤ 2

Figure S3
Van Krevelen Plots of various molecular components identified in hydrosoluble fractions (AQU2 and AQU4) and residual organic matter (RESOM) extracted from soil samples and their relative (%) abundance. Control = uncultivated soil; Maize = soil under maize monoculture; Mix = soil under maize-broad bean crop rotation.
AA: Aromatic acids; AC: Alcohols; AD: Amides; AL: Alkanes/alkenes; AM: Amines; BA: Benzoic Acids; BE: Benzoic Esters; DA: Dicarboxylic Acids; ES: Esters; ET: Ethers; FA: Fatty Acids; HA: Hydroxy Acids; HN: Heterocyclic Nitrogen compounds; HO: Heterocyclic Oxygen compounds; KE: Ketones; PA: Phenolic Acids; PE: Phenolic Esters; PH: Phenols; RA: Resin Acids; SA: Sugar Acids; SE: Sterols; SET: Sugar Ethers/Esters; ST: Steroids; SU: Sugars.
Standard deviation for all classes of compounds was ≤ 2

Figure S1

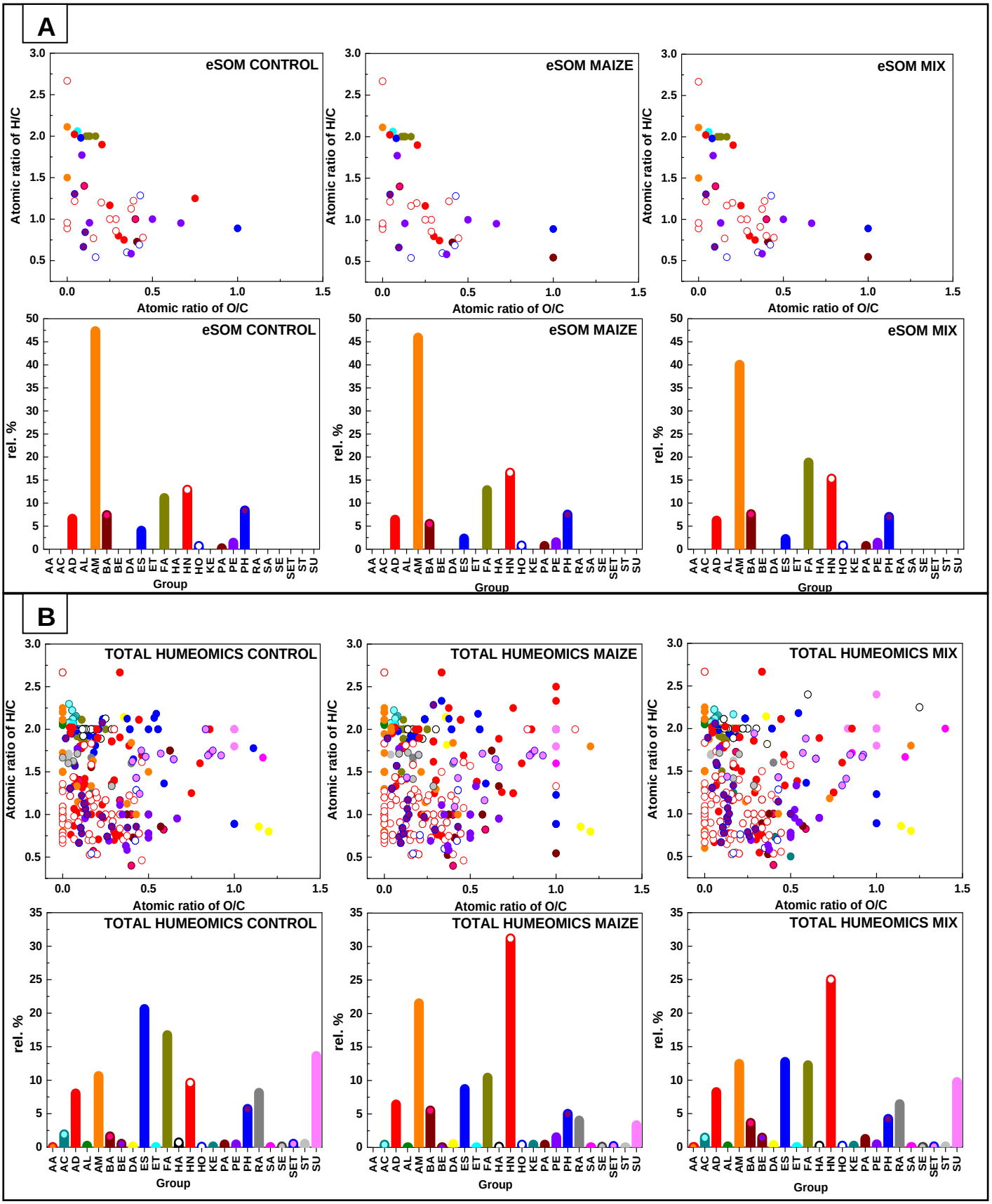
A
eSOM CONTROL
eSOM MAIZE
eSOM MIX
Atomic ratio of H/C
Atomic ratio of O/C
rel. %
Group
B
TOTAL HUMEOMICS CONTROL
TOTAL HUMEOMICS MAIZE
TOTAL HUMEOMICS MIX
AA AC AD AL AM BA BE DA ES ET FA HA HN HO KE PA PE PH RA SA SE SET ST SU
AA
AC
AD
AL
AM
BA
BE
DA
ES
ET
FA
HA
HN
HO
KE
PA
PE
PH
RA
SA
SE
SET
ST
SU

Figure S2

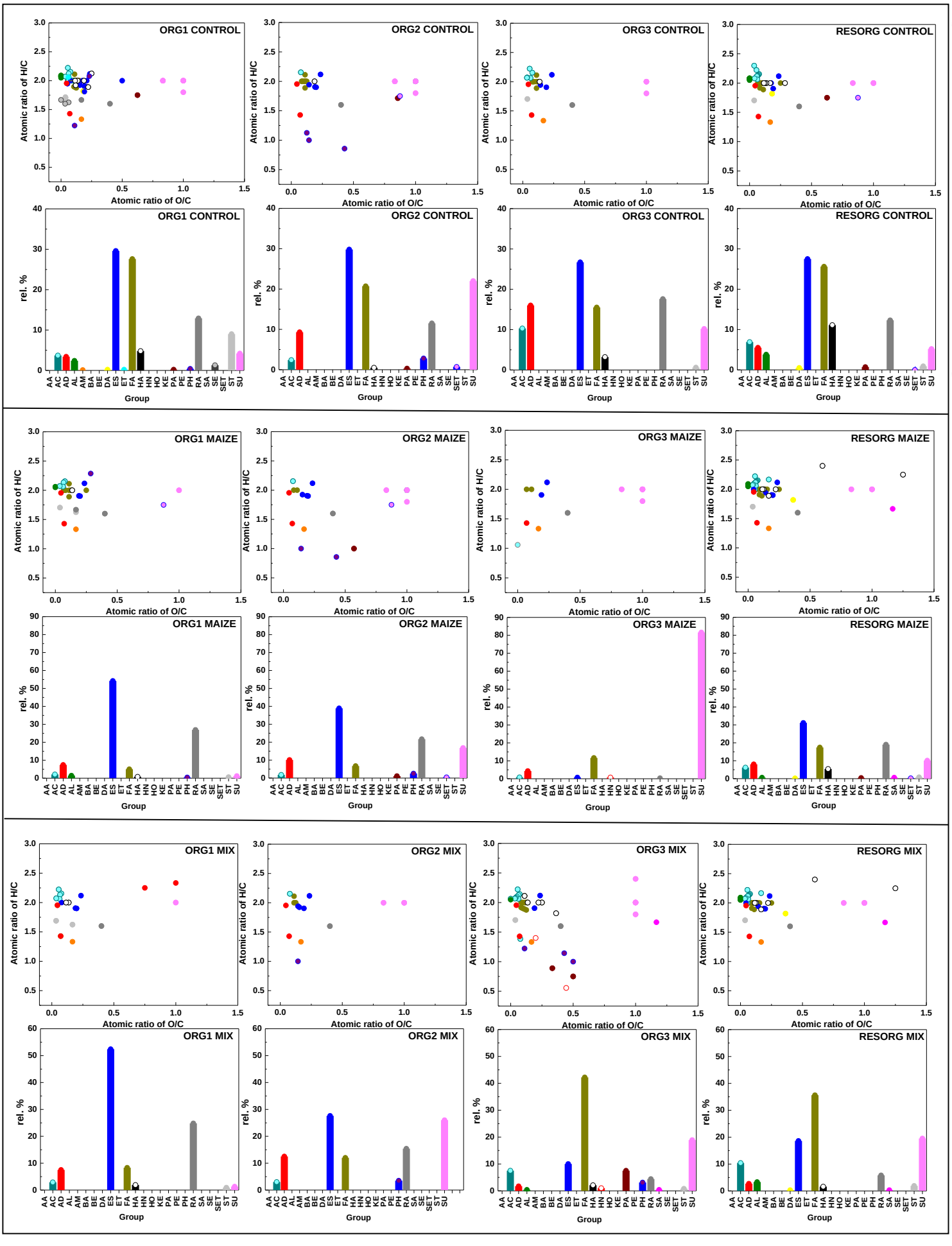
ORG1 CONTROL
ORG2 CONTROL
ORG3 CONTROL
RESORG CONTROL
ORG1 MAIZE
ORG2 MAIZE
ORG3 MAIZE
RESORG MAIZE
ORG1 MIX
ORG2 MIX
ORG3 MIX
RESORG MIX
Atomic ratio of H/C
Atomic ratio of O/C
rel. %
Group
AA
AC
AD
AL
AM
BA
BE
DA
ES
ET
FA
HA
HN
HO
KE
PA
PE
PH
RA
SA
SE
SET
ST
SU

Figure S3

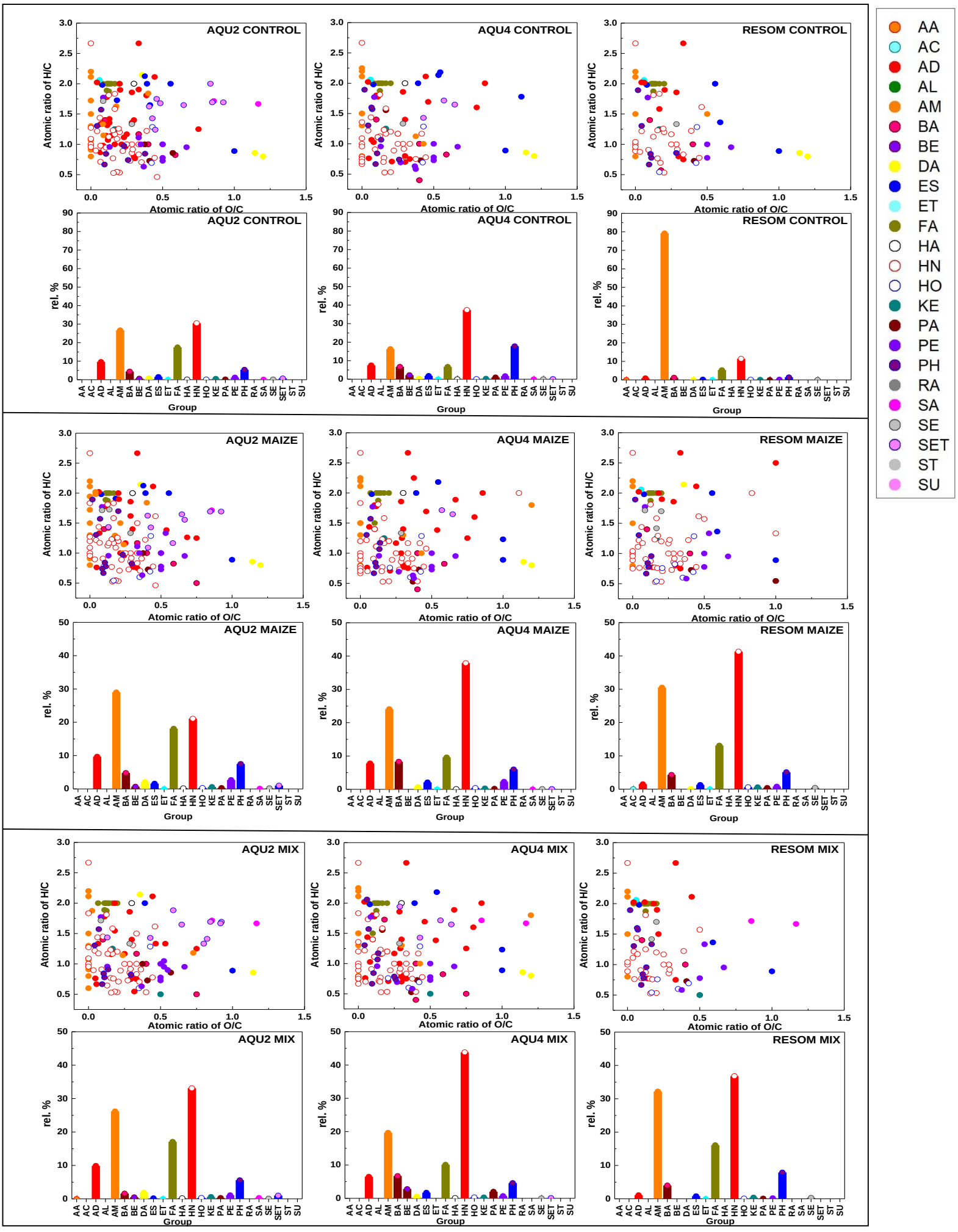
AQU2 CONTROL
AQU4 CONTROL
RESOM CONTROL
AQU2 MAIZE
AQU4 MAIZE
RESOM MAIZE
AQU2 MIX
AQU4 MIX
RESOM MIX
Atomic ratio of H/C
Atomic ratio of O/C
rel. %
Group
AA
AC
AD
AL
AM
BA
BE
DA
ES
ET
FA
HA
HN
HO
KE
PA
PE
PH
RA
SA
SE
SET
ST
SU

CHAPTER 5

Bioactivity of two different humic materials and their combination on plants growth as a function of their molecular proprieties

(Published in Plant and Soil Journal)

Plant Soil
https://doi.org/10.1007/s11104-021-05267-3

REGULAR ARTICLE

Bioactivity of two different humic materials and their combination on plants growth as a function of their molecular properties

Claudia Savarese · Vincenzo di Meo · Silvana Cangemi · Mariavittoria Verrillo · Davide Savy · Vincenza Cozzolino · Alessandro Piccolo

Received: 16 September 2021 / Accepted: 6 December 2021

Abstract

Background and aims Neutralization of adverse environmental effects of agriculture intensification to sustain population growth, requires ecologically sound alternatives for plant growth. We used as biostimulants towards germination of basil seeds and early growth of maize, two different humic materials: a potassium humate from leonardite (KH), and compost tea (CT) from a green compost made of coffee husks, and a 1:1 combination of the two (MIX). After their thorough chemical, molecular and conformational characterization, a relation between structure and bioactivity was investigated.

Results CT showed the largest bioactivity on either seed germination or maize plantlets growth due to its great content of polar bioactive molecules including oxidized lignin fragment, saccharides and peptides. The more hydrophobic KH, rich of alkyl and aromatic moieties, also exerted a significant bioactivity on maize, though to a lesser extent. The application of MIX to hydroponically grown maize plantlets showed a smaller bioactivity of polar CT molecules due to their entrapment into new suprastructures stabilized by hydrogen bonds formed with complementary functions of KH hydrophobic components. However, while the KH hydrophobicity in MIX ensured adhesion to roots, its conformational flexibility was still sufficient to provide a greater bioactivity than control, by releasing bioactive CT components capable to enhance both biomass yield and root elongation.

Conclusions Our study suggests that a combination of humic materials with diverse and well-characterized molecular properties may become a new tool to produce innovative and ecologically viable plant growth promoters, whose bioactivity may be modulated.

Keywords Humic matter · Compost tea · Green compost · Molecular and conformational characterization · Bioactivity · Seed germination · Maize plantlets

Responsible Editor: Tim S. George.

Supplementary Information The online version contains supplementary material available at https://doi.org/10.1007/s11104-021-05267-3.

C. Savarese (✉) · V. di Meo · D. Savy · V. Cozzolino · A. Piccolo
Department of Agricultural Sciences, Università di Napoli Federico II, Via Università 100, 80055 Portici, Italy
e-mail: claudia.savarese@unina.it

S. Cangemi · M. Verrillo · D. Savy · V. Cozzolino · A. Piccolo (✉)
Interdepartmental Research Centre of Nuclear Magnetic Resonance for the Environment, Agri-Food and New Materials (CERMANU), Università di Napoli Federico II, Via Università 100, 80055 Portici, Italy
e-mail: alessandro.piccolo@unina.it

Published online: 28 January 2022

Introduction

Food production to support a predicted global population of 10 billion by 2050 is the major challenge of the twenty-first century. Demand for food is expected to increase 2–5 fold by 2030 and food production is estimated to rise by 60% in the coming decades to meet population growth (St.Clair and Lynch 2010), thereby determining an agriculture intensification with its negative social and environmental impacts. Several works highlighted both SOM degradation and soil fertility reduction under traditional tillage practices and prolonged mono-cultivation as major problems (Chendev et al. 2015; Drosos and Piccolo 2018; Savarese et al. 2021). Likewise, intensive application of N/P mineral fertilizers and chemical pesticides resulted in an increase of waters contamination and plant susceptibility to pathogens, while negatively affecting the structure and composition of soil micro-flora (Liebman and Davis 2000; Geisseler and Scow 2014).

The use of plant biostimulants of biological origin, either with or without plant growth promoting microorganisms (PGPMs), may well represent a sustainable and ecological approach to stimulate plant growth at very low dosages while concomitantly ensuring high levels of agricultural productivity (du Jardin 2015; Yakhin et al. 2017; Savy et al. 2020). Among biostimulants, humic substances (HS) isolated from different sources are successfully and increasingly applied in ecological agricultural practices (Canellas et al. 2015; Jindo et al. 2020). In fact, HS have similar molecular and conformational properties as those found in soil humus (Piccolo et al. 2019), being the end product of the biotic transformation of plant and animal tissues and resulting in a supramolecular assembly of relatively small (<1000 Da) heterogeneous molecules held together by multiple weak interactions (Piccolo 2002). It is known that HS increase plant development, productivity, and tolerance to abiotic/biotic stresses through their interaction with different bio-chemical mechanisms and physiological processes in plants (Nardi et al. 2007; Canellas and Olivares 2014; Canellas et al. 2015). This biostimulant activity of HS has been related to the incorporation of hormone-like molecules into their supramolecular structure, which can be disrupted by low molecular weight organic acid, like those commonly exuded by plants (Nardi et al. 2007; Savy et al. 2017; Piccolo et al. 2019).

Humic Substances may differ in their composition and activity, depending on their original raw materials, such as leonardite or lignite, oxidized coal, composted biomasses or bio refinery-derived residues. Their salt forms as potassium humates (KH), are the main commercially available humic substances. Their efficiency in the amelioration of soil chemical, physical and biological proprieties, as well as their biostimulant activity towards both plant productivity and resistance to stress conditions, have been widely demonstrated (Piccolo et al. 1997; Kumar and Singh 2017; Conselvan et al. 2017; Ertani et al. 2019). However, HS from renewable resources, such as from composted biomasses or bio-refinery wastes, are being progressively shown to possess equal if not larger bioactivity (Savy et al. 2017; Monda et al. 2018). Moreover, compost-derived products, such as compost tea (CT), the water-soluble fraction obtained by immersion of compost in water for few days, with or without forced aeration (Eudoxie and Martin 2019), allow a more sustainable agricultural production by enhancing soil biodiversity, and nutrients availability for plant growth (Darby et al. 2006; Naidu et al. 2013). Recently, CT was found to increase both plant yield and stress resistance (Zaccardelli et al. 2018), suppress several plant pathogens (Koné et al. 2010; Dionne et al. 2012; MohdDin et al. 2018), and exert a systematic antimicrobial activity (Sang and Kim 2011; Verrillo et al. 2021a).

Despite the growing importance of CT for agricultural applications, the diverse composition of composts and the variable solubilisation of humic molecules in either water or alkaline solution still prevent to clarify a structure-activity relationship of HS (Savy et al. 2020). However, it is of great research interest the development of novel biostimulant products whose activity can be predicted based on their chemical and molecular characteristics. The objective of the present work was hence to verify the stimulating capacity towards basil seeds germination and maize early growth of two different well molecularly characterized humic materials, such a commercial KH from leonardite and a CT from a green compost, alone and in their 1:1 combination in aqueous solution.

Materials and methods

Potassium Humates and compost tea extraction

Potassium Humates (KH) used for experimentation was provided by Hymato Products Ltd., Hungary. The

product was obtained by a KOH alkaline extraction from a leonardite ore and supplied in form of dried granules of about 0.5 mm–1 mm size. It was 100% water soluble and was applied as received.

Green compost was produced in the composting facility of the experimental farm of the University of Napoli Federico II at Castel-Volturno (CE). Compost was obtained by 45-days composting process of 4×6 m static pile under forced air insufflation, followed by a two-month curing period. The composting pile consisted in residues of coffee production (coffee husks) (70% w/w) added with horticultural fresh residues (30% w/w). The compost was left to mature for 30 more days and then randomly sampled to collect 1 Kg. The compost sample was air dried, sieved at 2 mm and stored a 4 °C for further extraction processes.

Compost Tea (CT) was obtained from a green compost based on coffee husks as reported earlier (Verrillo et al. 2021a). Briefly, 200 g of compost was weighed into a gauze bag and suspended in 1 L of distilled water in a plastic Becker (w/v 1/5). The compost containing gauze bag was subjected to air insufflation at regular intervals (15 min every 3 h) with an automatic aeration pump device. After seven days of aeration, the extraction was stopped, and compost tea solution was freeze-dried.

Chemical and elemental analysis

The electrical conductivity (EC) and the pH were measured by conventional methods in a water suspension (1:10 w/v) of KH from leonardite and CT from green compost. Elemental composition (C, H, N, and S) was determined using 2 mg of each humic material by an UNICUBE elemental analyser (Elementar Analysensysteme GmbH, Germany).

Total concentration of macro- (Ca, Mg, K) and micro- (Cu, Zn, Mn) elements was determined by digesting 250 mg of each sample with 6 mL of HNO_3 (65%) and 2 mL of H_2O_2 (35%) in a Milestone 900 microwave oven at 600 W for 24 min. Solution were diluted to 25 mL with distilled water and analysed by an atomic absorption spectrometer (AAnalyst 700, Perkin-Elmer). The P content was measured calorimetrically in the same digested samples by the molybdenum blue assay method (Murphy and Riley 1962). All analyses were carried out in triplicate. Total elemental content, pH, and Electrical Conductivity (EC) of both the KH product and CT are reported in Table 1.

DRIFT spectroscopy and thermogravimetric analysis

Infrared spectra were recorded on a Perkin-Elmer Frontier Fourier transform infrared spectrometer using a Perkin-Elmer Diffuse Reflectance Fourier Transform (DRIFT) accessory, by accumulating 32 scans with a resolution of 4 cm^{-1} from 4000 to 650 cm^{-1} wave numbers. Before DRIFT analysis, freeze-dried samples of KH, CT, and MIX samples were diluted with KBr powder (5/150, w/w) in an agate mortar.

Thermogravimetric analysis (TGA) and differential scanning calorimetry (DSC) curves of KH, CT, and MIX samples were obtained by air combustion of 10 mg of each humic sample in a simultaneous thermal analyzer (STA 6000-Perkin Elmer). The initial and final temperatures were 30 °C and 700 °C, respectively, with an increasing temperature rate of 10 °C min^{-1}.

Table 1 Chemical characteristics of Potassium Humates (KH) from leonardite and Compost Tea (CT) from green compost

	KH	CT
pH	8.8	7.8
EC (μS/cm)	55	130
% (w/w)		
C	48.11 ± 0.1	32.01 ± 0.4
H	4.06 ± 0.5	4.41 ± 0.1
N	1.23 ± 0.06	4.25 ± 0.04
S	0.69 ± 0.04	1.30 ± 0.1
C/N[a]	45.8	8.8
H/C[a]	1.0	1.6
$g.kg^{-1}$		
P	0.37 ± 0.01	3.73 ± 0.02
Ca	0.66 ± 0.1	1.92 ± 0.6
Mg	1.42 ± 0.1	3.53 ± 0.1
K	50.44 ± 2.4	73.89 ± 1.0
Fe	13.66 ± 1.0	2.28 ± 0.02
$mg.kg^{-1}$		
Cu	28.01 ± 1.0	247.46 ± 1.0
Zn	29.46 ± 1.0	93.61 ± 1.9
Mn	74.16 ± 2.3	50.44 ± 1.0

[a]Atomic ratio

^{13}C-CPMAS-NMR spectroscopy

A 300 MHz Bruker Avance spectrometer (Bruker Bio Spin GmbH, Rheinstetten, Germany), equipped with a 4 mm wide-bore MAS probe, was used to run solid-state NMR spectra of KH from leonardite, CT from green compost and the 1:1 mixture of KH with CT (MIX). Each fine-powdered sample (5 mg) was loaded into 4-mm zirconia rotor, stoppered by a Kel-F cap, and spun at a rate of 13,000 ± 1 Hz. ^{13}C-NMR spectra were acquired through the Cross-Polarization Magic-Angle-Spinning (CPMAS) technique, by using 2 s of recycle delay, ^{1}H-power for CP 92.16 W: ^{1}H 90° pulse 2.85 µs, ^{13}C power for CP 150.4 W, 1 ms of contact time, 30 ms of acquisition time and 4000 scans. The ^{13}C-CPMAS pulse sequence was conducted by using a ^{1}H RAMP pulse to account for the *non*-homogeneity of the Hartmann–Hahn condition. The Fourier transform was performed with 4 k data point and an exponential apodization of 100 Hz line broadening. All NMR spectra were processed by using MestReC NMR Processing Software (v.4.8.6.0, Cambridgesoft, Cambridge, Massachusetts, USA). For the interpretation of ^{13}C-CPMAS-NMR spectra, the overall chemical shift range was divided into the following main resonance intervals: alkyl-C (0 ppm–45 ppm); methoxy-C and N-alkyl-C (45 ppm–60 ppm); O-alkyl-C (60 ppm–110 ppm); unsubstituted and alkyl-substituted aromatic-C (110 ppm–145 ppm); O-substituted aromatic-C (145 ppm–160 ppm); carboxyl- and carbonyl-C (160 ppm–200 ppm) (Spaccini and Piccolo 2009). The percent relative contribution of a specific functional group (*i*) was determined by dividing the area of each spectral region (Res*i*) by the sum of all spectral areas: Rel*i* % = (Res*i* / Σ Res*i*) × 100. In order to highlight the structural features of humic materials, four dimensionless indexes were calculated from the relative abundance of specific components: O-Alkyl ratio A/OA = [(0–45)/(60–110)]; Aromaticity index ARM = [(110–160)/(0–190)]; Hydrophobic index HB/HI = [(0–45) + (110–160)]/(60–110) + (160–190)]; Lignin ratio LigR = [(45–60)/(145–160)] (Monda et al. 2017; Verrillo et al. 2021a, b).

Offline pyrolysis TMAH-GC-MS

The off-line pyrolysis coupled with GC-MS analysis was performed as reported by Vinci et al. (2019). Briefly, about 500 mg of humic sample were placed in a quartz boat with 1 mL of a 25% tetramethylammonium hydroxide (TMAH) methanol solution. The quartz boat was introduced into a Pyrex tubular reactor (50 cm × 3.5 cm i.d.), and heated at 400 °C in a Barnstead Thermolyne 21,100 tubular furnace for 30 min. The gaseous products released from thermochemolysis were flowed into two chloroform (50 mL) traps in series, kept in ice/salt baths. The chloroform solutions were combined and rotoevaporated to dryness. The residue was dissolved in 1 mL of chloroform and transferred in a glass vial for GC–MS analysis. The GC–MS analyses were conducted with a Perkin Elmer Autosystem XL equipped with an RTX-5MS WCOT capillary column (Restek, 30 m × 0.25 mm; film thickness, 0.25 mm) and coupled, through a heated transfer line (250 °C), to a PE Turbomass-Gold quadrupole mass spectrometer. The chromatographic separation was achieved with the following temperature program: 60 °C (1 min isothermal), rate 7 °C min^{-1} to 320 °C (10 min isothermal). Helium was used as carrier gas at 1.90 mL min^{-1}, the injector temperature was at 250 °C, and the split-injection mode had a 30 mL min^{-1} of split flow. Mass spectra were obtained in EI mode (70 eV), by scanning in the range 45 m–650 m/z, with a cycle time of 0.2 s. Compound identification was based on comparison of mass spectra with the NIST-library database and published spectra.

High performance size exclusion chromatography (HPSEC)

The HPSEC of the three humic samples was carried out by using a PolySep™ GFC-P3000 300 × 7.80 mm (Phenomenex, USA). The elution flow rate was set at 0.6 mL min^{-1} and the eluent was 0.05 mol L^{-1} NaCl added with 4.6 mmol L^{-1} NaN_3. Both mobile phase and sample solutions were filtered through 0.45 μm cellulose acetate filter prior to the analysis. Humic samples were dissolved in the eluent solution at a concentration of 0.6 g L^{-1} and 100 μL of this solution were injected into the SEC system. Thereafter, the pH of the humic solutions was lowered to 3.5 by adding a few microlitres of glacial acetic acid (AcOH). After filtration through 0.45 μm Millipore filter, the humic solutions were injected again in the HPSEC systems. A UV detector (Perkin Elmer LC295) set at 280 nm was used to detect peaks elution, while a nominal

column calibration was carried out by using sodium polystyrene sulfonates of known molecular masses. Chromatograms were acquired and elaborated by using a Unipoint Gilson Software, while the calculations of Weight Average (Mw) and Number Average (Mn) molecular weights and polydispersity (P) were performed by the Origin software (v. 9.1, Originlab), as described elsewhere (Savy et al. 2017).

Germination test

The germination assay was performed in a growth-chamber at 25 °C in dark conditions by setting the relative humidity at 85%. Twenty Basil seeds (*Ocinum basilicum* Italian Large Leaf ILL) were placed on a filter paper in a Petri dish (9 cm diameter) and moistened with 10 mL of either distilled water (control) or aqueous solutions of KH from leonardite and CT from green compost (50 $mg.L^{-1}$). The solutions were adjusted to pH 7 before use. All treatments were carried out in five replicates. After 5 days of incubation, Win-Rhizo software (version 2016, Regent Instruments, Inc.) was used to measure germination rate, roots, and epicotyls length (Verrillo et al. 2021b). The percentage of relative seed germination (RSG) was calculated in reference to control as follows:

$$\text{RSG}\ (\%) = \frac{\text{no. seeds germinated by KH and CT}}{\text{no. seeds germinated by control}} * 100$$

Growth of maize seedlings

Maize seeds (*Zea mays* L. var. Limagrain) were soaked in tap water overnight and germinated in the dark at 25 °C on filter paper moistened with distilled water. After germination, maize seedlings (five days old) with uniform size, shape and healthy aspect were selected, trasferred into 10 plastic test tubes, and added with 18 mL of a modified Hoagland solution (Hoagland and Arnon 1950) composed of: 40 µM KH_2PO_4, 200 µM $Ca(NO_3)_2$, 200 µM KNO_3, 200 µM $MgSO_4$, 10 µM FeNaEDTA, 4.6 µM H_3BO_3, 0.036 µM $CuCl_2 \bullet 2H_2O$, 0.9 µM $MnCl_2 \bullet 4H_2O$, 0.09 µM $ZnCl_2$, 0.01 µM $NaMoO_3 \bullet 2H_2O$. Tubes with seedlings were placed in a climate chamber that maintained 16 h of light per day, air temperature at 25 °C, and relative humidity at 75%. After 7 days from transplanting, 18 mL of either distilled water (control) or aqueous solutions of KH from leonardite and CT from green compost (50 $mg.L^{-1}$) were added to the growing seedlings. Aqueous solutions of the MIX sample at three different concentration (25, 50, 100 mgL^{-1}) were also tested. All solutions were adjusted to pH 7 before use. After 96 h, plants were harvested and the fresh and dry weights for shoots and roots were determined. Seedling's roots from growth experiments were first scanned with an Epson Perfection V700 modified flatbed scanner, and, then, their length was measured by the WinRhizo software, version 2016 (Regent Instruments, Inc.) (Monda et al. 2017).

Statistical analysis

The significant difference between mean values obtained from all measurements of either germination and early growth tests was determined by the one-way analysis of variance (ANOVA), and validated applying the least significant differences (LSD) test at $p < 0.05$ by using the XLSTAT software (Addinsoft, v. 2014). In order to evaluate the possible bioactivity of the two humic materials and their mixture on plants growth, a principal component analysis (PCA) was applied by using the XLSTAT software (Addinsoft, v. 2014). PCA was processed using both phenological and analytical data as an exploratory tool to identify which variables mostly affected the humic samples bioactivity and to predict the correlation with their molecular features.

Results

Chemical characterization

The percent elemental composition in leonardite KH and CT from green compost is reported in Table 1. Total carbon and nitrogen contents were respectively greater and smaller in KH than in CT. These results are in line with the elemental composition reported earlier for these types of humic matter (Lodhi et al. 2013; Verrillo et al. 2021a). Interestingly, elemental analyses revealed differences in C/N and H/C ratios between the two HS, with a larger C/N ratio in KH than in CT (Table 1). These values suggest a large content of N-rich molecules, such as polysaccharides and peptidic moieties in the

compost extract (Monda et al. 2017; Verrillo et al. 2021a), as compared to C-rich components that are predominant in leonardite KH (Table 1). Moreover, KH showed a small value for the H/C ratio (Table 1), thus indicating an aromatic character that is in line with its geochemical origin (García et al. 2012). The slight increase of the H/C ratio in CT (Table 1) may derive from the incorporation and/or preservation of alkyl compounds during the composting process (Spaccini and Piccolo 2009).

As for macro- (P, K, Ca, Mg) and micro- (Fe, Cu, Zn, Mn) elements, a low content of all elements was detected in KH, except for K and Fe (Table 1), confirming previous reports on leonardite humic acids (Tahiri et al. 2016). Conversely, CT revealed a rich mineral composition, mainly due to high values of K, P, Mg and Cu (Table 1). A large solubilisation of P and K has already been noted in aqueous extracts from various compost-based biomasses (Pant et al. 2012; Pane et al. 2016), and especially when obtained by forced aeration (Xu et al. 2012).

DRIFT spectroscopy and thermal proprieties of humic materials

DRIFT spectra of leonardite KH, CT from green compost, and their 1.1 mixture (MIX) revealed a similar distribution of main functional groups (Fig. 1). The broad absorption band around 3000 cm–3400 cm^{-1} is attributed to the OH and NH stretching vibrations in alcohols, phenolic and carboxylic acids, and N-containing compounds, while the bands at 2934 cm^{-1} are referred to symmetric and asymmetric C-H stretching of methyl and methylene groups in aliphatic chains (Monda et al. 2017). In the 2400–2000 region, the band at 2191 cm^{-1}, appearing in KH and, even more intense, in the MIX sample, can be attributed to strongly H-bonded OH of carboxyls and phenols to complementary O and N containing groups (Piccolo and Stevenson 1982). In the central region, the bands around 1570 cm–1600 cm^{-1} may be related to either the amide bonds of peptides (Verrillo et al. 2021a), as well as to ring vibrations of aromatic moieties (aromatic C = C, strongly H-bonded C = O, C = C conjugated with C = O, or a combination of these) (Piccolo and Stevenson 1982). The bending of C-H and C-O bonds at 1445 cm^{-1} and 1360 cm^{-1}, respectively, confirm the inclusion of alkyl chains and carboxylates functions in aliphatic acids (Monda et al. 2017). The C-O stretching bands at 1200 and 1037 cm^{-1}, in both poly-alcoholic compounds and glycosidic bonds indicated the presence of carbohydrates. Additionally, CT signals in DRIFT spectra implied the solubilization from bulk compost of mainly polar and medium polar components, such as aliphatic acids, carbohydrates, and peptides (Verrillo et al. 2021a). The weak shoulder of aryl C-H stretching around 3030–80 cm^{-1} in all spectra, also suggested the presence of aromatic moieties. The broad band centered at 1030 cm^{-1} and the signals at 1120 and 1220 cm^{-1} are assigned to the C-O stretching of carbohydratic moieties in all samples.

Thermogravimetry can be used to evaluate the stability and maturity of compost and/or its derivatives. The TGA and DSC curves of KH, CT, and MIX samples are shown in Fig. 2. Despite minor differences, DSC curves reflected the different thermal behavior between KH and CT and how their molecular differences were balanced in MIX. The thermal profile of TGA curves (Fig. 2) showed a larger weight loss for CT with raising temperature than for KH. The CT thermogram revealed one distinct shoulder attributed to thermal degradation of aromatic and heterocyclic structures at about 550 °C. This exothermic peak is commonly related to the combustion of complex aromatic compounds such as lignin and/or other polyphenols (Plante et al. 2009; Monda et al. 2017). The same exothermic peak was shifted to higher temperatures (700 °C) in KH thermal curve, thereby indicating a greater thermal stability of this material (Nada et al. 2012). This may be attributed to the larger content of intermolecular hydrophobic interactions in KH, which determined an increased stability of its supramolecular structure (Buurman et al. 2002). The MIX sample showed an intermediate behaviour in both TGA and DSC curves, thereby suggesting that the CT components somewhat disrupted the molecular clusters stabilized in KH by multiple hydrophobic interactions, likely through formation of more energetic hydrogen bonds between the complementary functional groups present in both KH and CT. This explanation is supported by the noted occurrence of an intense absorption due to strong H-bonds at around 2200 cm^{-1} in the DRIFT spectrum of MIX.

Solid-state ^{13}C-NMR spectra of humic materials

The ^{13}C-CPMAS-NMR spectra of leonardite KH, CT from green compost and their 1:1 mixture (MIX) are

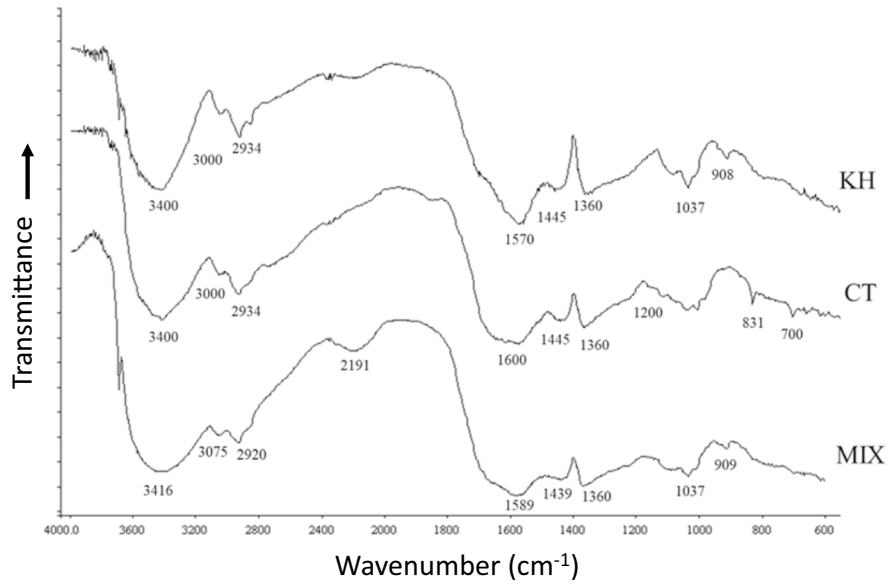

Fig. 1 FTIR-DRIFT spectra of potassium humates from leonardite (KH), compost tea from green compost (CT), and 1:1 mixture of both KH and CT (MIX)

shown in Fig. 3, whereas the relative distribution of signal areas is reported in Table 2. In all humic samples, spectra revealed a predominance of the Alkyl-C (0 ppm–45 ppm) region, accounting for 41.57, 27.95 and 30.36% of total area, for the KH, CT and MIX materials, respectively (Table 2). The large NMR resonances in this region can be attributed to CH_2- and CH_3- groups in aliphatic chains of lipid compounds, plant waxes and biopolyester (Spaccini and Piccolo 2009). The molecular composition of CT was also rich in mono- and polysaccharides components, responsible for the 60 ppm–110 ppm spectral region (Fig. 3) and accounting for 19.43% of total area (Table 2). In particular, the signal around 72 ppm is assigned to the overlapping of C-2, C-3, and C-5 carbons in the pyranosidic structures of cellulose and several hemicelluloses. The distinct bands in the 45 ppm–60 ppm region in the CT spectrum

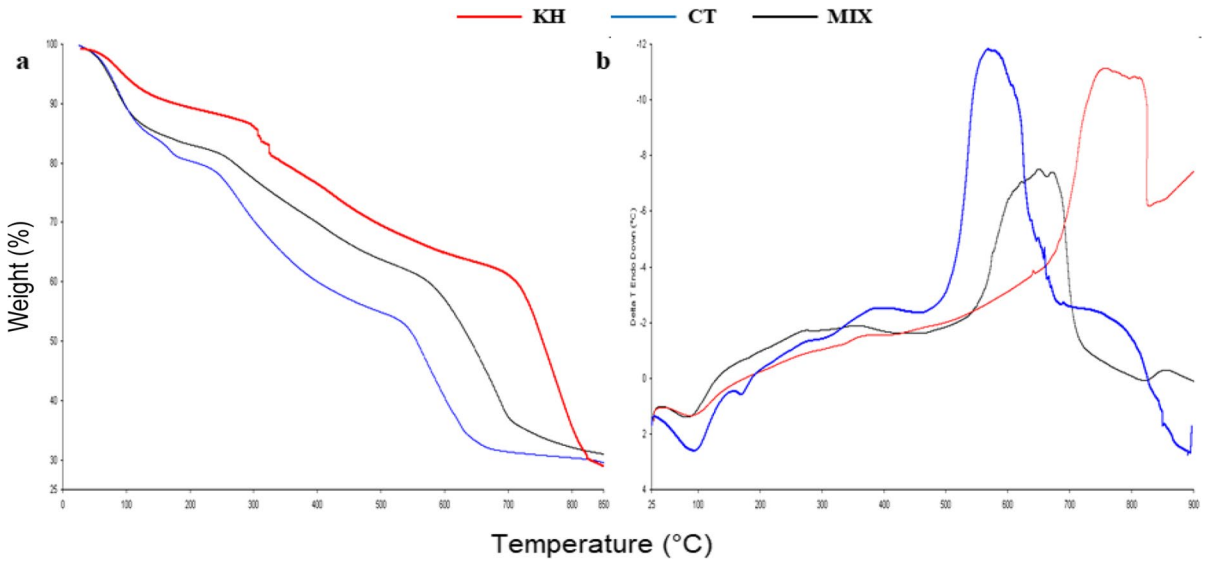

Fig. 2 Thermogravimetric (**A**) and differential scanning calorimetry (**B**) curves of potassium humates from leonardite (KH), compost tea from green compost (CT), and 1:1 mixture of both KH and CT (MIX)

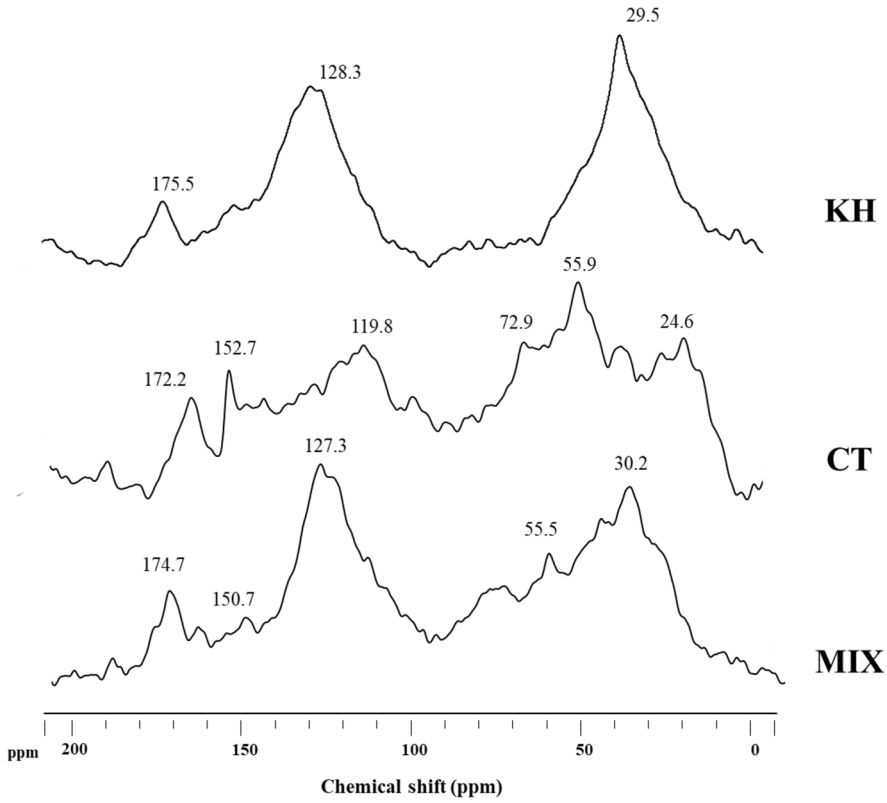

Fig. 3 ^{13}C-CPMAS-NMR spectra of potassium humates from leonardite (KH), compost tea from green compost (CT), and 1:1 mixture of both KH and CT (MIX)

Table 2 Relative distribution (%) of signals area over chemical shift regions (ppm) and structural indexes in ^{13}C-CPMAS-NMR spectra of Potassium Humates (KH) from leonardite, Compost Tea (CT) from green compost, and the 1:1 mixture of KH and CT (MIX)

Sample	^{13}C NMR regions						^{13}C NMR structural indexes			
	Alkyl-C (0–45)	CH_3O/CN (45–60)	O-alkyl-C (60–110)	Aryl-C (110–145)	O-aryl-C (145–160)	Carboxyl-C (160–190)	HB/HI[a]	A/OA[b]	ARM[c]	LigR[d]
KH	41.57	4.52	7.61	33.87	5.33	7.10	4.2	5.5	0.6	0.8
CT	27.95	16.49	19.43	17.91	5.59	12.64	1.1	1.4	0.3	2.9
MIX	30.36	9.34	10.75	32.73	6.29	10.54	2.3	2.8	0.6	1.5

[a]HB/HI = hydrophobicity index = [Σ (0–45) + (110–160) / Σ (45–60) + (60–110) + (160–190)]

[b]A/AO = alkyl/O-alkyl ratio = [(0–45) / (60–110)]

[c]ARM = aromaticity index = [(110–160) / Σ (0–45) + (45–60) + (60–110) + (160–190)]

[d]LR = lignin ratio = [(45–60) / (145–160)]

(Fig. 3) are instead attributed to methoxyl carbons in both guaiacyl and syringyl units of lignin fragments, and C-N functions in amino acids and peptide moieties (de Aquino et al. 2019), accounting for 16.49% of total spectral area for CT (Table 2). Interestingly, the 45–60 and 60 ppm–110 ppm spectral regions in KH accounted only for 4.52 and 7.61% of total area (Table 2), probably because of the relative predominant alkyl and aromatic components of this geochemically derived material (García et al. 2012). On the other hand, the MIX sample showed an intermediate content of these components (Fig. 3), which represented the 9.34 and 10.75% of the total area for CH_3O/CN (45–60) and O-alkyl-C (60–110) region, respectively (Table 2).

Moreover, the peaks extended along the 110 ppm–160 ppm spectral region indicate the presence of aryl-C in both lignin residues and other aromatic moieties (Fig. 3). These compounds represented the 39.20, 23.50 and 39.02% of the total spectral area for KH, CT and MIX, respectively (Table 2), confirming the large amount of aromatic and phenyl carbons commonly observed in leonardite humic acids (Monteil-Rivera et al. 2000; Imbufe et al. 2005; Qian et al. 2015). In particular, the signals within the 110 ppm–145 ppm region can be assigned to unsubstituted and C-substituted phenyl carbons, while the subsequent 145 ppm–160 ppm interval is commonly referred to the O-bearing C in hydroxyl- and methoxy-groups of aromatic rings in polyphenol compounds and lignin fragments (Monda et al. 2017; Verrillo et al. 2021a). Finally, the Carboxyl-C (160 ppm–190 ppm) spectral region accounted for 7.10, 12.64, and 10.54% of total area in KH, CT and MIX, respectively (Table 2). In this region, the signal around 175 ppm in all humic materials (Fig. 3) corresponds to either the carbonyl carbons of aliphatic acids or amide functional groups (Spaccini and Piccolo 2009).

The molecular differences among humic materials may be inferred by the structural indexes calculated from spectral areas, such as alkyl/O-alkyl (A/OA), aromaticity (ARM), hydrophobicity (HB/HI), and lignin ratio (LigR) (Table 2). Particularly, the larger values for A/OA, ARM and HB/HI indexes detected in KH than CT (Table 2), suggest a metastable conformational stability conferred by the multiple weak dispersive bonds established among the predominant hydrophobic compounds present in KH (Monda et al. 2017; Piccolo et al. 2019). Conversely, the smaller A/OA and greater LigR values shown by CT (Table 2) reveal a large content of polar and bioavailable components in this humic material, thereby implying a less stable supramolecular assembly in this compost extract (Pane et al. 2016; Monda et al. 2018). Finally, the MIX sample, representing the mixture of both KH and CT, displayed intermediate values of structural indices (Table 2), implying the expected balance among the molecular components of the original samples (Fig. 3).

Off-line Pyr-TMAH-GC-MS of humic materials

Thermochemolysis showed several differences in the molecular composition of the two humic materials (Table 3). The main components in the pyrogram of KH were long-chain fatty acid methyl esters (Table 3 and S1), reflecting the contribution of waxes of higher plants (Olivella et al. 2002). Linear hydrocarbons nC_{14}-nC_{30} alkanes, aromatic compounds and phenolic structures were also detected in Leonardite KH (Table 3 and S1), as observed in previous reports (Piccolo et al. 2002; Wang et al. 2017). The most abundant compounds in CT were instead lignin monomers, followed by N containing molecules, linear fatty acids, and lipid metabolites of microbial cells (Table 3 and S2). In contrast to NMR spectra, a relatively small amount of carbohydrates was found in CT (Table 3), probably due to the reduced analytical efficiency of thermochemolysis in detecting polyhydroxy molecules in complex matrices (Spaccini et al. 2013). The wide range of methyl ethers and esters of lignin derivatives (Table S2) were associated to the current symbols used to distinguish different lignin structural units: P, p-hydroxyphenyl; G, guaiacyl (3-methoxy, 4-hydroxyphenyl); S, syringyl (3,5-dimethoxy, 4- hydroxyphenyl) (Monda et al. 2017). The most represented lignin monomers in CT were the oxidized forms of di- and trimethoxy phenylpropane molecules such as benzaldehyde (G4, S4) and benzoic acid (G6, S6) (Table S2). The ratio of acidic

Table 3 Relative yield (%) of main thermochemolysis products released by Potassium Humates (KH) from leonardite and Compost Tea (CT) from green compost

Compounds (%)	KH	CT
Lignin	0.7	30.2
Aromatic compounds	5.6	3.6
Phenols	3.9	7.5
N derivatives	2.8	35.6
Carbohydrates	N.D.	1.5
Alcohols	1.1	0.1
Alka/Alke[a]	15.4	0.5
Dioic acids	6.3	N.D.
FAME[a]	56.9	15.9
Mic[a]	6.3	4.6
Sterols	1.2	0.5
Ad/Al_G [b]	N.D.	4.6
Ad/Al_S [b]	N.D.	5.2

[a]*Alka/Alke* alkanes and alkenes, *FAME* fatty acid methyl ester, *Mic* microbial origin

[b]$Ad/Al_G = G6/G4$; $Ad/Al_S = S6/S4$

structures over that of the corresponding aldehydes (Ad/AlG = G6/G4, Ad/AlS=S6/S4) are extensively used as indicators of the bio-oxidative transformation of lignin polymers (Monda et al. 2017; de Aquino et al. 2019). The large value of both Ad/Al ratios shown by CT (Table 3), suggests a solubilisation by water infusion of simple and oxidized molecules from the original compost into compost tea (Verrillo et al. 2021a). Similarly, the detection of N compounds in the CT pyrogram of compost extract (Table 3) is evidence of the transfer of peptide moieties in the aqueous solution of compost tea (de Aquino et al. 2019). Alkyl compounds found in CT were mainly methyl esters of linear fatty acids (FAME), such as linear saturated and unsaturated hexadecanoic and octadecanoic acids (Table S2), thus suggesting plant waxes as a prevalent source (Spaccini et al. 2013; de Aquino et al. 2019). Methyl branched short chain fatty acids were also detected in CT sample (Table S2), as an evidence of the intense microbial activity in the formation of both green compost and its CT (Spaccini and Piccolo 2009; Martinez-Balmori et al. 2013; Verrillo et al. 2021a).

The Pyr-TMAH-GC-MS results supported NMR data, in showing the strong influence of raw materials on the humic extracts. Alkyl and aromatic compounds were mainly detected in leonardite KH (Tables 2 and 3), in line with their geochemical origin (Qian et al. 2015; Wang et al. 2017), and their notable hydrophobicity (Piccolo et al. 2004). Conversely, Compost Tea from green compost showed a greater content of oxidized lignin derivatives, N-containing compounds, and polysaccharides than KH (Tables 2 and 3), as easily solubilized polar moieties from green compost into aqueous solutions (Monda et al. 2017; Verrillo et al. 2021a).

HPSEC of humic materials

Size exclusion chromatograms revealed that, at pH 7, CT had the largest apparent molecular dimension with a nominal Mw of 44.7 kDa, whereas the smallest size was shown by KH, and an intermediate size by MIX (Table 4). While a bimodal elution profile was shown for both CT and MIX, only one broad peak was observed in the KH size exclusion chromatogram (Fig. 4).

The HPSEC profile of samples was again evaluated after having lowered the solutions pH to 3.5 (Table 4). This approach is based on previous studies, which observed that upon AcOH addition, the chromatograms of humic matter showed a marked reduction of peaks intensity (the hypochromic effect), as well as a shift in elution volumes (Piccolo et al. 2001, 2002, 2003). This behaviour was attributed to poor stability of supramolecular associations of small molecules held together only by weak bonds, contrary to that of covalently stabilized macropolymers, whose conformation remains unaltered upon addition of few µL of AcOH (Piccolo et al. 2001). In fact, while metastable suprastructures are stabilized in neutral solutions by weak bonds, such as van der Waals forces, π- π and CH- π interactions, protonation of carboxyl groups at a lower pH entails the formation of stronger hydrogen bonds between the complementary oxygen-containing molecules, thereby producing smaller and more stable molecular associations with peaks having lower UV absorbance and larger elution volumes (Piccolo 2002).

At pH 3.5, a significant change in elution profile, namely with peaks reduced absorbance and increased elution volume, was noticed for all samples (Fig. 4), but especially for the most hydrophobic KH, whose single peak at pH 7 was fragmented, after AcOH addition, into five different absorbances eluting at greater elution volumes. The size distribution of the more polar CT was also significantly altered by AcOH treatment, though to a lesser extent than for KH. In the case of MIX, the elution profile at pH 7 resembled that of CT, but shifted to larger elution volumes, as if the insertion of polar CT molecules had somewhat lowered the dimension of the KH molecular associations but increased their conformational stability, since they were no longer disrupted into

Table 4 Weight-Average (Mw) and Number-Average (Mn) molecular weight, and Polydispersity (P), as calculated from UV-detected HPSEC chromatograms for Potassium Humate (KH from leonardite, Compost Tea (CT) from green compost, and the 1:1 mixture of KH and CT (MIX), before and after addition of acetic acid (AcOH). Standard deviation was <5%

Sample (peak interval, mL)	Mw	Mn	P
KH (4.4–15.4)	25,061	7772	3.2
KH + AcOH (4.4–15.4)	7234	1441	5.0
CT (4.7–17.6)	44,732	20,150	2.2
CT + AcOH (4.7–17.6)	26,254	10,964	2.4
MIX (5.6–15.0)	35,002	14,682	2.4
MIX + AcOH (5.6–15.0)	24,141	7937	3.0

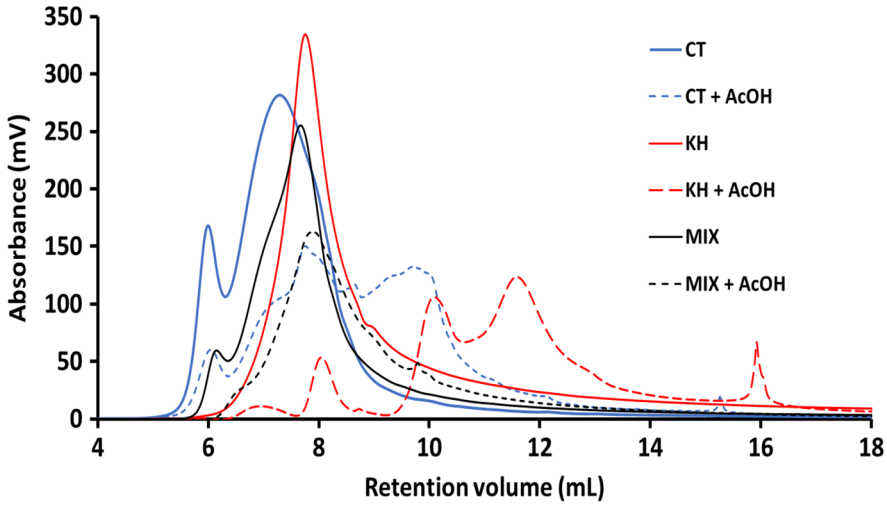

Fig. 4 HPSEC of Potassium Humates (KH), Compost Tea (CT) and the 1:1 mixture of both KH and CT (MIX), before and after addition of acetic acid (AcOH) to adjust their solutions from 7 to pH 3.5

smaller size clusters upon AcOH addition, as instead happened for KH and CT (Fig. 4). Despite the differences in elution profiles, all CT, KH and MIX samples showed a decrease in Mw and Mn, as well as an increase in P, after the AcOH treatment (Table 4).

These findings can be explained with the dynamics of the specific supramolecular structure of each sample. The most hydrophobic KH (Table 2) was stabilized at pH 7 by dispersive forces between apolar components, such as long chain fatty acids, alkyl, and aromatic compounds (Table 3). The lowering of pH with AcOH was very effective in breaking the hydrophobic interactions by forming stronger hydrogen bonds and dispersing the KH chromophores in smaller but more stable assemblies (Fig. 4). Conversely, the more hydrophilic CT extract (Table 2) resulted richer in residual oligosaccharides and oxidized lignin oligomers, as well as in N-containing compounds (Table 3), which determined a more variable supramolecular structure, whose conformation was less affected by pH change. While the oxidized lignin and oligosaccharidic residues maintained after AcOH addition their molecular clusters that eluted at smaller elution volumes than for KH, the oxygen and nitrogen containing components of CT well reacted with the added AcOH protons and formed new molecular associations of greater stability and exclusion volumes (Fig. 4).

When the KH and CT components were equally combined in the MIX sample, a new supramolecular arrangement was established (Fig. 4). This still showed an earlier exclusion absorbance, but shifted to larger elution volumes than for CT, and a more diffuse peak somewhat centred at a similar elution volume as for KH, but of reduced intensity. While the first MIX absorbance was due to partially altered associations of CT saccharidic and lignin residues, the second diffuse peak of lesser absorbance represents the supramolecular assembly composed by the combined KH hydrophobic components with CT oxygen and nitrogen containing compounds. This because the hydrogen bonds established among complementary functions in the MIX sample not only stabilized its conformation into smaller clusters but also separated the hydrophobic KH chromophores from each other, thereby decreasing their overall absorbance (Piccolo et al. 2002). This explanation is confirmed by the MIX elution profile after the AcOH treatment, whereby the additional protons were effective in disrupting the residual associations of the first peak, that was no more detected, but failed to alter the already well stabilized conformational arrangement of the second diffuse absorbance, that was only slightly shifted to larger elution volumes (Fig. 4).

Effect of humic materials on basil seeds germination

The potential bioactivity of each humic material of this study was preliminarily tested with a germination essay on *Ocinum basilicum* seeds at different concentrations (Table S3 and S4). These results showed not only the absence of any phytotoxic effect on seed germination rate, but also a positive response of both KH and CT samples in root and epicotyl elongation

of germinated seeds (Table S3 and S4). In particular, the maximum length stimulation of both radicles and epicotyls by KH was recorded at the concentration of 50 mg.L^{-1} (Table S3), whereas CT induced seeds root elongation and epicotyl development at both 50 and 100 mg.L^{-1} (Table S4). Thereafter, the bioactivity on basil seeds germination of both humic materials was tested in a similar assay at the best concentration of 50 mg.L^{-1} (Table 5). While CT significantly increased the epicotyl length 22.6% more than control, KH promoted a slightly less epicotyl development (14.5% more than control) (Table 5). Both CT and KH also showed a stimulation of root elongation by about 14.5 and 9.2% more than control, respectively (Table 5).

Table 5 Epicotyl and Root length (cm) and percent germination (RSG) of Ocinum basilicum seedlings treated with aqueous solution (50 mgL^{-1}) of Potassium Humates (KH) from leonardite and Compost Tea (CT) from green compost

Treatment	Epicotyl	Root	RSG
H_2O	0.62 ± 0.04^{b}	1.52 ± 0.10^{b}	100
KH	0.71 ± 0.07^{a}	1.66 ± 0.10^{a}	98
CT	0.76 ± 0.05^{a}	1.74 ± 0.11^{a}	101

Means of five replicates and standard deviation. Different letters in the same column indicate significant differences at $P < 0.05$. (LSD test)

Effect of humic materials on maize early growth

The bioactivity of both leonardite KH and CT from green compost, as well as their mixture was assayed towards the early growth of maize plantlets (Table 6). KH showed a progressive dose-response trend on seedlings development for all measured parameters (Table 6). In particular, the 25 and 100 mg.L^{-1} KH treatment did not generally differ from control, whereas a significantly greater performance was observed for the 50 mg.L^{-1} concentration, being root length (LR), total fresh (TFW) and dry weight (TDW) respectively 14.8, 9.4 and 12.5% larger than control (Table 6). Conversely, CT addition at 25 mg.L^{-1} concentration showed a generally positive effect on maize early growth, although not significantly different from control (Table 6), except for LR that was 11.9% significantly greater than for untreated plantlets (Table 6). An important index for assessing plant health is the shoot to root ratio (S/R), as estimated in the dry weight (DW) form. As compared to control, a general decreased in this index values was detected for all treated plantlets, with the exception of CT at 50 mg.L^{-1}, that showed the highest S/R DW ratio (Table 6).

We then compared the biostimulation on maize plantlets of humic materials alone at their most effective concentrations with that of their 1:1 mixture at three different concentrations (25, 50 and 100 mg.L^{-1}) (Table 7). Both KH and CT applied alone at 50 and 25 mg.L^{-1}, respectively, showed a generally

Table 6 Total Fresh Weight (TFW, g), Shoot Fresh Weight (SFW, g), Root Fresh Weight (RFW, g), Total Dry Weight (TDW, g), Shoot Dry Weight (SDW, g), Root Dry Weight (RDW, g), Shoot-to-Root Dry Weight ratio (S/R DW, g), and Root Length (RL, cm) for Maize seedlings treated with aqueous solutions of Potassium Humates (KH) from leonardite and Compost Tea (CT) from green compost at different concentrations (25, 50, 100 mg.L^{-1})

	Control H_2O	KH			CT		
		25	50	100	25	50	100
TFW	2.469 ± 0.19^{b}	2.281 ± 0.18^{b}	2.702 ± 0.21^{a}	2.406 ± 0.19^{b}	2.426 ± 0.35^{b}	2.266 ± 0.20^{b}	1.908 ± 0.16^{c}
SFW	$1.672 \pm 0.16^{a,b}$	1.521 ± 0.12^{b}	1.827 ± 0.18^{a}	$1.577 \pm 0.12^{a,b}$	1.581 ± 0.33^{b}	1.527 ± 0.19^{b}	1.248 ± 0.16^{c}
RFW	$0.797 \pm 0.05^{b,c}$	0.760 ± 0.08^{c}	0.875 ± 0.05^{a}	$0.829 \pm 0.08^{a,b}$	$0.845 \pm 0.06^{a,b}$	0.739 ± 0.06^{c}	0.660 ± 0.04^{d}
TDW	0.216 ± 0.01^{c}	$0.220 \pm 0.02^{b,c}$	0.243 ± 0.01^{a}	$0.225 \pm 0.01^{b,c}$	$0.231 \pm 0.02^{a,b}$	$0.220 \pm 0.02^{b,c}$	0.159 ± 0.02^{d}
SDW	0.188 ± 0.01^{c}	$0.193 \pm 0.01^{b,c}$	0.206 ± 0.01^{a}	$0.194 \pm 0.01^{b,c}$	$0.199 \pm 0.01^{a,b}$	$0.194 \pm 0.01^{b,c}$	0.135 ± 0.01^{d}
RDW	$0.028 \pm 0.01^{b,c,d}$	$0.027 \pm 0.01^{c,d}$	0.037 ± 0.01^{a}	$0.031 \pm 0.01^{b,c}$	$0.032 \pm 0.01^{a,b}$	$0.027 \pm 0.01^{c,d}$	0.025 ± 0.01^{d}
S/R DW	$6.729 \pm 1.44^{a,b}$	$7.301 \pm 1.19^{a,b}$	5.646 ± 0.48^{c}	$6.322 \pm 0.76^{b,c}$	$6.405 \pm 1.23^{b,c}$	7.633 ± 1.43^{a}	5.635 ± 0.88^{c}
RL	283.542 ± 18^{b}	262.876 ± 19^{c}	325.501 ± 12^{a}	315.931 ± 12^{a}	317.506 ± 19^{a}	265.655 ± 21^{c}	215.567 ± 19^{d}

Means of five replicates and standard deviation. Different letters in the same column indicate significant differences at $P < 0.05$. (LSD test)

larger fresh biomass (TFW, SFW, and RFW) and root length (RL) of maize plantlets, whereas the dry weight parameters (TDW, SDW, and RDW) were not significantly different from control (Table 7). In the case of RL, the maximum significant increase resulted 23 and 13% larger than control for KH and CT, respectively. In the case of MIX, the concentration of 50 mg.L^{-1} revealed the largest effect on maize plantlet, with RL being significantly greater than control but similar to the values for KH alone (Table 7). In contrast, the 25 and 100 mg.L^{-1} mixed concentrations performed worse than both the humic materials alone and control (H_2O), except for RL that maintained greater values than for maize plantlets treated only by water (Table 7). Finally, KH applied at the concentration of 50 mg.L^{-1} showed the largest value for the S/R DW ratio, whereas all other treatments decreased this index in comparison to the untreated plantlets (Table 7).

The bioactivity assay on maize seedlings indicated that the use of KH, CT and MIX materials generated significantly greater biomass production and root length than for control (Tables 6 and 7), in accordance with previously reported biostimulation benefits of leonardite humic acids and compost teas when applied alone (Ertani et al. 2019; Priya et al. 2021). However, the MIX treatments provided a more balanced shoot/root biomass ratios (Table 7), that appears to confer to plants an increased capacity to express growth across different stress conditions (Filho et al. 2020).

Correlation between the molecular features of humic materials and their bioactivity

The effect of the two humic materials and their mixture on maize early growth, as a function of their molecular features, was evaluated by a Principal Components Analysis (PCA) based on CPMAS-NMR and HPSEC data, as well as on results of bioactivity assays (Fig. 5). The first two principal components explained 95.96% of the total variance, with PC1 and PC2 accounting for 75.19 and 20.77%, respectively (Fig. 5). The treatments were well separated and distributed along the loading plot. In particular, the PC1 neatly separated KH from CT and MIX, based on the positive loadings of polydispersity, hydrophobicity and aromaticity, and the negative loadings of the LigR, Carboxylic-C and O-Alkyl-C content (Fig. 5). Interestingly, the HB/HI, ARM and P-AcOH indexes positively correlated to the total fresh and dry weight, the shoot to root ratio and the root length of maize treated plantlets (Fig. 5, Table S5). Meanwhile, the distribution of CT treatment on the negative side of PC1 in the lower left quadrant strongly correlated to the molecular dimension of this material and its large content of Carboxylic-C, O-Alkyl-C and oxidized lignin fragments (Fig. 5). On the other hand, these CT molecular features showed a negative correlation with dry biomasses and root length of maize

Table 7 Total Fresh Weight (TFW, g), Shoot Fresh Weight (SFW, g), Root Fresh Weight (RFW, g), Total Dry Weight (TDW, g), Shoot Dry Weight (SDW, g), Root Dry Weight (RDW, g), Shoot-to-Root Dry Weight ratio (S/R DW, g), and Root Length (RL, cm) for Maize seedlings treated with aqueous Solutions of Potassium Humates (KH) from leonardite (50 mgL^{-1}), Compost Tea (CT) from green compost (25 mg.L^{-1}), and 1:1 mixture of both KH and CT at different concentrations (25, 50, 100 mg.L^{-1})

	Control H_2O	KH 50	CT 25	MIX (1:1)		
				25	50	100
TFW	2.672 ± 0.21^{b}	2.934 ± 0.18^{a}	2.915 ± 0.16^{a}	2.194 ± 0.19^{c}	2.879 ± 0.18^{a}	2.145 ± 0.19^{c}
SFW	$1.731 \pm 0.21^{a,b}$	1.834 ± 0.21^{a}	1.878 ± 0.31^{a}	1.550 ± 0.18^{b}	1.913 ± 0.26^{a}	1.514 ± 0.15^{b}
RFW	0.944 ± 0.11^{c}	1.100 ± 0.12^{a}	$1.037 \pm 0.10^{a,b}$	0.644 ± 0.05^{d}	$0.965 \pm 0.12^{b,c}$	0.631 ± 0.06^{d}
TDW	$0.146 \pm 0.02^{a,b,c}$	0.169 ± 0.03^{a}	$0.142 \pm 0.01^{b,c}$	0.125 ± 0.02^{c}	$0.149 \pm 0.03^{a,b}$	0.124 ± 0.03^{c}
SDW	$0.111 \pm 0.02^{a,b,c}$	0.131 ± 0.02^{a}	$0.105 \pm 0.01^{b,c}$	0.092 ± 0.01^{d}	$0.112 \pm 0.03^{a,b}$	$0.092 \pm 0.03^{c,d}$
RDW	$0.035 \pm 0.01^{a,b}$	0.037 ± 0.01^{a}	0.038 ± 0.01^{a}	$0.034 \pm 0.01^{a,b}$	0.037 ± 0.01^{a}	0.032 ± 0.01^{b}
S/R DW	$3.202 \pm 0.44^{a,b}$	3.491 ± 0.22^{a}	2.790 ± 0.15^{c}	2.735 ± 0.36^{c}	$3.034 \pm 0.41^{b,c}$	2.846 ± 0.40^{c}
RL	326.676 ± 10^{d}	403.788 ± 11^{a}	370.490 ± 13^{b}	367.619 ± 12^{b}	402.918 ± 11^{a}	353.526 ± 14^{c}

Means of five replicates and standard deviation. Different letters in the same column indicate significant differences at $P < 0.05$. (LSD test)

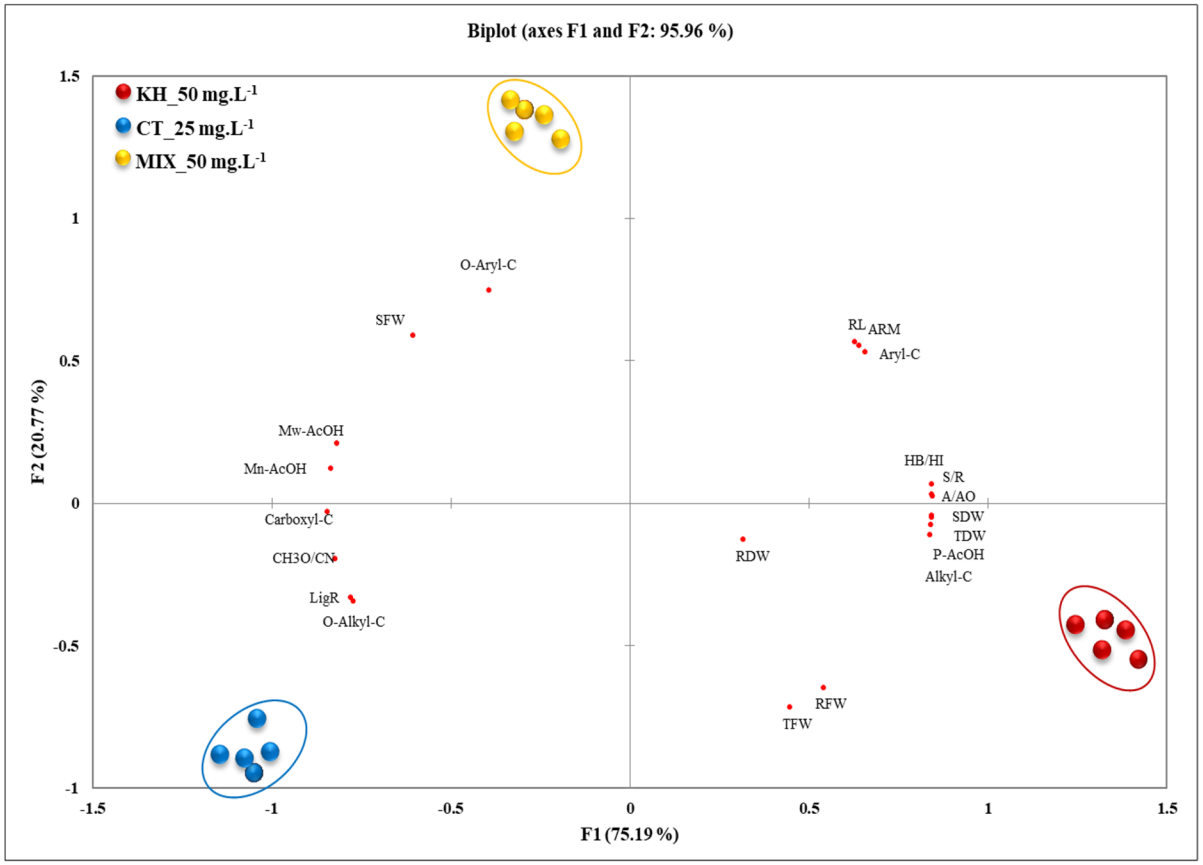

Fig. 5 PCA biplot of Potassium Humates (KH) from leonardite, Compost Tea (CT) from green compost, and 1:1 mixture of KH and CT (MIX), where molecular characteristics are correlated with bioactivity assay on maize plants. ^{13}C-NMR: Alkyl-C = 0 ppm–45 ppm; CH_3O/CN = 45 ppm–60 ppm; O-Alkyl = 60 ppm–110 ppm; Aryl-C = 110 ppm–145 ppm; O-Aryl-C = 145 ppm–160 ppm; Carboxylic-C = 160 ppm–190 ppm; HB/HI = Hydrophobicity index; A/AO = Alkyl ratio; ARM = Aromaticity index; LigR = Lignin ratio. HPSEC: Mw-AcOH = Weight average molecular weight after the addition of acetic acid; Mn-AcOH = Number average molecular weight after the addition of acetic acid; P = Polidispersity after the addiction of acetic acid. Plant parameters: TFW = Total fresh weight; SFW = Shoot fresh weight; RFW = Root fresh weight; TDW = Total dry weight; SDW = Shoot dry weight; RDW = Root dry weight; S/R = Shoot-to-Root dry weight ratio; RL = Root length

treated plantlets (Fig. 5, Table S5). Moreover, along the PC2, the MIX sample was clearly separated from KH and CT, according to its intermediate molecular size, as compared to the two humic materials alone (Fig. 5). In particular, the hydrophobicity of MIX, mainly derived from the aromatic-C of KH, positively correlated to the root length promotion of treated maize plants (Fig. 5 and Table S5), whereas the presence in MIX of polar bioavailable compounds (Carboxylic-C and CH_3O/CN) provided by CT, strongly correlated to the increase of the shoot fresh weight (Fig. 5, Table S5).

Discussion

Previous studies have accounted to a general hormone-like activity of humic materials the cause of seeds germination promotion (Canellas and Olivares 2014; Canellas et al. 2015; Savy et al. 2020). However, the different bioactivity of the two KH and CT humic extracts used here on basil seedlings may be specifically explained by their diverse molecular composition. The greatest stimulatory effect of CT on both root and epicotyl elongation (Table 4) may be related to either the presence of oxidized lignin

fragments or polar bioavailable compounds, such as oligo and monosaccharides and peptide clusters and/or amino acids (Tables 2 and 3) (Monda et al. 2017; de Aquino et al. 2019; Verrillo et al. 2021b). Furthermore, the smaller value reached by seeds root and epicotyl length upon the KH treatment (Table 4) may be accounted to the larger content of hydrophobic compounds in this material of geochemical origin (Tables 2 and 3). In fact, it has been observed that the hydrophobicity of humic molecules plays an important role in plants biostimulation, since it regulates the conformational stability of their self-assembly and the release of bioactive polar compounds therein contained (Piccolo et al. 2019). The large hydrophobicity of KH may thus limit the conformational flexibility of its suprastructure and the availability of compounds with bioactivity on seedlings. Conversely, the greater polarity of the molecules present in CT confers to this material a loose supramolecular association with greater molecular mobility and more effective bioactivity (Savy et al. 2015, 2020; Monda et al. 2017).

It has been already reported the plant biostimulation of both leonardite humic acids and compost teas (Ertani et al. 2011; Haghighi and Teixeira Da Silva 2013; Pane et al. 2016; Giménez et al. 2020) is exerted through the increase of both root length and activity of enzymes involved in nitrogen metabolism (Conselvan et al. 2017). Furthermore, the application of compost teas had been shown to positively affect plants productivity, leaf nutrient status, chlorophyll content and photosynthetic activity (Naidu et al. 2013). Our results also showed a significant increase over control of both fresh and dry shoot and root weights, and root length of maize seedlings treated with KH and CT at concentrations of 50 and 25 mg L^{-1}, respectively (Tables 6 and 7). The physical-chemical reason for the biostimulation effects of these humic materials was attributed to both their root adhesion capacity and conformational stability, whereby their hydrophobic components may form solution flexible associations, which, once adhered to root surfaces, may release polar molecular fragments to exert a bioactivity (Piccolo et al. 2019; Verrillo et al. 2021b).

Our findings on KH and CT effects on maize early growth may be similarly explained by their different molecular composition. It is reasonable to assume that the dose-response effect shown by KH on maize biomass and root elongation may be due to, first, a favoured adhesion of the KH suprastructure to maize incipient roots, that is effective from the 50 mg.L^{-1} concentration onward, and, then, to a release of bioactive molecules, that is maximum at 50 mg.L^{-1}. In fact, the KH supramolecular arrangement was shown to be easily disrupted into smaller associations by organic acids (Fig. 4, Table 4), as those exuded by plant roots, and this conformational behaviour resulted positively correlated to the increase of both biomass yield and root length of treated maize plants (Fig. 5). Conversely, biostimulation became limited at 100 mg.L^{-1} concentration when the KH conformation was too strongly stabilized by the great number of hydrophobic molecules in KH (Table 2 and Fig. 3) (Canellas et al. 2015; Savy et al. 2016; Piccolo et al. 2019). On the other hand, the observed larger hydrophilicity and readily bioavailability to plant roots of CT components may be responsible for the bioactivity of this material even at the smaller 25 mg.L^{-1} concentration (Table 2 and Fig. 3).

The bioactivity of the combined humic solutions (MIX) confirmed the role of the diverse molecular composition of KH and CT, although it indicated a prevalent effect of the hydrophobicity of KH over the bioavailability of CT components (Fig. 5). In fact, it appears that KH apolar domains were capable to effectively trap the CT O- and N-containing polar compounds (oxidized lignin phenols, saccharides, and peptides), which formed strong H-bonds with the alkanoic, and phenolic acids present in KH, as shown by DRIFT spectra (Fig. 1) and thermogravimetric results (Fig. 2). The biostimulation of the MIX solution at the concentration of 50 mg.L^{-1} was as effective as that of the KH treatment alone, while smaller and larger concentrations had also an effect but limited to RL. This observation suggests that the adhesion to roots surface ensured by the hydrophobicity of humic matter was the prevalent mechanism to convey trapped bioactive molecules to roots (Canellas et al. 2015; Monda et al. 2017). However, the capacity of humic samples to stimulate plant physiology and biochemistry further depends on the stability of the humic supramolecular associations, whose conformation may be altered by root-exuded organic acids (Piccolo et al. 2003), thereby liberating bioactive molecules. This seems to have been the case for the MIX sample that showed loading plot correlations in PC2 between shoot fresh weight, root length, and O-aryl C components, as well as decrease of molecular sizes (Mw-AcOH and Mn-AcOH) upon the organic acid treatment (Fig. 5).

Conclusion

The present work highlighted that two different humic materials, Potassium Humates from leonardite (KH) and Compost Tea from green compost (CT), exert significant biostimulation on plant growth when they are applied alone or in combination. In particular, while the highly polar CT stimulated both the epicotyl and root development of basil seeds, the effect of the mostly hydrophobic KH was less evident on seed germination. Moreover, the positive influence on the growth of maize seedlings was maximum for CT at a smaller concentration than for KH. However, when a combined solution of the two humic materials was added to hydroponically grown maize plantlets, the general increase on both biomass yield and root elongation was dictated by KH, thus indicating that the readily bioavailable CT compounds, such as oxidized lignin fragments, saccharides, and peptides, became trapped within MIX supramolecular structures stabilized by the hydrogen bonds formed with the complementary functions of hydrophobic KH components. In fact, this cage effect increased the bioactivity of the MIX treatment in respect to the CT applied alone. Our findings further indicate that polar molecules derived from the aerobic transformation of cellular materials during composting stimulate plant growth, but that the hydrophobicity of humic matter of geochemical origin is also an important factor for plant biostimulation, since it provides molecular adhesion to plant roots, and, depending on the conformational flexibility of the humic assembly, it enables a slow and effective release of bioactive molecules. This study thus indicates that a calibrated mixture of humic materials of selected molecular composition may represent an innovative and ecologically viable method to build up sustainable products with diverse mechanisms of plant biostimulation.

Acknowledgements This work was conducted in partial fulfilment of first author requirements, to achieve an "industrial" PhD degree, funded by the Ministry of University and Reasearch (MUR) of Italy.

Author contributions C. Savarese, V. Cozzolino, A. Piccolo designed the study. V. Di Meo prepared green compost, provided technical advice and support. S. Cangemi, M. Verrillo, D. Savy assisted in sample analyses and data collection. C. Savarese, A. Piccolo, V. Cozzolino interpreted data. C. Savarese, A. Piccolo wrote the manuscript,

Funding The research was financially supported by the Ministry of University and Research (MUR) of Italy.

Declarations

Conflict of interest The authors declare no conflict of interest.

References

Buurman P, van Lagen B, Piccolo A (2002) Increase in stability against thermal oxidation of soil humic substances as a result of self association. Org Geochem 33:367–381. https://doi.org/10.1016/S0146-6380(01)00167-X

Canellas LP, Olivares FL (2014) Physiological responses to humic substances as plant growth promoter. Chem Biol Technol Agric 1:1–11. https://doi.org/10.1186/2196-5641-1-3

Canellas LP, Olivares FL, Aguiar NO et al (2015) Humic and fulvic acids as biostimulants in horticulture. Sci Hortic (Amsterdam) 196:15–27. https://doi.org/10.1016/j.scienta.2015.09.013

Chendev YG, Sauer TJ, Ramirez GH et al (2015) History of east european chernozem soil degradation; protection and restoration by tree windbreaks in the russian steppe. Sustain 7:705–724. https://doi.org/10.3390/su7010705

Conselvan GB, Pizzeghello D, Francioso O et al (2017) Biostimulant activity of humic substances extracted from leonardites. Plant Soil 420:119–134. https://doi.org/10.1007/s11104-017-3373-z

Darby HM, Stone AG, Dick RP (2006) Compost and manure mediated impacts on Soilborne pathogens and soil quality. Soil Sci Soc Am J 70:347–358. https://doi.org/10.2136/sssaj2004.0265

de Aquino AM, Canellas LP, da Silva APS et al (2019) Evaluation of molecular properties of humic acids from vermicompost by 13 C-CPMAS-NMR spectroscopy and thermochemolysis–GC–MS. J Anal Appl Pyrolysis 141:104634. https://doi.org/10.1016/j.jaap.2019.104634

Dionne A, Tweddell R.J, Antoun H, Avis TJ (2012) Effect of non-aerated compost teas on damping-off pathogens of tomato. Can J Plant Pathol 34:51–57. https://doi.org/10.1080/07060661.2012.660195

Drosos M, Piccolo A (2018) The molecular dynamics of soil humus as a function of tillage. L Degrad Dev 29:1792–1805. https://doi.org/10.1002/ldr.2989

du Jardin P (2015) Plant biostimulants: definition, concept, main categories and regulation. Sci Hortic (Amsterdam) 196:3–14. https://doi.org/10.1016/j.scienta.2015.09.021

Ertani A, Francioso O, Tugnoli V et al (2011) Effect of commercial lignosulfonate-humate on Zea mays L. metabolism. J Agric Food Chem 59:11940–11948. https://doi.org/10.1021/jf202473e

Ertani A, Nardi S, Francioso O et al (2019) Metabolite targeted analysis and physiological traits of zea mays L. in response to application of a leonardite-humate and lignosulfonate-based products for their evaluation as potential biostimulants. Agronomy 9:1–18. https://doi.org/10.3390/agronomy9080445

Eudoxie G, Martin M (2019) Compost tea quality and fertility. In: Organic Fertilizers – History Production and Applications. Marcelo Larramendy and Sonia Soloneski IntechOpen. https://doi.org/10.5772/intechopen.86877

Filho JFDCL, Thomason WE, Evanylo GK et al (2020) Corn response to an integrated plant nutrition system (IPNS) with humic acid and biofertilizers. J Agric Sci 12:25. https://doi.org/10.5539/jas.v12n8p25

García C, Hernández T, Costa F, et al (2012) Soil science and plant nutrition comparison of humic acids derived from city refuse with more developed humic acids Comparison of Humic Acids Derived from City Refuse with More Developed Humic Acids. 0768: https://doi.org/10.1080/00380768.1992.10416498

Geisseler D, Scow KM (2014) Long-term effects of mineral fertilizers on soil microorganisms - a review. Soil Biol Biochem 75:54–63. https://doi.org/10.1016/j.soilbio.2014.03.023

Giménez A, Fernández JA, Pascual JA et al (2020) Application of directly brewed compost extract improves yield and quality in baby leaf lettuce grown hydroponically. Agronomy 10. https://doi.org/10.3390/agronomy10030370

Haghighi M, Teixeira Da Silva JA (2013) Amendment of hydroponic nutrient solution with humic acid and glutamic acid in tomato (Lycopersicon esculentum mill.) culture. Soil Sci Plant Nutr 59:642–648. https://doi.org/10.1080/00380768.2013.809599

Hoagland DR, Arnon DI (1950) Preparing the nutrient solution. Water-Culture Method Grow Plants without Soil 347:29–31

Imbufe AU, Patti AF, Burrow D et al (2005) Effects of potassium humate on aggregate stability of two soils from Victoria, Australia. Geoderma 125:321–330. https://doi.org/10.1016/j.geoderma.2004.09.006

Jindo K, Olivares FL, da Paixão Malcher DJ et al (2020) From lab to field: role of humic substances under open-field and greenhouse conditions as biostimulant and biocontrol agent. Front Plant Sci 11:1–10. https://doi.org/10.3389/fpls.2020.00426

Koné SB, Dionne A, Tweddell RJ et al (2010) Suppressive effect of non-aerated compost teas on foliar fungal pathogens of tomato. Biol Control 52:167–173. https://doi.org/10.1016/j.biocontrol.2009.10.018

Kumar D, Singh AP (2017) Efficacy of potassium Humate and chemical fertilizers on yield and nutrient availability patterns in soil at different growth stages of Rice. Commun Soil Sci Plant Anal 48:245–261. https://doi.org/10.1080/00103624.2016.1261884

Liebman M, Davis AS (2000) Integration of soil, crop and weed management in low-external-input farming systems. Weed Res 40:27–47. https://doi.org/10.1046/j.1365-3180.2000.00164.x

Lodhi A, Tahir S, Iqbal Z et al (2013) Characterization of commercial humic acid samples and their impact on growth of fungi and plants. Soil Environ 32:63–70

Martinez-Balmori D, Olivares FL, Spaccini R et al (2013) Molecular characteristics of vermicompost and their relationship to preservation of inoculated nitrogen-fixing bacteria. J Anal Appl Pyrolysis 104:540–550. https://doi.org/10.1016/j.jaap.2013.05.015

MohdDin ARJ, Hanapi SZ, Futamata H et al (2018) Utilization of compost tea for biochemical response assessment associated with resistance to phytopathogen causing leaf spot in Melicopeptelefolia. Org Agric 9:445–456. https://doi.org/10.1007/s13165-018-0235-9

Monda H, Cozzolino V, Vinci G et al (2017) Molecular characteristics of water-extractable organic matter from different composted biomasses and their effects on seed germination and early growth of maize. Sci Total Environ 590–591:40–49. https://doi.org/10.1016/j.scitotenv.2017.03.026

Monda H, Cozzolino V, Vinci G et al (2018) Biostimulation of the early growth of maize by the molecular Humeome extracted from different green composts. Plant Soil 429:407–424. https://doi.org/10.1007/s11104

Monteil-Rivera F, Brouwer EB, Masset S et al (2000) Combination of X-ray photoelectron and solid-state 13C nuclear magnetic resonance spectroscopy in the structural characterisation of humic acids. Anal Chim Acta 424:243–255. https://doi.org/10.1016/S0003-2670(00)01139-9

Murphy J, Riley JP (1962) A modified single solution method for the deter- mination of phosphate in natural waters. Anal Chim Acta 27:31–36

Nada WM, Van Rensburg L, Claassens S et al (2012) Evaluation of organic matter stability in wood compost by chemical and thermogravimetric analysis. Int. J Environ Res 6:425–434. https://doi.org/10.22059/ijer.2012.510

Naidu Y, Meon S, Siddiqui Y (2013) Foliar application of microbial-enriched compost tea enhances growth, yield and quality of muskmelon (Cucumis melo L.) cultivated under fertigation system. Sci Hortic (Amsterdam) 159:33–40. https://doi.org/10.1016/j.scienta.2013.04.024

Nardi S, Muscolo A, Vaccaro S et al (2007) Relationship between molecular characteristics of soil humic fractions and glycolytic pathway and Krebs cycle in maize seedlings. Soil Biol Biochem 39:3138–3146. https://doi.org/10.1016/j.soilbio.2007.07.006

Olivella MA, Del Ríío JC, Palacios J et al (2002) Characterization of humic acid from leonardite coal: an integrated study of PY-GC-MS, XPS and XANES techniques. J Anal Appl Pyrolysis 63:59–68. https://doi.org/10.1016/S0165-2370(01)00141-3

Pane C, Palese AM, Spaccini R et al (2016) Enhancing sustainability of a processing tomato cultivation system by using bioactive compost teas. Sci Hortic (Amsterdam) 202:117–124. https://doi.org/10.1016/j.scienta.2016.02.034

Pant AP, Radovich TJK, Hue NV et al (2012) Biochemical properties of compost tea associated with compost quality and effects on pak choi growth. Sci Hortic (Amsterdam) 148:138–146. https://doi.org/10.1016/j.scienta.2012.09.019

Piccolo A (2002) The supramolecular structure of humic substances: a novel understanding of humus chemistry and implications in soil science. Adv Agron 75:57–134. https://doi.org/10.1016/s0065-2113(02)75003-7

Piccolo A, Stevenson FJ (1982) Infrared spectra of Cu^{2+}, Pb^{2+}, and Ca^{2+} complexes of soil humic substances. Geoderma 27:195–208. https://doi.org/10.1016/0016-7061(82)90030-1

Piccolo A, Pietramellara G, Mbagwu J (1997) Use of humic substances as soil conditioners to increase aggregate stability. Geoderma 75:267–277. https://doi.org/10.1016/S0016-7061(96)00092-4

Piccolo A, Conte P, Cozzolino A (2001) Chromatographic and spectrophotometric properties of dissolved humic substances compared with macromolecular polymers. Soil Sci 166:174–185. https://doi.org/10.1097/00010694-200103000-00003

Piccolo A, Conte P, Trivellone E et al (2002) Reduced heterogeneity of a lignite humic acid by preparative HPSEC following interaction with an organic acid. Characterization of size-separates by Pyr-GC-MS and 1H-NMR spectroscopy. Environ Sci Technol 36:76–84. https://doi.org/10.1021/es010981v

Piccolo A, Conte P, Spaccini R et al (2003) Effects of some dicarboxylic acids on the association of dissolved humic substances. Biol Fertil Soils 37:255–259. https://doi.org/10.1007/s00374-003-0583-8

Piccolo A, Spaccini R, Nieder R et al (2004) Sequestration of a biologically labile organic carbon in soils by humified organic matter. Clim Chang 67:329–343. https://doi.org/10.1007/s10584-004-1822-1

Piccolo A, Spaccini R, Savy D, et al (2019) The Soil Humeome: Chemical Structure, Functions and Technological Perspectives. In: Sustainable Agrochemistry: A compendium of Technologies. Ed: Vaz S. Jr., Springer Nature, Heidelberg, pp. 183–222

Plante AF, Fernández JM, Leifeld J (2009) Geoderma application of thermal analysis techniques in soil science. Geoderma 153:1–10. https://doi.org/10.1016/j.geoderma.2009.08.016

Priya S, Mk K, Roshan C, Deepak K (2021) Effect of soil and foliar applications of compost tea on growth characters , quality and nutrient content of soybean [Glycine max . (L .) Merrill] under organic cultivation. J Pharmacogn Phytochem 10:2566–2569. E-ISSN: 2278–4136

Qian S, Ding W, Li Y et al (2015) Characterization of humic acids derived from Leonardite using a solid-state NMR spectroscopy and effects of humic acids on growth and nutrient uptake of snap bean. Chem Speciat Bioavailab 27:156–161. https://doi.org/10.1080/09542299.2015.1118361

Sang MK, Kim KD (2011) Biocontrol activity and primed systemic resistance by compost water extracts against anthracnoses of pepper and cucumber. Phytopathology 101:732–740. https://doi.org/10.1094/PHYTO-10-10-0287

Savarese C, Drosos M, Spaccini R et al (2021) Molecular characterization of soil organic matter and its extractable humic fraction from long-term field experiments under different cropping systems. Geoderma 383:114700. https://doi.org/10.1016/j.geoderma.2020.114700

Savy D, Cozzolino V, Vinci G et al (2015) Water-soluble lignins from different bioenergy crops stimulate the early development of maize (Zea mays, L.). Molecules 20:19958–19970. https://doi.org/10.3390/molecules201119671

Savy D, Cozzolino V, Nebbioso A et al (2016) Humic-like bioactivity on emergence and early growth of maize (Zea mays L.) of water-soluble lignins isolated from biomass for energy. Plant Soil 402:221–233. https://doi.org/10.1007/s11104-015-2780-2

Savy D, Mazzei P, Drosos M et al (2017) Molecular characterization of extracts from biorefinery wastes and evaluation of their plant biostimulation. ACS Sustain Chem Eng 5:9023–9031. https://doi.org/10.1021/acssuschemeng.7b01928

Savy D, Brostaux Y, Cozzolino V et al (2020) Quantitative structure-activity relationship of humic-like biostimulants derived from agro-industrial byproducts and energy crops. Front Plant Sci 11:1–13. https://doi.org/10.3389/fpls.2020.00581

Spaccini R, Piccolo A (2009) Molecular characteristics of humic acids extracted from compost at increasing maturity stages. Soil Biol Biochem 41:1164–1172. https://doi.org/10.1016/j.soilbio.2009.02.026

Spaccini R, Song XY, Cozzolino V et al (2013) Molecular evaluation of soil organic matter characteristics in three agricultural soils by improved off-line thermochemolysis: the effect of hydrofluoric acid demineralisation treatment. Anal Chim Acta 802:46–55. https://doi.org/10.1016/j.aca.2013.09.031

St.Clair SB, Lynch JP (2010) The opening of Pandora's box: climate change impacts on soil fertility and crop nutrition in developing countries. Plant Soil 335:101–115. https://doi.org/10.1007/s11104-010-0328-z

Tahiri A, Richel A, Destain J et al (2016) Comprehensive comparison of the chemical and structural characterization of landfill leachate and leonardite humic fractions. Anal Bioanal Chem 408:1917–1928. https://doi.org/10.1007/s00216-016-9305-6

Verrillo M, Salzano M, Cozzolino V et al (2021a) Bioactivity and antimicrobial properties of chemically characterized compost teas from different green composts. Waste Manag 120:98–107. https://doi.org/10.1016/j.wasman.2020.11.013

Verrillo M, Cozzolino V, Spaccini R et al (2021b) Humic substances from green compost increase bioactivity and antibacterial properties of essential oils in basil leaves. Chemical and Biological Technologies in Agriculture 8:1 8(1):1–14. https://doi.org/10.1186/S40538-021-00226-7

Vinci G, Mazzei P, Bridoux M et al (2019) Molecular characterization of organic matter in two calcareous soils: the effects of an acid decarbonation treatment. Anal Bioanal Chem 411:5243–5253. https://doi.org/10.1007/s00216-019-01903-1

Wang CF, Fan X, Zhang F et al (2017) Characterization of humic acids extracted from a lignite and interpretation for the mass spectra. RSC Adv 7:20677–20684. https://doi.org/10.1039/C7RA01497J

Xu D, Liu D, Tang Z et al (2012) Structure of chemical components in different compost extracts characterized by chromatogram and spectroscopy analysis and its influence on plant growth promotion. J Mater Cycles Waste Manag 14:325–333. https://doi.org/10.1007/s10163-012-0071-z

Yakhin OI, Lubyanov AA, Yakhin IA et al (2017) Biostimulants in plant science: a global perspective. Front Plant Sci 7. https://doi.org/10.3389/fpls.2016.02049

Zaccardelli M, Pane C, Villecco D et al (2018) Compost tea spraying increases yield performance of pepper (Capsicum annuum L.) grown in greenhouse under organic farming system. Ital J Agron 13:229–234. https://doi.org/10.4081/ija.2018.991

Supporting Information

The bioactivity of two different humic materials and their combination on plants growth as a function of their molecular properties

Claudia Savarese[1*], Vincenzo di Meo[1], Silvana Cangemi[2], Mariavittoria Verrillo[2], Davide Savy[1,2],Vincenza Cozzolino[1,2*], Alessandro Piccolo[1,2*]

[1] Department of Agricultural Sciences, Università di Napoli Federico II, Via Università 100, 80055 Portici, Italy

[2] Interdepartmental Research Centre of Nuclear Magnetic Resonance for the Environment, Agri-Food and New Materials (CERMANU). Università di Napoli Federico II, Via Università 100, 80055 Portici, Italy

*** Corresponding authors. E-mail addresses claudia.savarese@unina.it;**

alessandro.piccolo@unina.it

Table S1.
List of the main products released by thermochemolysis of Potassium Humates (KH) from leonardite.

RT[a]	Assignment	Origin[b]
6,58	Phenol, 4-methyl	Phenol
7,03	Benzene 1 methyl 4 methoxy	Lig P2
7,77	1,2-Di-methoxy benzene	Lig G1
8,06	Phenol, 2,6-dimethyl	Phenol
8,32	Phenol, 3.5-dimethyl	Phenol
8,77	N derivative	N
9,29	Phenol, 2-ethyl-4-methyl	Phenol
9,58	N derivative	N
10,79	Naphthalene, 1,2-dihydro-6-methyl	Aromatic
11,09	Phenol, 3,5-diethyl	Phenol
11,36	C14 alkane	Alkane
11,57	Naphthalene, 1-methyl	Aromatic
11,96	Naphthalene, 2-methyl	Aromatic
13,65	N derivative	N
14,14	C17 alkane	Alkane
14,25	N derivative	N
14,37	C 14 brached alkane	Alkane
14,62	Naphthalene, 1,5-dimethyl	Aromatic
15,05	Naphthalene, 1,6-dimethyl	Aromatic
16,07	C16 alcohol	Alcohol
17,22	C19 alkane	Alkane
17,41	Naphthalene, 2-(1-methylethyl)	Aromatic
17,50	Phenol, 2-5-bis(1,1-methylethyl)	Phenol
17,57	N derivative	N
18,11	Naphthalene, 2,3,6-trimethyl	Aromatic
19,57	Naphthalene, 1,4,6-trimethyl	Aromatic
20,03	C20 alkane	Alkane
22,57	C17 alcohol	Alcohol
23,49	C14 FAME	Lip
27,93	C21 alkane	Alkane
28,53	C16 iso FAME	Mic
30,19	C19 alcohol	Alcohol
32,67	C18:1 FAME	Lip
33,25	C18 iso FAME	Mic
34,75	C19:1 FAME	Mic
34,89	C22 alkane	Alkane
37,02	C23 alkane	Alkane
37,58	C20 FAME	Lip
38,96	C18:1 dioic acid DIME	Dioic acid
39,08	C24 alkane	Alkane
40,20	N derivative	N
41,04	C19:1 dioic acid DIME	Dioic acid
41,59	C22 FAME	Lip
42,96	C26 alkane	Alkane
43,49	C23 FAME	Lip
44,79	C27 alkane	Alkane
45,33	C24 FAME	Lip
46,57	C28 alkane	Alkane
47,10	C25 FAME	Lip
48,29	C29 alkane	Alkane

48,82	C26 FAME	Lip
49,96	C30 alkane	Alkane
50,33	C23:1 dioic acid DIME	Dioic acid
50,47	C27 FAME	Lip
52,09	C28 FAME	Lip
53,66	C29 FAME	Lip
55,19	C30 FAME	Lip
55,67	Triterpenol (pentacyclcic)	Sterol
56,73	Triterpenol (pentacyclcic)	Sterol
61,79	Sterol	Sterol

[a] Retetion time (min).

[b] N nitrogen derivatives; Lig lignin, P p-hydroxyphenyl, G guayacil, S syringyl; FAME fatty acid methyl ester; Mic microbial origin; DIME dimethyl ester.

Table S2

List of the main products released by thermochemolysis of Compost Tea (CT) from green compost.

RT[a]	**Assignment**	**Origin[b]**
6.60	3,4-Methylpropylsuccinimide	N
6.79	Benzene, 1-OMe	Lig P1
7.25	N derivative	N
8.13	1,2-Di-OMe benzene	Lig G1
8.45	Benzene 1-ME 4-Ome	Lig P2
8.92	Phenol, 2-ethyl	Phenol
9.49	4-Ammino-1-methyl-5nitropyrazole	N
10.40	N derivative	N
10.91	Benzenepropanoic acid, methyl ester	Phenol
11.80	N derivative	N
12.37	N derivative	N
12.76	N derivative	N
13.38	1H-indole,1,3-dimethyl	N
13.54	1,2,3-Tri-OMe benzene	Lig S1
13.68	Benzoic acid, 4-OMe,ME	Lig P6
14.17	Carbohydrate derivative (m/z 88, 101, 130)	Carb
14.41	N derivative	N
15.16	N derivative	N
15.46	2H-Indol-2-Oone, 1,3-dihydro-1-methyl	N
15.64	1H-Indole, 5-methoxy-2-methyl	N
15.84	N derivative	N
16.90	Carbohydrate derivative (m/z 88, 101, 130)	Carb
17.14	Benzaldehyde, 3,4-di-OMe	Lig G4
17.78	1H-indole,1,3,5-trimethyl	N
18.03	Propnoic acid, 3-(2-hydroxy-5-methyl) hydrazide	Lig P12
18.31	Carbohydrate derivative (m/z 101, 129, 161)	Carb
18.52	N derivative	N
19.07	Ethanone, 1-(3,4-dimethoxyphenyl)	Lig G5
19.83	Benzoic acid, 3,4-di-OMe,ME	Lig G6
20.21	Benzaldehyde, 3,4,5-trimethoxy-	Lig S4
20.74	trans-2-(3,4-Di-OMe phenyl)-1-OMe ethylene	Lig G8
21.60	trans-1-OMe-1-(3,4-dimethoxyphenyl)-1-propene	Lig G11
22.80	N derivative	N
23.28	Benzoic acid, 3,4,5-triOMe,ME	Lig S6

23.82	trans-1-(3,4-Di-OMe phenyl)-3-OMe-1-propene	Lig G13
24.54	cis-1-(3,4,5-Tri-OMe phenyl)-2-OMe ethylene	Lig S7
24.84	N derivative	N
24.93	N derivative	N
25.09	1,2,3-tri-OMe-1-(3,4-dimethoxyphenyl)propane (threo/erythro)	Lig G14
25.29	C15 iso FAME	Mic
25.45	1,2,3-tri-OMe-1-(3,4-dimethoxyphenyl)propane (threo/erythro)	Lig G15
25.87	trans-1-(3,4,5-Tri-OMe phenyl)-3-OMe-1-Propene	Lig S13
26.80	Caffeine	N
26.95	2,3-Benzenedicarboxylic acid, bis(2-methylpropyl)ester	Aromatic
27.54	trans-3-(3,4-Di-OMe phenyl)-3-propenoic acid ME	Lig G18
27.65	C16 iso FAME	Mic
27.89	1,2,3-tri-OMe-1-(3,4,5-trimethoxyphenyl)propane (threo/erythro)	Lig S14
28.01	11-Hexadecanoic acid, ME	Lip
28.45	1,2,3-tri-OMe-1-(3,4,5-trimethoxyphenyl)propane (threo/erythro)	Lig S15
28.58	C16 FAME	Mic
29.36	N derivative	N
30.09	C17 iso FAME	Mic
30.28	C17 anteiso FAME	Mic
30.37	c17 cy FAME	Mic
30.67	cis-1-(3,4,5-Tri-OMe phenyl)-1,3-di-OMe propene	Lig S16
31.66	BENZENE, (1,2-dimethoxyethyl)	Aromatic
32.65	C18:1 FAME	Lip
32.78	C18:1 FAME	Lip
33.28	C18 iso FAME	Mic
35.10	cy C19 FAME	Mic
37.24	C24 alkane	Alkane
37.61	C20 FAME	Lip
41.61	C22 FFAME	Lip
47.21	C26-OMe	Alcohol
47.40	C24, 2-CH3,FAME	Mic
48.34	C36 alkane	Alkane
49.98	C37 alkane	Alkane
50.12	Sterol	Sterol
50.34	C28-CH3O	Alcohol
50.74	Sterol	Sterol
51.08	Sterol	Sterol
51.59	C38 akane	Alkane
52.27	C28 FAME	Lip
52.59	Sterol	Sterol
53.15	C39 alkane	Alkane
53.60	Sterol	Sterol

[a] Retetion time (min).

[b] N nitrogen derivatives; Lig lignin, P p-hydroxyphenyl, G guayacil, S syringyl; ME methyl ester; OMe methoxy; FAME fatty acid methyl ester; Mic microbial origin; DIME dimethyl ester.

Table S3.
Epicotyl and Root length (cm) and percent germination (RSG) of *Ocinum basilicum* seedlings treated with aqueous solution of Potassium Humates (KH) from leonardite at different concentrations (10, 25, 50, 100 mg.L^{-1}).[1]

Treatment	Epicotyl	Root	RSG
H_2O	0.69 ± 0.06^{c}	1.34 ± 0.15^{b}	100
KH 10	0.70 ± 0.07^{c}	1.33 ± 0.16^{b}	96
KH 25	$0.71 \pm 0.06^{b,c}$	1.34 ± 0.17^{b}	100
KH 50	0.81 ± 0.06^{a}	1.44 ± 0.17^{a}	106
KH 100	0.73 ± 0.07^{b}	1.34 ± 0.17^{b}	102

[1] Means of five replicates and standard deviation. Different letters in the same column indicate significant differences at $P < 0.05$. (LSD test).

Table S4.
Epicotyl and Root length (cm) and percent germination (RSG) of *Ocinum basilicum* seedlings treated with aqueous solution of Compost Tea (CT) from green compost at different concentrations (10, 25, 50, 100 mgL^{-1}).[1]

Treatment	Epicotyl	Root	RSG
H_2O	$0.70 \pm 0.07^{c,d}$	1.48 ± 0.24^{c}	100
CT 10	0.71 ± 0.06^{c}	1.49 ± 0.23^{c}	102
CT 25	0.68 ± 0.07^{d}	$1.51 \pm 0.24^{b,c}$	100
CT 50	0.76 ± 0.07^{b}	1.58 ± 0.24^{b}	102
CT 100	0.79 ± 0.06^{a}	1.67 ± 0.21^{a}	98

[1] Means of five replicates and standard deviation. Different letters in the same column indicate significant differences at $P < 0.05$. (LSD test).

Table S5.

Correlation matrix (Pearson) between the molecular characteristics of Potassium Humates (KH) from leonardite, Compost Tea (CT) from green compost, and the 1:1 mixture of KH and CT (MIX), and the results of bioactivity assay on maize plants. ^{13}C-NMR: Alkyl-C = 0-45; CH_3O/CN = 45-60; O-Alkyl = 60-110; Aryl-C = 110-145; O-Aryl-C = 145-160; Carboxylic-C = 160-190; HB/HI = Hydrophobicity index; A/AO = Alkyl ratio; ARM = Aromaticity index; LigR = Lignin ratio. HPSEC: Mw-AcOH = Weight-average molecular weight after the addition of acetic acid; Mn-AcOH = Number-average molecular weight after the addition of acetic acid; P = Polidispersity after the addiction of acetic acid. Plant parameters: TFW = Total fresh weight; SFW = Shoot fresh weight; RFW = Root fresh weight; TDW = Total dry weight; SDW = Shoot dry weight; RDW = Root dry weight; S/R = Shoot-to-Root dry weight ratio; RL = Root length.[1]

Variables	TFW	SFW	RFW	TDW	SDW	RDW	S/R	RL	Mw-AcOH	Mn-AcOH	P-AcOH	Alkyl-C	CH3O/CN	O-Alkyl-C	Aryl-C	O-Aryl-C	Carboxyl-C	HB/HI	A/AO	ARM	LigR
TFW	**1**	**-0.971**	**0.990**	**0.580**	**0.571**	0.291	0.497	-0.154	**-0.723**	**-0.648**	**0.604**	**0.635**	-0.319	-0.136	-0.121	**-0.997**	-0.499	0.459	0.504	-0.176	-0.156
SFW	**-0.971**	**1**	**-0.995**	**-0.758**	**-0.751**	-0.339	**-0.691**	-0.088	**0.867**	**0.811**	**-0.778**	**-0.802**	**0.537**	0.370	-0.121	**0.951**	**0.692**	**-0.659**	**-0.696**	-0.066	0.389
RFW	**0.990**	**-0.995**	**1**	**0.686**	**0.678**	0.321	**0.612**	-0.016	**-0.811**	**-0.746**	**0.708**	**0.736**	-0.447	-0.272	0.017	**-0.978**	**-0.613**	**0.577**	**0.618**	-0.038	-0.291
TDW	**0.580**	**-0.758**	**0.686**	**1**	**1.000**	0.361	**0.995**	**0.716**	**-0.982**	**-0.996**	**1.000**	**0.998**	**-0.957**	**-0.886**	**0.739**	**-0.518**	**-0.995**	**0.990**	**0.996**	**0.700**	**-0.895**
SDW	**0.571**	**-0.751**	**0.678**	**1.000**	**1**	0.360	**0.996**	**0.724**	**-0.980**	**-0.995**	**0.999**	**0.997**	**-0.960**	**-0.891**	**0.746**	-0.509	**-0.996**	**0.991**	**0.997**	**0.708**	**-0.900**
RDW	0.291	-0.339	0.321	0.361	0.360	**1**	0.350	0.189	-0.374	-0.368	0.364	0.367	-0.317	-0.274	0.200	-0.273	-0.350	0.343	0.351	0.182	-0.279
S/R	0.497	**-0.691**	**0.612**	**0.995**	**0.996**	0.350	**1**	**0.781**	**-0.959**	**-0.983**	**0.992**	**0.986**	**-0.981**	**-0.927**	**0.801**	-0.433	**-1.000**	**0.999**	**1.000**	**0.767**	**-0.935**
RL	-0.154	-0.088	-0.016	**0.716**	**0.724**	0.189	**0.781**	**1**	**-0.572**	**-0.653**	**0.695**	**0.665**	**-0.887**	**-0.958**	**0.999**	0.226	**-0.780**	**0.807**	**0.776**	**1.000**	**-0.952**
Mw-AcOH	**-0.723**	**0.867**	**-0.811**	**-0.982**	**-0.980**	-0.374	**-0.959**	**-0.572**	**1**	**0.995**	**-0.987**	**-0.993**	**0.886**	**0.783**	**-0.599**	**0.670**	**0.960**	**-0.946**	**-0.961**	**-0.553**	**0.796**
Mn-AcOH	**-0.648**	**0.811**	**-0.746**	**-0.996**	**-0.995**	-0.368	**-0.983**	**-0.653**	**0.995**	**1**	**-0.998**	**-1.000**	**0.929**	**0.843**	**-0.678**	**0.590**	**0.983**	**-0.974**	**-0.985**	**-0.636**	**0.854**
P-AcOH	**0.604**	**-0.778**	**0.708**	**1.000**	**0.999**	0.364	**0.992**	**0.695**	**-0.987**	**-0.998**	**1**	**0.999**	**-0.948**	**-0.872**	**0.718**	**-0.544**	**-0.992**	**0.985**	**0.993**	**0.679**	**-0.882**
Alkyl-C	**0.635**	**-0.802**	**0.736**	**0.998**	**0.997**	0.367	**0.986**	**0.665**	**-0.993**	**-1.000**	**0.999**	**1**	**-0.935**	**-0.852**	**0.690**	**-0.577**	**-0.986**	**0.978**	**0.987**	**0.649**	**-0.862**
CH3O/CN	-0.319	**0.537**	-0.447	**-0.957**	**-0.960**	-0.317	**-0.981**	**-0.887**	**0.886**	**0.929**	**-0.948**	**-0.935**	**1**	**0.982**	**-0.902**	0.249	**0.981**	**-0.988**	**-0.979**	**-0.877**	**0.986**
O-Alkyl-C	-0.136	0.370	-0.272	**-0.886**	**-0.891**	-0.274	**-0.927**	**-0.958**	**0.783**	**0.843**	**-0.872**	**-0.852**	**0.982**	**1**	**-0.967**	0.064	**0.927**	**-0.943**	**-0.924**	**-0.951**	**1.000**
Aryl-C	-0.121	-0.121	0.017	**0.739**	**0.746**	0.200	**0.801**	**0.999**	**-0.599**	**-0.678**	**0.718**	**0.690**	**-0.902**	**-0.967**	**1**	0.193	**-0.800**	**0.827**	**0.797**	**0.998**	**-0.962**
O-Aryl-C	**-0.997**	**0.951**	**-0.978**	**-0.518**	-0.509	-0.273	-0.433	0.226	**0.670**	**0.590**	**-0.544**	**-0.577**	0.249	0.064	0.193	**1**	0.434	-0.393	-0.439	0.247	0.084
Carboxyl-C	-0.499	**0.692**	**-0.613**	**-0.995**	**-0.996**	-0.350	**-1.000**	**-0.780**	**0.960**	**0.983**	**-0.992**	**-0.986**	**0.981**	**0.927**	**-0.800**	0.434	**1**	**-0.999**	**-1.000**	**-0.766**	**0.934**
HB/HI	0.459	**-0.659**	**0.577**	**0.990**	**0.991**	0.343	**0.999**	**0.807**	**-0.946**	**-0.974**	**0.985**	**0.978**	**-0.988**	**-0.943**	**0.827**	-0.393	**-0.999**	**1**	**0.999**	**0.794**	**-0.949**
A/AO	0.504	**-0.696**	**0.618**	**0.996**	**0.997**	0.351	**1.000**	**0.776**	**-0.961**	**-0.985**	**0.993**	**0.987**	**-0.979**	**-0.924**	**0.797**	-0.439	**-1.000**	**0.999**	**1**	**0.762**	**-0.932**
ARM	-0.176	-0.066	-0.038	**0.700**	**0.708**	0.182	**0.767**	**1.000**	**-0.553**	**-0.636**	**0.679**	**0.649**	**-0.877**	**-0.951**	**0.998**	0.247	**-0.766**	**0.794**	**0.762**	**1**	**-0.945**
LigR	-0.156	0.389	-0.291	**-0.895**	**-0.900**	-0.279	**-0.935**	**-0.952**	**0.796**	**0.854**	**-0.882**	**-0.862**	**0.986**	**1.000**	**-0.962**	0.084	**0.934**	**-0.949**	**-0.932**	**-0.945**	**1**

[1] Values in bold are different from 0 with a significant level alpha = 0.05.

CHAPTER 6

Combination of different humic biostimulants with a mycorhiza-based microbial inoculum improves plant productivity, nutrient uptake, and primary and secondary metabolism

ABSTRACT

Biostimulants of natural origin represent a growing ecological strategy to increase crops productivity, expecially when combined application with microbial bioeffectors. Here we reports the effect of Potassium Humates (KH) from leonardite and Compost Tea (CT) from green compost, either alone or in combination with a commercial microbial inoculum (M+), mainly based on mycorrhiza (Micosat TabPlus), on both productivity and nutritional status of lettuce plants, as well as on the primary and secondary metabolism of treated plants. The biomass production as well as the uptake of both macro- and micronutrients by lettuce plants significantly increased by soil microbial inoculation combined to mixed humic materials. Similarly, the synergistic interaction between humic biostimulants and beneficial microorganisms significantly affected the primary metabolism of lettuce, by increasing the biosynthesis of essential amino acids and carbohydrates. Moreover, the combined addiction of humic biostimulants and microbial bioeffectors ehanced the accumulation in lettuce leaves of important antioxidant polyphenolic compounds. These findings indicate that a calibrated mixture of humic bioactive molecules in combination with microbial consortia has the potential tool to improve crop productivity and both its nutritional and metabolic status.

Keywords: humic matter, compost tea, green compost, mycorhizza, microbial bioeffectors, molecular characterization, plant biostimulants, GC-MS, UHPLC-MS-IT-TOF.

Introduction

Over the past two decades, agricultural intensification was the principal strategy proposed to ensure the growing need for food production (Shennan et al., 2017). However, conventional agricultural practices, such as the extensive use of chemical products (i.e., fertilizers and pesticides), resulted in a negative impact on the environment and human health, by gradual increasing both water pollution and degradation of cultivated soils (Shahrajabian et al., 2021). It is therefore necessary to adopt innovative technologies that enhance the sustainability of agricultural production systems, by preserving soil fertility and minimizing the adverse environmental impact of current agricultural production (Drobek and Fr, 2019). A promising and eco-friendly approach may be the treatment of plants with plant biostimulants (PB) and microbial bioeffectors that are found increase significantly plants productivity at low amendaent rates and improve plants tolerance against a wide range of abiotic stress (du Jardin, 2015; Yakhin et al., 2017). A major calss of plant biostimulants are humic and fulvic acids, followed by protein hydrolysates, seaweed extracts, while bioeffectors are beneficial fungi (i.e., arbuscular mycorrhizal fungi and Trichoderma spp.) and plant growth-promoting bacteria (Canellas et al., 2015).

Humic substances (HS) are relatively small heterogeneous molecules resulting from the biotic transformation of plant and animal tissues and held together by multiple weak interactions in supramolecular associations (Piccolo 2002). HS are essential to maintain and improve soil physical, chemical and biological proprieties (Piccolo et al., 1997; Imbufe et al., 2005; Puglisi et al., 2009). Moreover, their direct influence on different bio-chemical mechanisms and physiological processes in plants has repeatedly underlined (Nardi et al. 2002; Canellas and Olivares 2014). It has been shown that the positive effect of both HS and humic-like-substances (HLS) on root elongation and lateral root emergence (Canellas et al., 2002, 2012; Savy et al., 2015, 2016), as well as on nutrient uptake

(Nardi 2000; Quaggiotti et al., 2004), is correlated to the growth and productivity of plants. Moreover, Jannin et al. (2012) demonstrated that the HS applications induce the overexpression of genes involved in the major metabolic plant functions (i.e. photosynthesis, nitrogen/sulphur, phytohormones, plant development), thus supporting the influence of humic materials on plants both primary and secondary metabolism (Nardi et al., 2007; Schiavon et al., 2010; Ertani et al., 2011). The mechanism implied in such biostimulantion has been related to the incorporation into the humic suprastructure of hormone-like molecules (Muscolo et al., 2007), which are released to affect plant bioactivity when the humic supramolecular conformation is altered by the effect of small-size organic acids, as those commonly exuded by plants (Savy et al. 2017 a,b; Piccolo et al. 2019). The main commercially available humic substances are leonardite Potassium Humates (KH), whose beneficial effect on both soil proprieties and plant productivity has been widely demonstrated (Piccolo et al. 1997; Kumar et al., 2013; Conselvan et al. 2017; Ertani et al. 2019). However, the use of HS from renewable resources, such as from composted biomasses or bio-refinery wastes, is spreading in organic farming worldwide due to their remarkable bioactivity (Monda et al. 2017, 2018; Spaccini et al., 2019). In this regard, compost tea (CT), the water-soluble fraction obtained by either aerated or non- aerated immersion of compost in water for few days, may have great potentials for a sustainable agricultural production (Eudoxie and Martin 2019). In fact, it has been shown that applications of CT has multiple benefits as either fertilizer or biostimulant (Naidu et al. 2013; Pane et al., 2016; Zaccardelli et al., 2018), and as foliar spray against plants pathogens or antimicrobial product (Koné et al. 2010; Verrillo et al. 2021 a,b). Moreover, Savarese et al. (2021) recently reported that the combined application of leonardite KH and CT from green compost on maize seedlings stimulated both root development and shoot growth thanks to a cage effect by which CT bioactive compounds are stored in the hydrophobic domains of KH suprastructures, and then liberated to stimulate plant roots activity.

Another important class of plants biostimulants are the microbial bioeffectors, which have shown a powerful role in increasing both productivity and nutrients uptake of plants, as well as in

mitigating stress conditions (Giovannini et al., 2020; Moradtalab et al., 2020; Miceli et al., 2021). Among them, arbuscular mycorrhizal fungi (AMF) promote plants performance by improving the uptake of mineral nutrients (Rouphael et al., 2015), while PGPB (plant growth-promoting bacteria) stimulate plant growth by increasing the nutrients availability or by producing bioactive hormone-like compounds (Backer et al., 2018). Furthermore, many authors have reported that the *Trichoderma* fungus xhibits multiple beneficial effects, such as plant growth stimulation, promotion of nutrient uptake, suppression of plant pathogens and induction of plant defence mechanism (Woo et al., 2014; López-Bucio et al., 2015; Brenda et al., 2020). Moreover, recent studies have pointed out the potential as plant biostimulants of microbial consortia, by combining rhizobacteria and rhizofungi, which mimic the structured biological networks existing in native soils, through the empowerment of the natural microbiome (Kong et al., 2018; Woo and Pepe 2018; Bradáčová et al., 2019). Likewise, mixed application of HS and microbial bioeffectors has been recently explored for their possible synergistic effect on both plant development and soil biodiversity (Filho et al., 2021). Indeed, the combined application of humic extracts and PGPB, AMF or *Trichoderma spp.* was found to determine a boost effect on plants productivity, nutrients uptake and the overall metabolome (Ferreira et al., 2017; Vinci et al., 2018 a,b; Canellas et al., 2019b; Torun et al., 2020; Cozzolino et al., 2021).

Therefore, it is of great research interest the development of functional products by combining different plant biostimulants. However, the effects of combined biostimulants on plants growth and physiology, as well as their mechanisms of action are still poorly explored (Olivares et al., 2017). Hence, the aim of the present work was to study the stimulatory effect of different non-microbial (leonardite KH and CT from green compost) biostimulants and a commercial (Micosat TabPlus) microbial inoculum (M+), applied to soil alone or in multiple combinations, towards both productivity and nutritional status of lettuce plants. Additionally, the changes in primary and secondary metabolism of treated and untreated plants were investigated by both GC-MS and UHPLC-MS-IT-TOF analysis, to evaluate the overall effect of such bio-treatments on the lettuce metabolome.

Materials and Methods

Materials

Potassium Humates (KH) used for experimentation was provided by Hymato Products Ltd, Hungary. The KH were obtained by a KOH alkaline extraction from leonardite and supplied in form of dried granules of about 0.5-1 mm size.

Green compost was produced in the composting facility of the experimental farm of the University of Napoli Federico II at Castel-Volturno (CE) and used for the extraction of Compost Tea (CT), as reported earlier (Savarese et al., 2021). Briefly, 200 g of compost was weighed into a gauze bag and suspended in 1 L of distilled water in a plastic becker (w/v 1/5). The compost containing gauze bag was subjected to air insufflation at regular intervals (15 min every 3 h) with an automatic aeration pump device. After seven days of aeration, the extraction was stopped, and compost tea solution was freeze-dried.

A detailed chemical and molecular characterization of these materials is reported in a previous study (Savarese et al., 2021).

The microbial inoculum employed here was formulated by CCS Aosta s.r.l., as the MICOSAT TABPLUS commercial product and consisted of Glomus coronatum GU 53, B. caledonium GM 24, G. mosseae GP 11, G. viscosum GC 41, Rhizophagus irregularis RI 31l (10 %), plus Trichoderma harzianum TH01, Trichoderma viride TV 03, Bacillus subtilis BA 41, Streptomyces spp. SB 19, and Pichia pastoris PP59 (7.5% 10.2x107 C.F.U./g).

The soil used in the pot experiment was collected from the surface layer (0–20 cm) of a farmland Vertic Xerofluvent clay-loam soil located at the Castel Volturno (CE) University of Naples experimental station. The soil showed a clay loam textural composition (44.6%, 28% and 27.4% sand, silt and clay, respectively), an alkaline pH (8.6) and a content of 1.11 g kg^{-1} of total nitrogen, 10.5 g kg^{-1} of organic carbon, and 11 mg kg^{-1} of $NaHCO_3$-extractable phosphorous.

*Pot exp*eriment

The pot experiment was performed from March to May 2019, under greenhouse conditions (25–33 °C, daily temperature range). Lettuce plants (*Lactuca sativa* L. cv. capita "Meraviglia d'inverno") were grown on a mixture of soil/sand substrate (2:1 w/w, 1 kg pot^{-1}) sieved at 5 mm, and thoroughly homogenized. The basal nutrients supplied in powder form to the substrate of each individual pot and evenly mixed consisted of 100 mg N kg^{-1} as calcium nitrate $Ca(NO_3)_2$, and of 75 mg P kg^{-1} and 160 mg K kg^{-1} added as dipotassium hydrogen phosphate (K_2HPO_4). The KH and CT were tested individually and in combination (1:1) (MIX) at the rate of 169 $mgKg^{-1}$, applied once as water suspension at transplant, when the soil was also inoculated by applying 250 mg of the commercial microbial product (M+) per pot. The same rate of microbial inoculum was added again after one month of plant growth, corresponding to final total concentration of 0.5 gKg^{-1}. The synergistic effect of humic materials and microbial inoculum was tested with the following experimental design: CTRL: Control (H_2O); CTRL_M+: Control plus microbial inoculum; KH: Potassium Humates from leonardite; KH_M+: Potassium Humates from leonardite plus microbial inoculum; CT: Compost Tea from green compost; CT_M+: Compost Tea from green compost plus microbial inoculum; MIX: KH plus CT; MIX_M+: KH plus CT plus microbial inoculum. All treatments were replicated five times, for a total of 40 pots. After two months of plant growth, the leaves were harvested by cutting the plant base at 1 cm above the soil surface with a sharp knife. The leaves were first rinsed with tap water and then with deionized water. Biomass was determined (fresh and dry weight) to provide the plants yield for each treatment. The dried biomass was stored for mineral analysis, while three fresh leaves were immediately frozen in liquid nitrogen, and stored at –80 °C for metabolic analysis.

Mineral content analysis

Dried lettuce leaves were ground using a PM 20-ball mill (Retsch) before undergoing chemical analyses. Total N and S concentration in plant tissues was determined using 3 mg of each sample by an UNICUBE elemental analyser (Elementar Analysensysteme GmbH, Germany). Total

concentration of macro- (Ca, Mg, K) and micro- (Cu, Zn, Mn, Fe) elements in the plant tissues was ascertained by digesting 0.5 g of each sample with 6 mL of HNO_3 (65%) and 2 mL of H_2O_2 (35%) in a Milestone 900 microwave oven at 600 W for 24 min. Solutions were diluted to 25 mL with distilled water and analysed by an atomic absorption spectrometer (AAnalyst 700, Perkin-Elmer). The P content was measured calorimetrically in the same digested samples by the molybdenum blue assay method (Murphy and Riley 1962). All analyses were carried out in triplicate.

Extraction of primary metabolites and GC-MS determination

Lettuce leaves stored at −80 °C were freeze-dried and homogenized with a mortar. Then, 10 mg of homogenized plant samples were weighed into 2 mL Eppendorf tubes. The metabolites extraction was performed adding on dried samples 1 mL of water/methanol/chloroform mixture (1:3:1 ratio) pre-cooled at -20 °C. Ribitol and Dodecanoic acid at the concentration of 13 mg L^{-1} were used as internal standards. Plant samples were vortexed for 2 minutes and incubated for 2 hours at –20 °C to increase extraction yields. After extraction, samples were incubated for 15 minute at 70 °C in order to inhibit the possible activity of possible enzymes, vortexed and centrifuged for 10 min at 12000 rpm and at 4 ° C. Then, 900 µL of supernatant were recovered, transferred into 2 mL Eppendorf tubes and mixed with 400 µL of Milli Q water to allow separation of polar and apolar phases. The chloroform phase was used to determinate lipids, while the methanol/water upper phase was employed for polar compounds analyses. All extracts were stirred for 30 s and centrifuged for 10 min at 4 °C at 12000 rpm. Finally, 200 µL of each phase was transferred into 1.5 mL glass tubes for GC–MS analyses, dried under nitrogen and stored at -80 °C. All analyses were carried out in triplicate.

Derivatization for GC–MS analyses was conducted by suspending dried samples in 50 µL of a solution of methoxyamine hydrochloride solubilized in pyridine (20 mg mL^{-1}), that was gently shaken for 90 min at 30°C. After methoximation, samples were silylated for 30 min at 37°C by using 50 µL of N-methyl-N-trimethylsilyltrifluoroacetamide (MSTFA).

Then, 2 µL of each fully derivatized sample were analyzed through an Agilent 7683B Injector coupled to an Agilent HP6890 Series gas chromatograph system and a quadrupole 5973 Agilent Mass spectometer. The GC was carried out by RTX-5MS WCOT capillary column (Restek, 30 m × 0.25 mm; film thickness, 0.25 mm) that was coupled, through a heated transfer line (250 °C), to a mass spectrometer. The gas chromatographic elution was carried out by applying a 1 min of isothermal phase at 70 °C, followed by a temperature increase from 80 to 300°C (rate of 15°C min-1) and by a 10 minutes long isothermal phase at 300°C. Helium was the carrier gas at 1 mLmin^{-1}, as well as the injector temperature was set at 250 °C and the split flow applied for the split-injection mode was 25 mL min^{-1}. Mass spectra were obtained in the EI mode (70 eV), scanning in the range included within 50 and 650 m/z, with a cycle time of 0.2 scan s^{-1}. The identification of mass spectra of polar and apolar compounds was carried out by analyzing standard compounds as well as by evaluating the mass spectra reported in the library NIST 11.

Extraction of phenolic metabolites and determination by UHPLC-MS-IT-TOF

About 30 mg of freeze-dried lettuce leaves were weighed into 1.5 mL Eppendorf tube and mixed with 400 µL of methanol/water mixture (8:2) pre-cooled at -20 °C. Umbelliferon at the concentration of 10 mg L^{-1} was used as internal standard. Plant samples were vortexed for 2 minutes and incubated overnight (16 h) at – 20 °C to increase extraction yields.The mixture was centrifuged for 15 min at 12000 rpm at 4 ° C, and 300 µL of supernatant were transferred into a new 1.5 mL Eppendorf tube. The residue was similarly extracted once again with 400 µL of MeOH. Supernatants of both extractions were combined, vortexed for 2 minutes and centrifuged for 15 min at 12000 rpm at 4 ° C. Then, 100 µL of supernatant were transferred into a new 1.5 mL Eppendorf tube and added with 25 µL of 0.1 % Formic acid. The mixture was vortexed for 2 minutes and centrifuged for 15 min at 12000 rpm at 4 ° C. Finally, a volume of 100 µL was collected and transferred into 200 µL glass vials for UHPLC-MS-IT-TOF analyses. All analyses were carried out in triplicate.

Secondary metabolites were determined by a Shimadzu Nexera UHPLC system, consisting of a CBM-20A controller , a DGU-20A5r degasser, a binary solvent system LC-20AD, a SIL-20Axr autosampler and a column heater system CTO-20A. Chromatographic separation was performed with a Kinetex EVO C18 column (150 x 2.1mm, 2.6 μm particle size) coupled to a guard column with the same stationary phase, both from Phenomenex. The chromatographic conditions were the following: 2.0 μL injected sample, column maintained at 35.0 °C, flow rate of mobile phase at 0.3 $mLmin^{-1}$. The mobile phase was a binary system of 0.1% formic acid aqueous solution (A) and acetonitrile containing 0.1% formic acid (B). The gradient elution was as it follows: 0-0.5 min, 1% B; 0.5-4.0 min, 13% B; 4.0-10.0 min, 45% B held for 2.0 min; 12.0-14.0 min, 60% B and then held for 1.5 min. The system was riequilibrated by again reaching 1% B in 16.5 min and held it for 4.5 min before the next injection step.

The UHPLC system was coupled online to a hybrid IT-TOF mass spectrometer from Shimadzu Corp. (Tokyo, Japan), equipped with an electrospray ionization (ESI) source operating in negative mode under the following conditions: N_2 nebulizing gas flow of 1.5 $Lmin^{-1}$; interface voltage at 3.5 kV; curved desorption line (CDL) interface temperature of 200 °C; block heater temperature, 200 °C; detector voltage 1.57 kV; drying gas pressure of 110 kPa. Full scan MS data were acquired in the range of 80–1000 m/z (octopole ion accumulation time of 20 ms; IT, (repeat = 3). MS/MS experiments were conducted in a data dependent acquisition using a mass range of 50-900 m/z; precursor ions were acquired in the range 150–900 m/z; peak width, 1 Da; ion accumulation time, 40 ms; Collision induced dissociation (CID) energy, 50%, collision gas 50%, repeat = 1; execution trigger (BPC) intensity, at 95% stop level. LC–MS data elaboration was performed by the LCMSsolution software (Version 3, Shimadzu), the Formula Predictor software (Version 1.2, Shimadzu) and MetID solution software (Version 1.2, Shimadzu).

Statistical analysis

A normality test (Kolmogorov–Smirnov) was performed on the dataset derived from mineral analysis. Significant differences between the means were determined by one and two-ways analysis of variance, while application of LSD test to differentiate among results was given at the $P < 0.05$ probability level using the XLStat software v.9.0 (Addinsoft).

The semi-quantitative evaluation of both GC- and LC-chromatograms was obtained by normalizing the area of each peak to the area of the internal standard and further modulating it to the sample fresh weight (mg). The Principal Component Analysis (PCA) was used here to reduce the dimensionality of the dataset and concomitantly preserve the useful information expressed in terms of variable variance. The XLStat software, version 9.0 (Addinsoft) was used to process the PCA of the total dataset composed of 38 and 23 variables obtained by GC-MS analysis of polar and apolar phases, respectively, and 23 variables derived from UHPLC-MS-IT-TOF analysis of phenolic metabolites. Data were checked for normality and homogeneity of variance and transformed where necessary. Significant differences in metabolites amount among treatments were tested by one-way ANOVA, followed by LSD test (significant for p-values < 0.05 at a significance α of 0.05). The Heatmapping was elaborated by the Heatmapper software (Babicki et al. 2016). Each Heatmap score represented the average value of nine replicates.

Results

Plant growth and nutrient content

All treatments significantly increased plant biomass compared to the control (CTRL) (Figure 1). Without the microbial inoculum, the largest effect on plants yield was obtained for the MIX treatment, that is the combination of KH and CT, with an increased shoot dry weight of 33 %, as compared to control (Figure 1b), whereas the application of the same materials alone showed an increase of only 15 % (Figure 1b). The same trend was visible in the shoot fresh weight (Figure 1a). The inoculation with the microbial product (M+) significantly affected lettuce productivity. With M+ addition, the shoot biomass raised for all treatments (Figure 1). In particular, the combination of KH

and CT with the microbial inoculum (MIX_M+) showed the largest shoot fresh and dry weight, which increased by 41 and 52 %, respectively, in comparison to control (Figure 1).

Figure 1.
Shoot fresh (**a**) and dry (**b**) weight of lettuce plants treated with different biostimulants. CTRL: Control; KH: Potassium Humates from leonardite; CT: Compost Tea from green compost; MIX: KH plus CT; M+: plus microbial inoculum (Micosat TABPLUS). Dark grey indicates the microbial inoculation. Bars indicate standard deviation of means (n = 5). Different letters above the bars indicate significantly different means according to LSD test ($p < 0.05$).

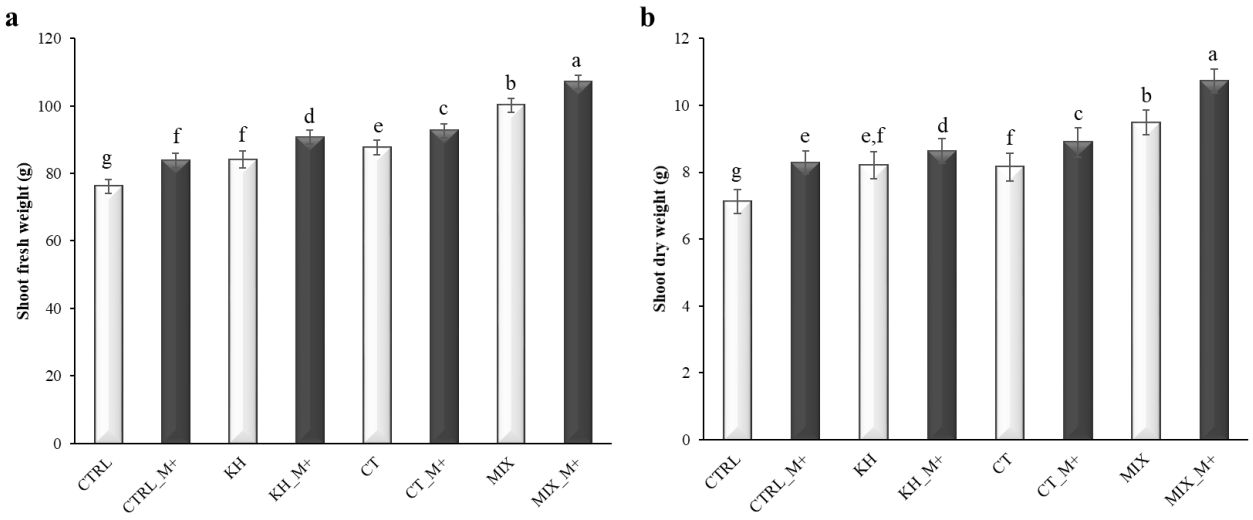

The mineral status of lettuce plants resulted also affected by both the individual application of the microbial inoculum and biostimulants, and by their combination (Table 1 and 2). As shown in Figure 2, the effect on macronutrients uptake varied with the treatment. In absence of the microbial inoculum, the individual application of CT significantly increased leaf concentration (mg g^{-1}) of P, K, Ca, and Mg (Figure 2 c, e, i, m), whereas the combined MIX treatment provided a significant improvement of N and S leaf concentration (mg g^{-1}) (Figure 2 a, g). Moreover, plants treated with MIX showed a greater macronutrients leaf content (mg $plant^{-1}$ DW) than both control and plants under single KH and CT applications (Figure 2 b, d, f, h, l, n). The inoculation with the microbial product (M+) significantly affected the macronutrients status of lettuce plants (Table 1), increasing their uptake when applied either alone, except for CT, or in combination with the biostimulants (Figure 2). In particular, the MIX_M+ treatment showed the largest effect on both macronutrients leaf concentration (mg g^{-1}) and content (mg $plant^{-1}$ DW) (Figure 2). Moreover, plants under MIX_M+

reveales an increase in N, P, K, S, Ca and Mg leaf content (mg plant^{-1} DW) of 55.2, 74.8, 33.9, 70.2, 140.8, and 73.6 %, respectively, more than control plants (Figure 2 b, d, f, h, l, n).

The individual application of biostimulants slightly affected the micronutrients content of treated leaves, as compared to control (Figure 3), whereas microbial inoculation (M+) greatly improved their uptake by lettuce plants (Table 2 and Figure 3). In particular, the addition of KH togheter with the microbial product (KH_M+) significantly increased both leaf concentration (mg Kg^{-1}) and content (mg plant^{-1} DW) of Cu and Fe (Figure 3 a, b, g, h). On the other hand, the concentration of Zn and Mn remarkably raised in plants under the MIX_M+ treatment (Figure 3 c, d, e, f). In fact, plants treated with MIX_M+ showed the greatest leaf content (mg plant^{-1} DW) of Zn, Mn and Fe, which increased of 50, 98 and 85 %, respectively, more than for control (Figure 3 d, f, h).

Table 1.
Two-way ANOVA results on the influence of biostimulants application (B), microbial inoculation (M+) and interaction between biostimulants and microbial inoculum (B*M+) on both leaf macronutrients concentration **(**mg g^{-1}**)** and content **(**mg $plant^{-1}$ Dry Weight**)** of lettuce plants.

			Leaf concentration (mg g^{-1})			**Leaf content (mg $plant^{-1}$ DW)**	
Element	**Treatment**	**df**	**F**	**P**	**df**	**F**	**P**
N	B	3	57.690	< **0.0001**	3	381.638	< **0.0001**
	M+	1	5.105	**0.031**	1	137.908	< **0.0001**
	B*M+	3	5.042	**0.006**	3	20.164	< **0.0001**
	Error	32			32		
P	B	3	138.844	< **0.0001**	3	1114.484	< **0.0001**
	M+	1	58.672	< **0.0001**	1	145.501	< **0.0001**
	B*M+	3	141.013	< **0.0001**	3	297.230	< **0.0001**
	Error	32			32		
K	B	3	77.655	< **0.0001**	3	1895.467	< **0.0001**
	M+	1	8.830	**0.006**	1	2042.292	< **0.0001**
	B*M+	3	53.015	< **0.0001**	3	369.684	< **0.0001**
	Error	32			32		
S	B	3	37.466	< **0.0001**	3	279.772	< **0.0001**
	M+	1	4.422	**0.043**	1	42.462	< **0.0001**
	B*M+	3	1.058	0.380	3	10.518	< **0.0001**
	Error	32			32		
Ca	B	3	916.008	< **0.0001**	3	7489.782	< **0.0001**
	M+	1	532.634	< **0.0001**	1	5673.479	< **0.0001**
	B*M+	3	898.377	< **0.0001**	3	2648.269	< **0.0001**
	Error	32			32		
Mg	B	3	94.341	< **0.0001**	3	2291.876	< **0.0001**
	M+	1	0.654	0.452	1	971.719	< **0.0001**
	B*M+	3	112.707	< **0.0001**	3	285.756	< **0.0001**
	Error	32			32		

Table 2.
Two-way ANOVA results on the influence of biostimulants application (B), microbial inoculation (M+) and interaction between biostimulants and microbial inoculum (B*M+) on both leaf micronutrients concentration **(**mg g^{-1}**)** and content **(**mg $plant^{-1}$ Dry Weight**)** of lettuce plants.

			Leaf concentration (mg Kg^{-1})			**Leaf content (mg $plant^{-1}$ DW)**	
Element	**Treatment**	**df**	**F**	**P**	**df**	**F**	**P**
Cu	B	3	229.870	< **0.0001**	3	51.013	< **0.0001**
	M+	1	44.925	< **0.0001**	1	287.139	< **0.0001**
	B*M+	3	88.736	< **0.0001**	3	55.373	< **0.0001**
	Error	32			32		
Zn	B	3	259.732	< **0.0001**	3	706.522	< **0.0001**
	M+	1	16.050	**0.0003**	1	2212.979	< **0.0001**
	B*M+	3	310.818	< **0.0001**	3	1014.692	< **0.0001**
	Error	32			32		
Mn	B	3	903.346	< **0.0001**	3	3851.439	< **0.0001**
	M+	1	1445.613	< **0.0001**	1	4348.142	< **0.0001**
	B*M+	3	216.628	< **0.0001**	3	229.508	< **0.0001**
	Error	32			32		
Fe	B	3	5778.256	< **0.0001**	3	6768.731	< **0.0001**
	M+	1	20099.934	< **0.0001**	1	27180.559	< **0.0001**
	B*M+	3	1369.361	< **0.0001**	3	10.307	< **0.0001**
	Error	32			32		

Figure 2.

Effect of the biostimulants on macronutrients composition of lettuce leaves. Leaf nitrogen concentration and content (**a,b**), leaf phosphorus concentration and content (**c,d**), leaf potassium concentration and content (**e,f**), leaf sulphur concentration and content (**g,h**), leaf calcium concentration and content (**i,l**), leaf magnesium concentration and content (**m,n**). CTRL: Control; KH: Potassium Humates from leonardite; CT: Compost Tea from green compost; MIX: KH plus CT; M+: plus microbial inoculum (Micosat TABPLUS). Dark grey indicates the microbial inoculation. Bars indicate standard deviation of means (n = 9). Different letters above the bars indicate significantly different means according to LSD test ($p < 0.05$).

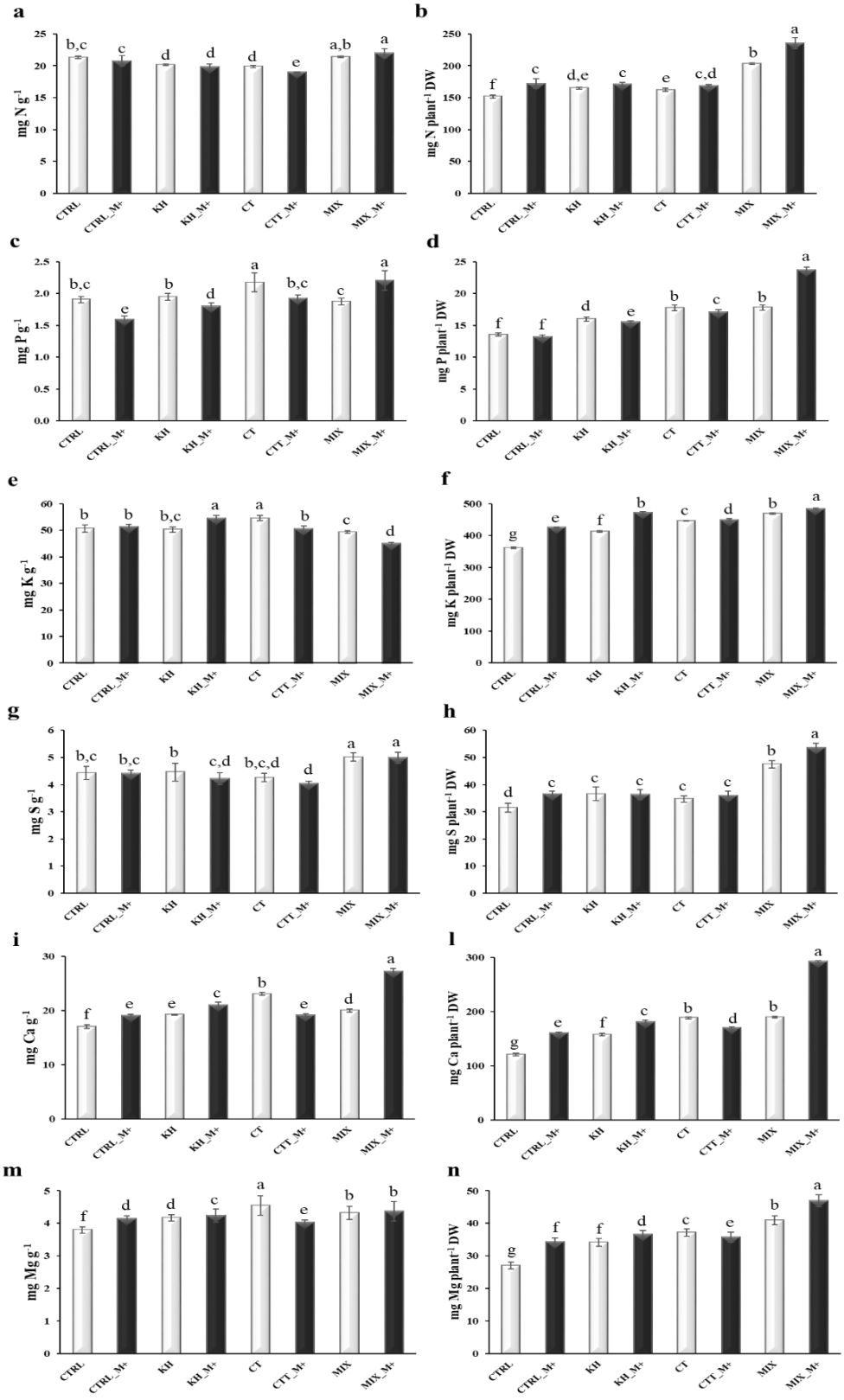

Figure 3.

Effect of the biostimulants on micronutrients composition of lettuce leaves. Leaf copper concentration and content (**a,b**), leaf zinc concentration and content (**c,d**), leaf manganese concentration and content (**e,f**), leaf iron concentration and content (**g,h**). CTRL: Control; KH: Potassium Humates from leonardite; CT: Compost Tea from green compost; MIX: KH plus CT; M+: plus microbial inoculum (Micosat TABPLUS). Dark grey indicates the microbial inoculation. Bars indicate standard deviation of means (n = 9). Different letters above the bars indicate significantly different means according to LSD test ($p < 0.05$).

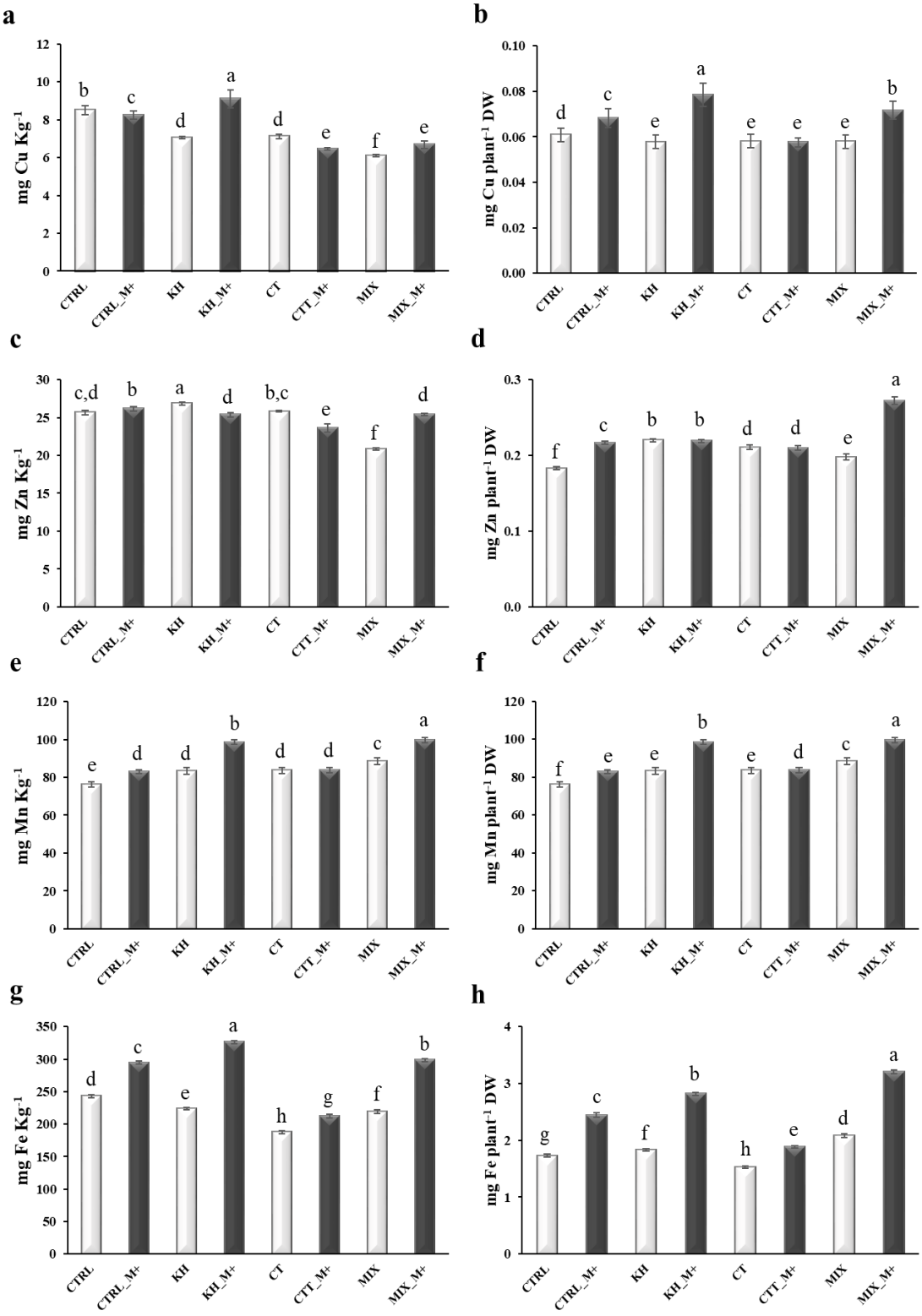

Primary metabolism

Differences in primary metabolism of lettuce plants grown under biostimulants, alone or in combination with the microbial inoculum, were assessed by GC-MS. The main identified compounds in the polar fraction of leaves extracts were saccharides (mono- and di- saccharides), amino and organic acids (Table S1 and Figure S1). To detect the effects of treatments on the leaves metabolome, the GC-MS data of polar plants extracts were elaborated by the Principal Components Analysis (PCA). The PCA of plants inoculated with the microbial product (M+) in combination with different biostimulants explained 72.59 % of the total variance, with PC1 and PC2 accounting for 52.94 and 19.65 %, respectively (Figure 4a). The treatments were well separated and distributed in the loading plot. In particular, the first PC neatly separated CT and CT_M+ treatments from other ones, based on the lower amount of almost all identified metabolites, except cellobiose and glycerol (Figure 4a and Table 3). Moreover, along the second PC the control and KH treatments, alone or in combination with the microbial inoculum (M+), were clearly separated from CT and MIX application, due to a larger amount in the corresponding leaves extracts of myo-inositol and organic acids such as malic, citric and fumaric acid (Figure 4a and Table 3). Finally, the distribution of MIX and MIX_M+ treatments in the lower right quadrant on the positive side of PC1 was significantly correlated to a large amino acids content, particularly alanine, GABA and glutamic acid, and main carbohydrates such as fructose, galactose and glucose (Figure 4a and Table 3).

The Heatmap derived from metabolomics data confirmed that the relative amount of identified metabolites varied as a function of treatments, thus determining a different placement of plant samples in the score-plot (Figure 4b). The application of leonardite KH increased the accumulation of organic acids (Figure S5), mostly malic and citric acid (Table 3), whereas CT treatments mainly enhanced the biosynthesis of cellobiose and glycerol (Table 3). Moreover, plants under the MIX treatment showed a greater amount than for control of amino acids, such as aspartic and glutamic acid (Table 3), and carbohydrates like fructose and glucose (Table 3 and Figure 4b). It is notworthy that the inoculation with the microbial product (M+) significantly affected the primary metabolism of polar

compounds, especially when applied in combination with the MIX treatment (Figure 4b). Plants under MIX_M+ treatment exhibited a larger amount of almost all amino acids and saccharides (Figure S4 and S6) than lettuce plants treated with all other biostimulants (Figure 4b).

GC-MS analysis was also applied to identify the metabolites extracted in the apolar fraction of lettuce leaves under different treatments. The main identified compounds were long-chain fatty acids, alcohols, sterols, and terpenes (Table S2 and Figure S2). When GC-MS data of apolar metabolic extracts were evaluated by Principal Component Analysis (PCA), it was found that the two first principal components captured 64.52 % of total variance, and showed a certain separation among treatments (Figure 5a). The PC1 (43.75 % of total variance) allowed to distinguish among the CT, KH_M+, MIX and MIX_M+ treatments, due to more abundant metabolites such as myristic acid, docosanol, stearic acid and sterols (Figure 5a and Table 3). The placement of KH, CTRL and CTRL_M+ along the negative values of PC1 was due to a lesser amount of all identified metabolites in the corresponding leaves extracts, except for amyrin, germanicol and lupenol (Figure 5a and Table 3). Moreover, the PC2 (20.78 % of total variance) neatly separated plants under CT and CT_M+ from the other treatments, based on a greater amount of long-chain fatty acids, mainly linoleic and linolenic acid (Figure 5a and Table 3). These results were confirmed by applying the Heatmap elaboration on the metabolomics data (Figure 5b). In particular, untreated plants (CTRL) and plants under microbial inoculation alone (CTRL_M+) and leonardite Potassium Humates (KH) application showed a similar lipidic profile (Figure 5b), whereas the combined application of KH and M+ significantly enhanced the biosynthesis of fatty acids (Figure S7), mainly lauric and myristic acid (Table 3). On the other hand, the application of Compost Tea (CT), either alone or in combination with the microbial inoculum (CT_M+), remarkably raised the concentration of long-chain fatty acids (Figure 5b and S7), principally linoleic and α-linolenic acid (Table 3). Interestingly, the lipidic profile of leaves treated with MIX was not so different from the application of CT alone (Figure 5b). Conversely, the addition of the microbial inoculum to the mixed humic material (MIX_M+) significantly affected the

concentration of all identified metabolites (Figure 5b), mainly long-chain fatty alcohols and sterols (Table 3 and Figure S8).

Table 3.
Relative abundance (metabolite-to-internal standard total area ratio, a/is) of main discriminant variables from PCA of both GC-MS and UHPLC-MS-IT-TOF metabolomics data of lettuce plants treated with different biostimulants. CTRL: Control; KH: Potassium Humates from leonardite; CT: Compost Tea from green compost; MIX: KH plus CT; M+: plus microbial inoculum (Micosat TABPLUS). Values are the means of nine replicates ± standard deviation. Different letters indicate significant differences according to LSD test ($p < 0.05$).

Metabolite	**Relative abundance (a/is)**							
	CTRL	**CTRL_M+**	**KH**	**KH_M+**	**CT**	**CT_M+**	**MIX**	**MIX_M+**
Amino acids								
Alanine	0.144 ± 0.01 ^{d,e}	0.158 ± 0.01 ^{c,d}	0.161 ± 0.01 ^{c,d}	0.167 ± 0.01 ^{c}	0.155 ± 0.01 ^{c,d}	0.127 ± 0.01 ^{e}	0.234 ± 0.01 ^{b}	0.234 ± 0.01 ^{a}
Serine	0.173 ± 0.01 ^{d}	0.197 ± 0.01 ^{c}	0.157 ± 0.01 ^{e}	0.168 ± 0.01 ^{d}	0.108 ± 0.01 ^{f}	0.112 ± 0.01 ^{f}	0.220 ± 0.01 ^{b}	0.240 ± 0.01 ^{a}
Proline	1.109 ± 0.07 ^{b}	1.038 ± 0.08 ^{b}	0.745 ± 0.03 ^{d}	0.853 ± 0.05 ^{c}	0.451 ± 0.06 ^{e}	0.352 ± 0.06 ^{f}	0.918 ± 0.06 ^{c}	1.238 ± 0.09 ^{a}
GABA	0.05 ± 0.001 ^{b}	0.05 ± 0.001 ^{b}	0.04 ± 0.001 ^{c}	0.05 ± 0.001 ^{b}	0.03 ± 0.001 ^{c,d}	0.03 ± 0.001 ^{d}	0.05 ± 0.001 ^{b}	0.07 ± 0.001 ^{a}
Aspartic acid	0.342 ± 0.05 ^{b}	0.308 ± 0.05 ^{c}	0.285 ± 0.02 ^{c}	0.313 ± 0.05 ^{b,c}	0.187 ± 0.04 ^{d}	0.184 ± 0.05 ^{d}	0.397 ± 0.05 ^{a}	0.402 ± 0.04 ^{a}
Glutamic acid	0.631 ± 0.03 ^{b}	0.630 ± 0.01 ^{b}	0.598 ± 0.05 ^{b}	0.610 ± 0.06 ^{b}	0.478 ± 0.02 ^{c}	0.459 ± 0.06 ^{c}	0.832 ± 0.03 ^{a}	0.811 ± 0.06 ^{a}
Organic acids								
Malic acid	19.01 ± 0.6 ^{c,d,e}	18.57 ± 0.9 ^{d,e,f}	21.39 ± 0.6 ^{a}	20.47 ± 0.4 ^{b}	18.33 ± 0.7 ^{e,f}	17.96 ± 0.4 ^{f}	19.15 ± 0.8 ^{c,d}	19.28 ± 0.6 ^{c}
Citric acid	1.826 ± 0.2 ^{d}	2.096 ± 0.2 ^{c}	2.732 ± 0.3 ^{a}	2.427 ± 0.6 ^{b}	1.649 ± 0.5 ^{,e}	1.816 ± 0.6 ^{d}	1.867 ± 0.3 ^{d}	2.274 ± 0.6 ^{b}
Fumaric acid	0.256 ± 0.05 ^{b}	0.307 ± 0.01 ^{a}	0.267 ± 0.01 ^{b}	0.259 ± 0.01 ^{b}	0.194 ± 0.03 ^{d}	0.182 ± 0.07 ^{d}	0.217 ± 0.02 ^{c}	0.225 ± 0.01 ^{c}

Tartaric acid	1.08 ± 0.2 ^{c,d}	1.012 ± 0.1 ^{d,e}	1.301 ± 0.4 ^{b}	1.465 ± 0.5 ^{a}	0.841 ± 0.2 ^{f}	0.864 ± 0.4 ^{e,f}	0.967 ± 0.2 ^{d,e,f}	1.215 ± 0.2 ^{b,c}
Threonic acid	0.161 ± 0.02 ^{b}	0.171 ± 0.01 ^{a}	0.152 ± 0.03 ^{c}	0.165 ± 0.02 ^{a,b}	0.126 ± 0.01 ^{e}	0.133 ± 0.03 ^{d}	0.162 ± 0.02 ^{b}	0.170 ± 0.01 ^{a}
Cinnamic acid	0.252 ± 0.02 ^{e}	0.1257 ± 0.01 ^{e}	0.266 ± 0.01 ^{d}	0.298 ± 0.01 ^{a,b}	0.294 ± 0.01 ^{b}	0.273 ± 0.03 ^{d}	0.303 ± 0.03 ^{a}	0.284 ± 0.02 ^{c}
Saccharides								
Glycerol	0.309 ± 0.03 ^{d,e}	0.284 ± 0.05 ^{e}	0.379 ± 0.02 ^{a,b}	0.333 ± 0.03 ^{c,d}	0.359 ± 0.04 ^{b,c}	0.394 ± 0.05 ^{a}	0.311 ± 0.03 ^{d,e}	0.302 ± 0.07 ^{e}
Fructose	28.26 ± 1.4 ^{c,d}	27.12 ± 1.5 ^{d,e}	26.01 ± 0.5 ^{e}	28.79 ± 0.6 ^{c}	27.89 ± 0.6 ^{c,d}	25.66 ± 0.7 ^{f}	33.36 ± 1.0 ^{b}	37.59 ± 0.7 ^{a}
Glucose	10.42 ± 0.5 ^{c}	11.04 ± 0.8 ^{b,c}	9.05 ± 0.5 ^{d}	10.29 ± 0.6 ^{c}	8.87 ± 0.8 ^{d}	8.91 ± 0.4 ^{d}	11.78 ± 0.2 ^{a,b}	11.97 ± 0.4 ^{a}
Galactose	28.12 ± 1.1 ^{b}	29.10 ± 0.8 ^{b}	26.21 ± 0.4 ^{c}	27.78 ± 1.0 ^{b}	26.21 ± 0.5 ^{c}	25.66 ± 0.6 ^{c}	31.48 ± 0.7 ^{a}	30.71 ± 0.8 ^{a}
Myo-inositol	15.63 ± 1.0 ^{a}	15.25 ± 0.8 ^{a,b}	15.48 ± 0.7 ^{a,b}	15.64 ± 0.8 ^{a}	12.99 ± 0.6 ^{c}	13.47 ± 0.7 ^{c}	13.82 ± 0.8 ^{c}	14.24 ± 0.5 ^{b,c}
Cellobiose	0.416 ± 0.03 ^{b,c}	0.445 ± 0.03 ^{b,c}	0.428 ± 0.03 ^{b,c}	0.399 ± 0.04 ^{b,c}	0.530 ± 0.03 ^{a}	0.531 ± 0.03 ^{a}	0.453 ± 0.05 ^{b}	0.398 ± 0.01 ^{c}
Trehalose	0.702 ± 0.04 ^{a}	0.567 ± 0.08 ^{c}	0.677 ± 0.07 ^{a,b}	0.683 ± 0.07 ^{a}	0.676 ± 0.03 ^{a,b}	0.686 ± 0.05 ^{a}	0.696 ± 0.03 ^{a}	0.618 ± 0.02 ^{b,c}
Lipids								
Myristic acid	3.61 ± 0.3 ^{c,d}	3.34 ± 0.2 ^{d,e}	3.62 ± 0.3 ^{c,d}	6.43 ± 0.3 ^{a}	4.21 ± 0.2 ^{b}	3.16 ± 0.1 ^{e}	3.86 ± 0.2 ^{b,c}	4.20 ± 0.2 ^{b}
Stearic acid	1.316 ± 0.2 ^{c,d}	1.273 ± 0.1 ^{d}	1.285 ± 0.2 ^{c,d}	1.441 ± 0.2 ^{b}	1.472 ± 0.1 ^{a,b}	1.236 ± 0.6 ^{d}	1.386 ± 0.3 ^{b,c}	1.552 ± 0.3 ^{a}
Linoleic acid	1.16 ± 0.1 ^{d,e}	1.091 ± 0.1 ^{e,f}	1.024 ± 0.1 ^{f}	1.26 ± 0.2 ^{c,d}	1.48 ± 0.2 ^{a,b}	1.538 ± 0.1 ^{a}	1.303 ± 0.2 ^{c}	1.434 ± 0.2 ^{b}
Linolenic acid	1.196 ± 0.2 ^{c,d}	0.949 ± 0.1 ^{e}	0.929 ± 0.3 ^{e}	0.969 ± 0.1 ^{e}	1.590 ± 0.2 ^{b}	1.835 ± 0.3 ^{a}	1.114 ± 0.4 ^{d}	1.259 ± 0.3 ^{c}

Hexadecenol	0.444 ± 0.05 ^{e}	0.47 ± 0.01 ^{e}	0.512 ± 0.01 ^{d}	0.456 ± 0.03 ^{e}	0.583 ± 0.01 ^{c}	0.451 ± 0.01 ^{e}	0.623 ± 0.03 ^{b}	0.722 ± 0.01 ^{a}
Docosanol	0.812 ± 0.01 ^{d}	0.959 ± 0.03 ^{c}	1.266 ± 0.2 ^{a}	1.095 ± 0.1 ^{b}	0.856 ± 0.06 ^{c,d}	0.621 ± 0.02 ^{e}	1.094 ± 0.1 ^{b}	1.321 ± 0.1 ^{a}
β-Sitosterol	1.34 ± 0.2 ^{c,d}	1.30 ± 0.2 ^{d}	1.29 ± 0.2 ^{d}	1.40 ± 0.2 ^{c}	1.55 ± 0.2 ^{b}	1.38 ± 0.1 ^{c,d}	1.63 ± 0.1 ^{b}	1.84 ± 0.1 ^{a}
β-amyrin	0.471 ± 0.02 ^{a}	0.374 ± 0.04 ^{c,d}	0.415 ± 0.07 ^{b,c}	0.433 ± 0.02 ^{a,b}	0.403 ± 0.02 ^{b,c}	0.385 ± 0.03 ^{c,d}	0.358 ± 0.02 ^{d}	0.384 ± 0.04 ^{c,d}
Phenolic compounds								
p-Coumaroylquinic acid	8.52 ± 0.3 ^{e}	10.13 ± 0.3 ^{d}	10.39 ± 0.7 ^{b,c}	11.47 ± 0.4 ^{b,c}	12.38 ± 0.7 ^{a,b}	12.99 ± 0.6 ^{a}	13.21 ± 0.3 ^{a}	11.89 ± 0.3 ^{c,d}
Feruloylquinic acid	0.341 ± 0.04 ^{c}	0.390 ± 0.05 ^{a,b}	0.391 ± 0.04 ^{a,b}	0.420 ± 0.06 ^{a}	0.210 ± 0.03 ^{d}	0.336 ± 0.02 ^{c}	0.370 ± 0.03 ^{b,c}	0.337 ± 0.07 ^{c}
Caffeoyltartaric p-coumaroyl acid	2.23 ± 0.2 ^{c}	2.25 ± 0.2 ^{c}	2.33 ± 0.3 ^{c}	2.68 ± 0.2 ^{b}	1.76 ± 0.1 ^{c}	2.68 ± 0.2 ^{b}	2.87 ± 0.3 ^{a}	1.86 ± 0.1 ^{d}
Chlorogenic acid	4.17 ± 0.9 ^{d}	5.87 ± 0.4 ^{b,c}	5.43 ± 0.6 ^{c}	5.75 ± 0.5 ^{b,c}	5.41 ± 0.5 ^{c}	6.01 ± 0.7 ^{b}	6.71 ± 0.4 ^{a}	5.81 ± 0.3 ^{b,c}
Coutaric acid	1.71 ± 0.1 ^{a,b}	1.75 ± 0.1 ^{a,b}	1.77 ± 0.2 ^{a}	1.69 ± 0.1 ^{a,b}	1.63 ± 0.2 ^{b}	1.78 ± 0.1 ^{a}	1.79 ± 0.1 ^{a}	1.71 ± 0.1 ^{a,b}
Chicoric acid	4.11 ± 0.3 ^{d}	5.28 ± 0.3 ^{c}	4.24 ± 0.4 ^{d}	6.24 ± 0.6 ^{a,b}	5.04 ± 0.9 ^{c}	6.68 ± 0.8 ^{a}	6.07 ± 0.8 ^{b}	6.07 ± 0.8 ^{b}
Luteolin-7-glucoside	1.35 ± 0.1 ^{c}	1.49 ± 0.1 ^{b}	1.50 ± 0.1 ^{b}	1.44 ± 0.1 ^{b,c}	1.77 ± 0.2 ^{a}	1.81 ± 0.1 ^{a}	1.84 ± 0.1 ^{a}	1.88 ± 0.1 ^{a}
Luteolin-7-glucuronide	3.37 ± 0.4 ^{e}	3.56 ± 0.2 ^{d,e}	3.11 ± 0.3 ^{f}	3.66 ± 0.3 ^{c,d}	3.08 ± 0.2 ^{f}	4.11 ± 0.2 ^{a,b}	4.22 ± 0.3 ^{a}	3.91 ± 0.3 ^{b,c}
Quercetin-3-O-glucoside	5.15 ± 0.7 ^{c}	6.11 ± 0.4 ^{b}	6.24 ± 0.6 ^{b}	6.62 ± 0.7 ^{b}	6.36 ± 0.3 ^{b}	7.86 ± 0.6 ^{a}	7.82 ± 0.7 ^{a}	7.72 ± 0.4 ^{a}
Esculetin-6-O-glucoside	0.630 ± 0.05 ^{d}	1.019 ± 0.08 ^{c}	0.963 ± 0.1 ^{c}	0.971 ± 0.07 ^{c}	0.958 ± 0.1 ^{c}	1.121 ± 0.1 ^{b}	1.247 ± 0.04 ^{a}	0.926 ± 0.1 ^{c}

Figure 4.

a) PCA biplot based on metabolites identified by GC-MS in the polar fraction of leaves extracts from lettuce plants treated with different biostimulants. The combination of the shapes and colors indicate different treatments. Light-Circle: single biostimulant; Dark-triangle: biostimulant plus microbial inoculum (M+). Red: Control (CTRL); Blue: Potassium Humates from leonardite (KH); Green: Compost Tea from green compost (CT); Yellow: KH plus CT (MIX). **b)** Heatmap resulting from metabolomics data. Each row represents a metabolite feature and each column represents a treatment. The row Z-score or scaled expression value of each feature is plotted in yellow-green-blue-red color scale. The red color of the tile indicates high abundance and yellow indicates low abundance. The PCA and Heatmap scores represent the average value of nine replicates. [1]

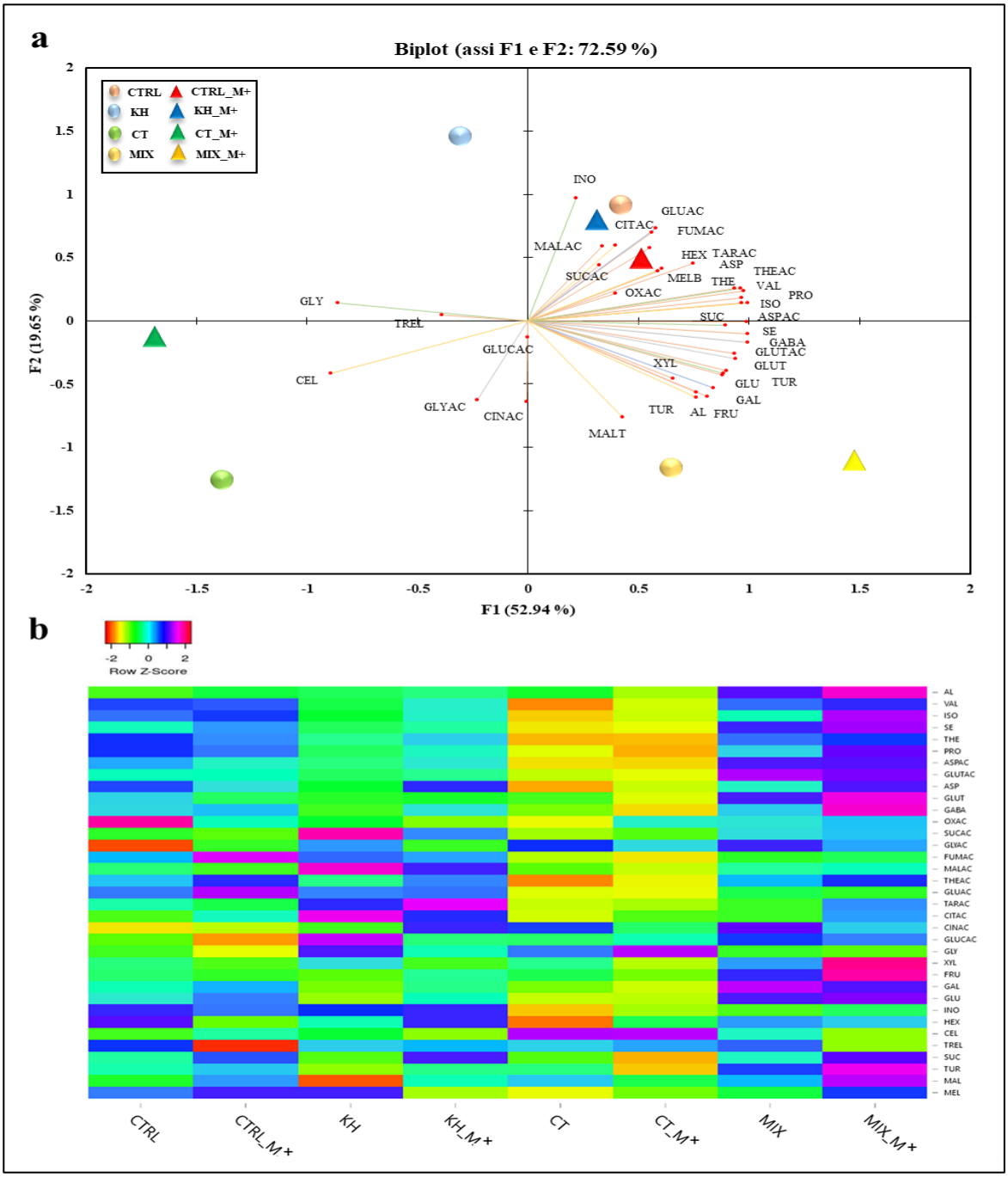

[1]AL: alanine; VAL: valine; ISO: isoleucine; SE: serine; THE: threonine; PRO: proline; ASPAC: aspartic acid; GLUTAC: glutamic acid; ASP: asparagine; GLUT: glutamine; GABA: 4-aminobutyrric acid; OXAC: oxalic acid; SUCAC: succinic acid; GLYAC: glyceric acid; FUMAC: fumaric acid; MALAC: malic acid; THEAC: threonic acid; GLUAC: glutaric acid; TARAC: tartaric acid; CITAC: citric acid; CINAC: cinnamic acid; GLUCAC: glucuronic acid; GLY: glycerol; XYL: xylose; FRU: fructose; GAL: galactose; GLU: glucose; INO: myo-inositol; HEX: hexose; CEL: cellobiose; TREL: trehalose; SUC: sucrose; TUR: turanose; MAL: maltose; MELB: melibiose.

Figure 5.

a) PCA biplot based on metabolites identified by GC-MS in the apolar fraction of leaves extracts from lettuce plants treated with different biostimulants. The combination of the shapes and colors indicate different treatments. Light-Circle: single biostimulant; Dark-triangle: biostimulant plus microbial inoculum (M+). Red: Control (H_20); Blue: Potassium Humates from leonardite (KH); Green: Compost Tea from green compost (CT); Yellow: KH plus CT (MIX). **b)** Heatmap resulting from metabolomics data. Each row represents a metabolite feature and each column represents a treatment. The row Z-score or scaled expression value of each feature is plotted in yellow-green-blue-red color scale. The red color of the tile indicates high abundance and yellow indicates low abundance. The PCA and Heatmap scores represent the average value of nine replicates. [1]

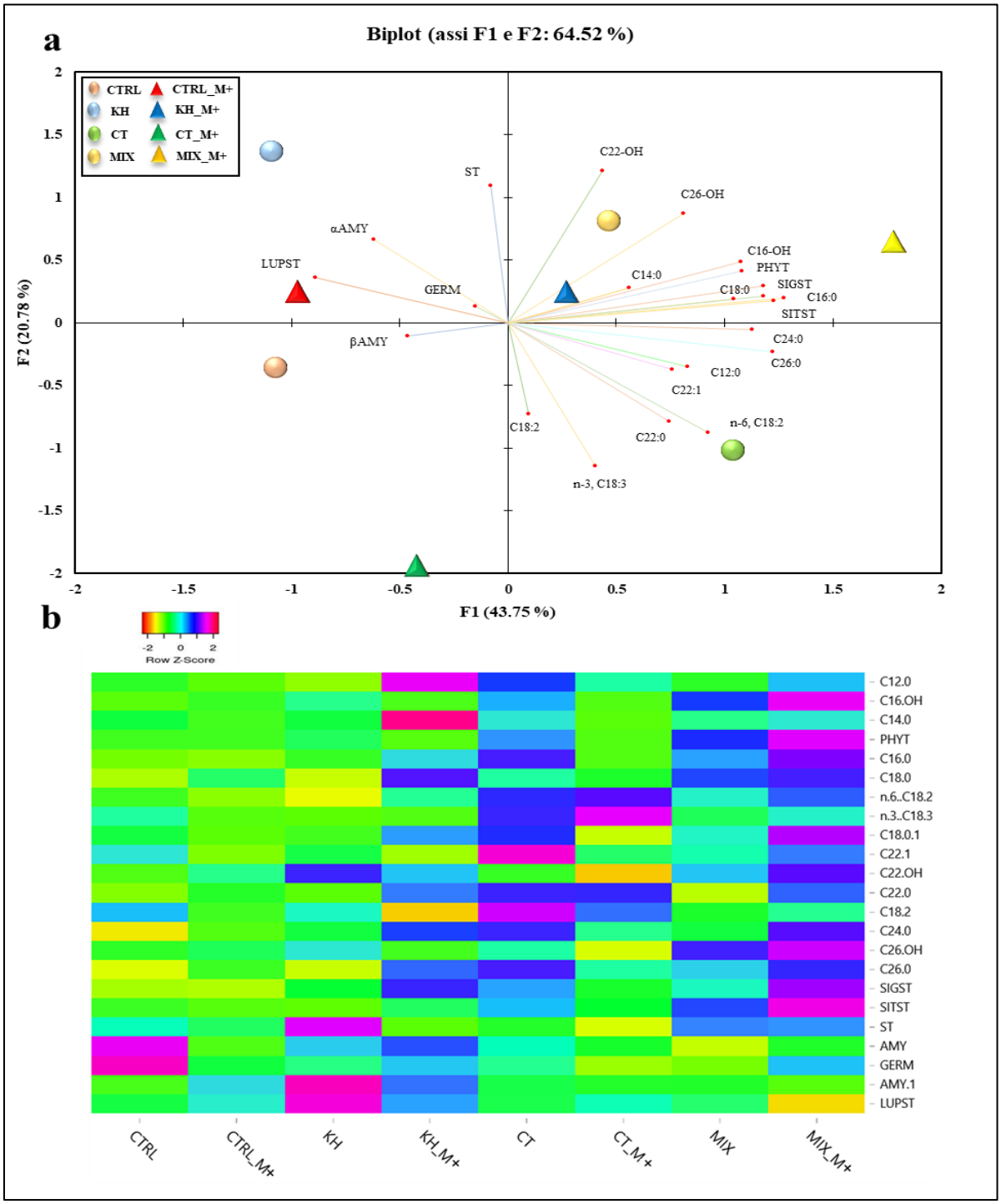

[1]C12:0 lauric acid; C16-OH hexadecenol; C14:0 mirystic acid; PHYT phytol acetate; C16:0 palmitic acid; C18:0 stearic acid; n-6, C18:2 α-linoleic acid; n-3, C18:3 linolenic acid; C22:1 erucic acid; C22-OH docosanol; C22:0 docosanoic acid; C18:2 linoleic acid; C24:0 tetracosanoic acid; C26-OH hexacosanol; C26:0 hexacosanoic acid; SIGST sigmasterol; SITST sitosterol; ST steroid; αAMY α-amyrin; βAMY β-amyrin; GERM germanicol; LUPST lupenol acetate.

Polyphenols metabolism

The polyphenols metabolism in lettuce plants grown under different treatments were assessed by UHPLC-MS-IT-TOF. Identification of polyphenols was carried out by comparing the fragmentation patterns with the data present in literature. Molecular formulae were calculated by both the Formula Predictor software and MetID solution software (Shimadzu), setting a low tolerance so that most of the identified compounds were in the first position in the list of possible candidates. Results are shown in Table S3 in order of peak elution. The main identified compounds in the metabolic extracts were hydroxycinnamic and hydroxybenzoic acids, followed by flavones, flavonols and coumarins (Table S3). The most abundant compounds among hydroxycinnamic acids, peaks 11 and 15 (Figure S3) showed two intense fragment ions at m/z 191 (quinic acid ion) and m/z 163 (p-coumaric acid ion), which were identified as chlorogenic and p-coumaroylquinic acid, respectively (Table S3). Moreover, isomeric form of dicaffeoyltartaric acid (chicoric acid) was found at m/z 473.0714 (Figure S3), which yielded MS/MS fragment ions at m/z 311 and 293, indicating the successive loss of the caffeoyl moiety and caffeic acid, respectively, from the precursor ion (Table S3). On the other hand, glycosylated quercetin (flavonol) and luteolin (flavone) were the most representative compounds among the detected flavonoids. In particular, peak 22 and 23 were identified as luteolin-7-glucuronide and quercetin-3-glucuronide (Figure S3), based on the corresponding fragment ions shown at m/z 285 and 301, respectively (Table S3). The semi-quantitative analysis of leaves polyphenols was performed by normalizing the extracted ion area of the most abundant identified compounds to the area of the internal standard (Figure S3).

These metabolomics data were then processed by Principal Component Analysis (PCA), to detect the effect of different treatments on the polyphenols profile of leaves. The two first principal components explained 74.82 % of the total variance, with PC1 and PC2 accounting for 59.59 and 15.23 %, respectively (Figure 6a). The PC1 neatly distinguished plants treated with the microbial inoculum (M+) in combination with KH, CT or their mixture (MIX), from control samples (CTRL and CTRL_M+), and plants under the individual applications of both KH and CT (Figure 6a). This

separation was due to a greater amount of all identified compounds in plants treated with MIX, and to metabolites such as chicoric acid, chlorogenic acid and luteolin-7-glucoside, which were more abundant in plants under KH_M+, CT_M+ and MIX_M+ treatments, respectively (Table 3). Moreover, along the PC2 the CT and MIX_M+ treatments were clearly separated from other ones (Figure 6a), based on the lesser amount of hydroxycinnamic acids, such feruloylquinic acid and caffeoyltartaric-p-coumaroyl acid, in the corresponding leaves extracts (Table 3). The Heatmap deriving from these metabolomics data confirmed that the net dissimilarity in the relative amount of these compounds was a function of treatments (Figure 6b). In particular, plants treated only with the microbial inoculum (CTRL_M+) or under the individual application of both KH and CT showed a metabolic profile similar to that of untreated plants (Figure 6b), which was characterized by a reduced biosynthesis of polyphenols compounds (Figure S9 and S10). Conversely, the MIX treatment significantly affected the leaves metabolome (Figure 6b), by increasing the amount of all identified metabolites (Figure S9 and S10). Moreover, the combined application of MIX with the microbial inoculum (MIX_M+) determined a significant increase of the accumulation of flavonoids in the corresponding leaves extracts (Figure 6b and S10), mainly luteolin-7-glucoside and quercetin-3-O-glucoside (Table 3).

Figure 6.

a) PCA biplot based on metabolites identified by LCMS-IT-TOF in the leaves extracts from lettuce plants treated with different biostimulants. The combination of the shapes and colors indicate different treatments. Light-Circle: single biostimulant; Dark-triangle: biostimulant plus microbial inoculum (M+). Red: Control (H_20); Blue: Potassium Humates from leonardite (KH); Green: Compost Tea from green compost (CT); Yellow: KH plus CT (MIX). **b)** Heatmap resulting from metabolomics data. Each row represents a metabolite feature and each column represents a treatment. The row Z-score or scaled expression value of each feature is plotted in yellow-green-blue-red color scale. The red color of the tile indicates high abundance and yellow indicates low abundance. The PCA and Heatmap scores represent the average value of nine replicates. [1]

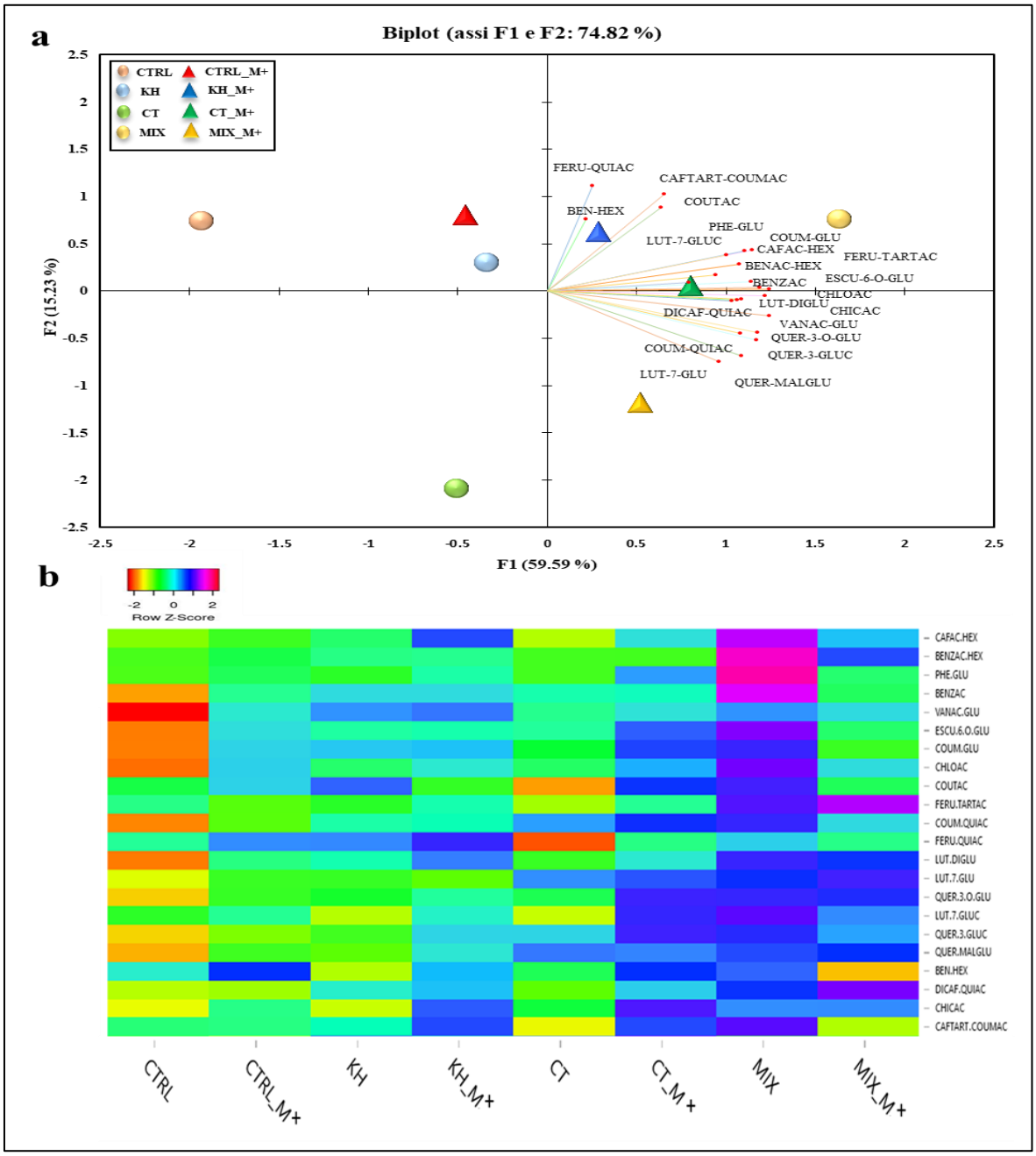

[1]CAFAC-HEX: Dihydrocaffeic acid hexose; BENAC-HEX: Dihydroxybenzoic acid hexose; PHE-GLU: 4-hydroxyphenylacetyl glucoside; BENZAC: Hydroxybenzoic acid derivative; VANAC-GLU: Vanillic acid glucoside; ESCU-6-O-GLU: Esculetin 6-O-glucoside; COUM-GLU: p-coumaroyl glucoside; CHLOAC: Chlorogenic acid; COUTAC: Coutaric acid; FERU-TARTAC: Feruloyl tartaric acid; COUM-QUIAC: p-coumaroylquinic acid; FERU-QUIAC: Feruloylquinic acid; LUT-DIGLU: Luteolin diglucoside; LUT-7-GLU: Luteolin 7-glucoside; QUER-3-O-GLU: Quercetin 3-O-glucoside; LUT-7-GLUC: Luteolin 7-glucuronide; QUERC-3-GLUC: Quercetin 3-glucuronide; QUERC-MALGLU: Quercetin malonylglucoside; BEN-HEX: Hydroxybenzoyl dihydroxybenzoyl hexose; DICAF-QUIAC: Dicaffeoylquinic acid; CHICAC: Chicoric acid; CAFTART-COUMAC: Caffeoyltartaric-p-coumaroyl acid.

Discussion

Effect of different biostimulants treatments on plants growth and nutrition

The application of a mixed biostimulant composed of leonardite Potassium Humates (KH) and Compost Tea (CT) from green compost in combination with the microbial inoculum (MIX_M+) resulted in greatest effect on growth of lettuce plants (Figure 1). The MIX_M+ significantly increased shoot dry weight of 52 and 30 % more than control samples (CTRL and CTRL_M+), 31 and 13 % more than each application of biostimulants (KH, CT and MIX), and 24 and 21 % more than the KH_M+ and CT_M+ combinations, respectively (Figure 1b). Additionally, the MIX_M+ treatment positively affected the uptake of both macro- and micro-nutrients by lettuce plants (Figure 2 and 3), being the N, P, K, S, Ca and Mg leaf content (mg plant^{-1} DW) by 55, 75, 34, 70, 141, and 74 % respectively, larger than non-treated plants (Figure 2 b, d, f, h, l, n), and the Mn and Fe content in lettuce leaves greater of about 98 and 85 %, respectively, than control samples (Figure 3 d, f, h).

The promotion of both plants productivity and nutrient status by the individual application of KH, CT, and beneficial microorganisms (i.e. AMF, PGPB and Trichderma spp.) has been widely demonstrated on different crops (Taha & Osmar, 2018; Priya et al., 2021; Saia et al., 2020). Mahdi et al. (2021) have recently shown an increase of N, P, K and Ca uptake following the application of leonardite KH, with a consequent improvement of all growth traits of faba bean plants, whereas Mohamed et al. (2021) reported that addition of compost tea to soil significantly enhanced Zn and Mn content of pepper leaves. Moreover, it is well known that the extra-radical mycelium of AMF can facilitate the uptake and transfer of mineral nutrients from soil to their host plants (Giovannini et al., 2021), and PGPB can stimulate plant growth by either increasing nutrients availability or by producing bioactive hormone-like compounds (Hayat et al., 2010). Furthermore, *Trichoderma spp*. was found to boost the growth and productivity of lettuce plants through multiple mechanisms of action, such as the solubilisation of soil micronutrients and the modulation of root growth by producing metabolites with hormone-like activities (Fiorentino et al., 2018). Recently, several authors have also highlighted the synergistic effects of AMF and PGPB when applied in combination, due to

an increased colonization of rhizospheric fungi on host plant roots, concomitant production of metabolites that improve cell permeability, and enhancment of root exudation that in turn stimulate further the growth of AMF hyphae (Saia et al., 2019; Moreira et al., 2020). Colla et al. (2015) and Bonini et al. (2020) also reported that the combination of AMF and *Trichoderma spp.* significantly increased the productivity of several crops, while improving the whole plants nutritional status.

As for the combination of humic materials and beneficial microorganisms, Olivares et al. (2017) well explained that HS-induced changes in root morphology and architecture may increase the surface area available for PGPB adsorption and establishment, thus favouring both their survival and colonization capacity. Likewise, in a recent study Cozzolino et al. (2021) showed that the combined application of humic acids, beneficial bacteria and two mycorrhizal fungi increased both maize growth and nutrient uptake (expecially P), and also positively influenced the native microbial community. Here, we similarly observed that the MIX_M+ treatment containing AMF, PGPB and T*richoderma spp.* determined a significant increase of both productivity and nutrient uptake in lettuce plants (Figure 1, 2 and 3). Therefore, our findings indicate the potential role of humic extracts in supporting the activity of beneficial microorganisms by promoting their roots colonization capacity and enhancing plants nutrition (Schoebitz et al., 2016; Filho et al., 2020). Moreover, our results also suggest an overall ability of the MIX combined treatment of humic materials to promote lettuce growth (Figure 1), and confirmed previous findings by Savarese et al (2021) on the synergistic effect of leonadite KH in combination with CT from green compost on both root development and shoot production of maize seedlings. The biostimulant activity of the MIX treatment may be related to the protection of polar bioavailable CT compounds into the hydrophobic domains of leonardite KH, which may provide not only a molecular adhesion to plant roots but also the sufficiently loos conformation of the humic supramolecular assembly to allow the release of bioactive molecules once in contact with organic acids exuded by roots (Savarese et al., 2021).

Effect of different biostimulants treatments on primary metabolism

The largest effect on plants growth and nutritional state observed for the MIX treatment with or without combination to the microbial inoculum (MIX_M+), was also reflected by the primary metabolomics analysis of both polar and apolar fraction of lettuce leaves extracts (Figure 4 and 5).

An overall increase of amino acids biosynthesis, mainly alanine, glutamine, aspartic and glutamic acid, was detected in MIX_M+ treated plants (Table 3 and Figure 4). Amino acids play an indispensable role in the metabolic pathways governing plant growth. The increase in alanine and aspartic acid content, which are involved in the carbon assimilation/fixation pathway, has already been reported after application of both single humic acids and combined microbial-humic treatments (Aguiar et al., 2018; Othibeng et al. 2021), as an indication of improved photosynthetic activity that promots lettuce growth. Additionally, aspartate is a metabolically reactive amino acid that serves as nitrogen donor in numerous aminotransferase reactions and is the precursor of essential amino acids such as threonine, lysine, isoleucine, and methionine (Coruzzi et al., 2015). In particular, the considerable amount of threonine and valine in the untreated lettuces compared to those under the biostimulants treatments (Figure S4) may suggest a state of plants stress, since these two amino acids are involved in the BCAAs pathway, which are abundantly synthesized in response to abiotic stresses (Joshi et al., 2010). On the other hand, the significant increase of glutamine and glutamic acid in the leaves extract of MIX_M+ treated plants (Table 3) is in line with the already reported role of humic materials in the upregulation of key enzymes involved in N assimilation, such as glutamine synthetase and glutamate synthase (Ertani et al., 2011, 2019). In fact, glutamate and glutamine are the initial assimilation products of nitrogen in plants, and perform several functions as substrates in protein biosynthesis, being both carrier and donor of N for the biosynthesis of amino acids, nucleotidic bases, and a host of other N-containing compounds (Coruzzi et al., 2015). Other observed variations in the amino acidic profile included an increase of serine, proline, and GABA levels in MIX_M+ treated plants (Table 3 and Figure 4). Apart from its proteinogenic function, serine plays an essential role in signalling mechanisms, plant photorespiration and biosynthesis of several biomolecules required for cell proliferation (Ros et al., 2014). Similarly, GABA acts as a signal to stimulate plant tissues to

either accumulate or reduce energy and control C/N balance in plants (Michaeli and Fromm 2015), whereas proline is commonly recognized as an important osmolite that regulates plants response to a variety of abiotic stresses (Kavi-Kishor et al., 2014). Othibeng (2021) and Vinci (2018 a,b) have already reported an increase of serine and GABA levels in plants treated, respectively, with humic acids and a combination of beneficial microrganisms and compost. Moreover, Aguiar and colleagues (2018) recently related the increase in proline accumulation following the combined application of humic acids and PGPB to the promotion of glutamate/glutamine synthesis in treated plants.

Regarding the organic acids biosynthesis, MIX and MIX_M+ treated plants showed no significant differences from control samples (Figure S5), except for a considerable amount of cinnamic acid in leaves treated with the mixed humic biostimulants (Table 3). This phenolic acid is synthetized in plants from phenylalanine through the action of the PAL/TAL (phenylalanine (tyrosine) ammonia-lyase) enzyme, whose activity is recognized to increase following the application of humic substances (Schiavon et al., 2010). Although the presence of phenylalanine in leaves extracts was not detected (Table S1), the remarkable production of cinnamic acid by MIX treated plants suggests an increase in the polyphenols metabolism with the application of mixed humic biostimulants. On the other hand, treatment with leonardite KH and the microbial inoculum (M+), either alone or in combined application (KH_M+), significantly increased the accumulation of malic, citric and fumaric acid compared to untreated plants (Table 3 and Figure 4). The TCA-related compounds are essential for several plants physiological processes, such as photosynthesis, photorespiration, nitrogen metabolism, reductant transport and the maintenance of photosynthetic redox balance (Araújo et al., 2012). Humic substances are known to upregulate the enzymes involved in the tricarboxylic acids (TCA) cycle (Nardi et al., 2007). Similarly, it has been recently shown the role of microbial inoculants in the promotion of organic acids accumulation, especially in the case of an observed improvement of tomato quality (Bona et al., 2017, 2018). Furthermore, Canellas et al. (2019) lately reported a promotion of TCA-related compounds biosynthesis by the combined application of humic acids and PGPB, which is in line with the increase of organic acids accumulation

observed here in KH_M+ treated plants (Figure S5). An overall increase of saccharides in lettuce leaves, mainly fructose, glucose and galactose (Table 3 and figure 4), was also detected following the application of the MIX_M+ treatment (Figure S6). Soluble sugars, such as fructose and glucose, play a central role in plants structure and metabolism. According to Rosa et al (2009) and Zeeman (2015), soluble sugars are involved in several metabolic events and act as molecular signals that regulate genes involved in photosynthesis, disaccharides metabolism and osmolyte synthesis. Although it is well known the increase of sugars accumulation in leaves induced by humic substances or microbial inoculants (Merlo et al., 1991; Nwodo et al., 2012; van Tol de Castro et al. 2021), their combined application led to conflicting results. Canellas et al (2013) showed that free carbohydrate content in leaf extracts was 60 % less than control in maize plants treated with HS and PGPB, whereas Vinci et al. (2018 a,b) found in the same specie an accumulation of glucose and fructose following the combined application of compost with beneficial bacteria or *Trichoderma spp*. In the latter work, authors attributed the overproduction of soluble sugars to an efficient microorganisms-plant-compost synergism that led in treated plants to an increase in photosynthetic activity and growth of shoots. This hypothesis seems to well fit into our positive results obtained in lettuce plants with the MIX_M+ treatment, which improved the overall plants productivity, nutritional status and metabolism more than other treatments. Interestingly, high levels of myo-inositol were found in control samples, while CT and CT_M+ treated plants showed an accumulation of cellobiose in leaves (Table 3 and Figure 4). Myo-inositol derivatives have been recognized as signal compounds in plants, as well as key metabolites under unfavourable conditions (Valluru and Van den Ende, 2011), thus suggesting an outset of stress in untreated plants (Figure S6). On the other hand, the ehanced production of cellobiose in plants under both CT and CT_M+ treatments (Table 3), is in line with the increase of carbohydrates biosynthesis already reported for the application of compost teas, which positively correlated with large content of N, P and K in treated plants (Ali, 2015; Abou-el-hassan and El-batran, 2020).

The lipid metabolism was significantly affected by both non-microbial and microbial treatments (Figure 5). The application of leonardite KH or CT from green compost in separate combination with the microbial inoculum (M+) greatly increased the accumulation of fatty acids (Figure S7), whereas the MIX_M+ treatment remarkably improved the biosynthesis of fatty alcohols and sterols (Figure S8). Lipids have essential functions in plants as the main structural components of cell membrane, substantial chemical reserve of free energy and as cell signal messengers (Suh et al., 2015). In our study, plants under KH_M+ treatment synthetized a considerable amount of lauric and myristic acid, while CT_M+ showed an accumulation of both linoleic and α-linolenic acid in treated leaves (Table 3 and Figure S7). These long-chain fatty acids are important constituent of storage lipids in plants, and the combined application of humic acids and PGPB has been reported to increase their biosynthesis in both maize and sugarcane seedlings (Canellas et al., 2019b). Similarly, Aguiar et al. (2018) previously revealed that plants accumulation of long-chain fatty alcohols are also enhanced by mixed humic-microbial biostimulants, which is in line with the considerable amount of hexadecenol, docosanol and hexacosanol found in MIX_M+ treated plants (Table 3 and Figure S8). The same authors also found a large concentration of β-sitosterol in sugarcane leaves treated with HA and PGPB. This lipid compound is the main plants sterol involved into cellulose elongation chain, and significantly increased in lettuce plants under the MIX_M+ application (Table 3). Finally, leaves of untreated plants showed an accumulation of β-amyrin and germanicol (Table 3 and Figure 5). Since terpenoids biosynthesis has recently been related to salts stress plants response (Basyuni et al., 2009), this may suggest an initial stress condition of control samples that did not occure under threatments with biostimulants and the microbial inoculum.

Therefore, our results suggest an overall capacity of leonardite KH and CT from green compost, applied either alone (MIX) or in combination with a microbial inoculum (MIX_M+), to positively affect the primary metabolism of lettuce plants (Figure 4 and 5). Hence, the present study confirms earlier findings of the role on plants physiology played by humic materials and their synergistic interaction with beneficial microorganisms (Trevisan et al., 2011; Canellas and Olivares

2014). This biostimulant activity of HS has been commonly attributed to the incorporation of hormone-like molecules into their supramolecular structure, which can alter several plants physiological processes (Nardi et al., 2002; Canellas et al., 2015; Pizzeghello et al., 2020), while a relationship between the molecular structure of humic substances and their bioactivity is the objective of many recent attempts (Savy et al., 2020; Monda et al., 2021). In fact, it has been shown that bioactive polar humic molecules can interact with cell membrane in root surfaces and stimulate plants growth, while the conformational stability of the humic suprastructures defines the type and intensity of bioactivity in plants (García et al., 2019). Similarly, we have previously observed that the promotion of maize seedlings growth by combined application of leonardite KH and CT from green compost was positively correlated with the molecular and physical-chemical features of mixed humic materials (Savarese er al., 2021). In particular, the protection of the readily bioavailable CT compounds by the KH hydrophobic components appears to be a key mechanism in the correct conformational stability of the humic assembly that enables the release of bioactive molecules to plant roots (Savarese et al., 2021). These findings may also explain the improvement of leaves metabolic activity observed here in lettuce plants under the MIX treatment (Figure 4 and 5). Moreover, Olivares et al. (2017) reported that the synergistic interaction between humic materials and beneficial microorganisms determines a boost effect on plants growth. These authors well explained that the morphological adaptation of plants root system induced by HS, which includes the stimulation of both lateral roots formation and border cells release from tips, may improve the colonization ability of microorganisms. Furthermore, physiological changes such as the increase of organic acids exudation by plants treated with HS could also favour the survival of beneficial microorganisms in the soil environment, by facilitating their exploitation of soil carbon sources (Canellas et al., 2019a). These evidence seem to well fit the significant effect on leaves primary metabolism observed here by the combination of the microbial inoculum with the mixture of both KH and CT humic materials (Figure 4 and 5).

Effect of different biostimulants treatments on secondary metabolism

The advantage in using UHPLC to separate polyphenolic compounds have recently been highlighted (Abu-Reidah et al., 2013). Our results showed that UHPLC-MS-IT-TOF analysis of metabolic leaves extracts allowed the identification of hydroxycinnamic acids and flavonols as the main phenolic compounds in lettuce plants (Table S1 and Figure S1), right in line with previous studies conducted on the same specie and with similar techniques (Pepe et al., 2015). In particular, the application of the MIX treatment provided the largest effect on the secondary metabolism of treated plants (Figure 6). The accumulation of cinnamic acid derivatives, mainly chlorogenic and coutaric acid, as well as of flavonoids, such as the glucoside conjugates of both luteolin and quercetin, increased in MIX treated leaves significantly more than in all the other treatments (Table 3). It has been generally recalled above the role of humic substances in the upregulation of PAL/TAL activity, the enzyme that catalyzes the first committed step in the biosynthesis of polyphenols in plants (Schiavon et al., 2010). Conselvan et al. (2017) recently indicated that PAL activity can be also stimulated by the application of leonardine humic acids on lettuce seedlings, with a consequent accumulation of hyroxycinnamic acids, such as p-coumaric and chlorogenic acid. Moreover, Cruz et al. (2014) reported an increase in total phenolic compounds of lettuce plants treated with espresso coffee residues. These findings are in accordance with the overproduction of polyphenols compounds observed by treating lettuce plants with a mixture of leonardite KH and CT from coffee wastes compost (Figure 6). These polyphenols have been commonly recognized as antioxidant molecules in plants, playing a major role in ensuring plant growth under abiotic stresses (Shinozaki et al., 2015). Under unfavourable growth conditions, such as drought or salinity stress, the generation of Reactive Oxygen Species (ROS) is one of the primary responses in plants, causing significant cell damage (Djoukeng et al., 2008). Massive ROS production is potentially harmful, if not controlled by antioxidant mechanism, since it can induce photosynthetic pigment bleaching, degradation and alteration of protein structure and function, lipid peroxidation and damage to organic molecules, including DNA and RNA (Apel and Hirt, 2004). The overproduction of antioxidants compounds such as ascorbic acid, glutathione and polyphenols is the major response of plants to the oxidative stress

(Arbona et al., 2013). Among these molecules, hydroxycinnamic acids are precursors of lignins, which constitute an important stress defence mechanism, especially at the root level where can modulate cell wall composition and stiffness (Peterson et al., 2010). Similarly, flavonoids such as luteolin 7-O and quercetin 3-O glycosides are potent free radical scavengers/antioxidants that effectively prevent ROS generation (Brunetti et al., 2013). Another important mechanism of plants response to oxidative stress is the activation of enzymatic antioxidant systems. Enzymatic antioxidants such as superoxide dismutase (SOD), catalase (CAT) and glutathione peroxidase (GPX) are activated in plants to reduce the concentration of hydrogen peroxide and superoxide (Canellas et al., 2020). In this regard, Cordeiro et al. (2011) showed that the treatment with HS stimulated catalase activity in plants, whereas García et al. (2016) have demonstrated the role of humic extracts in the upregulation of peroxidase that reduces the cells ROS concentration, thereby restoring the cytosolic redox homeostasis. In the latter study, the antioxidant defence induced in plants by HS was shown to be related to their biostimulant activity, as they lead to a state of eustress whose final effect is somehow beneficial to plants. Moreover, Monda et al. (2021) recently reported that molecules present in the supramolecular structure of HS such as lignin-derived fragments, condensed aromatic structures and lipids, are potentially involved in the modulation of ROS level in plant by priming their defence systems, thus resulting in increased root exploration and antioxidant production. In line with this, we earlier observed that the balanced molecular composition of mixed humic materials, characterized by both lignin derivatives from CT and aromatic components from KH, was positively correlated to the bioactivity on maize seedlings growth (Savarese et al., 2021). Therefore, it is reasonable to assume that the overall enhancement by the MIX treatment of lettuce secondary metabolism (Figure 6) may arise from the mixture of humic extracts containing different type of bioactive molecules, whose stable supramolecular assembly guarantees a protection from biotic degradation but also their availability to plants following an alteration of the humic conformational arrangent upon the action of root-exuded organic aicds.

Furthermore, consumers' interest in lettuce has increased dramatically in recent years due to the considerable content of phytochemicals, such as polyphenols, with a positive role on human health. Phenolic compounds alone and vegetables containing polyphenoles have shown beneficial effects against several human diseases (Kim et al., 2016). Cheng et al. (2014) showed the anti-diabetic effect of lettuce rich in phenolic compounds, especially chlorogenic acid, which determined less glucose content in blood. Moreover, Lee et al. (2009) indicated the decrease of total plasma cholesterol in mice fed with red-pigmented lettuce, highlighting the potential role of this vegetable against the risk of cardiovascular disease. Pepe et al. (2015) also outlined that polyphenols such as hydroxycinnamic acids derivatives, flavonols and coumarins in green lettuce have a potential anti-oxidant and anti-inflammatory effect on J774A.1 macrophages stimulated by Escherichia coli lipopolysaccharide. The composition and abundance of these beneficial compounds in lettuce is highly variable and may be influenced by several factors such as cultivation practices, genetic makeup and harvesting stage (Adesso et al., 2016; Assefa et al., 2019). In fact, Ismail et al. (2019) have shown that transformation of *rol* genes significantly alters the metabolome of *L. sativa* by improving the biosynthesis of bioactive compounds, whereas Yung et al. (2017) reported the increase in total polyphenols accumulation, mainly luteolin and quercetin glycosides, by treating lettuce plants with exogenous glycine. Our results also revealed that the application of mixed humic materials (MIX) stimulated the production of polyphenols in lettuce leaves (Figure 6), thus suggesting that the combination of different biostimulants may become an innovative potential tool to modulate plants secondary metabolism for the development of novel functional foods.

Conclusions

The present work showed that the combination of non-microbial biostimulants and microbial bioeffectors is a potential tool not only to increase plants productivity and nutritional status, but also to positively affect the overall plant metabolome. In particular, the combined application of mixed leonardite Potassium Humates (PH) and Compost Tea (CT) from green compost with a microbial

inoculum (M+) resulted in a most significant effect on lettuce yield, and on both leaf mineral status and primary metabolism. The synergistic interaction between humic materials and microbial consortia significantly enhanced the plants uptake of both macro- and micronutrients compared to their individual application, with a consequent increase of lettuce biomass production. These results indicate the potential role of humic substances (HS) in supporting the survival of beneficial microorganisms in the soil environment, as well as in promoting their colonization capacity (Olivares et al., 2017; Cozzolino et al., 2021). Moreover, the treatment with the humic mixture in combination with the microbial inoculum stimulated the accumulation in lettuce leaves of essential amino acids sand the production of saccharides.

Additionally, we evaluated the changes in the polyphenolic secondary metabolism of treated and untreated lettuce plants by UHPLC-MS-IT-TOF analysis. These compounds are potent free radical scavengers/antioxidants that prevent ROS generation effectively, thus explaining the growing in understanding their role in plants resistance to stressful conditions and in improving human health. We found that the mixture of KH and CT materials significantly increased leaf content of both hydroxycinnamic acids and flavonoids compared to other treatments. This stimulatory effect of the mixed humic materials could be related to an optimum balanced molecular composition of bioactive molecules and hydrophobic domains capable of modulating the humic molecular bioactivity. Therefore, this study indicates that the a calibrate mixture of humic extracts containing different type of bioactive molecules and their combination with beneficial microorganisms is a potential tool to improve both the productivity and nutritional status of plants, as well as to modulate plants metabolome for the development of novel functional crops.

Acknowledgements: This work was conducted in partial fulfilment of first author requirements, to achieve an “industrial” PhD degree, funded by the Ministry of University and Reasearch (MUR) of Italy.

References

Abou-el-hassan, S., and El-batran, H. S. (2020). Integration of Some Bio Compounds with Compost Tea to Produce Sweet Corn without Mineral Fertilizers. *Middle East J. Agric. Res.*, 645–652. doi:10.36632/mejar/2020.9.3.51.

Abu-Reidah, I. M., Contreras, M. M., Arráez-Román, D., Segura-Carretero, A., and Fernández-Gutiérrez, A. (2013). Reversed-phase ultra-high-performance liquid chromatography coupled to electrospray ionization-quadrupole-time-of-flight mass spectrometry as a powerful tool for metabolic profiling of vegetables: Lactuca sativa as an example of its application. *J. Chromatogr. A* 1313, 212–227. doi:10.1016/j.chroma.2013.07.020.

Adesso, S., Pepe, G., Sommella, E., Manfra, M., Scopa, A., Sofo, A., et al. (2016). Anti-inflammatory and antioxidant activity of polyphenolic extracts from Lactuca sativa (var. Maravilla de Verano) under different farming methods. *J. Sci. Food Agric.* 96, 4194–4206. doi:10.1002/jsfa.7622.

Aguiar, N. O., Olivares, F. L., and Novotny, E. H. (2018). Changes in metabolic profiling of sugarcane leaves induced by endophytic diazotrophic bacteria and humic acids. 1–28. doi:10.7717/peerj.5445.

Ali, O. A. M. (2015). Role of Humic Substances and Compost Tea in Improvement of Endogenous Hormones Content, Flowering and Yield and its Components of Faba Bean (Vicia faba L.). *Ann. Agric. Sci. Moshtohor* 53, 373–384. doi:10.21608/assjm.2015.109889.

Apel, K., and Hirt, H. (2004). Reactive oxygen species: Metabolism, oxidative stress, and signal transduction. *Annu. Rev. Plant Biol.* 55, 373–399. doi:10.1146/annurev.arplant.55.031903.141701.

Araújo, W. L., Nunes-Nesi, A., Nikoloski, Z., Sweetlove, L. J., and Fernie, A. R. (2012). Metabolic control and regulation of the tricarboxylic acid cycle in photosynthetic and heterotrophic plant tissues. *Plant, Cell Environ.* 35, 1–21. doi:10.1111/j.1365-3040.2011.02332.x.

Arbona, V., Manzi, M., de Ollas, C., and Gómez-Cadenas, A. (2013). Metabolomics as a tool to investigate abiotic stress tolerance in plants. *Int. J. Mol. Sci.* 14, 4885–4911. doi:10.3390/ijms14034885.

Assefa, A. D., Choi, S., Lee, J. E., Sung, J. S., Hur, O. S., Ro, N. Y., et al. (2019). Identification and quantification of selected metabolites in differently pigmented leaves of lettuce (Lactuca sativa L.) cultivars harvested at mature and bolting stages. *BMC Chem.* 13, 1–15. doi:10.1186/s13065-019-0570-2.

Babicki, S., Arndt, D., Marcu, A., Liang, Y., Grant, J.R., Maciejewski, A., and Wishart, D.S. (2016). Heatmapper: web-enabled heat mapping for all. *Nucleic Acids Res* 44:147–153.

Backer, R., Rokem, J. S., Ilangumaran, G., Lamont, J., Praslickova, D., Ricci, E., et al. (2018). Plant

growth-promoting rhizobacteria: Context, mechanisms of action, and roadmap to commercialization of biostimulants for sustainable agriculture. *Front. Plant Sci.* 871, 1–17. doi:10.3389/fpls.2018.01473.

Basyuni, M., Baba, S., Inafuku, M., Iwasaki, H., Kinjo, K., and Oku, H. (2009). Expression of terpenoid synthase mRNA and terpenoid content in salt stressed mangrove. *J. Plant Physiol.* 166, 1786–1800. doi:10.1016/j.jplph.2009.05.008.

Bona, E., Cantamessa, S., Massa, N., Manassero, P., Marsano, F., Copetta, A., et al. (2017). Arbuscular mycorrhizal fungi and plant growth-promoting pseudomonads improve yield, quality and nutritional value of tomato: a field study. *Mycorrhiza* 27, 1–11. doi:10.1007/s00572-016-0727-y.

Bona, E., Todeschini, V., Cantamessa, S., Cesaro, P., Copetta, A., Lingua, G., et al. (2018). Combined bacterial and mycorrhizal inocula improve tomato quality at reduced fertilization. *Sci. Hortic. (Amsterdam).* 234, 160–165. doi:10.1016/j.scienta.2018.02.026.

Bonini, P., Rouphael, Y., Miras-Moreno, B., Lee, B., Cardarelli, M., Erice, G., et al. (2020). A Microbial-Based Biostimulant Enhances Sweet Pepper Performance by Metabolic Reprogramming of Phytohormone Profile and Secondary Metabolism. *Front. Plant Sci.* 11, 1–13. doi:10.3389/fpls.2020.567388.

Bradáčová, K., Florea, A. S., Bar-Tal, A., Minz, D., Yermiyahu, U., Shawahna, R., et al. (2019). Microbial Consortia versus Single-Strain Inoculants: An advantage in PGPM-assisted tomato production? *Agronomy* 9. doi:10.3390/agronomy9020105.

Brenda, S., Di, F., Moreno-gav, A., Gea, F. J., and Santos, M. (2020). Role of Trichoderma aggressivum f . europaeum as Plant-Growth Promoter in Horticulture. 1–15.

Brunetti, C., Di Ferdinando, M., Fini, A., Pollastri, S., and Tattini, M. (2013). Flavonoids as antioxidants and developmental regulators: Relative significance in plants and humans. *Int. J. Mol. Sci.* 14, 3540–3555. doi:10.3390/ijms14023540.

Canellas, L. P., Balmori, D. M., Médici, L. O., Aguiar, N. O., Campostrini, E., Rosa, R. C. C., et al. (2013). A combination of humic substances and Herbaspirillum seropedicae inoculation enhances the growth of maize (Zea mays L.). *Plant Soil* 366, 119–132. doi:10.1007/s11104-012-1382-5.

Canellas, L. P., Canellas, N. O. A., Luiz Eduardo, L. E. S., Olivares, F. L., and Piccolo, A. (2020). Plant chemical priming by humic acids. *Chem. Biol. Technol. Agric.* 7, 1–17. doi:10.1186/s40538-020-00178-4.

Canellas, L. P., Dobbss, L. B., Oliveira, A. L., Chagas, J. G., Aguiar, N. O., Rumjanek, V. M., et al. (2012). Chemical properties of humic matter as related to induction of plant lateral roots. *Eur.*

J. Soil Sci. 63, 315–324. doi:10.1111/j.1365-2389.2012.01439.x.

Canellas, L. P., and Olivares, F. L. (2014). Physiological responses to humic substances as plant growth promoter. *Chem. Biol. Technol. Agric.* 1, 1–11. doi:10.1186/2196-5641-1-3.

Canellas, L. P., Olivares, F. L., Aguiar, N. O., Jones, D. L., Nebbioso, A., Mazzei, P., et al. (2015). Humic and fulvic acids as biostimulants in horticulture. *Sci. Hortic. (Amsterdam).* 196, 15–27. doi:10.1016/j.scienta.2015.09.013.

Canellas, L. P., Olivares, F. L., Canellas, N. O. A., Mazzei, P., and Piccolo, A. (2019a). Humic acids increase the maize seedlings exudation yield. *Chem. Biol. Technol. Agric.* 6, 1–14. doi:10.1186/s40538-018-0139-7.

Canellas, L. P., Olivares, F. L., Okorokova-Façanha, A. L., and Façanha, A. R. (2002). Humic acids isolated from earthworm compost enhance root elongation, lateral root emergence, and plasma membrane H+-ATPase activity in maize roots. *Plant Physiol.* 130, 1951–1957. doi:10.1104/pp.007088.

Canellas, N. O. A., Olivares, F. L., and Canellas, L. P. (2019b). Metabolite fingerprints of maize and sugarcane seedlings: searching for markers after inoculation with plant growth-promoting bacteria in humic acids. *Chem. Biol. Technol. Agric.* 6, 1–10. doi:10.1186/s40538-019-0153-4.

Cheng, D. M., Pogrebnyak, N., Kuhn, P., Krueger, C. G., Johnson, W. D., and Raskin, I. (2014). Development and phytochemical characterization of high polyphenol red lettuce with anti-diabetic properties. *PLoS One* 9, 1–10. doi:10.1371/journal.pone.0091571.

Colla, G., Rouphael, Y., Di Mattia, E., El-Nakhel, C., and Cardarelli, M. (2015). Co-inoculation of Glomus intraradices and Trichoderma atroviride acts as a biostimulant to promote growth, yield and nutrient uptake of vegetable crops. *J. Sci. Food Agric.* 95, 1706–1715. doi:10.1002/jsfa.6875.

Conselvan, G. B., Pizzeghello, D., Francioso, O., Di Foggia, M., Nardi, S., and Carletti, P. (2017). Biostimulant activity of humic substances extracted from leonardites. *Plant Soil* 420, 119–134. doi:10.1007/s11104-017-3373-z.

Cordeiro, F. C., Santa-Catarina, C., Silveira, V., and De Souza, S. R. (2011). Humic acid effect on catalase activity and the generation of reactive oxygen species in corn (Zea mays). *Biosci. Biotechnol. Biochem.* 75, 70–74. doi:10.1271/bbb.100553.

Coruzzi, G., Last, R., Dudareva, N., and Amrhein, N. (2015). Amino Acids. In: Buchanan B., Gruissem W. and Jones R., Eds., Biochemistry and Molecular Biology of Plants, American Society of Plant Biologists (2nd ed.), Wiley-Blackwell, 289-336.

Cozzolino, V., Monda, H., Savy, D., Di Meo, V., Vinci, G., and Smalla, K. (2021). Cooperation among phosphate-solubilizing bacteria, humic acids and arbuscular mycorrhizal fungi induces

soil microbiome shifts and enhances plant nutrient uptake. *Chem. Biol. Technol. Agric.* 8, 1–19. doi:10.1186/s40538-021-00230-x.

Cruz, R., Gomes, T., Ferreira, A., Mendes, E., Baptista, P., Cunha, S., et al. (2014). Antioxidant activity and bioactive compounds of lettuce improved by espresso coffee residues. *Food Chem.* 145, 95–101. doi:10.1016/j.foodchem.2013.08.038.

Djoukeng, J.D., Arbona, V., Argamasilla, R., and Gomez-cadenas, A. (2008). Flavonoid profiling in leaves of citrus genotypes under different environmental situations flavonoid profiling in leaves of Citrus genotypes. *J. Agric. Food Chem.* 56, 11087–11097.

Drobek, M., and Fr, M. (2019). Plant Biostimulants : Importance of the Quality and Yield of Horticultural Crops and the Improvement of Plant Tolerance to Abiotic Stress — A Review.

du Jardin, P. (2015). Plant biostimulants: Definition, concept, main categories and regulation. *Sci. Hortic. (Amsterdam).* 196, 3–14. doi:10.1016/j.scienta.2015.09.021.

Ertani, A., Francioso, O., Tugnoli, V., Righi, V., and Nardi, S. (2011). Effect of commercial lignosulfonate-humate on Zea mays L. metabolism. *J. Agric. Food Chem.* 59, 11940–11948. doi:10.1021/jf202473e.

Ertani, A., Nardi, S., Francioso, O., Pizzeghello, D., Tinti, A., and Schiavon, M. (2019). Metabolite targeted analysis and physiological traits of zea mays L. In response to application of a leonardite-humate and lignosulfonate-based products for their evaluation as potential biostimulants. *Agronomy* 9, 1–18. doi:10.3390/agronomy9080445.

Eudoxie, G., and Martin, M. (2019). Compost tea quality and fertility. In: Organic Fertilizers – History Production and Applications. Marcelo Larramendy and Sonia Soloneski *IntechOpen.* https://doi.org/10.5772/ intechopen.86877.

Ferreira, S., Olivares, F. L., and Canellas, L. P. (2017). The biostimulant manufactured using diazotrophic endophytic bacteria and humates is effective to increase sugarcane yield. *Chem. Biol. Technol. Agric.*, 1–6. doi:10.1186/s40538-017-0106-8.

Filho, J. F. D. C. L., Thomason, W. E., Evanylo, G. K., Zhang, X., Strickland, M. S., Chim, B. K., et al. (2020). The Synergistic Effects of Humic Substances and Biofertilizers on Plant Development and Microbial Activity: A Review. *Int. J. Plant Soil Sci.* 32, 56–75. doi:10.9734/ijpss/2020/v32i730306.

Fiorentino, N., Ventorino, V., Woo, S. L., Pepe, O., Rosa, A. De, Gioia, L., et al. (2018). Trichoderma -Based Biostimulants Modulate Rhizosphere Microbial Populations and Improve N Uptake Efficiency , Yield , and Nutritional Quality of Leafy Vegetables. 9, 1–15. doi:10.3389/fpls.2018.00743.

García, A. C., Santos, L. A., de Souza, L. G. A., Tavares, O. C. H., Zonta, E., Gomes, E. T. M., et al.

(2016). Vermicompost humic acids modulate the accumulation and metabolism of ROS in rice plants. *J. Plant Physiol.* 192, 56–63. doi:10.1016/j.jplph.2016.01.008.

García, A. C., van Tol de Castro, T. A., Santos, L. A., Tavares, O. C. H., Castro, R. N., Berbara, R. L. L., et al. (2019). Structure-Property-Function Relationship of Humic Substances in Modulating the Root Growth of Plants: A Review. *J. Environ. Qual.* 48, 1622–1632. doi:10.2134/jeq2019.01.0027.

Giovannini, L., Palla, M., Agnolucci, M., Avio, L., Sbrana, C., Turrini, A., et al. (2020). Arbuscular mycorrhizal fungi and associated microbiota as plant biostimulants: Research strategies for the selection of the best performing inocula. *Agronomy* 10. doi:10.3390/agronomy10010108.

Hayat, R., Ali, S., Amara, U., Khalid, R., and Ahmed, I. (2010). Soil beneficial bacteria and their role in plant growth promotion: A review. *Ann. Microbiol.* 60, 579–598. doi:10.1007/s13213-010-0117-1.

Imbufe, A. U., Patti, A. F., Burrow, D., Surapaneni, A., Jackson, W. R., and Milner, A. D. (2005). Effects of potassium humate on aggregate stability of two soils from Victoria, Australia. *Geoderma* 125, 321–330. doi:10.1016/j.geoderma.2004.09.006.

Jannin, L., Arkoun, M., Ourry, A., Laîné, P., Goux, D., Garnica, M., et al. (2012). Microarray analysis of humic acid effects on Brassica napus growth: Involvement of N, C and S metabolisms. *Plant Soil* 359, 297–319. doi:10.1007/s11104-012-1191-x.

Kavi Kishor, P. B., and Sreenivasulu, N. (2014). Is proline accumulation per se correlated with stress tolerance or is proline homeostasis a more critical issue? *Plant, Cell Environ.* 37, 300–311. doi:10.1111/pce.12157.

Kim, M. J., Moon, Y., Tou, J. C., Mou, B., and Waterland, N. L. (2016). Nutritional value, bioactive compounds and health benefits of lettuce (Lactuca sativa L.). *J. Food Compos. Anal.* 49, 19–34. doi:10.1016/j.jfca.2016.03.004.

Koné, S. B., Dionne, A., Tweddell, R. J., Antoun, H., and Avis, T. J. (2010). Suppressive effect of non-aerated compost teas on foliar fungal pathogens of tomato. *Biol. Control* 52, 167–173. doi:10.1016/j.biocontrol.2009.10.018.

Kong, W., Meldgin, D. R., Collins, J. J., and Lu, T. (2018). Designing microbial consortia with defined social interactions. *Nat. Chem. Biol.* 14, 821–829. doi:10.1038/s41589-018-0091-7.

Kumar, D., Singh, A. P., Raha, P., Rakshit, A., Singh, C. M., and Kishor, P. (2013). Potassium Humate: A Potential Soil Conditioner and Plant Growth Promoter. *Int. J. Agric. Environ. Biotechnol.* 6, 441. doi:10.5958/j.2230-732x.6.3.015.

Joshi, V., Joung, J.G., Fei, Z., and Jander, G. (2010). Interdependence of threonine, methionine and isoleucine metabo- lism in plants: accumulation and transcriptional regulation under abiotic stress. *J Amino Acids.* 39, 933–947.

Lee, J. H., Felipe, P., Yang, Y. H., Kim, M. Y., Oh, Y. K., Sok, D. E., et al. (2009). Effects of dietary supplementation with red-pigmented leafy lettuce (Lactuca sativa) on lipid profiles and antioxidant status in C57BL/6J mice fed a high-fat high-cholesterol diet. *Br. J. Nutr.* 101, 1246–1254. doi:10.1017/S0007114508073650.

López-Bucio, J., Pelagio-Flores, R., and Herrera-Estrella, A. (2015). Trichoderma as biostimulant: Exploiting the multilevel properties of a plant beneficial fungus. *Sci. Hortic. (Amsterdam).* 196, 109–123. doi:10.1016/j.scienta.2015.08.043.

Mahdi, A. H. A., Badawy, S. A., Latef, A. A. H. A., Hosary, A. A. A. E., Razek, U. A. A. El, and Taha, R. S. (2021). Integrated Effects of Potassium Humate and Planting Density on Growth, Physiological Traits and Yield of Vicia faba L. Grown in Newly Reclaimed Soil. *Agronomy* 11. doi:10.3390/agronomy11030461.

Merlo, L., Ghisi, R., Rascio, N., and Passera, C. (1991). Effects of humic substances on carbohydrate metabolism of maize leaves. *Can J Plant Sci* 71, 419–425.

Miceli, A., Moncada, A., and Vetrano, F. (2021). Use of microbial biostimulants to increase the salinity tolerance of vegetable transplants. *Agronomy* 11. doi:10.3390/agronomy11061143.

Michaeli, S., and Fromm, H. (2015). Closing the loop on the GABA shunt in plants: Are GABA metabolism and signaling entwined? *Front. Plant Sci.* 6, 1–7. doi:10.3389/fpls.2015.00419.

Mohamed, M. H. M., Sami, R., Al-mushhin, A. A. M., Mohamed, M., Ali, E., El-desouky, H. S., et al. (2021). Yeast Extract , and Foliar Spray with Seaweed Extract on Sweet Pepper Plants under Greenhouse Conditions. 1–23.

Monda, H., Cozzolino, V., Vinci, G., Spaccini, R., and Piccolo, A. (2017). Molecular characteristics of water-extractable organic matter from different composted biomasses and their effects on seed germination and early growth of maize. *Sci. Total Environ.* 590–591, 40–49. doi:10.1016/j.scitotenv.2017.03.026.

Monda, H., Cozzolino, V., Vinci, G., Drosos, M., and Piccolo, A. (2018). Biostimulation of the early growth of Maize by the molecular Humeome extracted from different green composts. *Plant and Soil* 429:407-424. https://doi.org/10.1007/s11104.

Monda, H., McKenna, A. M., Fountain, R., and Lamar, R. T. (2021). Bioactivity of Humic Acids Extracted From Shale Ore: Molecular Characterization and Structure-Activity Relationship With Tomato Plant Yield Under Nutritional Stress. *Front. Plant Sci.* 12, 1–17. doi:10.3389/fpls.2021.660224.

Moradtalab, N., Ahmed, A., Geistlinger, J., Walker, F., Höglinger, B., Ludewig, U., et al. (2020). Synergisms of Microbial Consortia, N Forms, and Micronutrients Alleviate Oxidative Damage and Stimulate Hormonal Cold Stress Adaptations in Maize. *Front. Plant Sci.* 11, 1–19. doi:10.3389/fpls.2020.00396.

Moreira, H., Pereira, S. I. A., Vega, A., Castro, P. M. L., and Marques, A. P. G. C. (2020). Synergistic effects of arbuscular mycorrhizal fungi and plant growth-promoting bacteria benefit maize growth under increasing soil salinity. *J. Environ. Manage.* 257, 109982. doi:10.1016/j.jenvman.2019.109982.

Murphy, J., and Riley, J.P. (1962). A modified single solution method for the deter- mination of phosphate in natural waters. *Anal Chim Acta* 27:31–36.

Muscolo, A., Sidari, M., Francioso, O., Tugnoli, V., and Nardi, S. (2007). The auxin-like activity of humic substances is related to membrane interactions in carrot cell cultures. *J. Chem. Ecol.* 33, 115–129. doi:10.1007/s10886-006-9206-9.

Naidu, Y., Meon, S., and Siddiqui, Y. (2013). Foliar application of microbial-enriched compost tea enhances growth, yield and quality of muskmelon (Cucumis melo L.) cultivated under fertigation system. *Sci. Hortic. (Amsterdam).* 159, 33–40. doi:10.1016/j.scienta.2013.04.024.

Nardi, S., Muscolo, A., Vaccaro, S., Baiano, S., Spaccini, R., and Piccolo, A. (2007). Relationship between molecular characteristics of soil humic fractions and glycolytic pathway and krebs cycle in maize seedlings. *Soil Biol. Biochem.* 39, 3138–3146. doi:10.1016/j.soilbio.2007.07.006.

Nardi, S., Pizzeghello, D., Gessa, C., Ferrarese, L., Trainotti, L., and Casadoro, G. (2000). A low molecular weight humic fraction on nitrate uptake and protein synthesis in maize seedlings. *Soil Biol. Biochem.* 32, 415–419. doi:10.1016/S0038-0717(99)00168-6.

Nardi, S., Pizzeghello, D., Muscolo, A., and Vianello, A. (2002). Physiological effects of humic substances on higher plants. *Soil Biol. Biochem.* 34, 1527–1536. doi:10.1016/S0038-0717(02)00174-8.

Nwodo, U. U., Green, E., and Okoh, A. I. (2012). Bacterial exopolysaccharides: Functionality and prospects. *Int. J. Mol. Sci.* 13, 14002–14015. doi:10.3390/ijms131114002.

Olivares, F. L., Busato, J. G., Paula, A. M. De, Lima, S., Aguiar, N. O., and Canellas, L. P. (2017). Plant growth promoting bacteria and humic substances : crop promotion and mechanisms of action. *Chem. Biol. Technol. Agric.*, 1–13. doi:10.1186/s40538-017-0112-x.

Othibeng, K., Nephali, L., Ramabulana, A. T., Steenkamp, P., Petras, D., Kang, K. Bin, et al. (2021). A metabolic choreography of maize plants treated with a humic substance-based biostimulant under normal and starved conditions. *Metabolites* 11. doi:10.3390/metabo11060403.

Pane, C., Palese, A. M., Spaccini, R., Piccolo, A., Celano, G., and Zaccardelli, M. (2016). Enhancing

sustainability of a processing tomato cultivation system by using bioactive compost teas. *Sci. Hortic. (Amsterdam).* 202, 117–124. doi:10.1016/j.scienta.2016.02.034.

Pepe, G., Sommella, E., Manfra, M., De Nisco, M., Tenore, G. C., Scopa, A., et al. (2015). Evaluation of anti-inflammatory activity and fast UHPLC-DAD-IT-TOF profiling of polyphenolic compounds extracted from green lettuce (Lactuca sativa L.; Var. Maravilla de Verano). *Food Chem.* 167, 153–161. doi:10.1016/j.foodchem.2014.06.105.

Peterson, M., Hans, J., and Matern, U. (2010). Biosynthesis of phenypropanoids and related compounds. In: Wink M., Ed., Biochemistry of Plant Secondary Metabolism (2nd ed.), *Annual Plant reviews*, Vol. 40, Wiley-Blackwell, 182-230.

Piccolo, A., Pietramellara, G., and Mbagwu, J. (1997). Use of humic substances as soil conditioners to increase aggregate stability. *Geoderma* 75:267-277.

Piccolo, A. (2002). The supramolecular structure of humic substances: A novel understanding of humus chemistry and implications in soil science. *Adv. Agron.* 75, 57–134. doi:10.1016/s0065-2113(02)75003-7.

Piccolo, A., Spaccini, R., Savy, D., Drosos, M., Cozzolino, V. (2019). The Soil Humeome: Chemical Structure, Functions and Technological Perspectives. In: Sustainable Agrochemistry: A compendium of Technologies. Ed: Vaz S. jr., *Springer Nature*, Heidelberg, pp. 183-222.

Pizzeghello, D., Schiavon, M., Francioso, O., Dalla Vecchia, F., Ertani, A., and Nardi, S. (2020). Bioactivity of Size-Fractionated and Unfractionated Humic Substances From Two Forest Soils and Comparative Effects on N and S Metabolism, Nutrition, and Root Anatomy of Allium sativum L. *Front. Plant Sci.* 11, 1–17. doi:10.3389/fpls.2020.01203.

Priya, S., Mk, K., Roshan, C., and Deepak, K. (2021). Effect of soil and foliar applications of compost tea on growth characters , quality and nutrient content of soybean [Glycine max . (L .) Merrill] under organic cultivation. *J. Pharmacogn. Phytochem.* 10, 2566–2569.

Puglisi, E., Fragoulis, G., Del Re, A. A. M., Spaccini, R., Piccolo, A., Gigliotti, G., et al. (2008). Carbon deposition in soil rhizosphere following amendments with compost and its soluble fractions, as evaluated by combined soil-plant rhizobox and reporter gene systems. *Chemosphere* 73, 1292–1299. doi:10.1016/j.chemosphere.2008.07.008.

Quaggiotti, S., Ruperti, B., Pizzeghello, D., Francioso, O., Tugnoli, V., and Nardi, S. (2004). Effect of low molecular size humic substances on nitrate uptake and expression of genes involved in nitrate transport in maize (Zea mays L.). *J. Exp. Bot.* 55, 803–813. doi:10.1093/jxb/erh085.

Rosa, M., Prado, C., Podazza, G., Interdonato, R., González, J. A., Hilal, M., et al. (2009). Soluble sugars-metabolism, sensing and abiotic stress a complex network in the life of plants. *Plant Signal. Behav.* 4, 388–393. doi:10.4161/psb.4.5.8294.

Ros, R., Muñoz-Bertomeu, J., and Krueger, S. (2014). Serine in plants: Biosynthesis, metabolism, and functions. *Trends Plant Sci.* 19, 564–569. https://doi.org/10.1016/j.tplants.2014.06.003.

Rouphael, Y., Franken, P., Schneider, C., Schwarz, D., Giovannetti, M., Agnolucci, M., et al. (2015). Arbuscular mycorrhizal fungi act as biostimulants in horticultural crops. *Sci. Hortic. (Amsterdam).* 196, 91–108. doi:10.1016/j.scienta.2015.09.002.

Saia, S., Aissa, E., Luziatelli, F., Ruzzi, M., Colla, G., Ficca, A. G., et al. (2020). Growth-promoting bacteria and arbuscular mycorrhizal fungi differentially benefit tomato and corn depending upon the supplied form of phosphorus. *Mycorrhiza* 30, 133–147. doi:10.1007/s00572-019-00927-w.

Saia, S., Colla, G., Raimondi, G., Di Stasio, E., Cardarelli, M., Bonini, P., et al. (2019). An endophytic fungi-based biostimulant modulated lettuce yield, physiological and functional quality responses to both moderate and severe water limitation. *Sci. Hortic. (Amsterdam).* 256, 108595. doi:10.1016/j.scienta.2019.108595.

Savarese, C., di Meio, V., Cangemi, S., Verrillo M., Savy D., Cozzolino, V., and Piccolo, A. (2021). Bioactivity of two different humic materials and their combination as a function of theri molecular proprieties. *Plant and Soi*l (In press).

Savy, D., Brostaux, Y., Cozzolino, V., Delaplace, P., du Jardin, P., and Piccolo, A. (2020). Quantitative Structure-Activity Relationship of Humic-Like Biostimulants Derived From Agro-Industrial Byproducts and Energy Crops. *Front. Plant Sci.* 11, 1–13. doi:10.3389/fpls.2020.00581.

Savy, D., Canellas, L., Vinci, G., Cozzolino, V., and Piccolo, A. (2017a). Humic-Like Water-Soluble Lignins from Giant Reed (Arundo donax L.) Display Hormone-Like Activity on Plant Growth. *J. Plant Growth Regul.* 36, 995–1001. doi:10.1007/s00344-017-9696-4.

Savy, D., Cozzolino, V., Nebbioso, A., Drosos, M., Nuzzo, A., Mazzei, P., et al. (2016). Humic-like bioactivity on emergence and early growth of maize (Zea mays L.) of water-soluble lignins isolated from biomass for energy. *Plant Soil* 402, 221–233. doi:10.1007/s11104-015-2780-2.

Savy, D., Cozzolino, V., Vinci, G., Nebbioso, A., and Piccolo, A. (2015). Water-soluble lignins from different bioenergy crops stimulate the early development of maize (Zea mays, L.). *Molecules* 20, 19958–19970. doi:10.3390/molecules201119671.

Savy, D., Mazzei, P., Drosos, M., Cozzolino, V., Lama, L., and Piccolo, A. (2017b). Molecular Characterization of Extracts from Biorefinery Wastes and Evaluation of Their Plant Biostimulation. *ACS Sustain. Chem. Eng.* 5, 9023–9031. doi:10.1021/acssuschemeng.7b01928.

Schiavon, M., Pizzeghello, D., Muscolo, A., Vaccaro, S., Francioso, O., and Nardi, S. (2010). High molecular size humic substances enhance phenylpropanoid metabolism in maize (Zea mays L.). *J. Chem. Ecol.* 36, 662–669. doi:10.1007/s10886-010-9790-6.

Shinozaki, S., Uemura, M., Bailey-Serres, J., Bray, E.A., and Weretilnyk, E. (2015). Responses to abiotic stress. In: Buchanan B., Gruissem W. and Jones R., Eds., Biochemistry and Molecular Biology of Plants, American Society of Plant Biologists (2nd ed.), Wiley-Blackwell, 1051-1099.

Schoebitz, M., López, M. D., Serrí, H., Martínez, O., and Zagal, E. (2016). Combined application of microbial consortium and humic substances to improve the growth performance of blueberry seedlings. *J. Soil Sci. Plant Nutr.* 16, 1010–1023. doi:10.4067/S0718-95162016005000074.

Shahrajabian, M. H., Chaski, C., Polyzos, N., and Petropoulos, S. A. (2021). Biostimulants application: A low input cropping management tool for sustainable farming of vegetables. *Biomolecules* 11. doi:10.3390/biom11050698.

Shennan, C., Krupnik, T. J., Baird, G., Cohen, H., Forbush, K., Lovell, R. J., et al. (2017). Organic and Conventional Agriculture: A Useful Framing? *Annu. Rev. Environ. Resour.* 42, 317–346. doi:10.1146/annurev-environ-110615-085750.

Spaccini, R., Cozzolino, V., Di Meo, V., Savy, D., Drosos, M., and Piccolo, A. (2019). Bioactivity of humic substances and water extracts from compost made by ligno-cellulose wastes from biorefinery. *Sci. Total Environ.* 646, 792–800. doi:10.1016/j.scitotenv.2018.07.334.

Suh, M.C., Hahne, G., Liu, J.R., and Stewart, N. (2015). Plant lipid biology and biotechnology. *Plant Cell Rep*. 34, 517–8. 10.1007/s00299-015-1780-2.

Taha, S. S., and Osman, A. S. (2018). Influence of potassium humate on biochemical and agronomic attributes of bean plants grown on saline soil. *J. Hortic. Sci. Biotechnol.* 93, 545–554. doi:10.1080/14620316.2017.1416960.

Trevisan, S., Botton, A., Vaccaro, S., Vezzaro, A., Quaggiotti, S., and Nardi, S. (2011). Humic substances affect Arabidopsis physiology by altering the expression of genes involved in primary metabolism, growth and development. *Environ. Exp. Bot.* 74, 45–55. doi:10.1016/j.envexpbot.2011.04.017.

Valluru, R., and Van den Ende, W. (2011). Myo-inositol and beyond - Emerging networks under stress. *Plant Sci.* 181, 387–400. doi:10.1016/j.plantsci.2011.07.009.

van Tol de Castro, T. A., Berbara, R. L. L., Tavares, O. C. H., Mello, D. F. da G., Pereira, E. G., Souza, C. da C. B. de, et al. (2021). Humic acids induce a eustress state via photosynthesis and nitrogen metabolism leading to a root growth improvement in rice plants. *Plant Physiol. Biochem.* 162, 171–184. doi:10.1016/j.plaphy.2021.02.043.

Verrillo, M., Cozzolino, V., Spaccini, R., and Piccolo, A. (2021a). Humic substances from green compost increase bioactivity and antibacterial properties of essential oils in Basil leaves. *Chem. Biol. Technol. Agric.* 8, 1–14. doi:10.1186/s40538-021-00226-7.

Verrillo, M., Salzano, M., Cozzolino, V., Spaccini, R., and Piccolo, A. (2021b). Bioactivity and antimicrobial properties of chemically characterized compost teas from different green composts. *Waste Manag.* 120, 98–107. doi:10.1016/j.wasman.2020.11.013.

Vinci, G., Cozzolino, V., Mazzei, P., Monda, H., Savy, D., Drosos, M., et al. (2018a). Effects of Bacillus amyloliquefaciens and different phosphorus sources on Maize plants as revealed by NMR and GC-MS based metabolomics. *Plant Soil* 429, 437–450. doi:10.1007/s11104-018-3701-y.

Vinci, G., Cozzolino, V., Mazzei, P., Monda, H., Spaccini, R., and Piccolo, A. (2018b). An alternative to mineral phosphorus fertilizers: The combined effects of Trichoderma harzianum and compost on Zea mays, as revealed by 1 H NMR and GC-MS metabolomics. *PLoS One* 13, 1–15. doi:10.1371/journal.pone.0209664.

Woo, S. L., Pepe, O., and Fertilizers, V. S. P. (2018). Microbial Consortia : Promising Probiotics as Plant Biostimulants for Sustainable Agriculture. 9, 7–12. doi:10.3389/fpls.2018.01801.

Yakhin, O. I., Lubyanov, A. A., Yakhin, I. A., and Brown, P. H. (2017). Biostimulants in plant science: A global perspective. *Front. Plant Sci.* 7. doi:10.3389/fpls.2016.02049.

Zaccardelli, M., Pane, C., Villecco, D., Maria Palese, A., and Celano, G. (2018). Compost tea spraying increases yield performance of pepper (Capsicum annuum L.) grown in greenhouse under organic farming system. *Ital. J. Agron.* 13, 229–234. doi:10.4081/ija.2018.991.

Zeeman S. (2015). Carbohydrate Metabolism. In: Buchanan B., Gruissem W. and Jones R., Eds., Biochemistry and Molecular Biology of Plants, American Society of Plant Biologists (2nd ed.), Wiley-Blackwell, 567-608.

Supporting Information

Table S1.

List of primary metabolites from lettuce leaves identified by GC-MS. The identification of compounds was carried out by analyzing standard compounds (STD) as well as by evaluating the mass spectra reported in the library (NIST 11).

N°	Metabolites	R.T.[a]	MS fragmentation (m/z)	References
1	Alanine	14.31	73-116-147-190	NIST
2	Oxalic acid	15.47	73-74-147-148-149	NIST
3	Valine	17.74	73-144-147-218	NIST
4	Glycerol TMS	19.52	73-117-147-205-299	NIST
5	Isoleucine	19.97	73-147-158-218	NIST
6	Succinic acid	20.57	73-147-172-247	NIST
7	Glyceric acid	21.03	73-103-147-189-292	NIST
8	Fumaric acid	21.58	73-133-147-245	NIST
9	Serine	21.84	73-147-204-218	NIST
10	Threonine	22.51	73-117-147-218-219	NIST
11	Malic acid	25.18	73-147-233-245	NIST
12	Proline	25.82	73-147-156-157	NIST
13	Aspartic acid	25.95	73-100-147-232	NIST
14	4-aminobutyric acid	26.14	73-130-147-230	NIST
15	Threonic acid	27.19	73-147-205-220-292	NIST
16	Glutaric acid	27.66	73-147-198-304	NIST
17	Glutamic acid	29.32	73-128-147-246	NIST
18	Tartaric acid	30.13	73-147-219-292	NIST
19	Xylose	30.88	73-103-147-217-307	NIST , STD
20	Asparagine	31.19	73-116-147-132-188-231	NIST
21	**Ribitol**	**32.78**	**73-103-147-217-319**	**IS[b]**
22	Glutamine	33.72	73-147-156-245	NIST
23	Citric acid	34.59	73-147-273-347-363	NIST
24	Fructose	35.44	73-103-133-147-217-307	NIST , STD
25	Fructose	35.60	73-103-133-147-217-308	NIST , STD
26	Galactose	35.82	73-147-205-217-319	NIST , STD
27	Glucose	36.05	73-147-160-205-319	NIST , STD
28	Myo-Inositol	36.55	73-147-191-217-305-318	NIST , STD
29	Hexose	36.90	73-147-191-204-205	NIST
30	Myo-Inositol	38.11	73-147-191-217-305-318	NIST , STD
31	Cinnamic acid	38.62	73-147-219-396	NIST
32	Cellobiose	40.22	73-147-204-217-361	NIST , STD
33	Glucuronic acid	40.78	73-147-205-217-292-375	NIST
34	Trehalose	42.49	73-147-191-204-217-362	NIST , STD
35	Sucrose	42.90	73-169-217-361-362	NIST , STD
36	D-Turanose	43.22	73-147-217-361-450	NIST
37	D-Turanose	43.35	73-147-217-361-450	NIST
38	Maltose	46.40	73-147-204-217-305-361	NIST , STD
39	Melibiose	46.75	73-103-129-204-217-361	NIST , STD

[a] Retention Time (min)

[b] IS = Internal Standard.

Table S2.

List of lipids from lettuce leaves identified by GC-MS. The identification of compounds was carried out by evaluating the mass spectra reported in the library (NIST 11).

N°	Metabolites	R.T.[a]	MS fragmentation (m/z)	References
1	Dodecanoic acid	24.75	73-75-117-129-132-257	NIST
2	3,7,11,15-Tetramethyl-2-hexadecen-1-ol	26.48	55-57-68-81-82-95-123	NIST
3	Tetradecanoic acid	26.61	73-75-117-129-132-145-285	NIST
4	Phytol acetate	27.01	57-68-82-95-123	NIST
5	Palmitic acid	28.82	73-75-117-129-132-145-313	NIST
6	11-Octanedecanoic acid	29.37	55-69-74-83-97-264	NIST
7	Linoleic acid	30.39	67-73-75-81-95-129-337	NIST
8	Linolenic acid	30.45	75-79-95-108-129-335	NIST
9	Stearic acid	30.69	73-75-117-129-132-145-341	NIST
10	**Dodecanedioic acid, bis(tert-butyldimethylsilyl) ester**	**31.94**	**73-75-129-401-402**	**IS [b]**
11	Erucic acid	32.79	55-69-83-97-111	NIST
12	1-Docosanol	33.21	57-75-83-103-383	NIST
13	Docosanoic acid	33.89	73-75-117-129-132-145-397	NIST
14	Linoleic acid, 2,3-bis-(O-trimethylsilyl)-propyl ester	35.19	73-75-129-147-207-221	NIST
15	Tetracosanoic acid	35.31	73-75-117-129-132-145-425	NIST
16	1-Hexacosanol	36.05	57-75-83-439-440	NIST
17	Hexacosanoic acid	36.68	73-75-117-129-132-145-453	NIST
18	Sigmasterol	38.93	55-69-73-83-129-255	NIST
19	beta-Sitosterol	39.61	73-129-357-381-396-486	NIST
20	Pregn-5-en-20-one, 3,16-bis[(trimethylsilyl)oxy]-, (3β,16α)-	39.79	73-75-129-172-296-386	NIST
21	beta-Amyrin TMSE	39.96	73-190-203-218-219	NIST
22	Germanicol (Olean-18-en-3-ol)	40.06	131-177-189-204-205	NIST
23	alfa-Amyrin TMSE	40.55	73-189-190-218-219	NIST
24	Lup-20(29)-en-3-ol, acetate, (3β)-	41.85	73-95-109-189	NIST

[a]Retention Time (min)

[b] IS = Internal Standard.

Table S3.

List of polyphenolic metabolites from lettuce leaves identified by UHPLC-MS-IT-TOF. The identification of compound was performed by the LCMSsolution software (Version 3, Shimadzu), the Formula Predictor software (Version 1.2, Shimadzu) and MetID solution software (Version 1.2, Shimadzu).

N°	RT[a] (min)	Observed m/z ([M-H]⁻)	Calculated m/z ([M-H]⁻)	Molecular formula	Error (ppm)	Major fragments m/z ([M-H]⁻)	Proposed compound
1	5.49	343.1036	343.1035	C15H20O9	0.13	181.0506, 164.0404	Dihydrocaffeic acid hexose
2	5.79	315.0726	315.0722	C13H16O9	1.41	153.0201, 108.0233	Dihydroxybenzoic acid hexose
3	5.80	313.0927	313.0929	C14H18O8	-0.61	151.0409	4-hydroxyphenylacetyl glucoside
4	5.88	299.0776	299.0772	C13H16O8	1.11	137.027	Hydroxybenzoic acid derivative
5	6.04	359.0982	n.d.[c]	C15H20O10	n.d.[c]	197.0454, 153.0165	Syringic acid hexose
6	6.05	341.0892	n.d.[c]	C15H18O9	n.d.[c]	179.033, 135.0455	Caffeoyl hexose
7	6.10	329.0872	329.0878	C14H18O9	-1.99	167.0333	Vanillic acid glucoside
8	6.85	339.0721	339.0714	C15H16O9	-0.31	177.0188	Esculetin 6-O-glucoside
9	6.87	311.0409	n.d.[c]	C13H12O9	n.d.[c]	149.0078	Caffeoyltartaric acid
10	7.15	325.0925	325.0929	C15H18O8	-1.28	163.0384, 119.0532	P-Coumaroyl glucoside
11	7.53	353.0877	353.0878	C16H18O9	-0.23	191.0545, 179.0366, 135.0401	Caffeoylquinic acid (Chlorogenic acid)
12	7.75	295.0460	295.0459	C13H12O8	0.28	163.0405, 119.0504	Coumaroyltartaric acid (Coutaric acid)
13	7.71	639.124	n.d.[c]	C27H28O18	n.d.[c]	463.0866, 535.1141, 343.0450	Quercetin hexose glucuronide
14	8.08	325.0565	325.0565	C14H14O9	0.29	163.2930	Feruloyl tartaric acid
15	8.18	337.0925	337.0929	C16H18O8	-1.08	163.0378	p-Coumaroylquinic acid 1
16	8.42	337.0925	337.0929	C16H18O8	-1.08	163.0378	p-Coumaroylquinic acid 2
17	8.46	367.1032	367.1035	C17H20O9	-0.76	179.1910	Feruloylquinic acid
18	8.52	609.1456	609.1461	C27H30O16	-0.92	285.0397	Luteolin diglucoside
19	**8.75**	**161.0244**	**161.0244**	**C9H6O3**	**0.1**	**-**	**Umbelliferone (IS[b])**
20	9.05	447.0938	447.0933	C21H20O11	1.32	285.0382	Luteolin 7-glucoside
21	9.11	463.0887	463.0882	C21H20O12	0.97	301.0346, 300.0278	Quercetin 3-O-glucoside
22	9.32	461.0723	461.0725	C21H18O12	-0.54	285.039, 271.0214, 299.0192	Luteolin 7-glucuronide
23	9.35	477.0672	477.0675	C21H18O13	-0.66	301.0347	Quercetin 3-glucuronide
24	9.48	549.0888	549.0886	C24H22O15	0.29	505.0981	Quercetin malonylglucoside
25	9.56	435.0931	435.0933	C20H20O11	-0.54	315.0732, 153.0205, 152.0130	Hydroxybenzoyl dihydroxybenzoyl hexose
26	9.59	515.1196	515.1195	C25H24O12	0.15	353.0876, 191.0551	Dicaffeoylquinic acid
27	9.64	445.0728	n.d.[c]	C21H18O11	n.d.[c]	269.0451	Apigenin 7-O-glucuronide
28	9.75	475.0880	n.d.[c]	C22H20O12	n.d.[c]	284.0353, 299.0574	Hispidulin glucuronide
29	9.89	473.0720	473.0725	C22H18O12	-1.16	311.0387, 293.0324, 170.0375	Dicaffeoyltartaric acid (Chicoric acid)
30	10.60	457.0780	457.0776	C22H18O11	0.80	295.0498, 277.0364	Caffeoyltartaric-p-coumaroyl acid
31	12.53	499.1241	n.d.[c]	C25H23O11	n.d.[c]	353.0706, 191.0504, 337.087	p-Coumaroyl-Caffeoylquinic acid
32	14.60	491.0826	n.d.[c]	C22H20O13	n.d.[c]	271.3010	Isorhamnetin 3-O-glucuronide

[a] Retention Time (min)

[b] Internal Standard

[c] Not determined.

Figure S1.
GC-MS chromatogram of polar fraction of metabolic extract from lettuce leaves (control sample). Numbers refer to the identified compounds listed in Table S1.

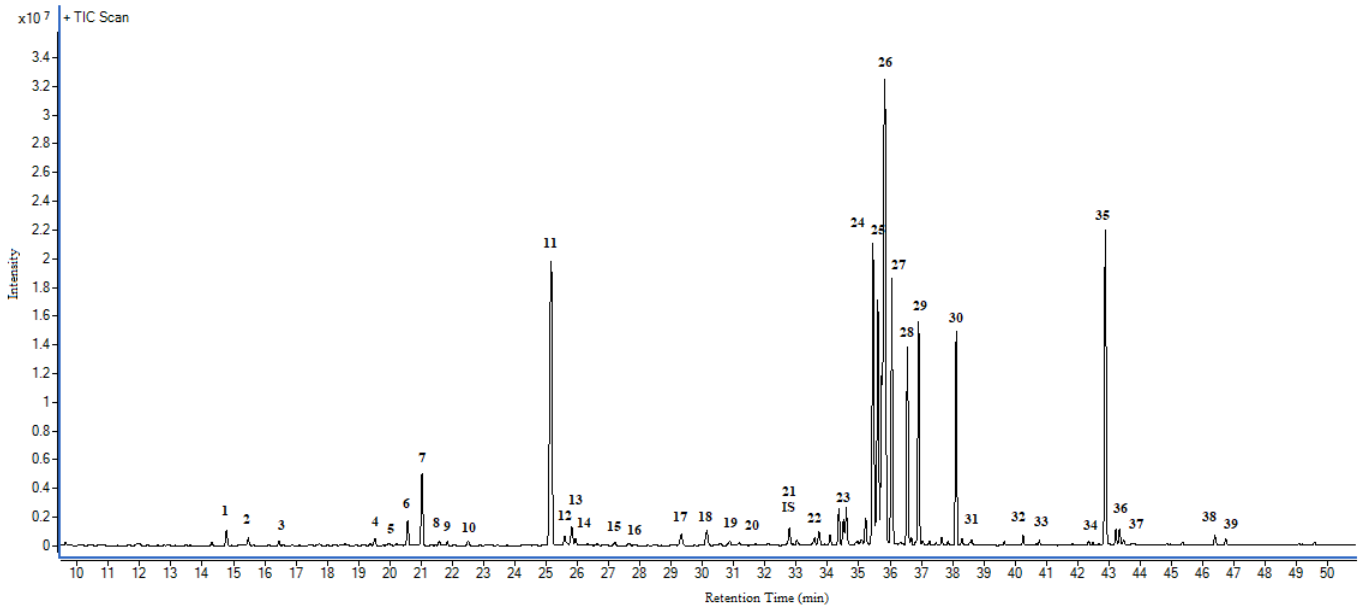

Figure S2.
GC-MS chromatogram of apolar fraction of metabolic extract from lettuce leaves (control sample). Numbers refer to the identified compounds listed in Table S2.

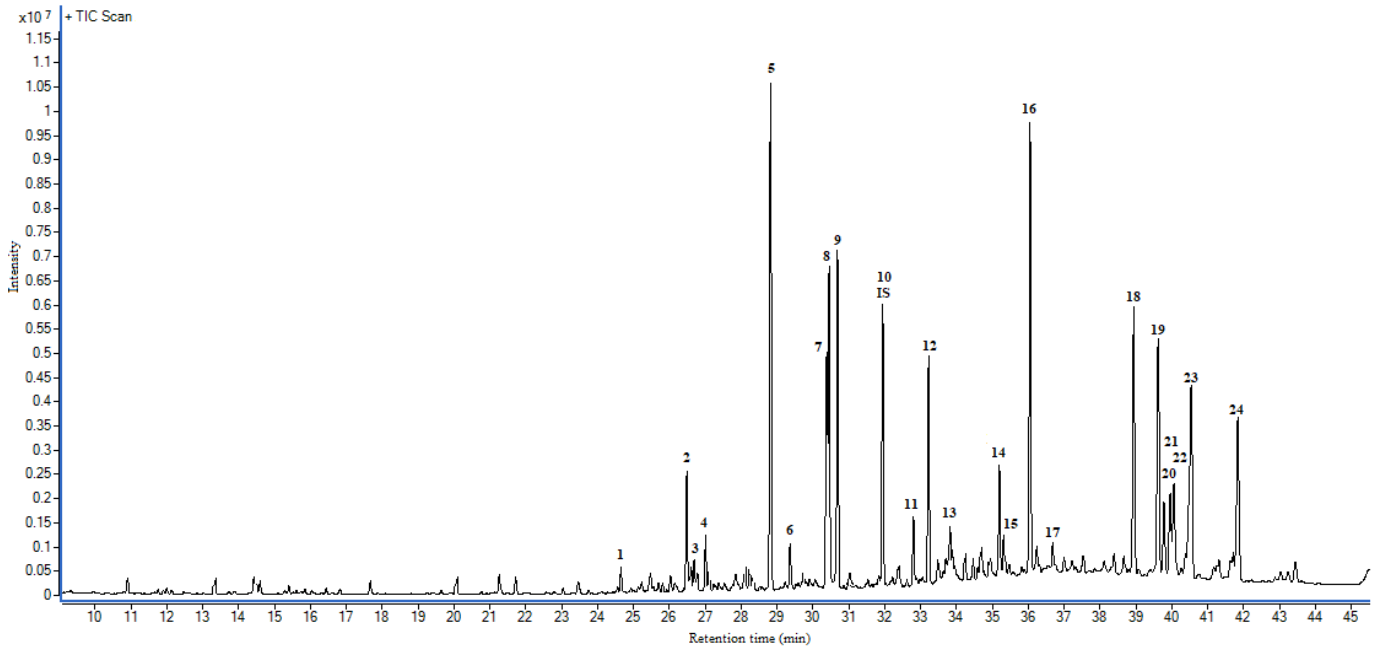

Figure S3.
UHPLC-MS-IT-TOF total ion chromatogram **(a)** and extracted ion chromatogram **(b)** of polyphenolic compounds detected in the metabolic extract from lettuce leaves (control sample). Numbers refer to the identified compounds listed in Table S3.

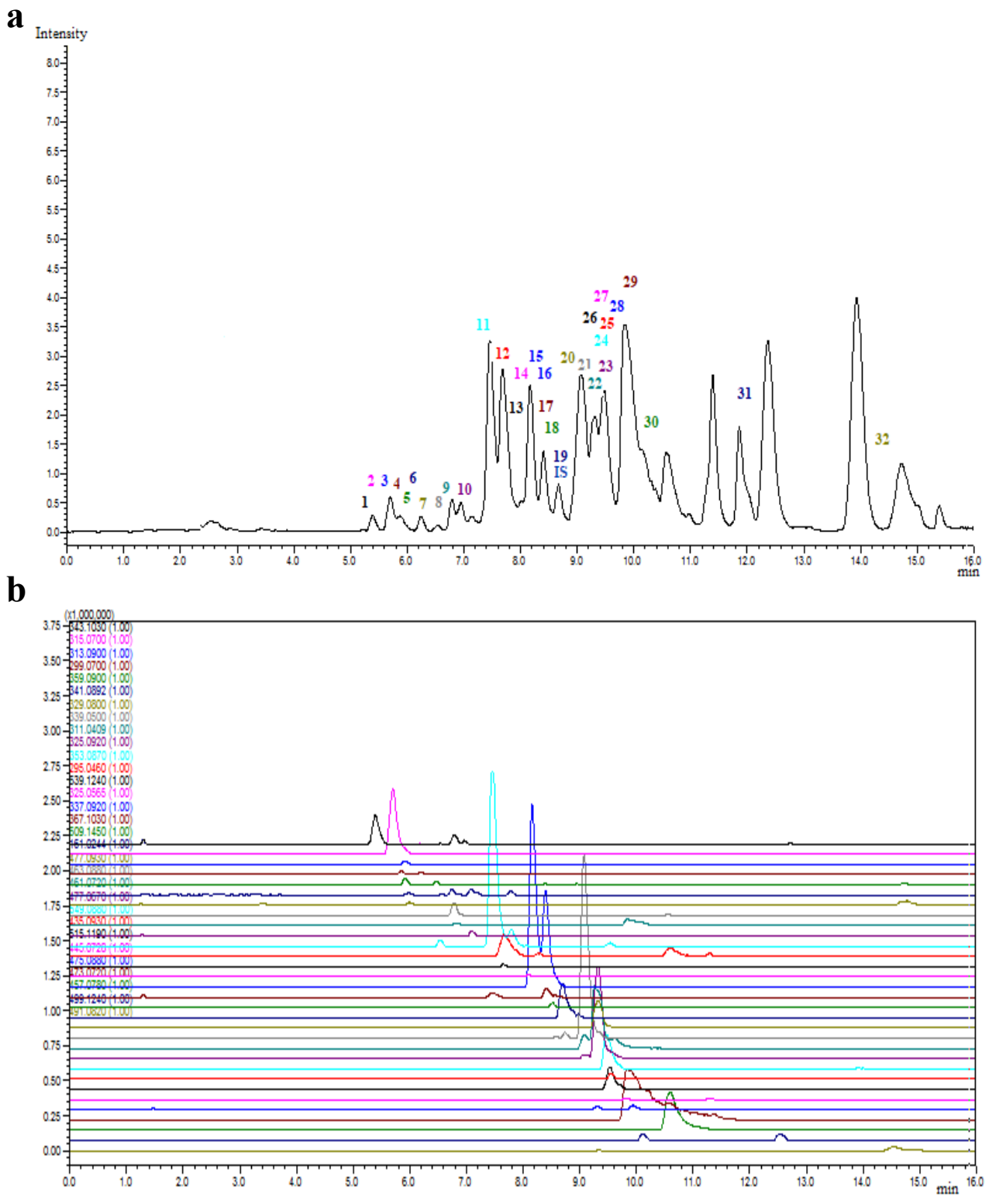

Figure S4.

Relative abundance (metabolite-to-internal standard total area ratio, a/is) of amino acids identified by GC-MS in the polar fraction of leaves extracts from lettuce plants treated with different biostimulants. CTRL: Control; KH: Potassium Humates from leonardite; CT: Compost Tea from green compost; MIX: KH plus CT; M+: plus microbial inoculum (Micosat TABPLUS). Dark grey indicates the microbial inoculation. Bars indicate standard deviation of means (n = 9). Different letters above the bars indicate significantly different means according to LSD test ($p < 0.05$).

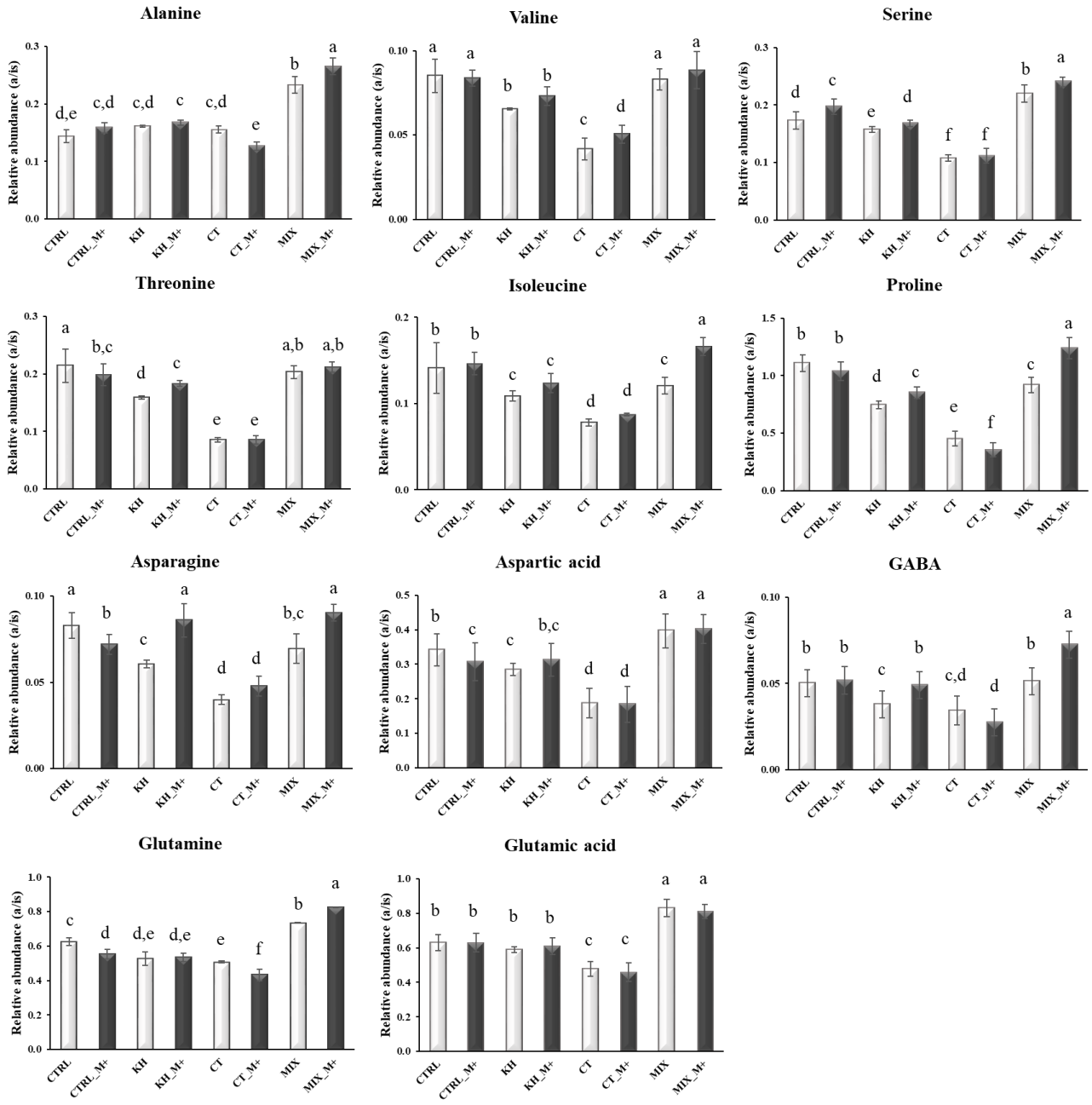

Figure S5 .

Relative abundance (metabolite-to-internal standard total area ratio, a/is) of organic acids identified by GC-MS in the polar fraction of leaves extracts from lettuce plants treated with different biostimulants. CTRL: Control; KH: Potassium Humates from leonardite; CT: Compost Tea from green compost; MIX: KH plus CT; M+: plus microbial inoculum (Micosat TABPLUS). Dark grey indicates the microbial inoculation. Bars indicate standard deviation of means (n = 9). Different letters above the bars indicate significantly different means according to LSD test ($p < 0.05$).

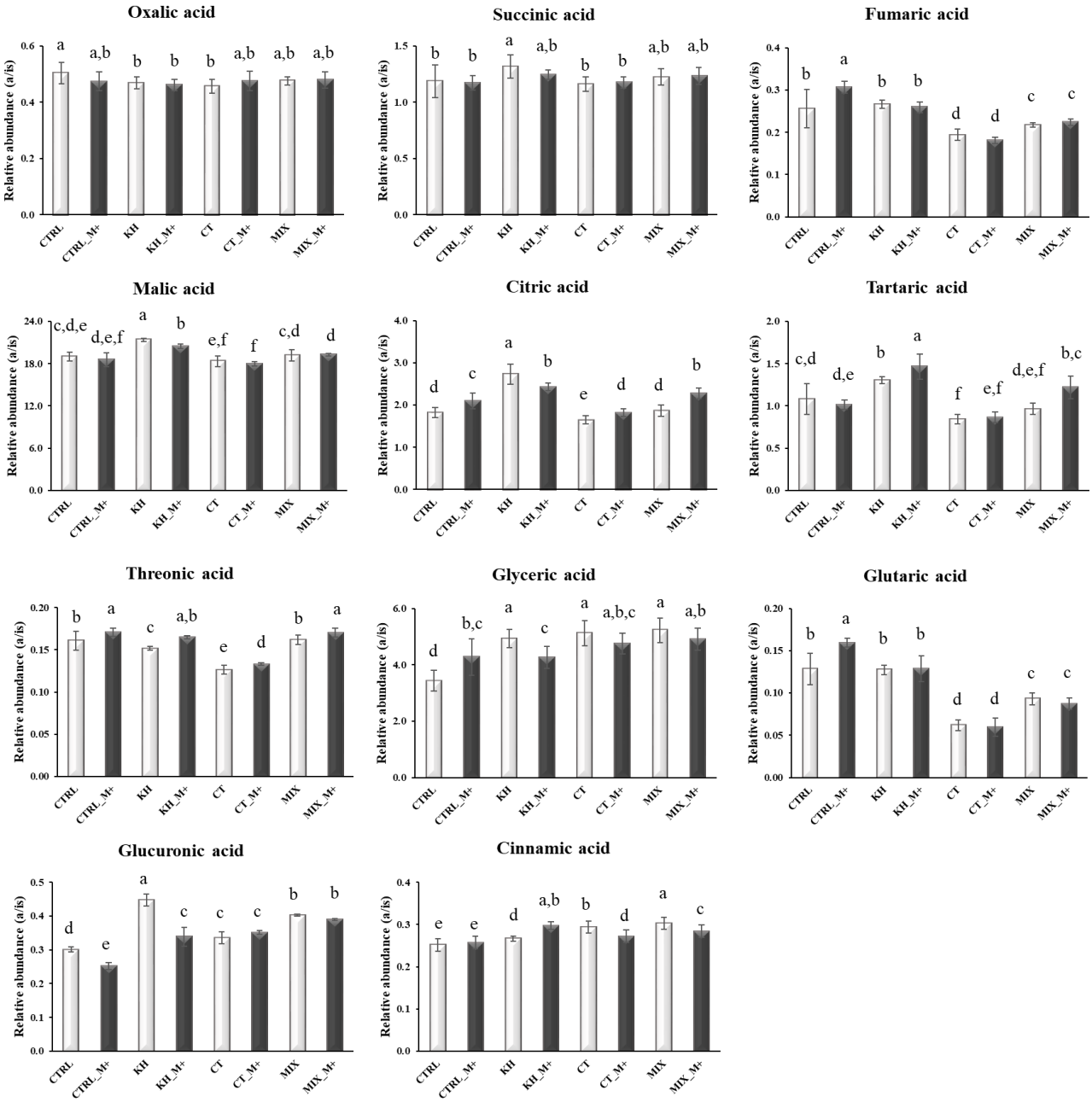

Figure S6 .

Relative abundance (metabolite-to-internal standard total area ratio, a/is) of saccharides identified by GC-MS in the polar fraction of leaves extracts from lettuce plants treated with different biostimulants. CTRL: Control; KH: Potassium Humates from leonardite; CT: Compost Tea from green compost; MIX: KH plus CT; M+: plus microbial inoculum (Micosat TABPLUS). Dark grey indicates the microbial inoculation. Bars indicate standard deviation of means (n = 9). Different letters above the bars indicate significantly different means according to LSD test ($p < 0.05$).

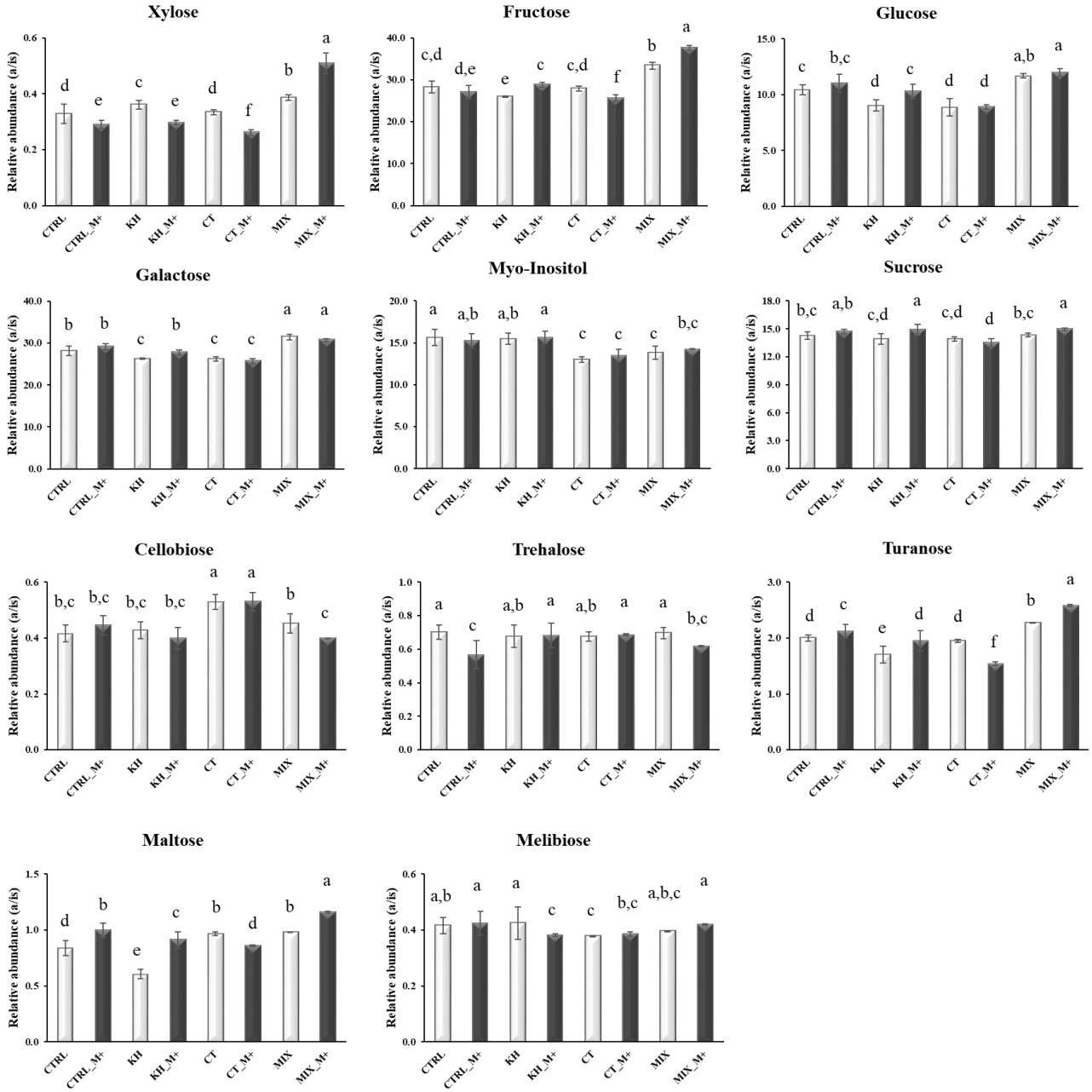

Figure S7.

Relative abundance (metabolite-to-internal standard total area ratio, a/is) of fatty acids identified by GC-MS in the apolar fraction of leaves extracts from lettuce plants treated with different biostimulants. CTRL: Control; KH: Potassium Humates from leonardite; CT: Compost Tea from green compost; MIX: KH plus CT; M+: plus microbial inoculum (Micosat TABPLUS). Dark grey indicates the microbial inoculation. Bars indicate standard deviation of means (n = 9). Different letters above the bars indicate significantly different means according to LSD test ($p < 0.05$).

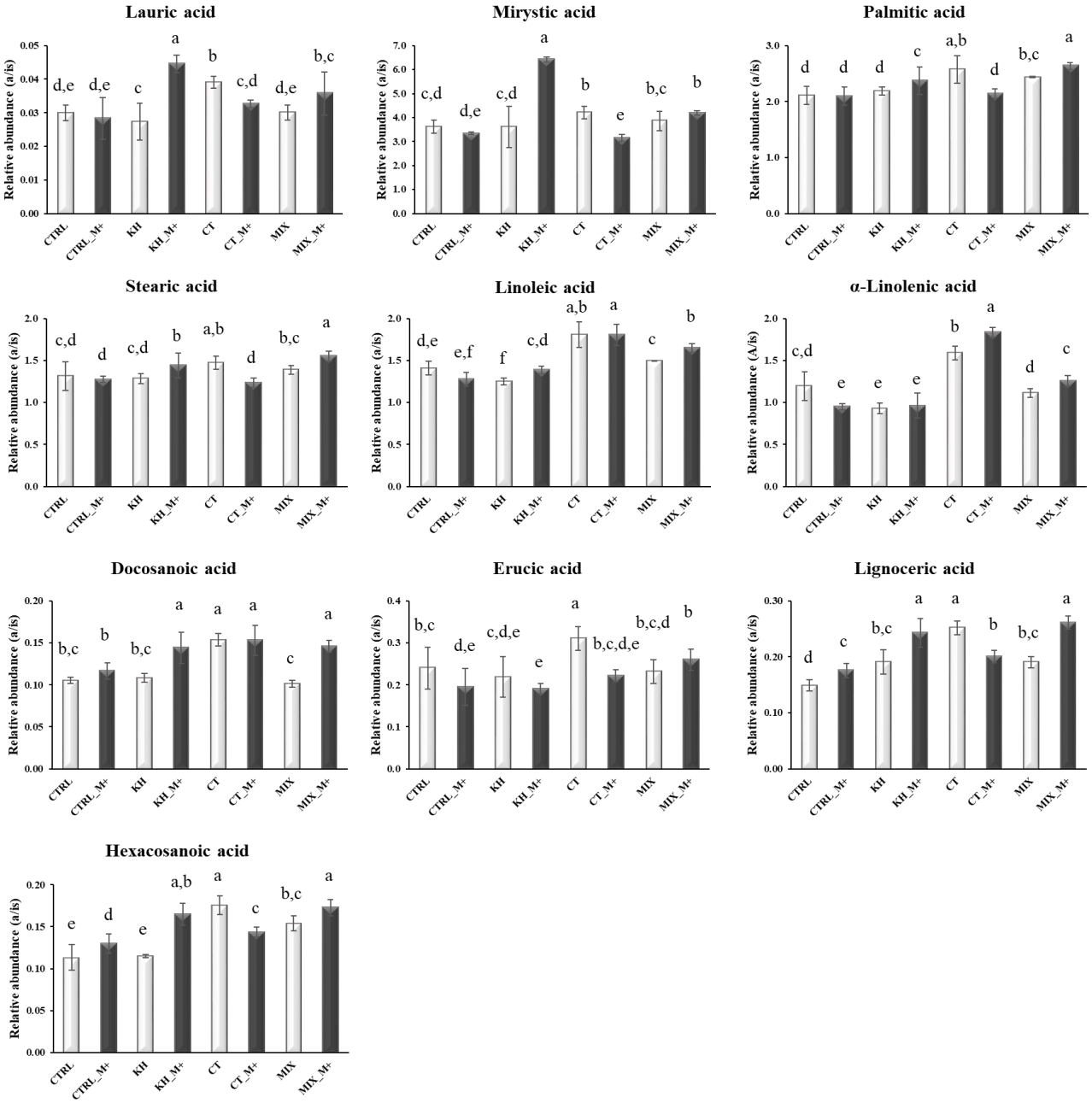

Figure S8.
Relative abundance (metabolite-to-internal standard total area ratio, a/is) of fatty alcohols, sterols and terpenes identified by GC-MS in the apolar fraction of leaves extracts from lettuce plants treated with different biostimulants. CTRL: Control; KH: Potassium Humates from leonardite; CT: Compost Tea from green compost; MIX: KH plus CT; M+: plus microbial inoculum (Micosat TABPLUS). Dark grey indicates the microbial inoculation. Bars indicate standard deviation of means (n = 9). Different letters above the bars indicate significantly different means according to LSD test ($p < 0.05$).

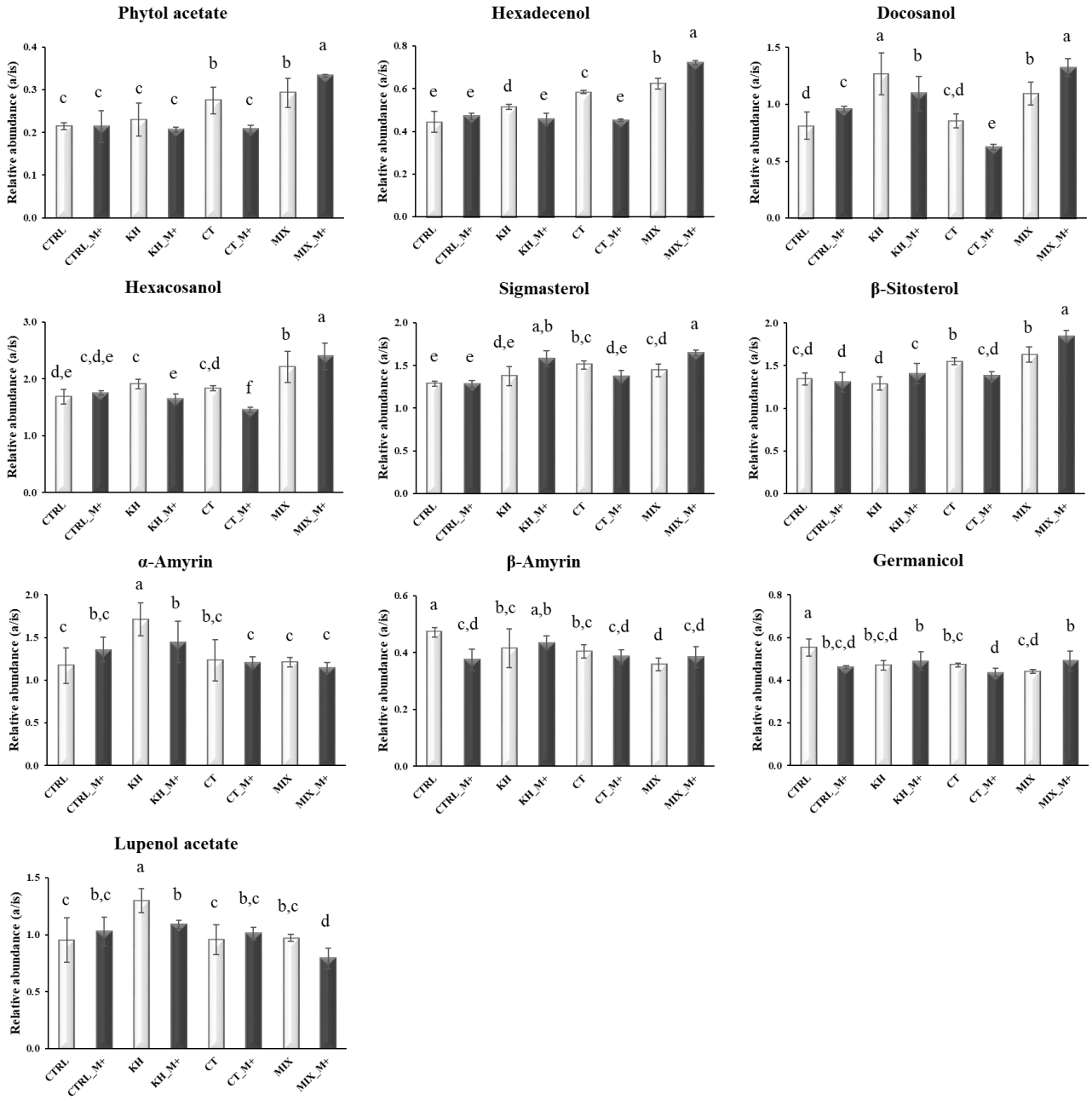

Figure S9.

Relative abundance (metabolite-to-internal standard total area ratio, a/is) of hydroxybenzoic and hydroxycinnamic acids identified by UHPLC-MS-IT-TOF in the leaves extracts from lettuce plants treated with different biostimulants. CTRL: Control; KH: Potassium Humates from leonardite; CT: Compost Tea from green compost; MIX: KH plus CT; M+: plus microbial inoculum (Micosat TABPLUS). Dark grey indicates the microbial inoculation. Bars indicate standard deviation of means (n = 9). Different letters above the bars indicate significantly different means according to LSD test ($p < 0.05$).

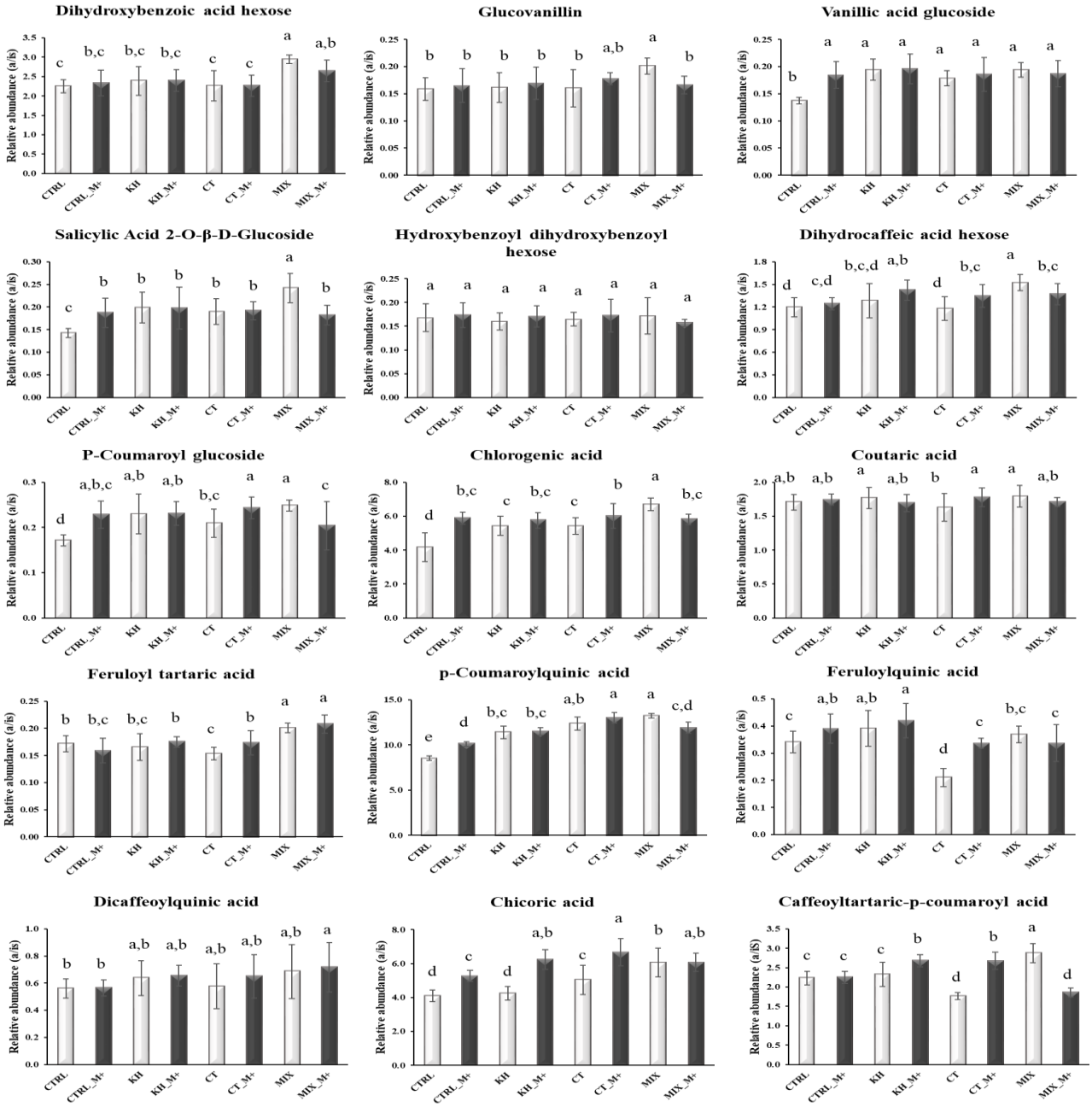

Figure S10.

Relative abundance (metabolite-to-internal standard total area ratio, a/is) of flavones, flavonols and coumarins by UHPLC-MS-IT-TOF in the leaves extracts from lettuce plants treated with different biostimulants. CTRL: Control; KH: Potassium Humates from leonardite; CT: Compost Tea from green compost; MIX: KH plus CT; M+: plus microbial inoculum (Micosat TABPLUS). Dark grey indicates the microbial inoculation. Bars indicate standard deviation of means (n = 9). Different letters above the bars indicate significantly different means according to LSD test ($p < 0.05$).

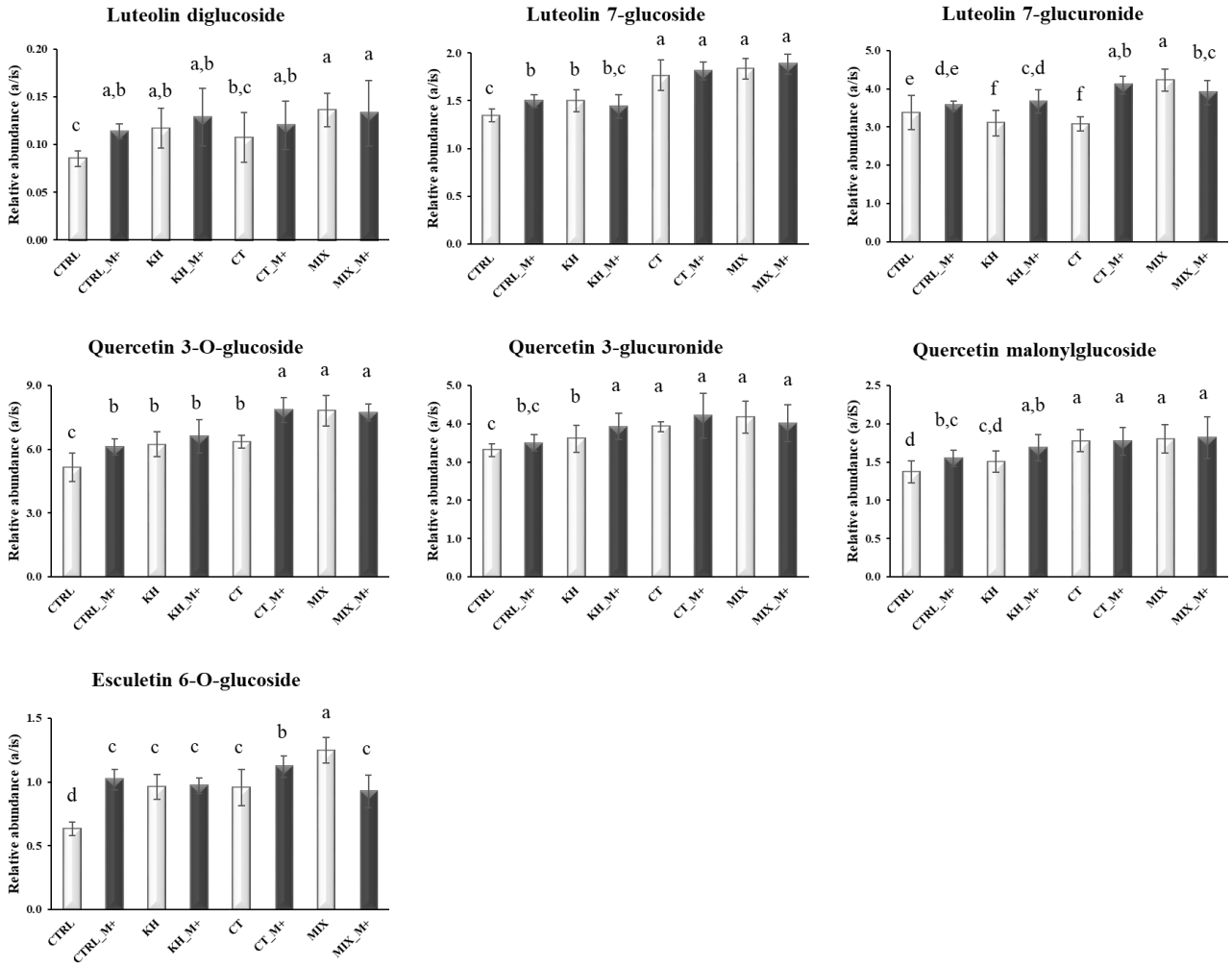

CHAPTER 7

Research in progress

Innovative application of bio-composite hydrogels

Abstract

A bio-composite hydrogel containing humic substances from green compost, sodium alginate and calcium nitrate as cross-linking agent was successfully fabricated by a 3D printer and used for soilless cultivation. Compared to pure alginate gel, the addition of humic substances improved the mechanical proprieties of the hydrogel, resulting in well-assembled and easly 3D printable structures. Furthermore, in both basil and lettuce seed germination experiments, the epicotyl and root lengh were enhanced by the addition of humic extracts to the alginate gel. These results indicate that humic substances have great potential to enhance the printability of alginate gels and improve plant growth as biostimulant materials, which implies that humic-hydrogels can be used as biomaterials for agricultural applications.

Keywords: hygrogels, bio-composite, humic substances, 3D printing, soilless cultivation.

1. Introduction

Soilless cultivation is a technology used for growing plants using alternative substrates instead of soil. Hydroponics is the most common method of soilless systems, although it requires much more water than soil cultivation, which is difficult in water-poor areas (Massa et al., 2020). An alternative to using water effectively is the employment of hydrogels (Vundavalli et al., 2015). Hydrogels are polymers with three-dimensional network structures having a water-hyper accumulation capacity of up to 100% of their own weights (Elshafie and Camel, 2021). Natural polymers have attracted increasing attention due to their unique properties such as biodegradability, environmental and ecological friendliness, low cost, and abundant sources (Guilherme et al., 2015). Natural hydrogels are widely used in the biomedical field for drug delivery (Peers et al., 2020), tissue engineering (Forget et al., 2017; Sivashankari et al., 2020), and biological engineering (Forget et al., 2013, 2016). In recent years, researchers have reported that hydrogels application has several benefits also in agriculture, such as conservation of soil water-holding capacity, lowering surface runoff, avoiding soil erosion, and improving the control of fertilizers and pesticides release (Abobatta, 2018). Moreover, it has been shown that hydrogel composites could be a viable alternative to the common methods used in soilless cultivation, since their porous structure, sufficient oxygen functional groups and suitable mechanical properties appear to be useful for promoting seed germination and plant growth (Tang et al., 2014; Cao and Li, 2021).

However, the potential applications of hydrogel bio-composites in agriculture are still poorly investigated, especially in combination with biostimulant materials. Plant Biostimulants (PB) represent a promising and eco-friendly strategy to increase plant growth with only very low dosages, while concomitantly ensuring high levels of agricultural productivity and food security (du Jardin, 2015; Yakhin et al., 2017). Among PB, humic materials may be innovatively used to formulate hydrogel bio-composites. Humic substances (HS) are composed of relatively small bioactive heterogeneous molecules held together in supramolecular assemblies by weak interactions (Piccolo, 2002; Nebbioso and Piccolo, 2011), and are widely used to enhance plants' productivity and

resistance to environmental stresses (Canellas et al., 2015). It has recently been highlighted that the introduction of HS into the hydrogel networks may increase their stabilization (Young et al., 2006). In fact, Nuzzo et al. (2020 a,b) lately reported that the molecular features of humic and humic-like substances affect the morphological and rheological properties of pectin hydrogels, thereby improving the ability to control the release of a previously incorporated model compound such as phloroglucinol. Therefore, the aim of the present work was to investigate the effect of humic substances from green compost (HS), on the formulation of an alginate hydrogel bio-composite, as well as their stimulatory proprieties on the germination of both basil and lettuce seeds.

Furthermore, in the present study we applied for the first time 3D printing to the development of innovative substrates for agricultural production. 3D printing belongs to the big family of Additive Manufacturing (AM) technologies, in which the object is generally a build up layer by layer from the bottom up from computer-assisted design (CAD) drawings by using a large variety of materials (powder, liquid, or sheets) (Vancauwenberghe et al., 2019; Falcone et al., 2022). Almost 30 years since its introduction, 3D printing is revolutionizing different processies in many industrial applications ranging from engineering to biomedical fields, and more recently, pharmaceutical and food products (Murphy and Atala, 2014; Vancauwenberghe et al., 2017, 2018; Capel et al., 2018). The selection and development of printing materials are based on several criteria, including flow-ability (easy manipulation and extrusion) and final rigidity (stability of the 3D structure) (Li et al., 2016; Hong et al., 2018). Sodium alginate (SA), a natural copolymer of mannuronic and glucuronic acid ((1,4) β-d-mannuronate (M) β-l-guluronate (G)) with different percentage ratio, is regarded as the most promising matrix for hydrogels 3D printing (Mallakpour et al., 2021). However, its application in the agricultural field is still limited (Elshafie and Camele, 2021). In this work, we hence attempted to design a novel hydrogel biomaterial through the combination of humic substances and alginate, and test its 3D printability for the development of innovative eco-frientdy substrate applicable to plants germination and growth.

2. Materials and Methods

2.1. Compost production and humic substances extraction

The green compost used in this study was produced in the composting facility of the experimental farm of the University of Napoli Federico II at Castel-Volturno (CE). Compost was obtained by 45-days composting process of 4 × 6 m static pile under forced air insufflation, followed by a two-month curing period. The composting pile consisted in residues of coffee production (coffee husks) (70% w/w) added with horticultural fresh residues (30% w/w). The compost was left to mature for 30 more days and then randomly sampled to collect 1 Kg. The compost sample was air dried, sieved at 2 mm and stored a 4 °C for further extraction processes.

Humic substances were extracted from the green compost as described elsewhere (Spaccini et al., 2019). Briefly, 200 g of air-dried compost was suspended in 1 L of 1M KOH solution in a polypropylene container and shaken overnight in a rotatory shaker. The supernatant containing humic matter was separated by centrifugation for 20 min at 7000 rpm, filtered through a Wathman 41 filter, brought to neutral pH using 1 M HCl, dialyzed until Cl-free against distilled water, and freeze-dried.

2.2. Chemical and Elemental Analysis of compost and humic substances

Elemental composition (C, H, N, and S) was determined using 2 mg of green compost and its humic extract (HS) by an UNICUBE elemental analyser (Elementar Analysensysteme GmbH, Germany).

Total concentration of macro- (Ca, Mg, K) and micro- (Cu, Zn, Mn) elements was determined by digesting 250 mg of samples with 6 mL of HNO_3 (65%) and 2 mL of H_2O_2 (35%) in a Milestone 900 microwave oven at 600 W for 24 min. Solutions were diluted to 25 mL with distilled water and analysed by an atomic absorption spectrometer (AAnalyst 700, Perkin-Elmer). The P content was measured calorimetrically in the same digested samples by the molybdenum blue assay method (Murphy and Riley 1962). All analyses were carried out in triplicate. Total elemental content of green compost and its humic extracts (HS) is reported in Table 1.

2.3. ^{13}C-CPMAS-NMR spectroscopy of compost and humic substances

A 300 MHz Bruker Avance spectrometer (Bruker Bio Spin GmbH, Rheinstetten, Germany), equipped with a 4 mm wide-bore MAS probe, was used to run solid-state NMR spectra of green compost and its humic extracts (HS). The fine-powdered samples (5 mg) were loaded into 4-mm zirconia rotor, stoppered by a Kel-F cap, and spun at a rate of 13000 ± 1 Hz. ^{13}C-NMR spectra were acquired through the Cross-Polarization Magic-Angle-Spinning (CPMAS) technique, by using 2 s of recycle delay, ^{1}H-power for CP 92.16 W: ^{1}H 90° pulse 2.85 µs, ^{13}C power for CP 150.4 W, 1 ms of contact time, 30 ms of acquisition time and 4000 scans. The ^{13}C-CPMAS pulse sequence was conducted by using a ^{1}H RAMP pulse to account for the *non*-homogeneity of the Hartmann–Hahn condition. The Fourier transform was performed with 4k data point and an exponential apodization of 100 Hz line broadening. The NMR spectrum was processed by using MestReC NMR Processing Software (v.4.8.6.0, Cambridgesoft, Cambridge, Massachusetts, USA). For the interpretation of ^{13}C-CPMAS-NMR spectra, the overall chemical shift range was divided into the following main resonance intervals: alkyl-C (0–45 ppm); methoxy-C and N-alkyl-C (45–60 ppm); O-alkyl-C (60–110 ppm); unsubstituted and alkyl-substituted aromatic-C (110–145 ppm); O-substituted aromatic-C (145–160 ppm); carboxyl- and carbonyl-C (160–200 ppm) (Spaccini and Piccolo, 2009). The percent relative contribution of a specific functional group (*i*) was determined by dividing the area of each spectral region (Res*i*) by the sum of all spectral areas: Rel*i* % = (Res*i* / Σ Res*i*) ×100. In order to highlight the structural features of green compost and its humic extract (HS), four dimensionless indexes were calculated from the relative abundance of specific components: O-Alkyl ratio A/OA = [(0–45)/(60–110)]; Aromaticity index ARM = [(110–160)/(0–190)]; Hydrophobic index HB/HI = [(0–45)+(110–160)]/(60–110) + (160–190)]; Lignin ratio LigR = [(45–60)/(145–160)] (Monda et al. 2017).

2.4. Preparation of bio-composite hydrogel

Stock solution of HS from green compost was prepared by dissolving 100 mg of powder in 100 mL of deionized water under magnetic stirring (700 rpm) for 30 min (final concentration 0.1 % w/v). The pH of aqueous solution was increased to 8-12 by adding KOH 5M (100-200 µL), for the complete solubilisation of HS. 2 g of Sodium alginate powder (Sigma-Aldrich) were dissolved in 66.4 mL of deionized water on a heated plate (60 °C) under magnetic stirring (700 rpm) for 30 min. After the complete solubilisation of alginate and cooling of the solution to room temperature, 10 mL of HS aqueous stock solution were added and the mixture was stirred (700 rpm) for another 30 min. The pH was checked to be around neutrality. Later, 23.6 mL of calcium nitrate tetra-hydrate (Sigma-Aldrich) solution 50.85 mM were added and the mixture was stirred (700 rpm) for 3 h, in order to obtain a homogeneous gel solution. The final concentration of sodium alginate, HS and $Ca(NO_3)_2$ in the hydrogel bio-composite was 2 % w/v, 0.01 % w/v and 12 mM, respectively.

2.5. 3D printing

The 3-D printing process was based on the extrusion of the hydrogel bio-composite at room temperature. Inkredible 3D bioprinter (CELLINK Inc, Sweden) was used to print the structures. The hydrogel was loaded into 3 mL printing cartridges (CELLINK Inc, Sweden) and connected to a controllable pressure regulator (0–200 kPa). The hydrogel printing flow rate was optimized by adjusting the extrusion pressure (109 kPa) and Z-axis of 0.1 mm from nozzle tip to print bed. The printed design was drawn on Inventor (Autodesk, 2018) and exported as an STL file. The files were then converted into G-code using Repetier Host (Hot-World GmbH) and Slic3R (Open Source). Preliminary experiments showed that the best filling was obtained with a rectilinear infill pattern and this was therefore used in all experiments (Figure 2). Layered scaffolds (0.3 mm) were printed on a Petri dish using a plastic nozzle (0.10-inch diameter). After printing, a 50 mM calcium nitrate tetrahydrate solution was sprayed on the structures, which were then incubated for 15 min.

Figure 2.
(a) Scheme of one of the printed structure defined in the Slic3r software. The yellow part is the object wall corresponding to outline defined by the perimeter; the red part represents the infill pattern. **(b)** Cross-section of one layer showing the print-head pathway.

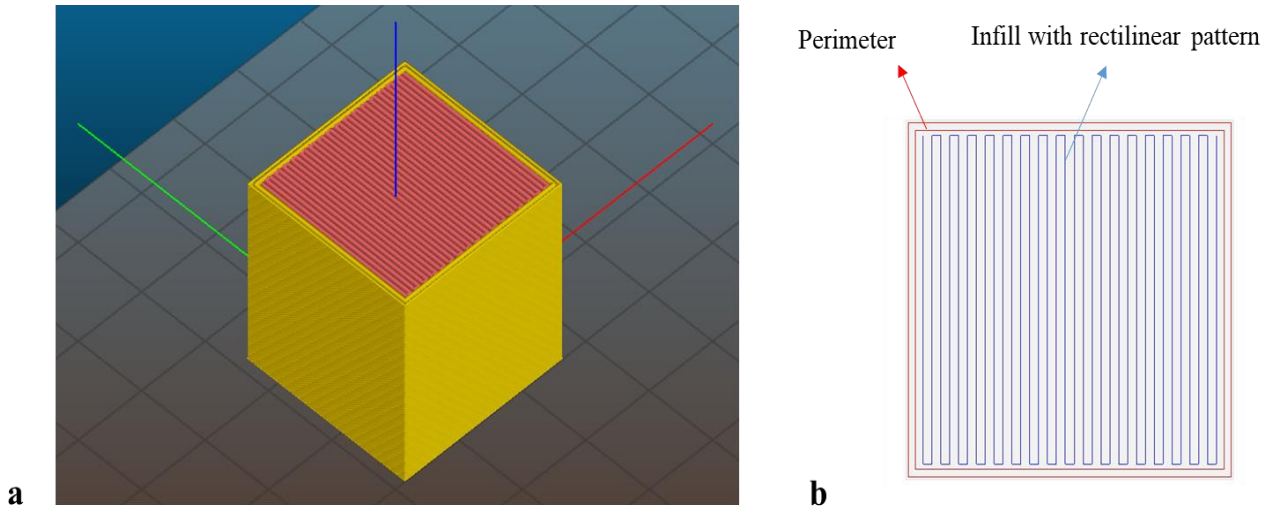

2.6. Germination test

The germination essays were performed in a growth-chamber at 25°C in dark conditions by setting the relative humidity at 85 %. Ten Basil (*Ocinum basilicum* Italian Large Leaf) or Lettuce (*Lactuca sativa L.*) seeds were placed on the printed hydrogel bio-composites, contained only sodium alginate (SA) or its mixture with HS solution, and moistened with 2 mL of distilled water. All treatments were carried out in five replicates. After 7 days of incubation, ImageJ software (64-bit, Open Source) was used to measure germinated seed, roots and epicotyls length.

2.7. Statistical Analysis

The significant difference between mean values obtained from all measurements of germination tests was determined by the one-way analysis of variance (ANOVA), and validated applying the least significant differences (LSD) test at $p < 0.05$ by using the XLSTAT software (Addinsoft, v. 2014). All data were tested for normality using the Shapiro-Wilk test.

3. Results and Discussion

3.1. Chemical and molecular characterization of compost and Humic Substances

The elemental composition and the nutrients content in green compost and its humic extracts (HS) are reported in Table 1. The carbon and nitrogen content were respectively smaller and larger in the humic extracts than in the green compost source (Table 1). In particular, the high C/N value of bulk compost may indicate plant residues as the major contributors to formation of the humified material (Campitelli and Ceppi, 2008), while the lower ratio found in HS suggests the incorporation of N-rich molecules, such as peptidies in the humic extract (Monda et al., 2018). On the other hand, no variation was found for the H/C ratio in both compost and HS, due to the accumulation of alkyl compounds during composting (Spaccini and Piccolo, 2009). Moreover, HS mainly contained an amount of K, Mg, Cu, and Mn (Table 1) in line with the elemental composition commonly found for humic extracts from composted biomasses (Jannin et al., 2012; Selim and Mosa, 2012).

The ^{13}C-CPMAS-NMR spectra of green compost and its humic extract (HS) are shown in Figure 1, while the relative distribution of signal areas is reported in Table 2. The broad resonance in the 0–45 ppm range, with distinct signals around 10, 30 and 31 ppm (Figure 1), reveals the presence of CH_2- and CH_3- groups in alkyl chains from various lipid compounds such as plant waxes and biopolyester (Spaccini and Piccolo, 2009). The signals in the 45–60 region at around 55 and 60 ppm (Figure 1), are instead attributed to methoxyl carbons in both guaiacyl and syringyl units of lignin fragments, as well as C-N functions in amino acids and peptide moieties (Scotti et al., 2016). The Alkyl-C and CH_3O/CN regions accounted respectively for 27.43 and 12.73 % of the total area in the bulk compost, 23.99 and 14.35 % in the corresponding HS (Table 2). The molecular composition of green compost was also rich in mono- and polysaccharides components, responsible for the 60-110 ppm spectral region (Figure 1) and accounting for 35.53 % of total area (Table 2). In particular, the signal around 72 ppm is assigned to the overlapping of C-2, C-3, and C-5 carbons in the pyranosidic structures of cellulose and several hemicelluloses, whereas the shoulder at 103 ppm is associated to the di-O-alkyl anomeric carbon 1 of glucose units (Spaccini et al., 2019). The spectra of HS from

green compost revealed a decrease in the O-Alkyl region, which accounted for 23.69 % of total area (Table 2). Moreover, the peaks extended along the 110–160 ppm spectral region indicate the presence of aryl-C in both lignin residues and other aromatic biomolecules (Figure 1). These compounds represented the 19.01 and 26.24 % of the total spectral area for compost and HS, respectively (Table 2), thus confirming the increase in aromatic structures, with a corresponding decrease of polysaccharide components, as already reported (Monda et al., 2018). In particular, the signals in the 145–160 ppm interval are assigned to O-substituted C in aromatic structures of lignin molecules and polyphenol compounds, while those in the 148–155 ppm range are specific to carbon 3, 4, and 5 in lignin aromatic ring, with carbon 3 and 5 being coupled to methoxyl substituent (Savy et al., 2015). Finally, the Carboxyl-C (160-190 ppm) spectral region accounted for 5.29 and 11.56 % of total area in the green compost and corresponding HS, respectively (Table 2). In this region, the signal around 170 ppm (Figure 1) corresponds to either the carbonyl carbons of aliphatic acids or amide functional groups (Spaccini and Piccolo, 2009). The main differences in molecular composition between green compost and its humic extract are summarized by the structural indices in Table 2. Larger values of hydrophobicity index (HB/HI), aromaticity (ARM) and alkyl-C/O-alkyl-C (A/OA) ratios are commonly associated to selective accumulation of recalcitrant compounds, and, thus, to progressive stabilization of organic biomasses (Piccolo et al., 2005). On the other hand, the lignin ratio (LigR) relates methoxyl to phenol carbons and assess the relative contribution of lignin-methoxyl substituents and/or C-N containing compounds, thus discriminating signals of lignin from those of other phenolic compounds (Monda et al., 2017). The values of HB/HI, ARM and A/OA indicate that the extracted humic substances are characterized by larger hydrophobicity in respect to the original compost (Table 2). An opposite trend of an improved incorporation of lignin moieties in HS was revealed by the small LigR values compared to the corresponding compost source (Table 2), whose higher lignin ratio implies a more abundant inclusion of C-N containing molecules (Spaccini and Piccolo, 2009). However, the largest percentage of methoxyl and phenolic C in HS (Table 2), may

suggest the presence of both lignin phenolic derivatives and labile nitrogen-containing compounds (Monda et al., 2018).

Table 1.
Elemental composition of green compost and its humic extract (HS).

	COMPOST	HS
		% (w/w)
C	37.16 ± 3.0	35.53 ± 1.0
H	5.29 ± 0.5	5.04 ± 0.9
N	3.37 ± 0.3	5.41 ± 0.9
S	0.83 ± 0.05	1.08 ± 0.1
C/N[a]	12.9	7.7
H/C[a]	1.7	1.7
		g/Kg
P	2.01 ± 0.05	1.89 ± 0.02
Ca	27.02 ± 1.2	3.01 ± 0.4
Mg	9.82 ± 0.9	5.24 ± 0.2
K	22.33 ± 2.0	13.38 ± 1.5
Fe	4.25 ± 0.3	2.73 ± 0.03
		mg/Kg
Cu	135.49 ± 2.0	370.32 ± 3.5
Zn	98.53 ± 5.0	108.73 ± 2.1
Mn	248.91 ± 2.5	122.45 ± 3.5

[a] Atomic ratio

Table 2.
Relative distribution (%) of signals area over chemical shift regions (ppm) and structural indexes in ^{13}C-CPMAS-NMR spectra of green compost and its humic extract (HS).

	^{13}C NMR regions						^{13}C NMR structural indexes			
Products	**Alkyl-C (0-45)**	**CH_3O/CN (45-60)**	**O-alkyl-C (60-110)**	**Aryl-C (110-145)**	**O-aryl-C (145-160)**	**Carboxyl-C (160-190)**	**HB/HI[a]**	**A/OA[b]**	**ARM[c]**	**LigR[d]**
COMPOST	27.43	12.73	35.53	15.43	3.58	5.29	0.9	0.8	0.2	3.6
HS	23.99	14.35	23.69	19.99	6.43	11.56	1.0	1.0	0.4	2.2

[a]HB/HI= hydrophobicity index = [Σ (0-45) + (110-160) / Σ (45-60) + (60-110) + (160-190)]
[b]A/AO = alkyl/O-alkyl ratio = [(0–45) / (60–110)]
[c]ARM = aromaticity index = [(110-160) / Σ (0-45) + (45-60) + (60-110) + (160-190)]
[d]LR = lignin ratio = [(45-60) / (145-160)]

Figure 1.
^{13}C-CPMAS-NMR spectra of green compost and its humic extract (HS).

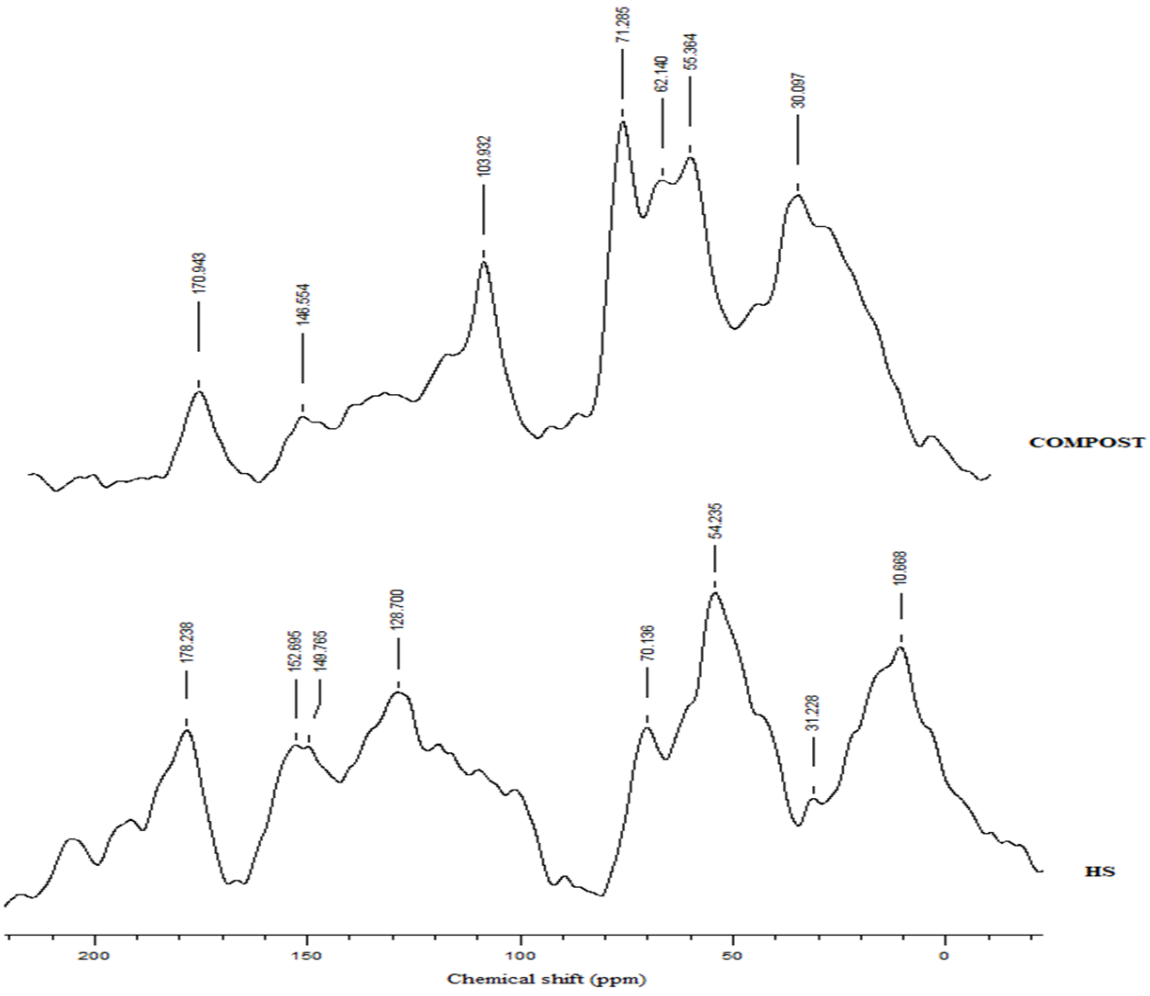

3.2. 3D printing of sodium alginate gel

The gelation of sodium alginate (SA) with calcium ions can be described with the "egg-box" model, which assumes the displacement of sodium by calcium ions from the binding sites, mainly the carboxyl groups of glucuronate blocks exploiting a zipper mechanism. Different polymeric network, with greater relative viscosity, can be obtained by adding increasing concentration of calcium chloride into the sodium alginate solution (Fang et al., 2007). Therefore, with the aim to obtain a homogeneous printable ink of alginate, capable to maintain its shape after the extrusion, a polymer pre-crosslinking operating procedure was performed adding to a fixed volume of sodium alginate (2 % w/v) solution the same volume of water in which different amounts of calcium nitrate were solubilized, from 10 to 20 mM (Figure 3). The printability conditions were carefully observed for each calcium-SA composition. These conditions were based on two visual observations: the deposition of the material and the 3-D shape stability during and after printing. The addition of calcium seemed to improve the build quality of the SA gel (Figure 3). However, three compositions (1, 3 and 4) showed lesser printability performance (Figure 3). First, irregular extrusion was observed following the addition of 15 mM of calcium nitrate, and, although this concentration appeared to result in a better build with shaper edges, the irregular extrusion sometimes caused structure defects such as the presence of cavities inside the object (Figure 3). Second, automatic stalling of the syringe pump occurred regularly with the 20 mM concentration of calcium nitrate, possibly due to the high viscosity (Figure 3). Finally, following the addition of only 10 mM calcium solution, a partial spreading was observed to occur during printing and the printed objects disassembled after the post treatment, thereby compromising their final 3-D shape (Figure 3). The best results were hence obtained from the SA gel with 12 mM calcium nitrate, whose printability was found to be optimal without needle occlusion and leading to compact structures after post-treatment (Figure 3). Vancauwenberghe et al. (2017) previously reported similar finding using the same 3D bio-printing of pectin gels with different amount of calcium ions. The best concentration was then used for preparing the hydrogel bio-composite, containing SA and humic substances (HS). 3D printing of the hydrogel resulted in well-

structured and easly printable objectes (Figure 4). Several structures were printed and the addition of HS appeared to increase the stabilization of the alginate gel, thus highlighting the potential versatility of the 3D technique (Figure 4). Nuzzo and collaborators (2020 a,b) recently showed the capacity of humic and humic-like substances to form hydrogels that changed the morphological and rheological properties of pectin gels. This hypothesis seems to well fit our positive results on the improved build quality of 3D-printed structures following the combination of humic substances with the SA gel (Figure 3 and 4).

Figure 3.
Printing tests for the identification of the best concentration of calcium nitrate in the sodium alginate gel. 1) 10 mM; 2) 12 mM; 3) 15 mM; 4) 20 mM.

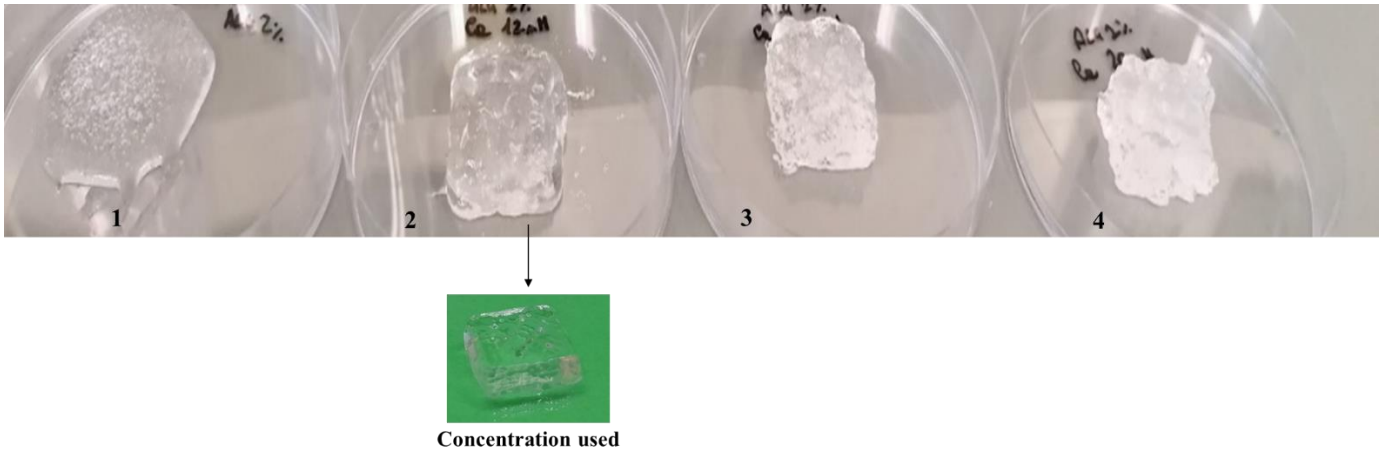

Figure 4.
3D bio-printing versatility of the hydrogel bio-composite containing sodium alginate (2 % w/v), humic substances from green compost (0.01 % w/v) and calcium nitrate 12 mM as cross-linking agent.

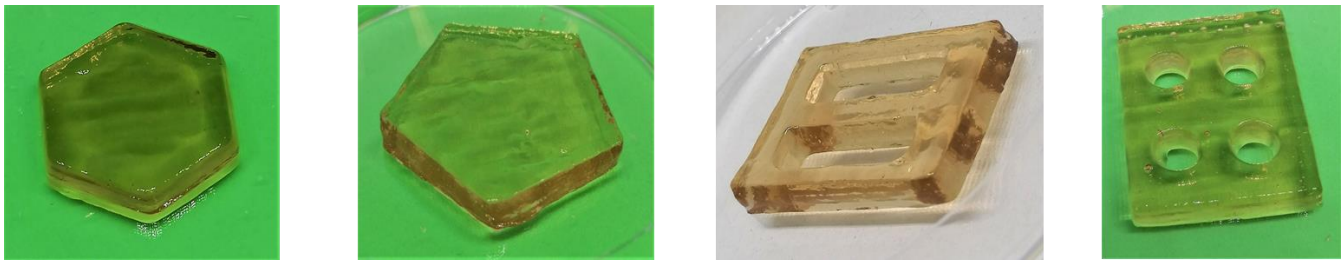

3.3. Seedlings growth on the hydrogel bio-composite

The potential use of the hydrogel bio-composite as substrate for soilless cultivation was evaluated by 3D printing two different structures, a compact cubic and a perforated rectangular one, which were used for growing basil and lettuce seedlings (Figure 4). The results of the bioactivity tests showed not only the absence of any phytotoxic effect on both basil and lettuce seeds germination, but also a positive response of the hydrogel bio-composite in root and epicotyl elongation of seedlings (Table 3 and 4). In particular, the addition of humic substances (HS) increased the epicotyl length of basil seeds by 8.5 % more than the alginate gel alone (SA), whereas no significant differences in root lenght were detected between SA and the humic-SA bio-composite hydrogel (Table 3). On the other hand, the combination of HS and SA positively affected both epicotyl and root elongation of lettuce seedlings, which increased by 13.5 and 22.6 %, respectively, in the bio-composite hydrogel as compared to the alginate gel alone (Table 4). The improved growth of both basil and lettuce seedlings in the bio-composite hydrogel may be related to the recognized hormone-like activity of humic materials that causes seeds germination promotion (Canellas et al., 2015; Savy et al. 2020). Humic substances have been described as supramolecular associations of relatively small and heterogeneous molecules, whose structural assemblies are stabilized by intermolecular weak hydrophobic interactions, hydrogen bonds and metal bridges (Piccolo, 2002). In particular, the hydrophobic domains in HS are assumed to randomly incorporate and preserve polar or medium polar bioactive molecules, which can be released following the supramolecular assembly disruption by low molecular weight organic acids such as those commonly extruded from plant roots (Piccolo et al., 1996, 1999, 2001; Savy et al., 2017; Piccolo et al., 2018). These bioactive molecules were found to possess a hormone-like activity (Muscolo et al., 1998), thus leading to a positive biological effect towards plant physiology and development (Nardi et al., 2007; Canellas and Olivares, 2014). Moreover, it has recently been shown that the presence of aromatic and/or hydrophobic components in humic supramolecular structure determines their closer and more effective interaction with plant roots, thus allowing these substances to better express their biological activity (Canellas et al., 2012; Savy et al.,

2016, 2017; Monda et al., 2017). Consequently, the effective HS bioactivity depends on an equilibrium of hydrophobic and hydrophilic components, which play a key role in the humic conformational flexibility (Monda et al., 2018; Piccolo et al., 2018). Therefore, the balance between polar molecules and hydrophobic structures found in humic substances from green compost (Table 2 and Figure 1) may explain the positive results obtained using the bio-composite hydrogel as a substrate for seedlings growth (Table 3 and 4; Figure 4). However, the potential development of porous structure and more suitable mechanical properties in the bio-composite by adding humic substances to the SA gel, as an additional cause of seed germination promotion and plant growth, may not be excluded (Tang et al., 2014; Cao and Li, 2021).

Figure 5.
(a) Basil and lettuce seedlings growth in different printed structures of sodium alginate gel (SA). **(b)** Basil and lettuce seedlings growth in different printed structures of hydrogel bio-composites containing sodium alginate and Humic substances from green compost (HS).

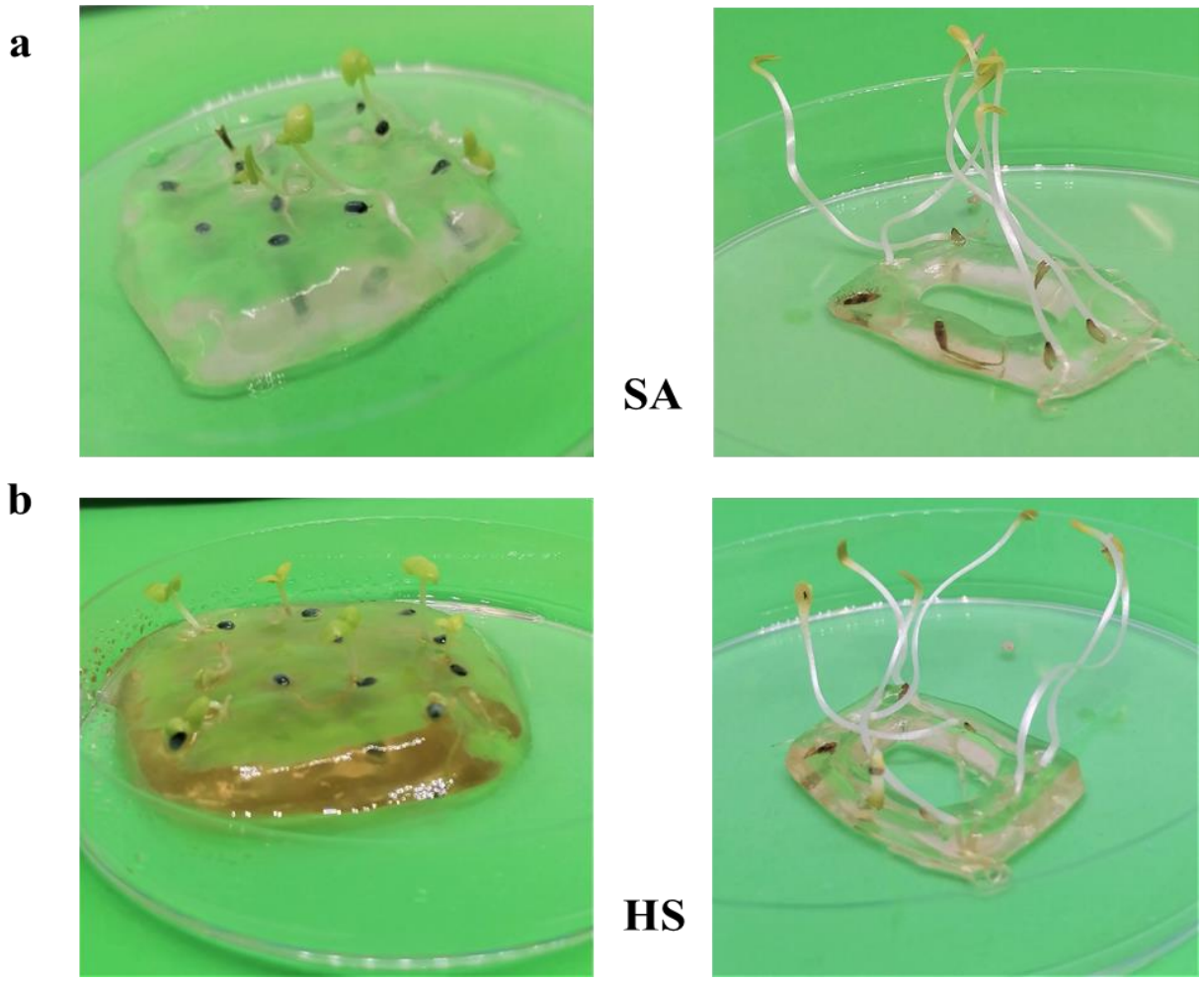

4. Conclusions

In this part of the thesis, develop during a research period abroad, the hypothesis of using a bio-composite hydrogel as substrate for soilless cultivation, caable of maintaining a specific shape after 3D bio printing, was successfully assessed and confirmed. The addition of humic substances from green compost improved the printability of the alginate gel, thus ensuring the right mechanical proprieties essential for 3D printing, and resulting in well-assembled and easly printable structures. This stabilization of the alginate gel had to be probably accounte to the influence of the humic substances' molecular features on the morphological and rheological properties of polymeric hydrogels. Moreover, the biostimulant activity of humic extracts toward plants development allowed an increased growth of both basil and lettuce seedlings in the bio-composite hydrogel, as compared to the sodium alginate alone. In particular, this plants growth stimulation by the bio-composite appears to be related to the balance between hydrophylic and hydrophobic components in the supramolecular structure of humic substances, that plays a key role in the humic conformational flexibility essential for the expression of their biological activity. Therefore, by simply scaling-up the volume of the shapes to be printed and using the same gel as the raw material of the system, it may be possible to adopt these bio-composites as substrates for soilless cultivation. However, further investigation of the molecular interaction between different humic materials and natural polymeric gels is still needed to better understand the potential innovative applications of humic-hydrogels in Agriculture.

References

Abobatta W (2018) Impact of hydrogel polymer in agricultural sector. Adv Agric Environ Sci Open Access 1:59–64. https://doi.org/10.30881/aaeoa.00011

Campitelli P, Ceppi S (2008) Effects of composting technologies on the chemical and physicochemical properties of humic acids. Geoderma 144:325–333. https://doi.org/10.1016/j.geoderma.2007.12.003

Canellas LP, Dobbss LB, Oliveira AL, et al (2012) Chemical properties of humic matter as related to induction of plant lateral roots. Eur J Soil Sci 63:315–324. https://doi.org/10.1111/j.1365-2389.2012.01439.x

Canellas LP, Olivares FL (2014) Physiological responses to humic substances as plant growth promoter. Chem Biol Technol Agric 1:1–11. https://doi.org/10.1186/2196-5641-1-3

Canellas LP, Olivares FL, Aguiar NO, et al (2015) Humic and fulvic acids as biostimulants in horticulture. Sci Hortic (Amsterdam) 196:15–27. https://doi.org/10.1016/j.scienta.2015.09.013

Cao L, Li N (2021) Activated-carbon-filled agarose hydrogel as a natural medium for seed germination and seedling growth. Int J Biol Macromol 177:383–391. https://doi.org/10.1016/j.ijbiomac.2021.02.097

Capel AJ, Rimington RP, Lewis MP, Christie SDR (2018) 3D printing for chemical, pharmaceutical and biological applications. Nat Rev Chem 2:422–436. https://doi.org/10.1038/s41570-018-0058-y

du Jardin P (2015) Plant biostimulants: Definition, concept, main categories and regulation. Sci Hortic (Amsterdam) 196:3–14. https://doi.org/10.1016/j.scienta.2015.09.021

Elshafie HS, Camele I (2021) Applications of absorbent polymers for sustainable plant protection and crop yield. Sustain 13:. https://doi.org/10.3390/su13063253

Falcone G, Mazzei P, Piccolo A, et al (2022) Advanced printable hydrogels from pre-crosslinked alginate as a new tool in semi solid extrusion 3D printing process. Carbohydr Polym 276:118746. https://doi.org/10.1016/j.carbpol.2021.118746

Fang Y, Al-Assaf S, Phillips GO, et al (2007) Multiple steps and critical behaviors of the binding of calcium to alginate. J Phys Chem B 111:2456–2462. https://doi.org/10.1021/jp0689870

Forget A, Arya N, Randriantsile R, et al (2016) Nonwoven Carboxylated Agarose-Based Fiber Meshes with Antimicrobial Properties. https://doi.org/10.1021/acs.biomac.6b01401

Forget A, Christensen J, Lüdeke S, et al (2013) Polysaccharide hydrogels with tunable stiffness and provasculogenic properties via α-helix to β-sheet switch in secondary structure. Proc Natl Acad Sci U S A 110:12887–12892. https://doi.org/10.1073/pnas.1222880110

Forget A, Staehly C, Ninan N, et al (2017) Oxygen-Releasing Coatings for Improved Tissue

Preservation. https://doi.org/10.1021/acsbiomaterials.7b00297

Guilherme MR, Aouada FA, Fajardo AR, et al (2015) Superabsorbent hydrogels based on polysaccharides for application in agriculture as soil conditioner and nutrient carrier: A review. Eur Polym J 72:365–385. https://doi.org/10.1016/j.eurpolymj.2015.04.017

Hong N, Yang GH, Lee JH, Kim GH (2018) 3D bioprinting and its in vivo applications. J Biomed Mater Res – Part B Appl Biomater 106:444–459. https://doi.org/10.1002/jbm.b.33826

Jannin L, Arkoun M, Ourry A, et al (2012) Microarray analysis of humic acid effects on Brassica napus growth: Involvement of N, C and S metabolisms. Plant Soil 359:297–319. https://doi.org/10.1007/s11104-012-1191-x

Li J, Chen M, Fan X, Zhou H (2016) Recent advances in bioprinting techniques: Approaches, applications and future prospects. J Transl Med 14:1–15. https://doi.org/10.1186/s12967-016-1028-0

Mallakpour S, Azadi E, Hussain CM (2021) State-of-the-art of 3D printing technology of alginate-based hydrogels—An emerging technique for industrial applications. Adv Colloid Interface Sci 293:102436. https://doi.org/10.1016/j.cis.2021.102436

Massa D, Magán JJ, Montesano FF, Tzortzakis N (2020) Minimizing water and nutrient losses from soilless cropping in southern Europe. Agric Water Manag 241:106395. https://doi.org/10.1016/j.agwat.2020.106395

Monda H, Cozzolino V, Vinci G, et al (2017) Molecular characteristics of water-extractable organic matter from different composted biomasses and their effects on seed germination and early growth ofmaize. Sci Total Environ 590–591:40–49. https://doi.org/10.1016/j.scitotenv.2017.03.026

Monda H, Cozzolino V, Vinci G, et al (2018) Molecular composition of the Humeome extracted from different green composts and their biostimulation on early growth of maize. Plant Soil 429:407–424. https://doi.org/10.1007/s11104-018-3642-5

Murphy J, Riley JP (1962) A modified single solution method for the deter- mination of phosphate in natural waters. Anal Chim Acta 27:31–36.

Murphy S V., Atala A (2014) 3D bioprinting of tissues and organs. Nat Biotechnol 32:773–785. https://doi.org/10.1038/nbt.2958

Muscolo A, Cutrupi S, Nardi S (1998) IAA detection in humic substances. Soil Bio Bioch 30:1199–1201.

Nardi S, Muscolo A, Vaccaro S, et al (2007) Relationship between molecular characteristics of soil humic fractions and glycolytic pathway and krebs cycle in maize seedlings. Soil Biol Biochem 39:3138–3146. https://doi.org/10.1016/j.soilbio.2007.07.006

Nebbioso A, Piccolo A (2011) Basis of a humeomics science: Chemical fractionation and molecular characterization of humic biosuprastructures. Biomacromolecules 12:1187–1199. https://doi.org/10.1021/bm101488e

Nuzzo A, Mazzei P, Drosos M, Piccolo A (2020a) Novel Humo-Pectic Hydrogels for Controlled Release of Agroproducts. ACS Sustain Chem Eng 8:10079–10088. https://doi.org/10.1021/acssuschemeng.0c01986

Nuzzo A, Mazzei P, Savy D, et al (2020b) Pectins of Di ff erent Degree of Methyl-Esterification. 1–13

Peers S, Montembault A, Ladavière C (2020) Chitosan hydrogels for sustained drug delivery. J Control Release 326:150–163. https://doi.org/10.1016/j.jconrel.2020.06.012

Piccolo A, Nardi S, Cancheri G (1996) Macro-molecular changes of soil humic substances in- duced by interactions with organic acids. Eur J Soil Sci 47:319–328.

Piccolo A, Conte P, Cozzolino A (1999) Effects of mineral and monocarboxylic acids on the molecular association of dissolved humic substances. Eur J Soil Sci 50:687–694.

Piccolo, A., Cozzolino, A., & Conte, P. (2001). Chromatographic and spectrophotometric properties of dissolved humic substances compared with macro-molecular polymers. *Soil Science* 166, 174–185.

Piccolo A (2002) The supramolecular structure of humic substances: A novel understanding of humus chemistry and implications in soil science. Adv in Agr *75:*57–134. https://doi.org/10.1016/s0065-2113(02)75003-7

Piccolo A, Conte P, Spaccini R, Mbagwu JSC (2005) Influence of land use on the characteristics of humic substances in some tropical soils of Nigeria. Eur J Soil Sci 56:343–352. https://doi.org/10.1111/j.1365-2389.2004.00671.x

Piccolo A., Spaccini R., Drosos M., Vinci G., Cozzolino V. The Molecular Composition of Humus Carbon: Recalcitrance and Reactivity in Soils. In: The Future of Soil Carbon. Its Conservation and Formation. Eds*:* Garcia C., Nannipieri P., Hernandez T. (2018), Elsevier, Amsterdam, pp, 87–124.

Savy D, Brostaux Y, Cozzolino V, et al (2020) Quantitative Structure-Activity Relationship of Humic-Like Biostimulants Derived From Agro-Industrial Byproducts and Energy Crops. Front Plant Sci 11:1–13. https://doi.org/10.3389/fpls.2020.00581

Savy D, Cozzolino V, Nebbioso A, et al (2016) Humic-like bioactivity on emergence and early growth of maize (Zea mays L.) of water-soluble lignins isolated from biomass for energy. Plant Soil 402:221–233. https://doi.org/10.1007/s11104-015-2780-2

Savy D, Cozzolino V, Vinci G, et al (2015) Water-soluble lignins from different bioenergy crops

stimulate the early development of maize (Zea mays, L.). Molecules 20:19958–19970. https://doi.org/10.3390/molecules201119671

Savy D, Mazzei P, Drosos M, et al (2017) Molecular Characterization of Extracts from Biorefinery Wastes and Evaluation of Their Plant Biostimulation. ACS Sustain Chem Eng 5:9023–9031. https://doi.org/10.1021/acssuschemeng.7b01928

Scotti R, Pane C, Spaccini R, et al (2016) On-farm compost: A useful tool to improve soil quality under intensive farming systems. Appl Soil Ecol 107:13–23. https://doi.org/10.1016/j.apsoil.2016.05.004

Selim EM, Ali Mosa A (2012) Fertigation of humic substances improves yield and quality of broccoli and nutrient retention in a sandy soil. J Plant Nutr Soil Sci 175:273–281. https://doi.org/10.1002/jpln.201100062

Sivashankari PR, Prabaharan M (2020) Three-dimensional porous scaffolds based on agarose/chitosan/graphene oxide composite for tissue engineering, Int J Biol Macromol 146 https://doi.org/222–231 10.1016/j.ijbiomac.2019.12.219

Spaccini R, Cozzolino V, Di Meo V, et al (2019) Bioactivity of humic substances and water extracts from compost made by ligno-cellulose wastes from biorefinery. Sci Total Environ 646:792–800. https://doi.org/10.1016/j.scitotenv.2018.07.334

Spaccini R, Piccolo A (2009) Molecular characteristics of humic acids extracted from compost at increasing maturity stages. Soil Biol Biochem 41:1164–1172. https://doi.org/10.1016/j.soilbio.2009.02.026

Tang H, Zhang L, Hu L, Zhang L (2014) Application of Chitin Hydrogels for Seed Germination, Seedling Growth of Rapeseed. J Plant Growth Regul 33:195–201. https://doi.org/10.1007/s00344-013-9361-5

Vancauwenberghe V, Baiye Mfortaw Mbong V, Vanstreels E, et al (2019) 3D printing of plant tissue for innovative food manufacturing: Encapsulation of alive plant cells into pectin based bio-ink. J Food Eng 263:454–464. https://doi.org/10.1016/j.jfoodeng.2017.12.003

Vancauwenberghe V, Katalagarianakis L, Wang Z, et al (2017) Pectin based food-ink formulations for 3-D printing of customizable porous food simulants. Innov Food Sci Emerg Technol 42:138–150. https://doi.org/10.1016/j.ifset.2017.06.011

Vancauwenberghe V, Verboven P, Lammertyn J, Nicolaï B (2018) Development of a coaxial extrusion deposition for 3D printing of customizable pectin-based food simulant. J Food Eng 225:42–52. https://doi.org/10.1016/j.jfoodeng.2018.01.008

Vundavalli R, Vundavalli S, Nakka M, Rao DS (2015) Biodegradable Nano-Hydrogels in Agricultural Farming - Alternative Source For Water Resources. Procedia Mater Sci 10:548–

554. https://doi.org/10.1016/j.mspro.2015.06.005

Yakhin OI, Lubyanov AA, Yakhin IA, Brown PH (2017) Biostimulants in plant science: A global perspective. Front Plant Sci 7:. https://doi.org/10.3389/fpls.2016.02049

Young C, Rekha PD, Lai W, Arun AB (2006) Encapsulation of Plant Growth-Promoting Bacteria in Alginate Beads Enriched With Humic Acid. https://doi.org/10.1002/bit

GENERAL CONCLUSIONS

The challenges associated with the development of sustainable agriculture to replace conventional agronomic practices require the integration of various approaches to provide a truly effective solution for maintaining crop productivity and environmental security. Therefore, this thesis followed different research lines that investigate potential eco-friendly strategies for a sustainable agriculture.

The first research lines focused on the effect of agricultural managements on both soil organic matter (SOM) and organic carbon (SOC). In particular, the molecular dynamics of organic matter in soils subjected to long-term field experiments (20 years) under conventional maize monoculture or maize-leguminous crop rotation were evaluated by both traditional analytical techniques and an innovative chemical sequential fractionation named Humeomics. The application of off-line pyrolysis TMAH-GC-MS (thermochemolysis) and solid-state ^{13}C NMR spectroscopy for the direct molecular characterization of OM components of both the bulk soils and their humic extracts revealed that the long-term cultivation under conventional tillage destabilizes SOM molecular conformation, though to a different extent, as a function of the cropping system (Chapter 3). Actually, 20 consecutive years of maize mono-cultivation led to alteration of the SOM hydrophobic composition, with a decrease in alkyl and aliphatic compounds (e.g. 47.4 % reduction in fatty acids), and an increase in hydrophilic labile components (42.2 %), while the crop-rotated soils showed a partial preservation of the pristine SOM composition by maintaining the content of hydrophobic and lipid constituents (only 1.8 % reduction). These results were further confirmed by the application on the same soil samples of Humeomics chemical fractionation, coupled to characterization of separated fractions by GC-MS and high-resolution Orbitrap LC-MS (Chapter 4). Particularly, Humeomics showed that the ratio of organosoluble to hydrosoluble components dropped significantly passing from untreated to long-term cultivated soils, thus revealing that traditional tillage not only reduced the total OC content of soils but also progressively depleted the hydrophobic components of soil humus and the capacity of

sequestering the labile/hydrophilic molecules. The loss of OC hydrophobic protection due to reduction of lipophilic components (such as long-chain fatty acids) under continuous maize was significantly mitigated in soil cropped with a maize-leguminous rotation, thus confirming at molecular level the long-standing perception of a greater ecological sustainability of crop rotation in respect to monoculture. The Humeomics fractionation enabled not only solubilization and characterization of a significant larger proportion of the soil Humeome than for the traditional single alkaline extraction (eSOM), but also detection of different types of humic molecules when the Humeome complex matrix was unraveled by progressively breaking weakly and strongly bound esters and highly recalcitrant ether linkages. In fact, hydrosoluble nitrogen containing compounds classes, such as amides, amines, and heterocyclic-N were detected in the more recalcitrant AQUs and RESOM fractions of both cropped soils, thus suggesting that some components of soil Humeome are more extractable when the protective complex molecular matrix is progressively altered or removed by the Humeomics fractionation. These N-containing compounds in cropped soils were mainly bound to iron, thereby implying that the formation of organo-mineral complexes represents a mechanism of nitrogen sequestration in agricultural soils. The first lines findings of this thesis hence highlight that a detailed molecular understanding of soil Humeoma is necessary to identify eco-friendly alternatives to conventional agriculture, particularly the Humeomics technique could be an innovative tool for new environmentally sustainable technologies in agriculture.

The second lines of this research involved the investigation on the combination of humic biostimulants with microbial bioeffectors as potential strategy to stimulate plant growth while concomitantly ensuring high levels of agricultural productivity and environmental security. To this purpose, the bioactivity of two different humic materials, a potassium humate from leonardite (KH) and compost tea (CT) from a green compost made of coffee husks, and their combination (1:1), was evaluated toward basil seeds germination and maize early growth (Chapter 5). After their thorough chemical and molecular characterization, a relation between structure and bioactivity was also investigated. The results of this experiment showed that the high polar CT stimulated both the epicotyl

and root development of basil seeds, while the mostly hydrophobic KH exerted a significant bioactivity on maize early growth. On the other hand, the application of a mixed solution of both humic materials to hydroponically grown maize plantlets resulted in a biostimulant effect similar to KH but greater than the individual CT treatment. This suggests that polar molecules derived from the aerobic transformation of cellular materials during composting stimulate plant growth, and that the hydrophobicity of geochemical humic matter is an important factor for plant biostimulation, since it provides molecular adhesion to plant roots, and, depending on the correct conformational stability of the humic assembly, it enables a slow and effective release of bioactive molecules. Actually, the molecular characterization of the humic materials allowed to explain the observed results by a cage effect of the readily bioavailable CT compounds, such as oxidized lignin fragments, saccharides, and peptides within the hydrophobic domains of the mainly apolar KH. These findings hence indicate that a calibrated mixture of humic materials of selected molecular composition may represent an innovative and ecologically viable method to build up sustainable products with diverse mechanisms of plant biostimulation. Moreover, in a second experiment the bioactivity of the same mixed humic biostimulants was investigated in synergy with microbial bioeffectors (Micosat TABPLUS, M+) on lettuce productivity, nutritional status and metabolism (Chapter 6). The synergistic interaction between KH, CT and M+ significantly increased lettuce biomass production and uptake of both macro- and micronutrients compared to their individual application. This humic-microbial combination (MIX_M+) also resulted in the highest effect on lettuce primary metabolism. In particular, the GC-MS analysis of leaves metabolites showed that MIX_M+ treatment stimulated the accumulation of essential amino acids such as glutamine, GABA, glutamic and aspartic acid, as well as the production of saccharides, mainly fructose, glucose and galactose. These results suggest a potential role of humic biostimulants in supporting the survival of beneficial microorganisms in the soil environment, as well as in promoting their colonization capacity, thereby improving their biological effect on plants health and development. Furthermore, the evaluation of lettuce secondary metabolism by UHPLC-MS-IT-TOF analysis in the same experiment revealed the effectiveness of

this technique for the study of polyphenolic compounds. Particularly, a significant increase leaf content of both cinnamic acid derivatives and flavonoids such as luteolin and quercetin glycosylates were detected in plants treated with the mixed humic materials compared to all other biostimulants. These outcomes further support that the cage effect of bioavailable CT compounds in the hydrophobic components of KH may has enhanced the conformational stability of the humic assembly essential for the release of bioactive molecules, thus increasing the biostimulant activity of the mixture than the individual application of the two humic material. Therefore, the findings of the second research lines of this thesis indicate that a calibrate mixture of humic extracts, containing different type of bioactive molecules, in combination with microbial consortia is a potential tool to tailor plants biostimulants for specific agronomic and industrial uses, as well as for the development of novel functional foods.

Finally, the third line of this doctoral research was to investigate the possible applications of innovative hydrogels based on humic matter from green compost to improve plant growth. The potential use of a hydrogel containing sodium alginate and humic extracts from green compost cross-linked by calcium nitrate and able of maintaining shape after 3D bio printing, as a substrate for soilless cultivation was explored. (Chapter 7). The preliminary results of this experimentation showed that the addiction of humic substances improved the printability of the alginate gel, ensuring the right mechanical proprieties essential for 3D printing, and thus resulting in well-assembled and easly printable structures. This stabilization of the alginate gel probably derived from the influence by the humic substances molecular features on morphological and rheological properties of polymeric hydrogels. Furthermore, the biostimulant activity of humic extracts toward plants development allowed an increased growth of both basil and lettuce seedlings in the hydrogel bio-composite compared to the sodium alginate alone. This stimulation of plants growth by the bio-composite appears to be releated to the balance between hydrophylic and hydrophobic components in the supramolecular structure of humic substances, which play a key role in the humic conformational flexibility essential for the expression of their biological activity. Therefore, by simply scaling-up the

volume of the shapes to be printed and using the same gel as the raw material of the system, it may be possible to adopt these bio-composites as substrates for soilless cultivation. The prelimiary findidings of the last reasearch line of this thesis may indicate that humic-hydrogels could be innovative biomaterials for several agricultural applications.

REFERENCES

Abd-Allah, E.F., Hashem, A., Alqarawi, A.A., Bahkali, A.H., & Alwhibi, M.S. (2015). Enhancing growth performance and systemic acquired resistance of medicinal plant Sesbania sesban (L.) Merr using arbuscular mycorrhizal fungi under salt stress. *Saudi Journal of Biological Science* 22, 274–283.

Abobatta, W. (2018). Impact of hydrogel polymer in agricultural sector. *Advances in Agriculture and Environmental Science: Open Access (AAEOA)*, *1*(2), 59–64. https://doi.org/10.30881/aaeoa.00011

Abou-el-hassan, S., & El-batran, H. S. (2020). Integration of Some Bio Compounds with Compost Tea to Produce Sweet Corn without Mineral Fertilizers. *Middle East Journal of Agriculture Research*, 645–652. https://doi.org/10.36632/mejar/2020.9.3.51

Ait-El-Mokhtar, M., Baslam, M., Ben-Laouane, R., Anli, M., Boutasknit, A., Mitsui, T., Wahbi, S., & Meddich, A. (2020). Alleviation of Detrimental Effects of Salt Stress on Date Palm (Phoenix dactylifera L.) by the Application of Arbuscular Mycorrhizal Fungi and/or Compost. *Frontiers in Sustainable Food Systems* 4, 1–19. https://doi.org/10.3389/fsufs.2020.00131

Álvaro-Fuentes, J., López, M.V., Cantero-Martinez, C., & Arrúe, J.L. (2008). Tillage effects on soil organic carbon fractions in mediterranean dryland agroecosystems. *Soil Science Society of American Journal* 72, 541. http://dx.doi.org/10.2136/sssaj2007.0164

Agnolucci, M., Avio, L., Pepe, A., Turrini, A., Cristani, C., Bonini, P., Cirino, V., Colosimo, F., Ruzzi, M., & Giovannetti, M. (2019). Bacteria associated with a commercial mycorrhizal inoculum: Community composition and multifunctional activity as assessed by illumina sequencing and culture-dependent tools. *Frontiers in Plant Science* 9, 1–13. https://doi.org/10.3389/fpls.2018.01956

Aguiar, N O, Novotny, E. H., Oliveira, A. L., Rumjanek, V. M., Olivares, F. L., & Canellas, L. P. (2013). Prediction of humic acids bioactivity using spectroscopy and multivariate analysis. *Journal of Geochemical Exploration*, *129*, 95–102. https://doi.org/10.1016/j.gexplo.2012.10.005

Aguiar, Natalia O, Olivares, F. L., & Novotny, E. H. (2018). *Changes in metabolic profiling of sugarcane leaves induced by endophytic diazotrophic bacteria and humic acids*. 1–28. https://doi.org/10.7717/peerj.5445

Aguirre, E., Leménager, D., Bacaicoa, E., Fuentes, M., Baigorri, R., Zamarreno, A.M., & García-Mina, J.M. (2009). The root application of a purified leonardite humic acid modifies the transcriptional regulation of the main physiological root responses to Fe deficiency in Fe-sufficient cucumber plants. *Plant Physiology and Biochemistry* 47, 215–223.

Andreux, F. (1996). Humus in world soils in: Humic substances in terrestrial ecosystems. Piccolo A. ed., Elsevier, Amsterdam, pp. 45-100.

Apel, K., & Hirt, H. (2004). Reactive oxygen species: metabolism, oxidative stress, and signal transduction. *Annual Review of Plant Biology* 55, 373–399.

Azevedo, R.A., & Lea, P.J. (2011). Research on abiotic and biotic stress—what next? *Annals of Applied Biology* 159, 317–319.

Backer, R., Rokem, J. S., Ilangumaran, G., Lamont, J., Praslickova, D., Ricci, E., Subramanian, S., & Smith, D. L. (2018). Plant growth-promoting rhizobacteria: Context, mechanisms of action, and roadmap to commercialization of biostimulants for sustainable agriculture. *Frontiers in Plant Science*, *871*(October), 1–17. https://doi.org/10.3389/fpls.2018.01473

Bai, Z., Caspari, T., Gonzalez, M. R., Batjes, N. H., Mäder, P., Bünemann, E. K., de Goede, R., Brussaard, L., Xu, M., Ferreira, C. S. S., Reintam, E., Fan, H., Mihelič, R., Glavan, M., & Tóth, Z. (2018). Effects of agricultural management practices on soil quality: A review of long-term experiments for Europe and China. *Agriculture, Ecosystems and Environment*, *265*(May), 1–7. https://doi.org/10.1016/j.agee.2018.05.028

Balota, E.L., Colozzi-Filho, A., Andrade, D.S., & Dick, R.P. (2003). Microbial biomass in soils under and crop rotation systems. *Biology and Fertility of Soils* 38, 15–20.

Bargaz, A., Lyamlouli, K., Chtouki, M., Zeroual, Y., & Dhiba, D. (2018). Soil Microbial Resources for Improving Fertilizers Efficiency in an Integrated Plant Nutrient Management System Soil Microbial Resources for Improving Fertilizers Efficiency in an Integrated plant nutrient management system. *Frontiers in Microbiology* 2018, 9, 1606. https://doi.org/10.3389/fmicb.2018.01606

Barthes, B., & Roose, E. (2002). Aggregate stability as an indicator of soil susceptibility to runoff and erosion validation at several levels. *Catena* 47, 133-149.

Battacharyya, D., Babgohari, M. Z., Rathor, P., & Prithiviraj, B. (2015). Seaweed extracts as biostimulants in horticulture. *Science Horticulture* 196, 39–48. doi: 10.1016/j. scienta.2015.09.012

Bashan, Y., Hernandez, J. P., Leyva, L. A., & Bacilio, M. (2002). Alginate microbeads as inoculant carriers for plant growth-promoting bacteria. *Biology and Fertility of Soils*, *35*(5), 359–368. https://doi.org/10.1007/s00374-002-0481-5

Bashan, Y., De-Bashan, L. E., Prabhu, S. R., & Hernandez, J. P. (2014). Advances in plant growth-promoting bacterial inoculant technology: formulations and practical perspectives (1998–2013). *Plant and Soil* 378, 1–33.

Beare, M. H. (1997). Fungal and bacterial pathways of organic matter decomposition and nitrogen mineralization in arable soil. Pp 37–70. En: Brussaard, L. and R. Ferrera- Cerrato (Eds). *Soil Ecology in Sustainable Agricultural Systems*. Lewis Publishers, Boca Raton, LA.

Benlhabib, O., Yazar, A., Qadir, M., Lourenço, E., & Jacobsen, S.E. (2014). How can we improve mediterranean cropping systems? *Journal of Agronomy and Crop* Science 200, 325–332. http://dx.doi.org/10.1111/jac.12066

Bharti, N., Barnawal, D., Wasnik, K., Tewari, S.K., & Kalra, A. (2016). Co-inoculation of Dietzia natronolimnaea and Glomus intraradices with vermicompost positively influences Ocimum basilicum growth and resident microbial community structure in salt affected low fertility soils. *Applied Soil Ecology* 100, 211–225.

Bitterlich, M., Rouphael, Y., Graefe, J., & Franken, P. (2018). Arbuscular mycorrhizas: a promising component of plant production systems provided favorable conditions for their growth. *Frontiers in Plant Science*, *9*(September), 1–6. https://doi.org/10.3389/fpls.2018.01329

Bradáčová, K., Florea, A. S., Bar-Tal, A., Minz, D., Yermiyahu, U., Shawahna, R., Kraut-Cohen, J.,

Zolti, A., Erel, R., Dietel, K., Weinmann, M., Zimmermann, B., Berger, N., Ludewig, U., Neumann, G., & Poşta, G. (2019). Microbial Consortia versus Single-Strain Inoculants: An advantage in PGPM-assisted tomato production? *Agronomy*, *9*(2). https://doi.org/10.3390/agronomy9020105

Brenda, S., Di, F., Moreno-gav, A., Gea, F. J., & Santos, M. (2020). *Role of Trichoderma aggressivum f . europaeum as Plant-Growth Promoter in Horticulture*. 1–15.

Bulgari, R., Cocetta, G., Trivellini, A., Vernieri, P., & Ferrante, A. (2015). Biostimulants and crop responses: a review. *Biological Agriculture &* Horticulture 31, 1-17. doi: 10.1080/01448765.2014.964649

Cambardella, C.A., & Elliot, E.T. (1992). Particulate soil organic matter changes across a grassland cultivation sequence. *Soil Science Society of American Journal* 56, 777-783.

Canellas, Luciano Pasqualoto, Olivares, F. L., Okorokova-Façanha, A. L., & Façanha, A. R. (2002). Humic acids isolated from earthworm compost enhance root elongation, lateral root emergence, and plasma membrane H+-ATPase activity in maize roots. *Plant Physiology*, *130*(4), 1951–1957. https://doi.org/10.1104/pp.007088

Canellas, L. P., Teixeira, L. R. L., Dobbss, L. B., Silva, C. A., Medici, L. O., Zandonadi, D. B., & Façanha, A. R. (2008). Humic acids crossinteractions with root and organic acids. *Annals of Applied Biology*, *153*(2), 157–166. https://doi.org/10.1111/j.1744-7348.2008.00249.x

Canellas, L.P., Piccolo, A., Dobbss, L.B., Spaccini, R., Olivares, F.L., Zandonadi, D.B., & Facanha, A.R. (2010) Chemical composition and bioactivity properties of size-fractions separated from a vermicompost humic acid. *Chemosphere* 78, 457–466.

Canellas, L.P., Dobbss, L.B., Oliveira, A.L., Chagas, J.G., Aguiar, N.O., Rumjanek, V.M., Novotny, E.H., Olivares, F.L., Spaccini, R., & Piccolo, A. (2012). Chemical properties of humic matter as related to induction of plant lateral roots. *European Journal of Soil Science* 63, 315–324.

Canellas, L.P., Martínez-Balmori, D., Médici, L.O., Aguiar, N.O., Campostrini, E., Rosa, R.C., Façanha, A., & Olivares, F.L. (2013). A combination of humic substances and Herbaspirillum seropedicae inoculation enhances the growth of maize (Zea mays L.). *Plant and Soil* 366, 119–32.

Canellas, Luciano P., & Olivares, F. L. (2014). Physiological responses to humic substances as plant growth promoter. *Chemical and Biological Technologies in Agriculture*, *1*(1), 1–11. https://doi.org/10.1186/2196-5641-1-3

Canellas, Luciano P., Olivares, F. L., Aguiar, N. O., Jones, D. L., Nebbioso, A., Mazzei, P., & Piccolo, A. (2015a). Humic and fulvic acids as biostimulants in horticulture. *Scientia Horticulturae*, *196*, 15–27. https://doi.org/10.1016/j.scienta.2015.09.013

Canellas, L.P., Silva, S.F., Olk, D., & Olivares, F.L. (2015b). Foliar application of Herbaspirillum seropedicae and humic acid increase maize yields. *Journal of Food Agriculture and* Environment 13, 146–53.

Canellas, Luciano Pasqualoto, & Olivares, F. L. (2017). Production of border cells and colonization of maize root tips by Herbaspirillum seropedicae are modulated by humic acid. *Plant and Soil*, *417*(1–2), 403–413. https://doi.org/10.1007/s11104-017-3267-0

Canellas, N. O. A., Olivares, F. L., & Canellas, L. P. (2019). Metabolite fingerprints of maize and sugarcane seedlings: searching for markers after inoculation with plant growth-promoting bacteria in humic acids. *Chemical and Biological Technologies in Agriculture*, *6*(1), 1–10. https://doi.org/10.1186/s40538-019-0153-4

Cao, L., & Li, N. (2021). Activated-carbon-filled agarose hydrogel as a natural medium for seed germination and seedling growth. *International Journal of Biological Macromolecules*, *177*, 383–391. https://doi.org/10.1016/j.ijbiomac.2021.02.097

Carletti, P., Masi, A., Spolaore, B., Polverino De Laureto, P., De Zorzi, M,, Turetta, L., Ferretti, M., & Nardi, S. (2008). Protein expression changes in maize roots in response to humic substances. *Journal of Chemical Ecology* 34, 804–818.

Carranca, C., Oliveira, A., Pampulha, E., & Torres, M.O. (2009). Temporal dynamics of soil nitrogen, carbon and microbial activity in conservative and disturbed fields amended with mature white lupine and oat residues. *Geoderma* 151, 50–59. http://dx.doi.org/10.1016/j.geoderma.2009.03.012

Castiglione, A.M., Mannino, G., Contartese, V., Bertea, C.M., & Ertani, A. (2021). Microbial Biostimulants as Response to Modern Agriculture Needs: Composition, Role and Application of These Innovative Products. *Plants* 10, 1533. https://doi.org/10.3390/ plants10081533

Chandra, D., Srivastava, R., Glick, B.R., & Sharma, A.K. (2018) Drought-Tolerant Pseudomonas spp. Improve the Growth Perfor- mance of Finger Millet (Eleusine coracana (L.) Gaertn) under Non-Stressed and Drought-Stressed Conditions. *Pedosphere* 28, 227–240.

Chiappero, J., del Rosario Cappellari, L., Alderete, L.G.S., Palermo, T.B., & Banchio, E. (2019). Plant growth promoting rhizobacteria improve the antioxidant status in Mentha piperita grown under drought stress leading to an enhancement of plant growth and total phenolic content. *Industrial Crops and Products* 139, 111553. https://doi.org/10.1016/j.indcrop.2019.111553

Celik, I. (2005). Land-use effects on organic matter and physical properties of soil in a southern Mediterranean highland of Turkey. *83*, 270–277. https://doi.org/10.1016/j.still.2004.08.001

Cely, M.V.T., Siviero, M.A., Emiliano, J., Spago, F.R., Freitas, V.F., Barazetti, A.R., Goya, E.T., Lamberti, G.D.S., Dos Santos, I.M.O., & De Oliveira, A.G. (2016). Inoculation of Schizolobium parahyba with mycorrhizal fungi and plant growth-promoting rhizobacteria increases wood yield under field conditions. *Frontiers in Plant Science* 7, 1708.

Cocetta, G., Passera, A., Vacchini, V., Shahzad, G. i. R., Cortellino, G., Picchi, V., Ferrante, A., Casati, P., & Piazza, L. (2021). Use of microbial inoculants during cultivation maintain the physiological, nutritional and technological quality of fresh-cut romaine lettuce. *Postharvest Biology and Technology*, *175*(November 2020), 111411. https://doi.org/10.1016/j.postharvbio.2020.111411

Colla, G., Nardi, S., Cardarelli, M., Ertani, A., Lucini, L., Canaguier, R., & Rouphael, Y. (2015a). Protein hydrolysates as biostimulants in horticulture. *Scientia Horticulturae*, *196*, 28–38. https://doi.org/10.1016/j.scienta.2015.08.037

Colla, G., Rouphael, Y., Di Mattia, E., El-Nakhel, C., & Cardarelli, M. (2015b). Co-inoculation of Glomus intraradices and Trichoderma atroviride acts as a biostimulant to promote growth, yield and nutrient uptake of vegetable crops. *Journal of the Science of Food and Agriculture*, *95*(8),

1706–1715. https://doi.org/10.1002/jsfa.6875

Colla, G., Hoagland, L., Ruzzi, M., Cardarelli, M., Bonini, P., Canaguier, R., & Rouphael, Y. (2017). Biostimulant action of protein hydrolysates: Unraveling their effects on plant physiology and microbiome. *Frontiers in Plant Science*, *8*(December), 1–14. https://doi.org/10.3389/fpls.2017.02202

Conselvan, G. B., Pizzeghello, D., Francioso, O., Di Foggia, M., Nardi, S., & Carletti, P. (2017). Biostimulant activity of humic substances extracted from leonardites. *Plant and Soil*, *420*(1–2), 119–134. https://doi.org/10.1007/s11104-017-3373-z

Conte, P., Spaccini, R., & Piccolo, A. (2004). State of the art of CPMAS 13C-NMR spectroscopy applied to natural organic matter. *Progress in Nuclear Magnetic Resonance Spectroscopy*. https://doi.org/10.1016/j.pnmrs.2004.02.002

Cozzolino, V., Di Meo, V., & Piccolo, A. (2013). Impact of arbuscular mycorrhizal fungi applications on maize production and soil phosphorus availability. *Journal of Geochemical Exploration*, *129*, 40–44. https://doi.org/10.1016/j.gexplo.2013.02.006

Cozzolino, V., Di Meo, V., Monda, H., Spaccini, R., & Piccolo, A. (2016). The molecular characteristics of compost affect plant growth, arbuscular mycorrhizal fungi, and soil microbial community composition. *Biology and Fertility of Soils*, *52*(1), 15–29. https://doi.org/10.1007/s00374-015-1046-8

Cozzolino, V., Savy, D., Piccolo, A., Monda, H., Vinci, G., & Drosos, M. (2018). Molecular composition of the Humeome extracted from different green composts and their biostimulation on early growth of maize. *Plant and Soil*, *429*(1–2), 407–424. https://doi.org/10.1007/s11104-018-3642-5

Cozzolino, V., Monda, H., Savy, D., Di Meo, V., Vinci, G., & Smalla, K. (2021). Cooperation among phosphate-solubilizing bacteria, humic acids and arbuscular mycorrhizal fungi induces soil microbiome shifts and enhances plant nutrient uptake. *Chemical and Biological Technologies in Agriculture*, *8*(1), 1–19. https://doi.org/10.1186/s40538-021-00230-x

de Aquino, A. M., Canellas, L. P., da Silva, A. P. S., Canellas, N. O., da S Lima, L., Olivares, F. L., Piccolo, A., & Spaccini, R. (2019). Evaluation of molecular properties of humic acids from vermicompost by 13 C-CPMAS-NMR spectroscopy and thermochemolysis–GC–MS. *Journal of Analytical and Applied Pyrolysis*, *141*(January), 104634. https://doi.org/10.1016/j.jaap.2019.104634

De Pascale, S., Rouphael, Y., & Colla, G. (2017). Plant biostimulants: Innovative tool for enhancing plant nutrition in organic farming. *European Journal of Horticultural Science*, *82*(6), 277–285. https://doi.org/10.17660/eJHS.2017/82.6.2

Diagne, N., Ndour, M., Djighaly, P.I., Ngom, D., Ngom, M.C.N., Ndong, G., Svistoonoff, S., & Cherif-Silini, H. (2020). Effect of Plant Growth Promoting Rhizobacteria (PGPR) and Arbuscular Mycorrhizal Fungi (AMF) on Salt Stress Tolerance of Casuarina obesa (Miq.). *Frontiers in Sustainable Food Systems* 4, 1–8. https://doi.org/10.3389/fsufs.2020.601004

Drążkiewicz, M. (1994). Distribution of microorganisms in soil aggregates: Effect of aggregate size. *Folia Microbioliologica* 39, 276–282. https://doi.org/10.1007/BF02814312

Drosos, M., Nebbioso, A., Mazzei, P., Vinci, G., Spaccini, R., & Piccolo, A. (2017). A molecular zoom into soil Humeome by a direct sequential chemical fractionation of soil. *Science of the Total Environment*, *586*, 807–816. https://doi.org/10.1016/j.scitotenv.2017.02.059

Drosos, M., & Piccolo, A. (2018). The molecular dynamics of soil humus as a function of tillage. *Land Degradation and Development*, *29*(6), 1792–1805. https://doi.org/10.1002/ldr.2989

Drosos, M., Vinci, G., Spaccini, R., & Piccolo, A. (2020). Molecular dynamics of organic matter in a tilled soil under short term wheat cultivation. *Soil and Tillage Research*, *196*(November 2019), 104448. https://doi.org/10.1016/j.still.2019.104448

Duer, M. J. (2002). Solid-state NMR spectroscopy. 1st ed, Blackwell Science, Oxford. https://doi.org/10.1039/b618332h

Du jardin, P. (2012). *Plant_Biostimulants_final_report_bio_2012_en.pdf* (p. 5).

du Jardin, P. (2015). Plant biostimulants: Definition, concept, main categories and regulation. *Scientia Horticulturae*, *196*, 3–14. https://doi.org/10.1016/j.scienta.2015.09.021

Elshafie, H. S., & Camele, I. (2021). Applications of absorbent polymers for sustainable plant protection and crop yield. *Sustainability (Switzerland)*, *13*(6). https://doi.org/10.3390/su13063253

Ekin, Z. (2019). Integrated use of humic acid and plant growth promoting rhizobacteria to ensure higher potato productivity in sustainable agriculture. *Sustainability (Switzerland)*, *11*(12). https://doi.org/10.3390/su10023417

Ertani, A., Cavani, L., Pizzeghello, D., Brandellero, E., Altissimo, A., Ciavatta, C., & Nardi, S. (2009). Biostimulant activities of two protein hydrolysates on the growth and nitrogen metabolism in maize seedlings. *Journal of Plant Nutrition and Soil Science* 172, 237–244.

Ertani, A., Francioso, O., Tugnoli, V., Righi, V., & Nardi, S. (2011). Effect of commercial lignosulfonate-humate on Zea mays L. metabolism. *Journal of Agricultural and Food Chemistry*, *59*(22), 11940–11948. https://doi.org/10.1021/jf202473e

Ertani, A., Nardi, S., Francioso, O., Pizzeghello, D., Tinti, A., & Schiavon, M. (2019). Metabolite targeted analysis and physiological traits of zea mays L. In response to application of a leonardite-humate and lignosulfonate-based products for their evaluation as potential biostimulants. *Agronomy*, *9*(8), 1–18. https://doi.org/10.3390/agronomy9080445

Eudoxie, G., & Martin, M. (2019). Compost tea quality and fertility. In: Organic Fertilizers – History Production and Applications. Marcelo Larramendy and Sonia Soloneski IntechOpen. https://doi.org/10.5772/ intechopen.86877

EU. (2019). Regulation of the European parliament and of the council laying down rules on the making available on the market of EU fertilising products and amending Regulations (EC) No 1069/2009 and (EC) No 1107/2009 and repealing Regulation (EC) No 2003/2003. https://eur-lex.europa.eu/legal- content/EN/TXT/?uri=OJ:L:2019:170:TOC

Fiorentino, N., Ventorino, V., Woo, S. L., Pepe, O., Rosa, A. De, Gioia, L., Romano, I., Lombardi, N., Napolitano, M., Colla, G., Rouphael, Y., & Elia, A. (2018). *Trichoderma -Based Biostimulants Modulate Rhizosphere Microbial Populations and Improve N Uptake Efficiency , Yield , and Nutritional Quality of Leafy Vegetables*. *9*(June), 1–15.

https://doi.org/10.3389/fpls.2018.00743

Forget, A., Christensen, J., Lüdeke, S., Kohler, E., Tobias, S., Matloubi, M., Thomann, R., & Prasad, V. S. (2013). Polysaccharide hydrogels with tunable stiffness and provasculogenic properties via α-helix to β-sheet switch in secondary structure. *Proceedings of the National Academy of Sciences of the United States of America*, *110*(32), 12887–12892. https://doi.org/10.1073/pnas.1222880110

Forget, A., Arya, N., Randriantsile, R., Miessmer, F., Buck, M., Ahmadi, V., Jonas, D., Blencowe, A., & Shastri, V. P. (2016). *Nonwoven Carboxylated Agarose-Based Fiber Meshes with Antimicrobial Properties*. https://doi.org/10.1021/acs.biomac.6b01401

Forget, A., Staehly, C., Ninan, N., Harding, F. J., Vasilev, K., Voelcker, N. H., & Blencowe, A. (2017). *Oxygen-Releasing Coatings for Improved Tissue Preservation*. https://doi.org/10.1021/acsbiomaterials.7b00297

Forte, A., Riondino, M., Fierro, A., Virzo, A., Fagnano, M., Fiorentino, N., Spaccini, R., Piccolo, A., Bertora, C., Alluvione, F., Zavattaro, L., Curtaz, A., Mendes da Silva, W., Grignani, C., (2009). GHGs-saving effects of minimum tillage, green manure and compost application on maize cropped soils in Northern and Southern Italy. In: Grignani, C., Acutis, M., Zavattaro, L., Bechini, L., Bertora, C., Marino Gallina, P., Sacco, D. (Eds.), Connecting different scales of N use in agriculture. Proceed. 16th Nitrogen workshop, Turin, Italy, pp. 155–156 (ISBN978-88-902754-2-5).

Garcia-Gil, J.C., Plaza, C., Soler-Rovira, P., & Polo, A. (2000). Long-term effects of municipal solid waste compost application on soil enzyme activities and microbial biomass. *Soil Biology and Biochemistry* 32, 1907–1913.

García, A.C., Santos, L.A., Izquierdo, F.G, Sperandio, M.V.L., Castro, R.N., & Berbara, R.L.L. (2012). Vermicompost humic acids as an ecological pathway to protect rice plant against oxidative stress. *Ecological Engineering* 47, 203–208. doi:10.1016/j.ecoleng.2012.06.011

García, A. C., Santos, L. A., de Souza, L. G. A., Tavares, O. C. H., Zonta, E., Gomes, E. T. M., García-Mina, J. M., & Berbara, R. L. L. (2016). Vermicompost humic acids modulate the accumulation and metabolism of ROS in rice plants. *Journal of Plant Physiology*, *192*, 56–63. https://doi.org/10.1016/j.jplph.2016.01.008

García, A. C., van Tol de Castro, T. A., Santos, L. A., Tavares, O. C. H., Castro, R. N., Berbara, R. L. L., & García-Mina, J. M. (2019). Structure-Property-Function Relationship of Humic Substances in Modulating the Root Growth of Plants: A Review. *Journal of Environmental Quality*, *48*(6), 1622–1632. https://doi.org/10.2134/jeq2019.01.0027

Giovannini, L., Palla, M., Agnolucci, M., Avio, L., Sbrana, C., Turrini, A., & Giovannetti, M. (2020). Arbuscular mycorrhizal fungi and associated microbiota as plant biostimulants: Research strategies for the selection of the best performing inocula. *Agronomy*, *10*(1). https://doi.org/10.3390/agronomy10010108

Gosh, K., & Schnitzer, M. (1980). Macromolecular structures of humic substances. *Soil Science* 129, 266-276.

Guilherme, M. R., Aouada, F. A., Fajardo, A. R., Martins, A. F., Paulino, A. T., Davi, M. F. T., Rubira, A. F., & Muniz, E. C. (2015). Superabsorbent hydrogels based on polysaccharides for application in agriculture as soil conditioner and nutrient carrier: A review. *European Polymer Journal*, *72*, 365–385. https://doi.org/10.1016/j.eurpolymj.2015.04.017

Guignard, C., Lemée, L., & Amblès, A. (2005). Lipid constituents of peat humic acids and humin. Distinction from directly extractable bitumen components using TMAH and TEAAc thermochemolysis. *Organic Geochemistry*, *36*(2), 287–297. https://doi.org/10.1016/j.orggeochem.2004.07.016

Hager, A. (2003). Role of the plasma membrane H+-ATPase in auxin-induced elongation growth: historical and new aspects. *Journal of Plant Research* 116, 483–505.

Haghighi, M., & Teixeira Da Silva, J. A. (2013). Amendment of hydroponic nutrient solution with humic acid and glutamic acid in tomato (Lycopersicon esculentum Mill.) culture. *Soil Science and Plant Nutrition*, *59*(4), 642–648. https://doi.org/10.1080/00380768.2013.809599

Hayes, M. H. B., & Swift, R. S. (1978). The chemistry of soil organic colloids in: The chemistry of soil constituents. Greenland & Hayes ed., pp. 179-320.

Hashem, A., Alqarawi, A.A., Radhakrishnan, R., Al-Arjani, A.B.F., & Aldehaish, H.A. (2018). Egamberdieva, D.; Abd Allah, E.F. Arbuscular mycorrhizal fungi regulate the oxidative system, hormones and ionic equilibrium to trigger salt stress tolerance in Cucumis sativus L. *Saudi Journal of Biological Science* 25, 1102–1114.

Hii, Y.S., Yen San, C., Lau, S.W., & Danquah, M.K. (2020). Isolation and characterisation of phosphate solubilizing microorganisms from peat. *Biocatalysis and Agricultural Biotechnology*, 26, 101643. https://doi.org/10.1016/j.bcab.2020.101643

Huang, X.F., Zhou, D., Guo, J., Manter, D.K., Reardon, K.F., & Vivanco, J.M. (2015). Bacillus spp.: From rainforest soil promote plant growth under limited nitrogen conditions. *Journal of Applied Microbiology* 118, 672–684. https://doi.org/10.1111/jam.12720

Huertas Tavares, O. C., Santos, L. A., Lima de Araújo, O. J., Coelho Bucher, C. P., García, A. C., Arruda, L. N., Regina de Souza, S., & Fernandes, M. S. (2019). Humic acid as a biotechnological alternative to increase N-NO3- or N-NH4+ uptake in rice plants. *Biocatalysis and Agricultural Biotechnology*, *20*(February), 101226. https://doi.org/10.1016/j.bcab.2019.101226

Hüttermann, A., Orikiriza, L.J.B., & Agaba, H. (2009). Application of superabsorbent polymers for improving the ecological chemistry of degraded or polluted Lands. *Clean Soil Air Water* 37, 517–526.

Ibraheim, S., Ali, A. S., & Bardisi, E. (2020). Effect of Compost Tea and some Nutrient Supplements on Growth and Yield of Two Potato Cultivars. *Journal of Plant Production*, *11*(11), 1055–1062. https://doi.org/10.21608/jpp.2020.122664

Insam, H. (1996). Microorganisms and humus in soils in: Humic substances in terrestrial ecosystems. Piccolo A. ed., Elsevier, Amsterdam, pp. 265-296.

Jannin, L., Arkoun, M., Ourry, A., Laîné, P., Goux, D., Garnica, M., Fuentes, M., Francisco, S. S., Baigorri, R., Cruz, F., Houdusse, F., Garcia-Mina, J. M., Yvin, J. C., & Etienne, P. (2012). Microarray analysis of humic acid effects on Brassica napus growth: Involvement of N, C and S metabolisms. *Plant and Soil*, *359*(1–2), 297–319. https://doi.org/10.1007/s11104-012-1191-x

Jindo, K., Martim, S. A., Navarro, E. C., Pérez-Alfocea, F., Hernandez, T., Garcia, C., Aguiar, N. O., & Canellas, L. P. (2012). Root growth promotion by humic acids from composted and non-composted urban organic wastes. *Plant and Soil*, *353*(1–2), 209–220. https://doi.org/10.1007/s11104-011-1024-3

Jindo, K., Soares, T. S., Peres, L. E. P., Azevedo, I. G., Aguiar, N. O., Mazzei, P., Spaccini, R., Piccolo, A., Olivares, F. L., & Canellas, L. P. (2016). Phosphorus speciation and high-affinity transporters are influenced by humic substances. *Journal of Plant Nutrition and Soil Science*, *179*(2), 206–214. https://doi.org/10.1002/jpln.201500228

Kang, S.M., Khan, A.L., Waqas, M., You, Y.H., Kim, J.H., Kim, J.G., Hamayun, M., & Lee, J. (2014). Plant growth-promoting rhizobacteria reduce adverse effects of salinity and osmotic stress by regulating phytohormones and antioxidants in Cucumis sativus. *Journal of Plant Interaction* 9, 673–682.

Kladivko, J.E. (2001). Tillage systems and soil ecology. *Soil Tillage Research* 61, 61–76.

Koné, S. B., Dionne, A., Tweddell, R. J., Antoun, H., & Avis, T. J. (2010). Suppressive effect of non-aerated compost teas on foliar fungal pathogens of tomato. *Biological Control*, *52*(2), 167–173. https://doi.org/10.1016/j.biocontrol.2009.10.018

Kour, D., Rana, K.L., Yadav, A.N., Yadav, N., Kumar, M., Kumar, V., & Vyas, P. (2020). Dhaliwal, H.S.; Saxena, A.K. Microbial biofertilizers: Bioresources and eco-friendly technologies for agricultural and environmental sustainability. *Biocatalysis and Agricultural Biotechnology*, 23, 101487. https://doi.org/10.1016/j.bcab.2019.101487

Kumar, D., & Singh, A. P. (2017). Efficacy of Potassium Humate and Chemical Fertilizers on Yield and Nutrient Availability Patterns in Soil at Different Growth Stages of Rice. *Communications in Soil Science and Plant Analysis*, *48*(3), 245–261. https://doi.org/10.1080/00103624.2016.1261884

Laranjeira, S., Fernandes-Silva, A., Reis, S., Torcato, C., Raimundo, F., Ferreira, L., Carnide, V., & Marques, G. (2021). Inoculation of plant growth promoting bacteria and arbuscular mycorrhizal fungi improve chickpea performance under water deficit conditions. *Applied Soil Ecology* 164, 103927. https://doi.org/10.1016/j.apsoil.2021.103927

Lal, R. (2004). Soil carbon sequestration impacts on global climate change and food security. *Science* 304, 1623-7. doi: 10.1126/science.1097396

Lal, R. (2011). Sequestering carbon in soils of agro-ecosystems. *Food Policy* 36, S33– S39. http://dx.doi.org/10.1016/j.foodpol.2010.12.001

Lally, R.D., Galbally, P., Moreira, A.S., Spink, J., Ryan, D., Germaine, K.J., & Dowling, D.N. (2017). Application of endophytic pseudomonas fluorescens and a bacterial consortium to brassica napus can increase plant height and biomass under greenhouse and field conditions. *Frontiers in Plant Science* 8, 1–10. https://doi.org/10.3389/fpls.2017.02193

Lamattina, L., García-Mata, C., Graziano, M., & Pagnussat, G.C. (2003) Nitric oxide: the versatility of an extensive signal molecule. *Annual Review of Plant Biology* 54, 109–136.

Lampurlanés, J., Plaza-Bonilla, D., Álvaro-Fuentes, J., & Cantero-Martínez, C. (2016). Long-term analysis of soil water conservation and crop yield under different tillage systems in Mediterranean rainfed conditions. *Field Crop Research* 189, 59–67. http://dx.doi.org/10.1016/j.fcr.2016.02.010

Lassaletta, L., & Aguilera, E. (2015). Soil carbon sequestration is a climate stabilization wedge: comments on Sommer and Bossio. *Journal of Environmental* Manage 153, 48–49. http://dx.doi.org/10.1016/j.jenvman.2015.01.038

Li, M., Cozzolino, V., Mazzei, P., Drosos, M., Monda, H., Hu, Z., & Piccolo, A. (2018). Effects of microbial bioeffectors and P amendements on P forms in a maize cropped soil as evaluated by 31P–NMR spectroscopy. *Plant and Soil*, *427*(1–2), 87–104. https://doi.org/10.1007/s11104-017-3405-8

López-Bucio, J., Pelagio-Flores, R., & Herrera-Estrella, A. (2015). Trichoderma as biostimulant: Exploiting the multilevel properties of a plant beneficial fungus. *Scientia Horticulturae*, *196*(January 2018), 109–123. https://doi.org/10.1016/j.scienta.2015.08.043

Lorito, M., Woo, S. L., Harman, G. E., & Monte, E. (2010). Translational research on Trichoderma: from 'omics to the field. *Annual Review of Phytopathology* 48, 395–417. doi: 10.1146/annurev-phyto-073009-114314

Lorito, M., & Woo, S. L. (2015). "Discussion agronomic," in Principles of Plant-Microbe Interactions, ed. B. Lugtenberg (Berlin: Springer International Publishing), 345–353. doi: 10.1007/978-3-319-08575-3_36

Lucini, L., Rouphael, Y., Cardarelli, M., Bonini, P., Baffi, C., & Colla, G. (2018). A Vegetal Biopolymer-Based Biostimulant Promoted Root Growth in Melon While Triggering Brassinosteroids and Stress-Related Compounds. *Frontiers in Plant Science*, *9*(April), 1–11. https://doi.org/10.3389/fpls.2018.00472

Mazzei, P. & Piccolo, A. (2015). Interactions between natural organic matter and organic pollutants as revealed by NMR spectroscopy. *Magnetic Resonance in Chemistry*, 53(9), 667–678. https://doi.org/10.1002/mrc.4209

Meftah Kadmiri, I., El Mernissi, N., Azaroual, S. E., Mekhzoum, M. E. M., Qaiss, A. E. K., & Bouhfid, R. (2020). Bioformulation of Microbial Fertilizer Based on Clay and Alginate Encapsulation. *Current Microbiology*, *78*(1), 86–94. https://doi.org/10.1007/s00284-020-02262-2

Miceli, A., Moncada, A., & Vetrano, F. (2021). Use of microbial biostimulants to increase the salinity tolerance of vegetable transplants. *Agronomy*, *11*(6). https://doi.org/10.3390/agronomy11061143

Monda, H., Cozzolino, V., Vinci, G., Spaccini, R., & Piccolo, A. (2017). Molecular characteristics of water-extractable organic matter from different composted biomasses and their effects on seed germination and early growth ofmaize. *Science of the Total Environment*, *590–591*, 40–49. https://doi.org/10.1016/j.scitotenv.2017.03.026

Monda, H., Cozzolino, V., Vinci, G., Drosos, M., & Piccolo, A. (2018) Biostimulation of the early growth of Maize by the molecular Humeome extracted from different green composts. *Plant and Soil* 429, 407-424. https://doi.org/10.1007/s11104

Monda, H., McKenna, A. M., Fountain, R., & Lamar, R. T. (2021). Bioactivity of Humic Acids Extracted From Shale Ore: Molecular Characterization and Structure-Activity Relationship With Tomato Plant Yield Under Nutritional Stress. *Frontiers in Plant Science*, *12*(May), 1–17. https://doi.org/10.3389/fpls.2021.660224

Mora, V., Bacaicoa, E., Zamarreño, A. M., Aguirre, E., Garnica, M., Fuentes, M., & García-Mina, J. M. (2010). Action of humic acid on promotion of cucumber shoot growth involves nitrate-related changes associated with the root-to-shoot distribution of cytokinins, polyamines and mineral nutrients. *Journal of Plant Physiology*, *167*(8), 633–642. https://doi.org/10.1016/j.jplph.2009.11.018

Moradtalab, N., Ahmed, A., Geistlinger, J., Walker, F., Höglinger, B., Ludewig, U., & Neumann, G. (2020). Synergisms of Microbial Consortia, N Forms, and Micronutrients Alleviate Oxidative Damage and Stimulate Hormonal Cold Stress Adaptations in Maize. *Frontiers in Plant Science*, *11*(April), 1–19. https://doi.org/10.3389/fpls.2020.00396

Morales-Corts, M. R., Pérez-Sánchez, R., & Gómez-Sánchez, M. Á. (2018). Efficiency of garden waste compost teas on tomato growth and its suppressiveness against soilborne pathogens. *Scientia Agricola*, *75*(5), 400–409. https://doi.org/10.1590/1678-992x-2016-0439

Moreira, H., Pereira, S. I. A., Vega, A., Castro, P. M. L., & Marques, A. P. G. C. (2020). Synergistic effects of arbuscular mycorrhizal fungi and plant growth-promoting bacteria benefit maize growth under increasing soil salinity. *Journal of Environmental Management*, *257*(September 2019), 109982. https://doi.org/10.1016/j.jenvman.2019.109982

Morsomme, P., & Boutry, M. (2000). The plant plasma-membrane H+-ATPase: structure, function and regulation. *Biochimica et Biophysica Acta* 1465, 1–16.

Merlo, L., Ghisi, R., Rascio, N., & Passera, C. (1991). Effects of humic substances on carbohydrate metabolism of maize leaves. *Canadian Journal of Plant Science* 71, 419–425.

Muscolo, A., Cutrupi, S., & Nardi, S. (1998). IAA detection in humic substances. *Soil Biology and Biochemistry* 30, 1199–1201.

Muscolo, A., Bovalo, F., Giomfriddo, F., & Nardi, S. (1999). Earthworm humi matter produces auxin-like on Daucus carota cell growth and nitrate metabolism. *Soil Biology and Biochemistry* 31, 1303–1311.

Nadeem, S.M., Ahmad, M., Zahir, Z.A., Javaid, A., & Ashraf, M. (2014). The role of mycorrhizae and plant growth promoting rhizobacteria (PGPR) in improving crop productivity under stressful environments. *Biotechnology Advances* 32, 429–448.

Naidu, Y., Meon, S., & Siddiqui, Y. (2013). Foliar application of microbial-enriched compost tea enhances growth, yield and quality of muskmelon (Cucumis melo L.) cultivated under fertigation system. *Scientia Horticulturae*, *159*, 33–40. https://doi.org/10.1016/j.scienta.2013.04.024

Nardi, S., Concheri, G., Pizzeghello, D., Sturaro, A., Rella, R., & Parvoli, G. (2000°). Soil organic matter mobilization by root exudates. *Chemosphere* 41, 653–658.

Nardi, S., Pizzeghello, D., Gessa, C., Ferrarese, L., Trainotti, L., & Casadoro, G. (2000b). A low molecular weight humic fraction on nitrate uptake and protein synthesis in maize seedlings. *Soil Biology and Biochemistry* 32, 415–419.

Nardi, S., Pizzeghello, D., Muscolo, A., & Vianello, A. (2002). Physiological effects of humic substances on higher plants. *Soil Biology and Biochemistry*, *34*(11), 1527–1536. https://doi.org/10.1016/S0038-0717(02)00174-8

Nardi, S., Muscolo, A., Vaccaro, S., Baiano, S., Spaccini, R., & Piccolo, A. (2007). Relationship between molecular characteristics of soil humic fractions and glycolytic pathway and krebs cycle in maize seedlings. *Soil Biology and Biochemistry*, *39*(12), 3138–3146. https://doi.org/10.1016/j.soilbio.2007.07.006

Nardi, S., Pizzeghello, D., Schiavon, M., & Ertani, A. (2016). Plant biostimulants: Physiological responses induced by protein hydrolyzed-based. *Scientia Agricola*, *73*(1), 18–23. https://doi.org/10.1590/0103-9016-2015-0006

Nardi, S., Schiavon, M., & Francioso, O. (2021). Chemical Structure and Biological Activity of Humic Substances Define Their Role as Plant Growth Promoters. *Molecules*, *26*(8). https://doi.org/10.3390/molecules26082256

Nawaz, A., Shahbaz, M., Asadullah, M., Imran, A., Marghoob, M.U., Imtiaz, M., & Mubeen, F. (2020). Potential of Salt Tolerant PGPR in Growth and Yield Augmentation of Wheat (Triticum aestivum L.) under Saline Conditions. *Frontiers in Microbiology* 11. https://doi.org/10.3389/fmicb.2020.02019

Nebbioso, Antonio, & Piccolo, A. (2011). Basis of a humeomics science: Chemical fractionation and molecular characterization of humic biosuprastructures. *Biomacromolecules*, *12*(4), 1187–1199. https://doi.org/10.1021/bm101488e

Nebbioso, Antonio, & Piccolo, A. (2012). Advances in humeomics: Enhanced structural identification of humic molecules after size fractionation of a soil humic acid. *Analytica Chimica Acta*, *720*, 77–90. https://doi.org/10.1016/j.aca.2012.01.027

Nebbioso, A., Piccolo, A., Lamshöft, M., & Spiteller, M. (2014). Molecular characterization of an end-residue of humeomics applied to a soil humic acid. *RSC Advances*, *4*(45), 23658–23665. https://doi.org/10.1039/c4ra01619j

Nebbioso, Antonio, Mazzei, P., & Savy, D. (2014). Reduced complexity of multidimensional and diffusion NMR spectra of soil humic fractions as simplified by Humeomics. *Chemical and Biological Technologies in Agriculture*, *1*(1), 1–9. https://doi.org/10.1186/s40538-014-0024-y

Nebbioso, Antonio, Vinci, G., Drosos, M., Spaccini, R., & Piccolo, A. (2015). Unveiling the molecular composition of the unextractable soil organic fraction (humin) by humeomics. *Biology and Fertility of Soils*, *51*(4), 443–451. https://doi.org/10.1007/s00374-014-0991-y

Neethu, T. M., Dubey, P. K., & Kaswala, A. R. (2018). Prospects and Applications of Hydrogel Technology in Agriculture. *International Journal of Current Microbiology and Applied Sciences*, *7*(05), 3155–3162. https://doi.org/10.20546/ijcmas.2018.705.369

Nephali, L., Piater, L. A., Dubery, I. A., Patterson, V., Huyser, J., Burgess, K., & Tugizimana, F. (2020). Biostimulants for plant growth and mitigation of abiotic stresses: A metabolomics perspective. *Metabolites*, *10*(12), 1–26. https://doi.org/10.3390/metabo10120505

Nuzzo, A., & Piccolo, A. (2013°). Enhanced catechol oxidation by heterogeneous biomimetic catalysts immobilized on clay minerals. *Journal of Molecular Catalysis* A 371, 8–14.

Nuzzo, A., & Piccolo, A. (2013b). Oxidative and photo-oxidative polymerization of humic suprastructures by heterogeneous biomimetic catalysis. *Biomacromolecules* 14, 1645–1652.

Nuzzo, A., Madonna, E., Mazzei, P., Spaccini, R., & Piccolo, A. (2016). In situ photo-polymerization of soil organic matter by heterogeneous nano-TiO2 and biomimetic metal- porphyrin catalysts. *Biology and Fertility of Soils* 52, 585–593.

Nuzzo, A., Spaccini, R., Cozzolino, V., Moschetti, G., & Piccolo, A. (2017). In situ polymerization of soil organic matter by oxidative biomimetic catalysis. *Chemical and Biological Technologies in Agriculture*, 1–7. https://doi.org/10.1186/s40538-017-0094-8

Nuzzo, A., Mazzei, P., Drosos, M., & Piccolo, A. (2020). Novel Humo-Pectic Hydrogels for Controlled Release of Agroproducts. *ACS Sustainable Chemistry and Engineering*, *8*(27), 10079–10088. https://doi.org/10.1021/acssuschemeng.0c01986

Nuzzo, A., Mazzei, P., Savy, D., Meo, V. Di, & Piccolo, A. (2020). *Pectins of Di ff erent Degree of Methyl-Esterification*. 1–13.

Ogle, S. M., Breidt, F. J., & Paustian, K. (2005). Land use and management of agricultural systems is known to change the storage of soil organic carbon (SOC) through variation in land use, tillage, cropping practices (intensity and types of crops), irrigation, fertilization, and other activities (Paustia. *Biogeochemistry*, *72*(1), 87–121. https://doi.org/10.1007/s10533-004-0360-2

Olivares, F.L., Aguiar, N.O., Rosa, R.C.C., & Canellas, L.P. (2015). Substrate biofortification in combination with foliar sprays of plant growth promoting bacteria and humic substances boosts production of organic tomatoes. *Scientia Horticulturae* 183, 100–108.

Olivares, F. L., Busato, J. G., Paula, A. M. De, Lima, S., Aguiar, N. O., & Canellas, L. P. (2017). Plant growth promoting bacteria and humic substances : crop promotion and mechanisms of action. *Chemical and Biological Technologies in Agriculture*, 1–13. https://doi.org/10.1186/s40538-017-0112-x

Ostle, N. J., Levy, P. E., Evans, C. D., & Smith, P. (2009). UK land use and soil carbon sequestration. *Land Use Policy*, *26*(SUPPL. 1), 274–283. https://doi.org/10.1016/j.landusepol.2009.08.006

Pane, C., Celano, G., Piccolo, A., Villecco, D., Spaccini, R., Palese, A.M., & Zaccardelli, M. (2015) Effects of on-farm composted tomato residues on soil biological activity and yields in a tomato cropping system. *Chemical and Biological Technologies in Agriculture* 2, 4.

Pane, C., Palese, A. M., Spaccini, R., Piccolo, A., Celano, G., & Zaccardelli, M. (2016). Enhancing sustainability of a processing tomato cultivation system by using bioactive compost teas. *Scientia Horticulturae*, *202*, 117–124. https://doi.org/10.1016/j.scienta.2016.02.034

Panuccio, M.R., Muscolo, A., & Nardi, S. (2001). Effect of humic substances on nitrogen uptake and assimilation in two species of pinus. *Journal of Plant Nutrition* 24, 693–704.

Pardey, P. G., Beddow, J. M., Hurley, T. M., Beatty, T. K. M., & Eidman, V. R. (2014). A Bounds Analysis of World Food Futures: Global Agriculture Through to 2050. *Australian Journal of Agricultural and Resource Economics*, *58*(4), 571–589. https://doi.org/10.1111/1467-8489.12072

Pathania, P., Rajta, A., Singh, P.C., & Bhatia, R. (2020). Role of plant growth-promoting bacteria in sustainable agriculture. *Biocatalysis and Agricultural Biotechnology*, 30, 101842. https://doi.org/10.1016/j.bcab.2020.101842

Pauly, N., Pucciariello, C., Mandon, K., Innocenti, G., Jamet, A., Baudouin, E., Frendo, P., & Puppo, A. (2006). Reactive oxygen and nitrogen species and glutathione: Key players in the legume-Rhizobium symbiosis. *Journal of Experimental Botany* 57, 1769–1776.

Pedranzani, H., Rodríguez-Rivera, M., Gutiérrez, M., Porcel, R., Hause, B., & Ruiz-Lozano, J.M. (2016). Arbuscular mycorrhizal symbiosis regulates physiology and performance of Digitaria eriantha plants subjected to abiotic stresses by modulating antioxidant and jasmonate levels. *Mycorrhiza* 26, 141–152.

Piccolo, A., & Mbagwu, J. S. C. (1990). Effects of different organic waste amendments on soil microaggregates stability and molecular sizes of humic substances. *Plant Soil* 123, 27-37.

Piccolo, A., Nardi, S., & Concheri, G. (1992). Structural characteristics of humus and biological activity. *Soil Biology and Biochemistry* 24, 273–380.

Piccolo, A. & Mbagwu, J.S.C. (1994). Humic substances and surfactants on the stability of two tropical soils. *Soil Science Society of American Journal* 58, 950-955.

Piccolo, A., Nardi, S., & Cancheri, G. (1996). Macro-molecular changes of soil humic substances induced by interactions with organic acids. *European Journal of Soil Science* 47, 319–328.

Piccolo, A. (1996). Humus and Soil Conservation. *Humic Substances in Terrestrial Ecosystems*, 225–264. https://doi.org/10.1016/b978-044481516-3/50006-2

Piccolo, A., Pietramellara, G., & Mbagwu, J. S. C. (1997°). Use of humic substances as soil conditioners to increase aggregate stability. *Geoderma*, *75*(3–4), 267–277. https://doi.org/10.1016/S0016-7061(96)00092-4

Piccolo, A, Pietramellara, G., & Mbagwu, J. S. C. (1997b). *Reduction in soil loss from erosion-susceptible soils amended with humic substances from oxidized coal*. *10*, 235–245.

Piccolo, A., & Mbagwu, J.S.C. (1999). Role of hydrophobic components of soil organic matter on the stability of soil aggregates. *Soil Science Society of American Journal* 63, 1801–1810.

Piccolo, A., Spaccini, R., Haberhauer, G., & Gerzabek, M. H. (1999a). Increased sequestration of organic carbon in soil by hydrophobic protection. *Naturwissenschaften*, *86*(10), 496–499. https://doi.org/10.1007/s001140050662

Piccolo, A., Conte, P., & Cozzolino, A. (1999b). Effects of mineral and monocarboxylic acids on the molecular association of dissolved humic substances. *European Journal of Soil Science* 50, 687–694.

Piccolo, A., Conte, P., & Cozzolino, A. (2000). Differences in high performance size exclusion chromatography between humic substances and macro-molecular polymers. In Humic Substances. Versatile Components of Plant, Soils and Water. E.A. Gabbhour and G. Davies (eds.).Royal Society of Chemistry, Cambridge, UK., Special Publication no. 259, pp. 111–124.

Piccolo, A., Cozzolino, A., & Conte, P. (2001). Chromatographic and spectrophotometric properties of dissolved humic substances compared with macro-molecular polymers. *Soil Science* 166, 174–185.

Piccolo, Alessandro. (2002). The supramolecular structure of humic substances: A novel

understanding of humus chemistry and implications in soil science. *Advances in Agronomy*, *75*, 57–134. https://doi.org/10.1016/s0065-2113(02)75003-7

Piccolo, Alessandro, Spaccini, R., Nieder, R., & Richter, J. (2004). Sequestration of a biologically labile organic carbon in soils by humified organic matter. *Climatic Change*, *67*(2–3), 329–343. https://doi.org/10.1007/s10584-004-1822-1

Piccolo, A., Conte, P., Spaccini, R., & Mbagwu, J. S. C. (2005). Influence of land use on the characteristics of humic substances in some tropical soils of Nigeria. *European Journal of Soil Science*, *56*(3), 343–352. https://doi.org/10.1111/j.1365-2389.2004.00671.x

Piccolo, A. (2012). The nature of soil organic matter and innovative soil managements to fight global changes and maintain agricultural productivity. In: Piccolo, A. (Ed.), Carbon Sequestration in Agricultural Soils: A Multidisciplinary Approach to Innovative Methods. Springer-Verlag Berlin Heidelberg, Berlin, pp. 1–20.

Piccolo, Alessandro, Spaccini, R., Cozzolino, V., Nuzzo, A., Drosos, M., Zavattaro, L., Grignani, C., Puglisi, E., & Trevisan, M. (2018). Effective carbon sequestration in Italian agricultural soils by in situ polymerization of soil organic matter under biomimetic photocatalysis. *Land Degradation and Development*, *29*(3), 485–494. https://doi.org/10.1002/ldr.2877

Piccolo, Alessandro, Spaccini, R., Drosos, M., Vinci, G., & Cozzolino, V. (2018). The molecular composition of humus carbon: Recalcitrance and reactivity in soils. In *The Future of Soil Carbon: Its Conservation and Formation*. Elsevier Inc. https://doi.org/10.1016/B978-0-12-811687-6.00004-3

Piccolo, Alessandro, Spaccini, R., Savy, D., & Drosos, M. (2019). *The Soil Humeome : Chemical Structure , Functions and Technological The Soil Humeome : Chemical Structure ,* (Issue May). https://doi.org/10.1007/978-3-030-17891-8

Plaza-Bonilla, D., Cantero-Martínez, C., & Álvaro-Fuentes, J. (2010). Tillage effects on soil aggregation and soil organic carbon profile distribution under Mediterranean semi-arid conditions. *Soil Use Manage* 26, 465–474. http:// dx.doi.org/10.1111/j.1475-2743.2010.00298

Priya, S., Mk, K., Roshan, C., & Deepak, K. (2021). Effect of soil and foliar applications of compost tea on growth characters , quality and nutrient content of soybean [Glycine max . (L .) Merrill] under organic cultivation. *Journal of Pharmacognosy and Phytochemistry*, *10*(1), 2566–2569.

Prove, B.J, Loch, R.J., Foley, J.L, Anderson, V.J., & Younger D.R. (1990). Improvements in aggregation and infiltration characteristics of a krasnozem under maize with direct drill and stubble retention. *Australian Journal of Soil Research* 28, 577-590.

Puglisi, E., Fragoulis, G., Del Re, A. A. M., Spaccini, R., Piccolo, A., Gigliotti, G., Said-Pullicino, D., & Trevisan, M. (2008). Carbon deposition in soil rhizosphere following amendments with compost and its soluble fractions, as evaluated by combined soil-plant rhizobox and reporter gene systems. *Chemosphere*, *73*(8), 1292–1299. https://doi.org/10.1016/j.chemosphere.2008.07.008

Quaggiotti, S., Ruperti, B., Pizzeghello, D., Francioso, O., Tugnoli, V., & Nardi, S. (2004). Effect of low molecular size humic substances on nitrate uptake and expression of genes involved in nitrate transport in maize (Zea mays L.). *Journal of Experimental Botany*, *55*(398), 803–813.

https://doi.org/10.1093/jxb/erh085

Quiroga, G., Erice, G., Aroca, R., Zamarreño, Á.M., García-Mina, J.M., & Ruiz-Lozano, J.M. (2018). Arbuscular mycorrhizal symbiosis and salicylic acid regulate aquaporins and root hydraulic properties in maize plants subjected to drought. *Agricultural Water Management* 202, 271–284. https://doi.org/10.1016/j.agwat.2017.12.012

Radzki, W., Gutierrez Mañero, F.J., Algar, E., Lucas García, J.A., García-Villaraco, A., & Ramos Solano, B. (2013). Bacterial siderophores efficiently provide iron to iron-starved tomato plants in hydroponics culture. Antonie Leeuwenhoek 104, 321–330.

Ramos, A.C., Olivares, F.L., Silva, L.S., Aguiar, N.O., & Canellas, L.P. (2015). Humic matter elicits proton and calcium fluxes and signaling dependent on Ca2+-dependent protein kinase (CDPK) at early stages of lateral plant root development. *Chemical and Biological Technologies in Agriculture* 2, 4.

Rasmussen, J. J., Wiberg-Larsen, P., Baattrup-Pedersen, A., Cedergreen, N., McKnight, U. S., Kreuger, J., Jacobsen, D., Kristensen, E. A., & Friberg, N. (2015). The legacy of pesticide pollution: An overlooked factor in current risk assessments of freshwater systems. *Water Research*, *84*, 25–32. https://doi.org/10.1016/j.watres.2015.07.021

Ray, D. K., Mueller, N. D., West, P. C., & Foley, J. A. (2013). Yield Trends Are Insufficient to Double Global Crop Production by 2050. *PLoS ONE*, *8*(6). https://doi.org/10.1371/journal.pone.0066428

Rochon, J.J., Doyle, C.J., Greef, J.M., Hopkins, A., Molle, G., Sitzia, M., Scholefield, D., & Smith, C.J. (2004). Grazing legumes in Europe: a review of their status, management, benefits, research needs and future prospects. *Grass Forage Science* 59, 197–214. http://dx.doi.org/10.1111/j.1365-2494.2004.00423

Ros, M., Hurtado-Navarro, M., Giménez, A., Fernández, J. A., Egea-Gilabert, C., Lozano-Pastor, P., & Pascual, J. A. (2020). Spraying agro-industrial compost tea on baby spinach crops: Evaluation of yield, plant quality and soil health in field experiments. *Agronomy*, *10*(3). https://doi.org/10.3390/agronomy10030440

Rouphael, Y., De Micco, V., Arena, C., Raimondi, G., Colla, G., & De Pascale, S. (2017). Effect of Ecklonia maxima seaweed extract on yield, mineral composition, gas exchange and leaf anatomy of zucchini squash grown under saline conditions. *Journal of Applied Phycology* 29, 459–470. doi: 10.1007/s10811-016- 0937-x

Rouphael, Y., & Colla, G. (2018). Synergistic biostimulatory action: Designing the next generation of plant biostimulants for sustainable agriculture. *Frontiers in Plant Science*, *871*(November), 1–7. https://doi.org/10.3389/fpls.2018.01655

Rouphael, Y., & Colla, G. (2020). Editorial: Biostimulants in Agriculture. *Frontiers in Plant Science*, *11*(February), 1–7. https://doi.org/10.3389/fpls.2020.00040

Rudawska, M.L., & Kieliszewska-Rokicka, B. (1997). Mycorrhizal formation by Paxillus involutus strains in relation to their IAA- synthesizing activity. *New Phytology* 1997, 137, 509–517.

Saia, S., Colla, G., Raimondi, G., Di Stasio, E., Cardarelli, M., Bonini, P., Vitaglione, P., De Pascale, S., & Rouphael, Y. (2019). An endophytic fungi-based biostimulant modulated lettuce yield, physiological and functional quality responses to both moderate and severe water limitation.

Scientia Horticulturae, *256*(March), 108595. https://doi.org/10.1016/j.scienta.2019.108595

Saia, S., Aissa, E., Luziatelli, F., Ruzzi, M., Colla, G., Ficca, A. G., Cardarelli, M., & Rouphael, Y. (2020). Growth-promoting bacteria and arbuscular mycorrhizal fungi differentially benefit tomato and corn depending upon the supplied form of phosphorus. *Mycorrhiza*, *30*(1), 133–147. https://doi.org/10.1007/s00572-019-00927-w

Saiz-Jimenez, C. (1996). In: A. Piccolo (Ed.), Humic Substances in Terrestrial Ecosystems. Elsevier Science, Amsterdam, The Netherlands, pp. 1–44.

Santos, M., Andrade, R. De, Melo, B. De, & Gallo, M. Del. (2021). *Humic Substances in Combination With Plant Growth-Promoting Bacteria as an Alternative for Sustainable Agriculture*. *12*(October), 1–14. https://doi.org/10.3389/fmicb.2021.719653

Sanz-Cobena, A., Lassaletta, L., Aguilera, E., Prado, A. del, Garnier, J., Billen, G., Iglesias, A., Sánchez, B., Guardia, G., Abalos, D., Plaza-Bonilla, D., Puigdueta-Bartolomé, I., Moral, R., Galán, E., Arriaga, H., Merino, P., Infante-Amate, J., Meijide, A., Pardo, G., … Smith, P. (2017). Strategies for greenhouse gas emissions mitigation in Mediterranean agriculture: A review. *Agriculture, Ecosystems and Environment*, *238*, 5–24. https://doi.org/10.1016/j.agee.2016.09.038

Savy, D., Cozzolino, V., Vinci, G., Nebbioso, A., & Piccolo, A. (2015). Water-soluble lignins from different bioenergy crops stimulate the early development of maize (Zea mays, L.). *Molecules*, *20*(11), 19958–19970. https://doi.org/10.3390/molecules201119671

Savy, D., Cozzolino, V., Nebbioso, A., Drosos, M., Nuzzo, A., Mazzei, P., & Piccolo, A. (2016). Humic-like bioactivity on emergence and early growth of maize (Zea mays L.) of water-soluble lignins isolated from biomass for energy. *Plant and Soil*, *402*(1–2), 221–233. https://doi.org/10.1007/s11104-015-2780-2

Savy, D., Mazzei, P., Drosos, M., Cozzolino, V., Lama, L., & Piccolo, A. (2017). Molecular Characterization of Extracts from Biorefinery Wastes and Evaluation of Their Plant Biostimulation. *ACS Sustainable Chemistry and Engineering*, *5*(10), 9023–9031. https://doi.org/10.1021/acssuschemeng.7b01928

Savy, D., Brostaux, Y., Cozzolino, V., Delaplace, P., du Jardin, P., & Piccolo, A. (2020). Quantitative Structure-Activity Relationship of Humic-Like Biostimulants Derived From Agro-Industrial Byproducts and Energy Crops. *Frontiers in Plant Science*, *11*(May), 1–13. https://doi.org/10.3389/fpls.2020.00581

Schiavon, M., Pizzeghello, D., Muscolo, A., Vaccaro, S., Francioso, O., & Nardi, S. (2010). High molecular size humic substances enhance phenylpropanoid metabolism in maize (Zea mays L.). *Journal of Chemical Ecology*, *36*(6), 662–669. https://doi.org/10.1007/s10886-010-9790-6

Schnitzer, M. (1972). "Humic substances in the environment". Marcel Dekker, New York.

Sexstone, A.J., Revsbech, N.P., Parkin, T.B., & Tiedje, J.M. (1985). Direct measurement of oxygen profiles and denitrification rates in soil aggregates. *Soil Science Society of American Journal* 49, 645-651.

Sestili, F., Rouphael, Y., Cardarelli, M., Pucci, A., Bonini, P., Canaguier, R., et al. (2018). Protein hydrolysate stimulates growth and N uptake in tomato coupled with N-dependent gene

expression involved in N assimilation. *Frontiers in Plant Science* 9, 1233. doi: 10.3389/fpls.2018.01233

Sharma, H. S. S., Fleming, C., Selby, C., Rao, J. R., & Martin, T. (2014). Plant biostimulants: A review on the processing of macroalgae and use of extracts for crop management to reduce abiotic and biotic stresses. *Journal of Applied Phycology*, *26*(1), 465–490. https://doi.org/10.1007/s10811-013-0101-9

Shennan, C., Krupnik, T. J., Baird, G., Cohen, H., Forbush, K., Lovell, R. J., & Olimpi, E. M. (2017). Organic and Conventional Agriculture: A Useful Framing? *Annual Review of Environment and Resources*, *42*, 317–346. https://doi.org/10.1146/annurev-environ-110615-085750

Siddiqui, Y., Islam, T. M., Naidu, Y., & Meon, S. (2011). The conjunctive use of compost tea and inorganic fertiliser on the growth, yield and terpenoid content of Centella asiatica (L.) urban. *Scientia Horticulturae*, *130*(1), 289–295. https://doi.org/10.1016/j.scienta.2011.05.043

Šimon, T., Javůrek, M., Mikanová, O., & Vach, M. (2009). The influence of tillage systems on soil organic matter and soil hydrophobicity. *Soil and Tillage Research*, *105*(1), 44–48. https://doi.org/10.1016/j.still.2009.05.004

Six, J., Elliott, E.T, & Paustian, K. (1999). Aggregate and soil organic matter dynamics under conventional and no-tillage systems. *Soil Science Society of American Journal* 63, 1350–1358.

Six, J., Elliott, E.T., & Paustian, K (2000). Soil macroaggregate turnover and microaggregate formation: a mechanism for C sequestration under no-tillage agriculture. *Soil Biology and Biochemistry* 32, 2099–2103.

Six, J., Bossuyt, H., Degryze, S., & Denef, K. (2004). A history of research on the link between (micro)aggregates, soil biota, and soil organic matter dynamics. *Soil Tillage Research* 79, 7–31. http://dx.doi.org/10.1016/j.still.2004.03.008

Šmejkalová, D., & Piccolo, A. (2005). Enhanced molecular dimension of a humic acid induced by photooxidation catalyzed by biomimetic metalporphyrins. *Biomacromolecules* 6, 2120–2125.

Šmejkalová, D., & Piccolo, A. (2006). Rates of oxidative coupling of humic phenolic monomers catalyzed by a biomimetic iron-porphyrin. *Environmental Science and Technology* 40, 1644–1649.

Smejkalova, D., & Piccolo, A. (2008). Aggregation and disaggregation of humic supramolecular assemblies by NMR diffusion ordered spectroscopy (DOSY-NMR). *Environmental Science and Technology* 42, 699-706.

Smith, S.E., & Read, D.J. (2008). Mycorrhizal Symbiosis, 3rd ed.; Academic Press: London, UK, 2008.

Smith, P., & Olesen, J.E. (2010). Synergies between the mitigation of, and adaptation to, climate change in agriculture. *Journal of Agricultural Science* 148, 543– 552. http://dx.doi.org/ 10.1017/s0021859610000341

Song, B., Liang, H., Sun, R., Peng, P., Jiang, Y., & She, D. (2020). Hydrogel synthesis based on lignin/sodium alginate and application in agriculture. *International Journal of Biological Macromolecules*, *144*, 219–230. https://doi.org/10.1016/j.ijbiomac.2019.12.082

Spaccini, R., Piccolo, A., Conte, P., Haberhauer, G., & Gerzabek, M. H. (2002). Increased soil organic

carbon sequestration through hydrophobic protection by humic substances. *Soil Biology and Biochemistry*, *34*(12), 1839–1851. https://doi.org/10.1016/S0038-0717(02)00197-9

Spaccini, R., Mbagwu, J. S. C., Conte, P., & Piccolo, A. (2006). Changes of humic substances characteristics from forested to cultivated soils in Ethiopia. *Geoderma*, *132*(1–2), 9–19. https://doi.org/10.1016/j.geoderma.2005.04.015

Spaccini, Riccardo, & Piccolo, A. (2007). Molecular characterization of compost at increasing stages of maturity. 2. Thermochemolysis-GC-MS and 13C-CPMAS-NMR spectroscopy. *Journal of Agricultural and Food Chemistry*, *55*(6), 2303–2311. https://doi.org/10.1021/jf0625407

Spaccini, Riccardo, Baiano, S., Gigliotti, G., & Piccolo, A. (2008). Molecular characterization of a compost and its water-soluble fractions. *Journal of Agricultural and Food Chemistry*, *56*(3), 1017–1024. https://doi.org/10.1021/jf0716679

Spaccini, Riccardo, & Piccolo, A. (2009). Molecular characteristics of humic acids extracted from compost at increasing maturity stages. *Soil Biology and Biochemistry*, *41*(6), 1164–1172. https://doi.org/10.1016/j.soilbio.2009.02.026

Spaccini, R., Piccolo, A. (2012). Carbon sequestration in soils by hydrophobic protection and in situ catalyzed photo-polymerization of soil organic matter (SOM): chemical and physical–chemical aspects of SOM in field plots. In: Piccolo A (ed) Carbon sequestration in agricultural soils. Springer Verlag, Heidelberg, pp 61–106.

Spaccini, Riccardo, Song, X. Y., Cozzolino, V., & Piccolo, A. (2013). Molecular evaluation of soil organic matter characteristics in three agricultural soils by improved off-line thermochemolysis: The effect of hydrofluoric acid demineralisation treatment. *Analytica Chimica Acta*, *802*, 46–55. https://doi.org/10.1016/j.aca.2013.09.031

Spaccini, R., Cozzolino, V., Di Meo, V., Savy, D., Drosos, M., & Piccolo, A. (2019). Bioactivity of humic substances and water extracts from compost made by ligno-cellulose wastes from biorefinery. *Science of the Total Environment*, *646*, 792–800. https://doi.org/10.1016/j.scitotenv.2018.07.334

Spedding, T.A., Hamel, C., Mehuys, G.R., & Madramootoo, C.A. (2004). Soil microbial dynamics in maize- growing soil under different tillage and residue management systems. *Soil Biology and Biochemistry* 36, 499–512.

Stevenson, F.J. (1994). Humus chemistry: genesis, composition, and reactions. 2nd ed. Wiley-Intersci., New York.

Sun, S., Sidhu, V., Rong, Y., & Zheng, Y. (2018). Pesticide Pollution in Agricultural Soils and Sustainable Remediation Methods: a Review. *Current Pollution Reports*, *4*(3), 240–250. https://doi.org/10.1007/s40726-018-0092-x

Tadini, A. M., Pantano, G., de Toffoli, A. L., Fontaine, B., Spaccini, R., Piccolo, A., Moreira, A. B., & Bisinoti, M. C. (2015). Off-line TMAH-GC/MS and NMR characterization of humic substances extracted from river sediments of northwestern São Paulo under different soil uses. *Science of the Total Environment*, *506–507*, 234–240. https://doi.org/10.1016/j.scitotenv.2014.11.012

Tang, H., Zhang, L., Hu, L., & Zhang, L. (2014). Application of Chitin Hydrogels for Seed Germination, Seedling Growth of Rapeseed. *Journal of Plant Growth Regulation*, *33*(2), 195–

201. https://doi.org/10.1007/s00344-013-9361-5

Tedersoo, L., Ko, U., Bahram, M., Sa, S., Do, M., May, T., Ryberg, M., & Abarenkov, K. (2018). High-level classification of the Fungi and a tool for evolutionary ecological analyses. *Fungal Diversity* 90, 135–159. https://doi.org/10.1007/s13225-018-0401-0

Thonar, C., Lekfeldt, J. D. S., Cozzolino, V., Kundel, D., Kulhánek, M., Mosimann, C., Neumann, G., Piccolo, A., Rex, M., Symanczik, S., Walder, F., Weinmann, M., de Neergaard, A., & Mäder, P. (2017). Potential of three microbial bio-effectors to promote maize growth and nutrient acquisition from alternative phosphorous fertilizers in contrasting soils. *Chemical and Biological Technologies in Agriculture*, *4*(1), 1–16. https://doi.org/10.1186/s40538-017-0088-6

Tisdall, J.M., & Oades, J.M. (1982). Organic matter and water-stable aggregates in soils. *Journal of Soil Science* 33, 141–163.

Traon, D. (2014). A Legal Framework for Plant Biostimulants and Agronomic Fertiliser Additives in the EU – Report to the European Commission, DG Enterprise & Industry D.G.E. European Commission & Industry, eds.

Trevisan, S., Botton, A., Vaccaro, S., Vezzaro, A., Quaggiotti, S., & Nardi, S. (2011). Humic substances affect Arabidopsis physiology by altering the expression of genes involved in primary metabolism, growth and development. *Environmental and Experimental Botany*, *74*(1), 45–55. https://doi.org/10.1016/j.envexpbot.2011.04.017

Vaccaro, S., Ertani, A., Nebbioso, A., Muscolo, A., Quaggiotti, S., Piccolo, A., & Nardi, S. (2015). Humic substances stimulate maize nitrogen assimilation and amino acid metabolism at physiological and molecular level. *Chemical and Biological Technologies in Agriculture*, *2*(1), 1–12. https://doi.org/10.1186/s40538-015-0033-5

van Tol de Castro, T. A., Berbara, R. L. L., Tavares, O. C. H., Mello, D. F. da G., Pereira, E. G., Souza, C. da C. B. de, Espinosa, L. M., & García, A. C. (2021). Humic acids induce a eustress state via photosynthesis and nitrogen metabolism leading to a root growth improvement in rice plants. *Plant Physiology and Biochemistry*, *162*, 171–184. https://doi.org/10.1016/j.plaphy.2021.02.043

Verrillo, M., Salzano, M., Cozzolino, V., Spaccini, R., & Piccolo, A. (2021°). Bioactivity and antimicrobial properties of chemically characterized compost teas from different green composts. *Waste Management*, *120*, 98–107. https://doi.org/10.1016/j.wasman.2020.11.013

Verrillo, M., Cozzolino, V., Spaccini, R., & Piccolo, A. (2021b). Humic substances from green compost increase bioactivity and antibacterial properties of essential oils in Basil leaves. *Chemical and Biological Technologies in Agriculture*, *8*(1), 1–14. https://doi.org/10.1186/s40538-021-00226-7

Vinale, F., Flematti, G., & Sivasithamparam K. (2009). Harzianic acid, an antifungal and plant growth promoting metabolite from Trichoderma harzianum. *Journal of Natural Products* 72(11), 2032-5.

Vinale, F., Ghisalberti, E.L., Flematti, G., Marra, R., Lorito, M., & Sivasithamparam, K. (2010). Secondary metabolites produced by a root- inhabiting sterile fungus antagonistic towards pathogenic fungi. *Letters in Applied Microbiology* 50(4), 380-5.

Vinci, G., Cozzolino, V., Mazzei, P., Monda, H., Savy, D., Drosos, M., & Piccolo, A. (2018°). Effects

of Bacillus amyloliquefaciens and different phosphorus sources on Maize plants as revealed by NMR and GC-MS based metabolomics. *Plant and Soil*, *429*(1–2), 437–450. https://doi.org/10.1007/s11104-018-3701-y

Vinci, G., Cozzolino, V., Mazzei, P., Monda, H., Spaccini, R., & Piccolo, A. (2018b). An alternative to mineral phosphorus fertilizers: The combined effects of Trichoderma harzianum and compost on Zea mays, as revealed by 1 H NMR and GC-MS metabolomics. *PLoS ONE*, *13*(12), 1–15. https://doi.org/10.1371/journal.pone.0209664

Vinci, G., Mazzei, P., Drosos, M., Zaccone, C., & Piccolo, A. (2020). Molecular characterization of ombrotrophic peats by humeomics. *Chemical and Biological Technologies in Agriculture*, *7*(1), 1–11. https://doi.org/10.1186/s40538-020-00184-6

Vinci, G., Cangemi, S., Bridoux, M., Spaccini, R., & Piccolo, A. (2021). Molecular properties of the Humeome of two calcareous grassland soils as revealed by GC/qTOF-MS and NMR spectroscopy. *Chemosphere*, *279*, 130518. https://doi.org/10.1016/j.chemosphere.2021.130518

Visser, S.A. (1986). Effetto delle sostanze umiche sulla crescita delle piante. In: Vaughan, D., Malcom, R.E. (Eds.), Soil Organic Matter and Biological Activity. Martinus Nijhoff, Dordrecht/Dr junk W. Publish- ers, Dordecht, The Netherlands, pp. 77–108.

Wang, X., Yost, R.S., & Linquist B.A. (2001). Soil aggregate size affects phosphorus desorption from highly weathered soils and plant growth. *Soil Science Society of American Journal* 65, 139-146.

Wang, Y.Y., Cheng, Y.H., Chen, K.E., & Tsay, Y.F. (2018). Nitrate transport, signaling, and use efficiency. *Annual Review of Plant Biology* 69, 85–122. https://doi.org/10.1146/annurev-arplant-042817-040056

Weber, J., Karczewska, A., Drozd, J., Licznar, M., Licznar, S., Jamroz, E., & Kocowicz, A. (2007) Agricultural and ecological aspects of a sandy soil as affected by the application of municipal solid waste composts *Soil Biology and Biochemistry* 39, 1294–1302.

Wershaw, R.L. (1986). A new model for humic materials and their interactions with hydrophobic chemicals in soil water and sediment-water systems. *Journal of Contaminant Hydrology* 1, 29-45.

West, T. O., & Post, W. M. (2002). Soil organic carbon sequestration rates by tillage and crop rotation: A global data analysis. *Soil Science Society of America Journal*, *66*(6), 1930–1946.

Woo, S. L., Ruocco, M., Vinale, F., Nigro, M., Marra, R., Lombardi, N., Pascale, A., Lanzuise, S., & Manganiello, G. (2014). *Trichoderma -based Products and their Widespread Use in Agriculture*. 71–126.

Woo, S. L., Pepe, O., & Fertilizers, V. S. P. (2018). *Microbial Consortia : Promising Probiotics as Plant Biostimulants for Sustainable Agriculture*. *9*(2003), 7–12. https://doi.org/10.3389/fpls.2018.01801

Yakhin, O. I., Lubyanov, A. A., Yakhin, I. A., & Brown, P. H. (2017). Biostimulants in plant science: A global perspective. *Frontiers in Plant Science*, *7*(January). https://doi.org/10.3389/fpls.2016.02049

Young, C., Rekha, P. D., Lai, W., & Arun, A. B. (2006). *Encapsulation of Plant Growth-Promoting Bacteria in Alginate Beads Enriched With Humic Acid*. https://doi.org/10.1002/bit

Zaccardelli, M., Pane, C., Villecco, D., Maria Palese, A., & Celano, G. (2018). Compost tea spraying increases yield performance of pepper (Capsicum annuum L.) grown in greenhouse under organic farming system. *Italian Journal of Agronomy*, *13*(3), 229–234. https://doi.org/10.4081/ija.2018.991

Xu, L., & Geelen, D. (2018). Developing biostimulants from agro-food and industrial by-products. *Frontiers in Plant Science* 9, 1567. https://doi.org/10.3389/fpls.2018.01567